Recirculated Process Water in the Flotation of Sulfides

Prepared by:

Michael Sekiette Ngau

In fulfilment of the requirements for the degree of Master of Science in Engineering

Department of Chemical Engineering

Faculty of Engineering and the Built Environment

University of Cape Town

31/12/2022

Plagiarism Declaration

I know that plagiarism is wrong. Plagiarism is using another's work and pretending it is one's own. I have used the University of Cape Town convention for citation and referencing. Each contribution to and quotation in this report from other people's work(s) has been attributed, cited and referenced. Any section taken from an internet source has been referenced to that source. This report is my own words (except where I have attributed it to others). I have not allowed and will not allow anyone to copy my work with the intention of passing it off as their work. I acknowledge that copying someone else's assignment or essay, or part of it, is wrong, and I declare that this is my own work.

Signed by Signed by candidate

Acknowledgement

I want to share my sincere gratitude to the following people who were integral in the preparation and execution of this project:

Associate Professor Kirsten C. Corin and Dr Malibongwe S. Manono for their supervision and understanding throughout this project. We always found a way to tackle any hurdles that came by. Thank you for entertaining my curiosity and facilitating and coordinating collaborations that ensured this project came to fruition. Thank you for the mentorship and patronage. I will never forget this opportunity.

The Centre for Minerals Research laboratory staff at the UCT: Shireen Govender, Refilwe Moalosi, Kenneth Maseko, Monde Bekaphi, Lorraine Nkemba, Gary Groenmeyer. Thank you for your sound advice and quick tips on improving the project. Thank you for the check-ups, motivating chats in the lab, and the brief but detailed history of the mineral processing field. I learned many techniques from you and plan to use them in all my endeavours.

Heather Sundstrom, thank you for your administrative patronage; I always felt reassured and calm after your correspondence.

My friend Matthew Dzingai, thank you for your motivation and advice throughout this journey. You preached perseverance and pushed me through to the end—many thanks.

Dr. Njeru, for being the unwitting accomplice and audience of one in the flagrant tales of the journey thus passed.

To my mother Rita Kavashe Nariangai, “ Ulichonipa ndio nguzo yangu, tugange yajayo.” Thank you, mama.

Synopsis

Mineral concentration is an important ore beneficiation step after comminution, utilised to create a mineral concentrate through physical separation from gangue. Froth flotation is commonly used as a mineral concentration process that separates minerals based on their surface properties (hydrophobicity). The separation efficiency of this process is aided by the presence of surfactants such as acids, oils, and salts. Industrial scale froth flotation is operated in units known as flotation cells, tanks and or columns to make up what is known as a concentrator. In a froth flotation process, a mineral-water slurry (about 80 % w/v) is aerated and agitated to develop two distinct phases: a froth and a pulp phase.

The valuable concentrate is collected in the froth phase. In South Africa, the Bushveld Igneous Complex (BIC) is a global powerhouse of Platinum Group Minerals (PGM) production located on Johannesburg's outskirts, a primarily arid region. Due to water scarcity, water use and disposal legislation and water reuse initiatives, most mines use water recycled on-site. Consequently, the efficiency and operating conditions are affected by the change in water quality and have promoted extensive research into the impact of changes in water quality on flotation performance. Water recycling introduces and accumulates inorganic species as suspended solids and ions (e.g., Ca^{2+}, Mg^{2+}, SO_4^{2-}, and Cl^-), which can interact with the ore and reagents used in froth flotation. The change in water quality due to water recycling has an impact on the mineral surface properties, activation of minerals, gangue entrainment, froth stability, settling rate and the ionic concentration of the pulp. An increase in electrostatic ion concentration leads to a more compressed electrical double layer between bubbles and particles, thus leading to greater bubble-particle attachment and higher froth stability, thus affecting both the pulp and froth phase phenomena. In the pulp phase, the ions present alter the surface charge leading to more particle collision and aiding their coagulation. Furthermore, ions interact with the mineral surface leading to a change in the surface properties, activating or acting as competitors for active sites with reagents. The change in pulp chemistry, i.e., changes in dissolved oxygen concentration or redox potential, have an impact on the reaction pathways at play, such as reagent / mineral and or galvanic interactions. Therefore, a change in water quality significantly impacts the operation efficiency of concentrators.

Several operations recycle water on-site. Water recovery from tailings dams is a lengthy process. However, short water recirculation occurs during plant operation, hence, may form a timeous water feed source. Short recycle waters from thickener and

dewatering units are a second recycle water source; however, constituents of such a water source may occur in an active state, hosting active reagents and ongoing chemical interactions. The focus of the study is to investigate the impact of short water recirculation on the recovery and grade of copper and nickel sulfides, solids and water recovery, entrained gangue, electrical conductivity (EC), dissolved oxygen concentration (DO), foam and froth stability, ionic concentration, and tailings settling rates in the flotation of a platinum bearing ore from the Upper Group Chromite (UG2) ore.

The investigation is conducted through sequential batch flotation using recovered water from the preceding batch flotation tailings pulp. Synthetic plant water of a set quality, typical of onsite process water was used as the fresh feed water (baseline water). After flotation, the recycled water is fed either to both the mill for ore comminution and the float cell for batch flotation or only to the float cell for batch flotation. These two circuit configurations supported the investigation into the impact of water recycling on milling and froth flotation. The initial water quality mimicked typical feed water quality based on relevant research and thereafter recycled water was used which showed a spike in common ions such as Ca^{2+}, Mg^{2+}, SO_4^{2-}, Cl^-. Flotation of the ore at a constant collector, depressant and frother dosage is the baseline condition for the experimental program. The presence of these ions in the water was investigated through electrical conductivity and discrete colorimetry. The settling rate of solids present in the tailings was monitored through real time spectroscopic analysis of tailing samples over time to establish both a maximum transparency and the rate of change in transparency over time. The solids, water, nickel and copper recoveries and grades paired with kinetic analysis of recovery, transparency, foam and froth rates are used to evaluate the flotation performance under the degrading water quality.

The residual collector and depressant in the recirculated water are tested using a UV/Vis Spectrophotometer. The concentrations of residual collector and depressant were significantly lower than their feed concentrations as was expected, therefore water recycling did not significantly inhibit reagent activity. This result indicates that the change in water quality did not inhibit the reagent efficiency or usage thereof as it pertains to interactions between reagents and mineral particles in the pulp phase. However, froth stability was significantly influenced by both the change in water quality and the presence of residual frother. In addition, the presence of residual depressant improved the coagulation of the tailings. In all the tests conducted, recycled water had a higher froth stability as compared to recovered water from the baseline floats. In addition, the higher the ionic concentration, the higher the froth stability of the tailings

water, as observed in float cell recirculated water. Short water recirculation led to an increase in the recovery and recovery rate (especially for Ni) of the Cu and Ni present in the ore, however due to an increase in entrainment the grade of the product was not improved. The coagulation of tailings was also affected by the ionic concentration. The increase in ionic concentration led to higher particle collision due to the increase in repulsive forces. The increase in ionic strength led to the development of more stable froths possibly owing to a decrease in bubble coalescence and reduced bubble rupture which are phenomenal with the use of highly inorganic electrolyte concentrated process water in flotation. This increase in froth stability was observed both in dynamic stability tests and in the increase in solids and water recovered during froth flotation. It was also seen that the amount of entrained gangue in the froth increased with water recirculation.

This study successfully showed that short water recycling leads to an increase in ionic concentrations due to ore dissolution in the mill and during froth flotation. The dissolved ions are primarily from the common gangue minerals found in the ore such as Ca^{2+}, Mg^{2+}, SO_4^{2-} and Cl^-. The choice of point of addition leads to a significant difference in performance and pulp chemistry; recycling water to comminution operations may lead to a depletion of DO % present while recycling water to the flotation cells may allow for the highest froth stability achievable. The higher ionic strength in the water quality improves the solids, water, and sulfide recovery and a higher solids load per unit water. However, as entrainment is non-selective, an increase in the amount of entrained gangue as seen in this study, may have a detrimental impact on the concentrate grade. Accumulation of ions brought about by water recirculation may lead to an increase in solids, water, sulfide mineral and gangue recoveries in a concentrator and downstream when a series of concentrators are in use. Therefore, short water recirculation can be utilised as a water re-use strategy. However, it will require water quality monitoring to ensure that the flotation performance is not adversely impacted. In addition, the study encourages the use of recycled water from tailings and thickeners as a source of process water as it is non-detrimental to the overall flotation performance.

Glossary

Control variables	These are variables that are not measured in a study but must be held constant, neutralized/ balanced, or eliminated to limiting biased impact on other variables.
Daltons	1/12 of the mass of an unbound neutral atom of carbon-12 in its nuclear and electronic ground state and at rest.
Dependent variables	Are variables that show the effect of manipulating or introducing the independent variable.
Extraneous variables	Factors in the research environment that may affect dependent variables but are not controlled.
Gangue	Collective name for valueless minerals
Independent variables	Are variables that the researchers have control over.
Ore deposit	Economic term that denotes a mineral deposit of enough extent and concentration to invite exploitation.
Wettability	The ability of a liquid to maintain contact with a solid surface by balancing the intermolecular interactions of the adhesive (liquid to the surface) and cohesive (liquid to liquid) (Moldoveanu and David, 2017).

Abbreviations

µm	-	micrometers microns
DO	-	Dissolved oxygen
EC	-	Electrical Conductivity
Eq	-	Equation
Fig	-	Figure
IS	-	Ionic strength
kg	-	Kilogram
M	-	Molarity
mL	-	milliliter
mm	-	millimeter
NFG	-	Naturally Floatable Gangue
PGE	-	Platinum Group Elements
PGM	-	Platinum Group Minerals
SPW	-	Synthetic Plant Water
w/w	-	mass fraction

Table of Contents

List of Figures

List of Tables

1 Introduction

1.1 Background

The scarcity of freshwater, exaggerated by increased freshwater withdrawals by a growing population, climate change reducing green and blue water resources, and legislative action for stringent environmental restrictions, has motivated industrial innovation in the usage of freshwater and handling of wastewaters. Although the Platinum Group Mining industry in South Africa consumes freshwater as a resource, it only accounted for 5% of the freshwater consumption in South Africa in 2010 (Haggard et al., 2015). However, mining sites are located in arid regions, compounding the impact of water scarcity on their operations (Haggard et al., 2015). The developed scarcity has led to the growth of alternative water sources, such as treated sewage water, ground water, and water management strategies, such as internal water recycling, reuse and freshwater withdrawal reduction. These strategies inadvertently affect water quality and may, in turn, affect flotation chemistry as species present in solution (biotic and abiotic) and water characteristics such as total dissolved solids (TDS) may differ from freshwater. Water recycling has become a significant input to the overall plant water use, accounting for between 60-65% of available water in 2015 (Buchspies et al., 2017).

Froth flotation, first patented in 1877, is a mineral processing step utilized to concentrate ore minerals based on their surface properties into valuable minerals and gangue in flotation concentrators circuits (Bradshaw, 1997; Bunyak, 2000). The crushed mineral slurry in the presence of water (about 80 % of the vessel), acids, oils and salts (formally known as flotation reagents) is; agitated and aerated to develop two distinct phases, the pulp and the froth phase; where the hydrophobic minerals are recovered from the froth phase as a concentrate and the hydrophilic recovered from the pulp phase as tailings (Napier-Munn and Wills, 2005). Mineral recovery is a function of flow mechanisms; true flotation, entrainment, drainage and entrapment; that are the bases of mineral surface properties and flow of air in the process. Reagent mineral and air interactions are integral to the flotation performance and are affected by pulp chemistry. Froth flotation in the industry utilizes a series of flotation cells, producing a mineral-rich concentrate that is utilized in downstream beneficiation processes. Froth flotation is an integral step in the mineral beneficiation process acting as the primary concentration step before pyrometallurgy and oxidation of the concentrate. Froth flotation is a water intensive process, with concentrator plants contributing 93 % of the fresh water withdrawals in Platinum Processing Plants (Haggard et al., 2015).

Water quality has a significant influence on the concentrator plant performance and extensive research into the impact of varying water quality and the species at play on flotation efficiency has been performed (Biçak et al., 2012a; Boujounoui et al., 2015; Finkelstein, 1999; Haran et al., 2008; Ikumapayi et al., 2012; Slatter et al., 2009). Change in water quality through water recirculation (water recycling) have been shown to impact various aspects of froth flotation leading to change in the mineral activation, gangue entrainment, froth stability, hydrophobicity of mineral surface, hydrophilicity of gangue and its depression, and the electrolyte concentration of the pulp (Biçak et al., 2012a; Boujounoui et al., 2015; Finkelstein, 1999; Haran et al., 2008; Ikumapayi et al., 2012; Slatter et al., 2009). Change in froth stability in froth flotation has an impact on the overall recovery, grade and selectivity of a concentrator, due to its impact on the flow mechanisms at play (Manono et al., 2012). Changes in the mineral surface properties, through mineral activation has an impact on the surface properties such as its floatability and reagent interaction, influencing the mineral recovery and grade in the concentrate. Changes in pulp chemistry, i.e. changes in dissolved oxygen concentration or redox potential, have an impact on the reaction pathways at play, such as reagent mineral and or galvanic interactions (Bruckard et al., 2011). Settling of the solid pulp in subsequent thickener units is also impacted by the electrolytic concentration of the water (Manono et al., 2018). The presence of selected ions in the pulp, i.e., Ca^{2+}, Mg^{2+}, SO_4^{2-}, and Cl^-, have an impact on the mineral and froth properties observed in froth flotation (Dzingai et al., 2021, 2020). Water recycling may also reduce reagent consumption by recovering unconsumed reagents retained in the water that is to be recycled (Bleiwas, 2012; Levay et al., 2001; Slatter et al., 2009).

It is for this reason that the use of recycled water as an alternative to freshwater has been noted to possibly impact flotation efficiency, selectivity and mineral recoveries and hence water quality has become a subject of many research studies (Biçak et al., 2012a; Boujounoui et al., 2015; Corin et al., 2011; Finkelstein, 1999; Haran et al., 2008; Ikumapayi et al., 2012; Slatter et al., 2009). Water recycling fits well into the mining industry's goals of achieving a zero-emission policy, minimizing interaction of the mine with its surroundings (Liu et al., 2013). It is on this basis that this study argues that an understanding of the impact of water recirculation, with a keen interest on the impact of recirculation on flotation outcomes while considering a small number of water quality variables.

1.2 Problem Statement

South African PGM mines use water from the Vaal River which suffers at least 3 months of severe water scarcity during a year, indicating that the mines are located in a water-stressed region (Haggard et al., 2015). The industry has also been motivated by society and policy towards more sustainable mineral processing with reduced emissions (Biçak et al., 2012a; Ikumapayi et al., 2012; Slatter et al., 2009). Thus, the industry has had to implement water recirculation as a water management strategy commonly used in processing plants in arid regions (Boujounoui et al., 2015; Slatter et al., 2009). The focus of the study will be to investigate the impact of short water recirculation on flotation efficiency. The project will simulate sulfide rougher flotation utilizing a reagent suite of collectors, depressants and frothers with simulated water re-circulation through water recovery from the tailings. The project will investigate the impact of point of addition of recirculated water (i.e., to the mill or the float cell.). While many operations recycle water on-site, water recovery from tailings dams is a lengthy process, short water recycles occur during plant operation, hence may form a timeous water feed source.

However short recirculated water varies greatly in quality to long water recycles, and is considered to be in an “active state” with mineral and reagents interactions still occurring (Liu et al., 2013; Slatter et al., 2009). Water recirculation leads to a build-up of ions present in solutions: impact of accumulation due to water recirculation is usually studied through as synthetic build-up of concentration and not through water recovery as proposed in this project.

Bulatovic, (2007: 1) states that “*In commercial plants, the control of flotation reagents is the most important part of the flotation strategy.*” Reagent costs in sulfide flotation operations typically run into tens of millions of dollars per annum presenting a good opportunity for cost improvement and improvement in flotation efficiency (Muzenda et al., 2013). Studies on reagent optimization have shown that typical plants may not be operating optimally due to disproportionate reagent doses leading to reagent misuse and reduced recovery (Muzenda et al., 2013). Water re-circulation reduces reagent consumption by recovering unconsumed reagents retained in wastewater (Bleiwas, 2012; Levay et al., 2001; Slatter et al., 2009).

This motivates the investigation of the impact of residual reagents, especially in short recycle systems where the reagents are still considered to be active. However, the impact of residual reagents on the grinding chemistry and pulp chemistry on flotation performance is still a matter of contention with Bruckard et al., (2011) proposing that

the water chemistry variation in the mill through the addition of reagents has no impact on the grinding chemistry or flotation performance. It is this niche in knowledge and literature that this project finds its relevance as an opportunity to develop new insights.

1.3 Scope

Froth flotation performance is controlled by several complex parameters. The overall rate of flotation performance is a balance of various competing mechanisms of collection, attachment and detachment (Jameson, 1984). Crozier, (1992) lists up to 25 identifiable parameters however Manono, (2012) proposes that these can be more fully described by over 100 variables. Klimpel, (1984) summarises them into twenty-five measurable parameters affecting a flotation system by dividing the major variables into three categories, equipment, chemical and operational components as shown in Fig 1-1.

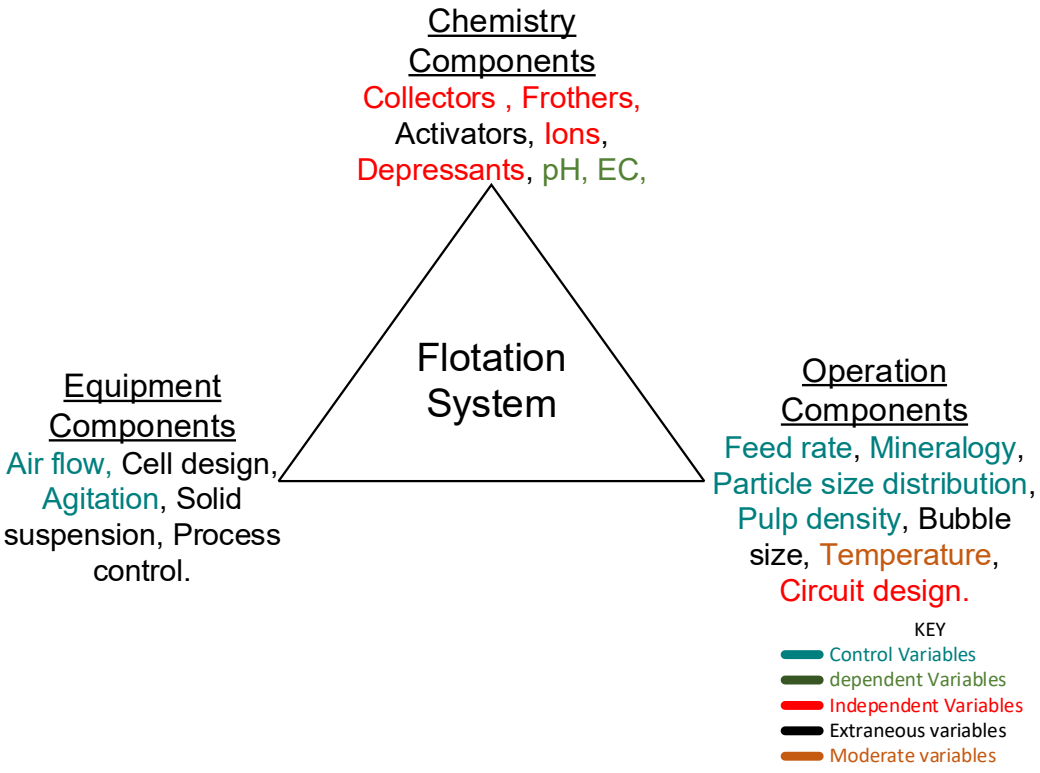

Fig 1-1. A summary of variables in the flotation system adapted from (Klimpel, 1984)

This project evaluates the impact of short water re-circulation on the flotation performance of a platinum bearing UG2 reef ore by analytical and quantitative analysis of the solids and water recoveries, valuable mineral recoveries and grades, froth stability, coagulation, pH and ionic strength (IS) during the flotation process.

The controlled variables in the project are milling media, reagent suite, physical flotation conditions and equipment used will be kept constant. The project is limited to water quality research on flotation, utilizing synthetic plant water. The control variables are kept constant based on standard practice for water quality batch flotation work: synthetic plant water (SPW) recipe; the mass of ore; airflow; agitation; feed rate; pulp density; mineralogy; particle size distribution; and reagent suite.

The temperature was chosen as a moderate variable; because it affects the strength of the relationship between dependent and independent variables, however, it is difficult to control. As the lab is a temperature-controlled environment, the temperature will only be monitored. The ore mineralogy and standard batch flotation work are summarized in Chapter 4. The project variables are summarized and elaborated in Fig 1-1.

The dependent variables will be monitored throughout the experiment using appropriate equipment to develop performance indicators about flotation efficiency. The dependent variables are pH, Oxidative Redox Potential (ORP), Dissolved Oxygen Concentration (DO %) and Electrical Conductivity (EC) and will be monitored at specific points in the experimental program as described in Chapter 4. The independent variable is the point of addition, developing a water recirculation loop and varying of the recirculated water. All other variables are beyond the scope of the project and can neither be controlled nor monitored during the experiment. The reagent suite and the ore used in the project are all outlined Fig 1-2. The inputs to the project are the water quality, ore type and the reagent suite, while the outputs include nickel (Ni) and copper (Cu) grades and recoveries; froth stability, ion concentration, EC, ORP, DO %, solids coagulation, reagent adsorption and pH producing information on the impact of short water recirculation and change water quality in froth flotation.

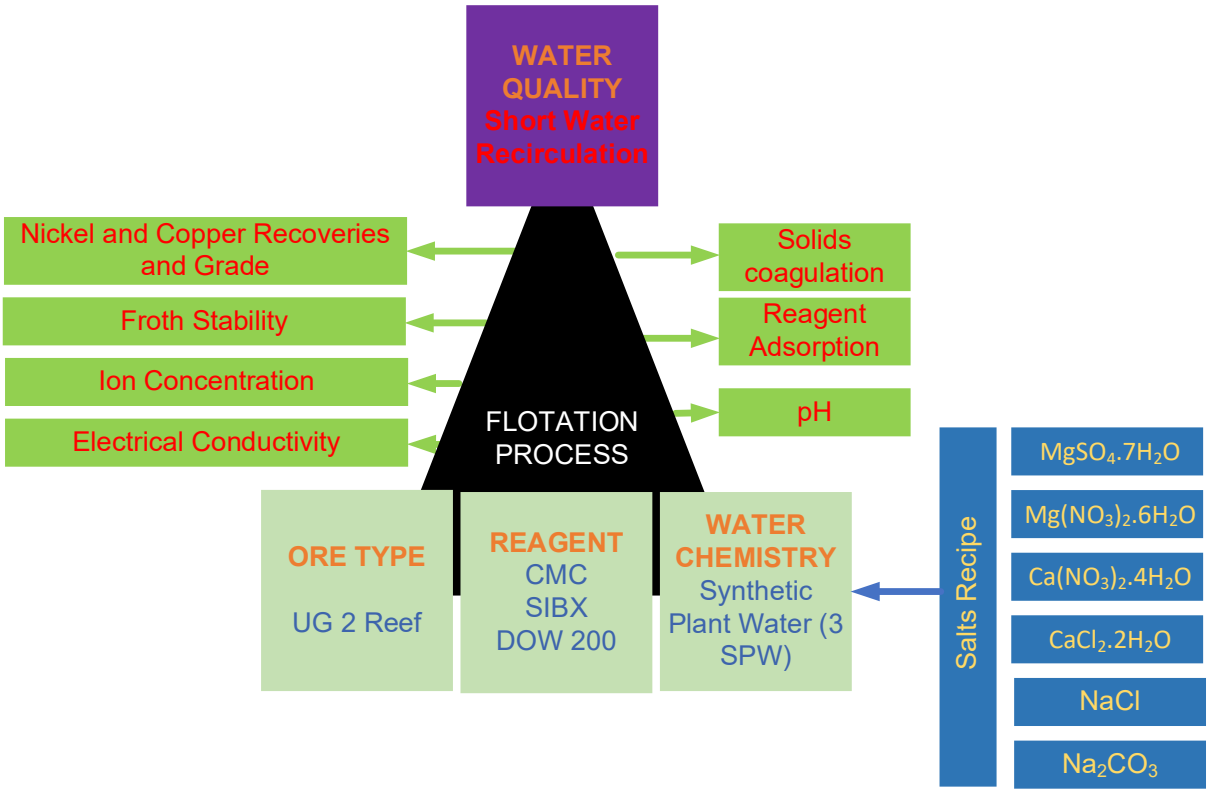

Fig 1-2. A schematic representation of the scope of this study.

1.4 Value of Work

The emergence of stringent laws and policy on water use across the manufacturing industry, with additional requirements on the minimization of mine water discharge and minimal freshwater feed from municipal sources, has motivated the use of water re-circulation as a water management strategy (Peters and Meybeck, 2000). Liu et al., (2013) presented a review on water quality research which identified a gap in knowledge regarding why water quality varies, the proposed project considers the impact of short water recirculation on water quality in terms of pH and EC. Although water re-circulation prevents environmental pollution from mine water discharge or effluent and is the best alternative to meet the demand for zero-wastewater effluent from operations, its impact on flotation performance is not fully understood. The project aims to provide valuable information to the discussion, and as a water sustainability project, it falls in line with goal 6, 8, 9, 11, 13, 14 and 15 of the United Nations (U.N.) sustainability development goals outlined in the 2030 Agenda for sustainable development summarized in Fig 1-3 from (Desa, 2016).

Fig 1-3. U.N. Sustainability Development Goals (Desa, 2016).

1.5 Importance, Applicability, Limits, and Uncertainty of the Short Water Reticulation Project

The use of synthetic plant water in the study is a limitation as it oversimplified and not a true representation of plant water and does not fully describe the complexity dynamicity, and instability of mining process water (Intergovernmental Panel on Climate Change, 2014; Miranda-Trevino et al., 2013; Wasserlauf and Dutrizac, 1984). However, the UCT SPW recipe developed was mine specific, developed for the Bushveld Ingenuous Complex, however the unstable, dynamic and complex of real plant water motivates the use of SPW in common practice in water quality research, noting the ore specificity of the water recipes to be used (Biçak et al., 2012a; Corin et al., 2011; Ikumapayi and Rao, 2015a; Manono et al., 2013, 2012; Wiese et al., 2005). In addition, through water recycling, the observed change in water quality in chemistry and physical properties shows the importance of ore specific synthetic water recipe to ensure all ions involved are accounted for.

Water recycling projects allow for investigations into the rate of change in water quality due to ore dissolution, residual reagent, suspended solids, and ion accumulation (Le et al., 2020). The water composition in the experiments will be compared to the standard synthetic plant water qualities that are used in water quality research.

The Water Recirculation Project allows for quantitative and qualitative analysis of the impact of water recycling on flotation performance. Mass balance on the froth flotation process allowed for investigation on the impact of Water Recycling on the selectivity and the recovery of the mineral processing step. The impact of ore dissolution on the water quality will be inferred though EC and TDS measurements, as well as GDACA for specific ion concentrations. Water re-circulation will impact the flotation performance. The impact on selectivity, recovery and flotation performance of the flotation process will be compared to correlations developed from literature at different concentrations in water (Biçak et al., 2012a; Boujounoui et al., 2015; Corin et al., 2011; Haran et al., 2008; Ikumapayi and Rao, 2015b; Khraisheh et al., 2005; Mailula et al., 2003; Manenzhe, 2018; Manono, 2012; Martinovic et al., 2005; Mhlanga, 2011; Slatter et al., 2009; V.P. Finkelstein, 1972). Finally, reproducibility of Water Recycling test work is imperative in validation of methodology with the purpose of motivating its addition into the standard test work done on site.

1.6 Limitations of Research Work in Flotation.

Flotation is a multi-faceted topic; however, the research approach is focused on a case to case basis (Liu et al., 2013). It is rare to see paralleled study on adsorption of collectors and collector induced adsorption (Finkelstein, 1999). The conditions of operation of some of the research work in the field have little or no relevance to flotation: acid to neutral pH; the amount of adsorption greater than those encountered in the industrial application; relatively long adsorption times (Finkelstein, 1999). The impact of hydroxide coatings on the mineral surface, mineral interaction before and after activation in the form of solid-solid and solid-fluid interactions has not been fully investigated. The careful nature of the lab work does not accurately simulate distortion and irregularities i.e., surface layer distortion in abrasion and grinding, leading to findings that are contrary to real systems in industry (Finkelstein, 1999). However, the whole body of research work done serves its importance in the potential that all cumulative work done can be put together to map out the most efficient flotation strategy and creation of integrated process prediction models.

2 Literature Review

2.1 Froth Flotation

First patented in 1877, froth flotation has become one of the most prominent recovery processes for sulfide minerals, utilized for the processing of much of the world's copper (Cu), Nickel (Ni), zinc (Zn) and lead-bearing minerals (Bradshaw, 1997; Bunyak, 2000). Froth flotation is a mineral processing step developed in response to; inefficient ore recovery methods, depleting high-grade ore bodies with the goal of developing high-grade mineral-rich concentrates from low-grade ore bodies (Bunyak, 2000; Hu, 2014). Froth flotation is a complex physicochemical separation process utilized to separate minerals (with similar density); whose surface properties differ greatly in wettability (Encyclopaedia Britannica, 2012). Flotation is aided through the use of surfactants that stabilize a froth formed on the surface of an agitated suspension of the minerals in the water into a valuable mineral-rich concentrate and a gangue collected in the tailings (Bunyak, 2000; Wills and Napier-Munn, 2006). Industrial-scale froth flotation utilizes mechanical cells or columns. In a flotation cell, appropriately sized and liberated solid particles of differing commercial values are suspended in water, treated with flotation reagents and subjected to aeration (Finch, 1995a, 1995b; Harris, 1982; Leja and Schulman, 1954).

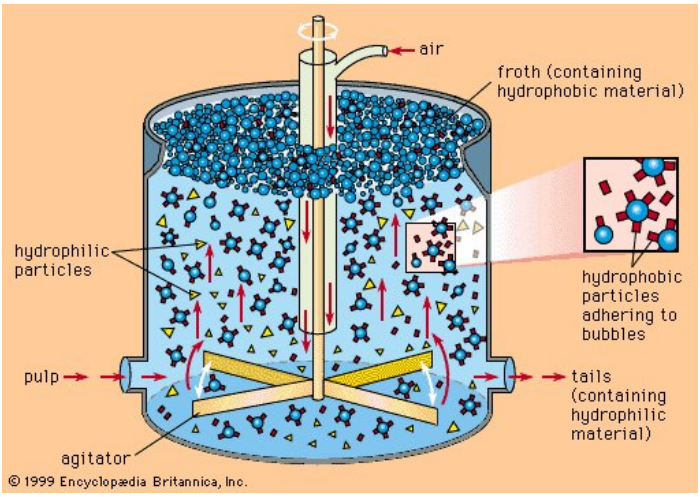

Fig 2-1. Schematic diagram of a flotation separation cell adapted from (Encyclopaedia Britannica, 2012)

The process environment is a water bath that is agitated to maintain and enhance phase interactions leading to bubble particle collisions by developing turbulence in the pulp phase and aerated with flotation gases, e.g., nitrogen, air etc., developing a

mineral rich froth phase. (Bunyak, 2000; Couper et al., 2005; Hintikka and Leppinen, 1995; Napier-Munn and Wills, 2005).

Froth flotation relies on surface properties of the valuable and gangue minerals, where the natural floatability of the minerals defines the principal flow of the flotation process; and takes advantage of the surface tension of liquids and the ability of minerals to attach to air bubbles (Bunyak, 2000; Wills and Napier-Munn, 2006). The three phases in flotation are the solids, water and air (Napier-Munn and Wills, 2005). Aeration in froth flotation leads to the development of distinct phases; the pulp phase where the mineral recovery occurs by particle attachment to air bubbles which rise and by coagulation of hydrophobic particles leading to settling, and the froth phase where the bubble-particle aggregates rise to the top of the cell, where the concentrated valuable minerals are separated from the bulk as shown in Fig 2-1. The recovery of materials in the froth phase from the pulp phase occurs through three mechanisms that lead to the recovery of minerals: true flotation, entrainment and physical entrapment (aggregation) (Napier-Munn and Wills, 2005). In the pulp phase particle agglomeration leads to change in mass, reducing buoyancy hence the particles settle this is known as coagulation.

True flotation is the only selective mechanism and is based on the surface properties of the minerals which are enhanced in the flotation process by use of flotation reagents (Napier-Munn and Wills, 2005). Entrainment is the non-selective recovery of both valuable and gangue particles carried up by the flow of water and air into the concentrate (Napier-Munn and Wills, 2005). Physical entrapment occurs when particles are trapped between other particles attached to bubbles in the froth phase (Napier-Munn and Wills, 2005). Froth flotation stability the differences in hydrophobic and hydrophilic properties of a mineral. A hydrophobic mineral is nonpolar and will attempt to avoid contact with water, thus being preferentially attracted to air bubbles (Schaschke and Carl, 2014). A hydrophilic mineral is preferentially attracted to water (Schaschke and Carl, 2014). Due to entrainment and naturally floatable gangue (unwanted minerals), a complete separation of valuable minerals from gangue is impossible, hence the need to use flotation reagents to assist in the flotation process. In addition to entrainment, gangue minerals can be carried to the froth phase by being locked to valuable hydrophobic particles through incomplete liberation (Becker, 2009; Corin et al., 2011). Similarly, valuable minerals can remain in the pulp as a result of being locked in hydrophilic and composite particles (Kawatra and Darling, 2011). The flotation reagents used are added to the pulp phase of the flotation process where they impact the hydrophobicity and hydrophilicity of the minerals and the properties of the process water (Becker et al., 2007; Chau, 2009). Reagent adsorption on the mineral

surface is almost instantaneous however some reagents require some time (conditioning time) for complete reaction with the mineral surface (Sweet, 1999).

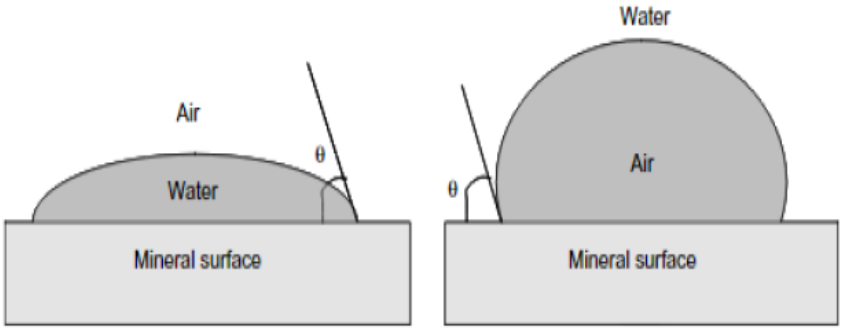

Fig 2-2. Particle-water (left) and Particle-bubble (right) attachment in the pulp phase adapted from (Celik and Somasundaran, 1980; Chau, 2009).

Chau, (2009) states that "*the primary requisite for flotation is the replacement of water at the mineral surface by an air bubble*." This develops the three major subprocesses in flotation: particle-bubble collision, adhesion of the mineral particle to air bubble, and detachment. The schematic of reagent-water-particle (left) and the particle-bubble (right) interaction in the agitated pulp phase is shown in Fig 2-2. The water collector phase surrounds the mineral during conditioning, improving mineral hydrophobicity, after aeration starts, the particle attaches itself to the air bubbles formed and rises from the pulp to the froth phase. Flotation reagents used are known as collectors, depressants and frothers as detailed in Section 2.2.

2.2 Flotation Reagents

As stated by Napier-Munn & Wills, (2005) "*Most minerals are not water-repellent in their natural state and flotation reagents must be added to the pulp. "* Flotation reagents are added to manipulate the pulp chemistry and enhance the differences in mineral surface hydrophobicity to facilitate the separation improving flotation recovery and grade (Becker et al., 2007; Muzenda et al., 2013; Wiese et al., 2005). The different reagents used in froth flotation are described below: Reagent efficiency is a function of their concentration in solution (Napier-Munn and Wills, 2005).

2.2.1 Collectors

Collectors are used in sulfide flotation to interact with valuable minerals to render them hydrophobic to increase recovery. Collectors are heterogeneous molecules that

contain an inorganic, active group (polar functional group), non-ionic hydrocarbon chain (Garrels and Christ, 1990; Lovell, 1982).

The polar functional group is hydrophilic and attaches itself to the mineral surface while the hydrocarbon attaches to the bubble (Garrels and Christ, 1990; King, 1982; Lovell, 1982). The most commonly used thiol collectors are xanthates and di-thiophosphates due to their high selectivity for sulfides and non-affinity for non-sulfide gangue minerals (Rao and Finch, 1988a). The molecular structure of a commonly used xanthate collector is shown in Fig 2-3.

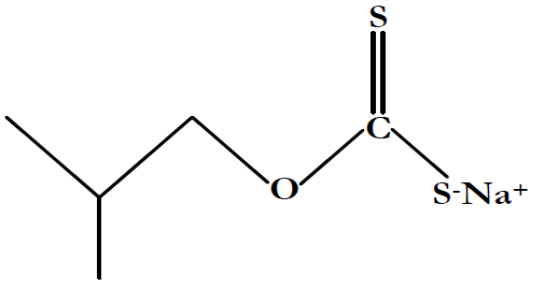

Fig 2-3: Molecular structure of sodium isobutyl xanthates (SIBX) obtained from (Fuerstenau, 1982)

Collectors are used in sulfide flotation to interact with valuable minerals to render them hydrophobic to increase recovery. The polar functional group is hydrophilic and attaches itself to the mineral surface while the hydrocarbon attaches to the bubble (Garrels and Christ, 1990; King, 1982; Lovell, 1982).

2.2.1.1 Xanthate Chemistry

Xanthates are widely used in the processing industry as reactants or additives in pesticides, rubber, cellulose and pharmaceuticals (Shen et al., 2016; Spottiswod and Kelly, 1982; Wills and Napier-Munn, 2006). In the mineral processing industry, they are used in the beneficiation of base metal sulfides (Cu, Ni, Zn, Fe), precious metal ores (Shen et al., 2016; Spottiswod and Kelly, 1982; Wills and Napier-Munn, 2006). Xanthates decomposition in aqueous solutions is a function of the system temperature, pH, residence time and UV exposure in the liquid phase (Dautzenberg et al., 1984; Mustafa et al., 2004; Rao and Finch, 1989; Sheni, 2016). The use of UV-Vis spectroscopy to evaluate the decomposition of xanthates has been used frequently throughout decomposition studies for xanthates. The Stopped Flow Techniques (STF) was first developed by Tornell to investigate decomposition of xanthates (Tornell, 1967, 1966a, 1966b). The method is still used in12 recent studies on decomposition

and stability of xanthates under the influence of time, pH, temperature and electrolyte concentration (Mustafa et al., 2004; Muzinda and Schreithofer, 2018; Shen et al., 2016).

Shen et al., (2016) discourages the use of the STF methodology as it does not allow for identification of gas phase decomposition products. It relies on the assumption that the only gas phase products is Carbon Disulfide (CS_2) and that the decrease in xanthate in solution is solely due to decomposition (Mustafa et al., 2004). Furthermore, the SFT methodology was not suitable for heterogenous mixtures (flotation pulp) and the UV-Vis band assignments for xanthates and its relevant compounds have never been agreed upon. For this reason, the use of gas chromatography mass spectroscopy (GC-MS), Fourier Transfer Infrared Spectroscopy (FTIR), capillary electrophoresis and the Raman method have been proposed by Shen et al., (2016); Muzinda & Schreithofer, (2018) as alternative methodologies for decomposition studies due to their ability to monitor gas phase products.

However Shen et al (2016), Mustafa et al (2004) and Tornell (1966b,a, 1967) yielded key findings that formulate insights into the decomposition chemistry of xanthates. Mustafa et al (2004) work on the stability of xanthates as a function of pH and temperature shed insights on the potential decomposition reactions occurring. The reaction mechanism of decomposition following a uni-molecular (i.e., xanthate and water first from xanthic acid which then decomposes) or bimolecular which is depicted in Eq. (2-1). Shen et al (2016) however postulates that due to the moderate acidity of xanthic acid, *p*Ka=2.23 for butyl xanthic acid, hence it dissociates under alkaline, neutral, and weakly acidic conditions. This theory is also adapted by Mustafa et al (2004) for the decomposition of potassium ethyl xanthate as shown in Eq. (2-2) & Eq. (2-3). This assumption allows us to model the decomposition of xanthates as a single order reaction.

$$(CH_3)_2CHCH_2OCS_2Na + H_2O \Leftrightarrow CS_2 + (CH_3)_2CHCH_2OH + NaOH \quad \text{Eq. (2-1)}$$

$$C_2H_5O\ CS_2K + H_2O \rightarrow C_2H_5OCS_2H + KOH \quad \text{Eq. (2-2)}$$

$$C_2H_5OCS_2K + H_2O \rightarrow KOH + C_2H_2OH + CS_2 \quad \text{Eq. (2-3)}$$

Xanthate (or alkyl dithiocarbonate, R-OCS_2) can decompose to produce oxidation and degradation products from residual xanthates (Muzinda and Schreithofer, 2018). Similar work on degradation residual of xanthates has also been performed by Muzinda & Schreithofer, (2018), and they based on absorbance at a wavelength 301 nm.

The decomposition of xanthates varies as a function of pH, decomposing faster as the pH decreases with a maximum at c.a. 2.2 (Shen et al., 2016). CS_2 generation, and hence SIBX degradation, decreases as a function of increasing pH as elaborated in Fig 6 Shen et al., (2016, p. 5).

2.2.2 Depressant

Depressants are utilized in PGM flotation to reduce the recovery of naturally floatable gangue and therefore improve concentrate grades (Corin et al., 2011; Dzvinamurungu et al., 2013; Ekmekçi et al., 2003; Mailula et al., 2003; Wiese et al., 2005). Desired minerals are naturally hydrophobic, hence reducing the true flotation of gangue can improve the selectivity of mineral flotation, leading to a higher grade concentrates (Corin et al., 2011; Dzvinamurungu et al., 2013; Ekmekçi et al., 2003; Mailula et al., 2003; Wiese et al., 2005). Depressants act by adsorption on to the surface of the mineral, rendering it hydrophilic, limiting its flotation. The most commonly used polysaccharide depressants are carboxymethyl cellulose (CMC), guar gum and dextrin (Khraisheh et al., 2005; Mailula et al., 2003; Martinovic et al., 2005). The structure of CMC shown in Fig 2-4 shows three hydroxyl groups on each hydro glucose unit of cellulose (Wang and Somasundaran, 2005). Unlike collectors, depressants do not degrade into toxic by-products, hence the degradation of residual depressant was not considered. Colorimetric treatment through the use of phenol and sulfuric acid was used to determine residual reagent concentrations in the water samples through the use a UV-Vis Spectrometer (Dubois et al., 1956).

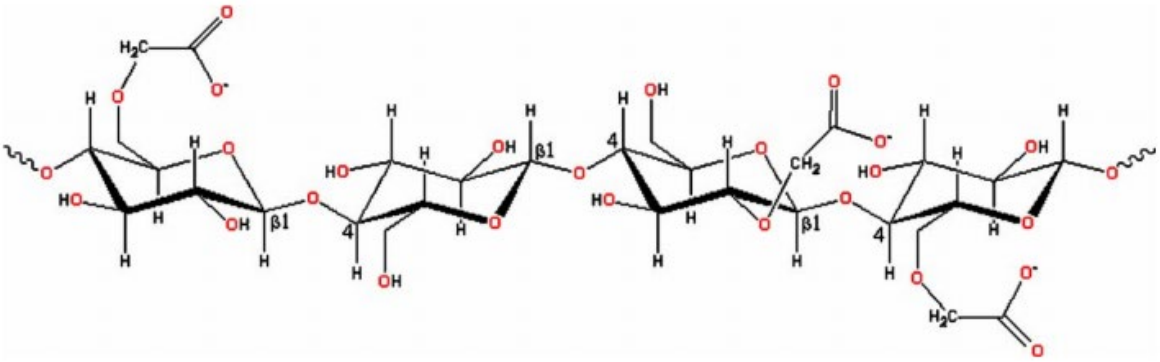

Fig 2-4: The monomeric structure of CMC obtained from (Wang and Somasundaran, 2005)

Flotation in the absence of depressant would display the grade and recovery developed at a maximum true flotation of gangue (NFG) accompanied by entrainment. Increasing the depressant dosage is considered to lead to a maximum selectivity, where all that floats can be floating by true flotation, therefore all gangue reporting to the froth can be considered true floating gangue, developing an overall entrainment factor. To determine the amount of natural floating gangue, the depressant dosage is increased to a maximum to limit the flotation of all gangue, and hence any gangue reporting to the concentrate is through entrainment as prescribed by Wiese and Harris, (2012), and hence develop the mass of entrained gangue per gram of water. I

2.2.3 Frothers

Frothers are surface-active solutes, usually non-ionic molecules, that absorb at the air-liquid interface and function in flotation is to facilitate air dispersion into fine bubbles and provide a large water-air interface of sufficient stability to facilitate transportation of hydrophobic material to the froth phase (Lovell, 1982; Pan et al., 2022; Ramos et al., 2013).

Frothers are made up of neutral molecules consisting of a medium-chain hydrocarbon and a polar group, usually a hydroxyl in the form of alcohol or glycol leading to a dual affinity for water and air (Pearse, 2005). Frothers have been shown to have an impact on the kinetics of bubble attachment (Klimpel, 1984; Klimpel and Isherwood, 1991). Polyether glycols are the most commonly used frothers in sulfide flotation due to their strong froth stabilizing effect which also enhances the particle-bubble attachment sub-process of flotation (Sweet et al., 1997).

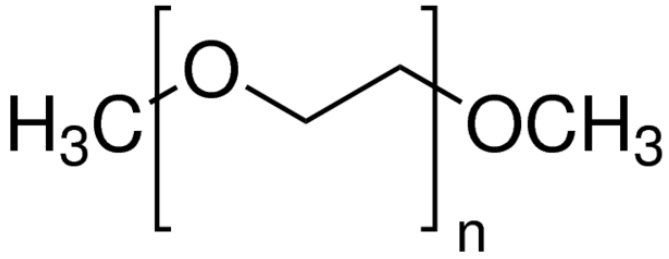

Fig 2-5: Polyether Glycol Structure (ethylene glycol dimethyl ether) obtained from (Merck, 2020)

2.3 Froth and Foam Stability

Froth stability is the ability of bubbles to resist coalescence and bursting, and plays a significant role in determining the flotation performance mineral grade and recovery (Barbian et al., 2005a, 2003; Farrokhpay, 2011; Pan et al., 2022). Bubble coalescence involves the thinning of bubbles leading to their rupture of the thin liquid film between bubbles. The term “foam” refers to two phase systems containing polyhedral gas bubbles with liquid films residing between bubbles while the “froth” is the three phase structure comprising of air bubbles, solids, and water (Farrokhpay, 2011; Pan et al., 2022). The foam capacity is an effective way to assess the performance through quantitative measurement of the height or volume of foam generated with the injection of gas (Pan et al., 2022). There are two commonly known tests for froth stability, dynamic or static tests. Dynamic tests develop the froth to an equilibrium point where the rate of formation equals the rate of decay, while static tests have a zero rate of formation and focus on the rate of collapse of the foam (Barbian et al., 2003). One of the methods developed based on a dynamic stability test is non-overflowing froth columns to develop stability parameters comparable to flotation performance.

One stability parameter developed is the ratio of steady state foam volume (V_f), estimated from the height of the foam (H_{max}) and the cross-sectional area of the vessel (A), to the injection gas flowrate (Q) as a measure of foaminess for dynamic froths, denoted as (∑) developed by Bickerman, (1973), as shown in Eq. (2-4).

$$\sum = \frac{\Delta V_f}{\Delta Q} = \frac{H_{max} * A}{Q} \qquad \text{Eq. (2-4)}$$

The dynamic foam stability (∑) is a measure of the average time gas remains entrained in the foam (Barbian et al., 2003; Pan et al., 2022). Other parameters are also

developed from kinetic measurements of the froth height, to establish a froth rise rate, by visually or electronically recording the froth height H(t) as a function of time (t) fitted by an exponential model of the form shown in equation developed by (Barbian et al., 2006, 2005b, 2003). The equilibrium maximum height (H_{max}) can be obtained from the experiment or inferred from data obtained in the rise period in which (H_{max}) and the characteristic bubble lifetime are fitted (τ).

$$H(t) = H_{max}(1 - e^{-\frac{t}{\tau}}) \qquad \text{Eq. (2-5)}$$

Variations in froth height (*H(t)*) as a function of time (d*H/dt*) at any particular time is develops the froth rising velocity *u(t)* which can be linked to the fraction of bubbles bursting on top of the surface of the froth, known as the stable fraction (*β*) as shown by models developed by Barbian et al., (2006, 2005a) for *u(t)* in Eq. (2-6) and developing the stable fraction (*β*) in Eq. (2-7) and Eq. (2-8).

$$u(t) = \frac{dH(t)}{dt} = \frac{H_{max}}{\tau} e^{-t/\tau} = \frac{H_{max} - H(t)}{\tau} \qquad \text{Eq. (2-6)}$$

$$u(t) = \frac{dH(t)}{dt} = \beta(H)\ \frac{Q}{A} \qquad \text{Eq. (2-7)}$$

Both the stable fraction and the rising velocity are related to a relationship between H(t) and H_{max} which are dependent on frother concentration, air flowrate, and position of the flotation cell down a bank of cells, hence an important factor in froth modelling and plant operation (Barbian et al., 2006, 2005a).

$$\beta(H) = \frac{dH(t)}{dt}\ \frac{Q}{A} = \frac{H_{max} - H(t)}{\tau}\frac{Q}{A} \qquad \text{Eq. (2-8)}$$

For a highly stable froth, *u(t)* is equal to the superficial gas velocity in the plup J_g , however due to bubble bursting, the rising velocity is progressively lower by a factor *β* that represents the fraction of air remaining in the froth at a given froth height H(t) (Barbian et al., 2006, 2005a).

2.4 Effects of Grinding Chemistry on Flotation Chemistry

Comminution is the size reduction of mined ore prior to froth flotation to provide fine particles, that ensure efficient bubble adhesion occurs with enough power to overcome the particle weight (Napier-Munn and Wills, 2005). These processes are done in two

stages, crushing, and grinding, to liberate the minerals from their associated gangue. Crushing is the dry processing of Run of Mine (ROM) to a suitable size range that can be transported to the concentrator (Napier-Munn and Wills, 2005).

Grinding is the wet processing of the crushed ore traditionally achieved by abrasion of the ore using rods (generally used in laboratory set-up) or balls in different milling equipment's (Napier-Munn and Wills, 2005). Usaini et al.,(2014) defined liberated valuable minerals as released from their associated gangue at the coarsest possible particle size. Grinding media has an impact on the pulp chemistry, surface properties and floatability of sulfide minerals mainly through electrochemical interactions, surface morphology and mechano-chemical reactions (Rao and Finch, 1988b; Wang and Xie, 1990).

Bruckard et al (2011) postulate that "*Galvanic interactions between sulfide minerals can occur, depending on mineralogy of the ore, can have an influence on the separation efficiency of the flotation.*"

The pulp chemical environment, pre-conditioning stages before flotation, reagent interactions during grinding and conditioning can influence the subsequent flotation process (Bruckard et al., 2011). During grinding, electrochemical corrosion occurs between the sulfide minerals present in the mill, where two or more dissimilar sulfide minerals are connected through an electrolyte, and interactions with the mill (Bradshaw et al., 2006; Qing You et al., 2007; Rao and Finch, 1988b). Sulfide minerals are generally nobler electrochemically than steel grinding media (rods) leading to the development of high rest potentials under most conditions (Rao and Natarajan, 1989; Rao et al., 1976). The mill acts as an anode, undergoing oxidation, loss of electrons, while the sulfide mineral acts as the cathode, undergoing reduction, gain of electrons (Bruckard et al., 2011). This leads to the development of galvanic cells where redox reactions occur due to the differences in open circuit potentials of the sulfide mineral and grinding media (Wang and Xie, 1990). Iron has the highest half-cell potential as shown in Eq. (2-9) and acts as an oxidizing agent, forming galvanic cells with copper, magnesium and calcium which are reduced in these reactions as shown in Eq. (2-10), Eq. (2-11) and Eq. (2-12).

$$Fe^{3+}_{(aq)} + e^- \rightarrow Fe^{2+}_{(aq)}\ E^o(V) = +0.77 \qquad \text{Eq. (2-9)}$$

$$Cu^{2+}_{(aq)} + 2e^- \rightarrow Cu_{(s)}\ E^o(V) = +0.153 \qquad \text{Eq. (2-10)}$$

$$Mg^{2+}_{(aq)} + 2e^- \rightarrow Mg_{(s)}\ E^o(V) = -2.363 \qquad \text{Eq. (2-11)}$$

$$Ca^{2+}_{(aq)} + 2e^- \rightarrow Ca_{(s)}\ E^o(V) = -2.866 \qquad \text{Eq. (2-12)}$$

Galvanic interactions are controlled by the mixed potential principle, with lower open-circuit potentials acting as anodes undergoing surface oxidation (Wang et al., 1989). This has motivated the study of electrochemical interactions of pyrite, chalcopyrite, galena and sphalerite minerals as well as studies on the effects of grinding chemistry on the flotation chemistry and overall flotation performance (Bradshaw et al., 2006; Jacques, 2017; Qing You et al., 2007; Rao and Finch, 1988b; Van Deventer et al., 1993; Wang and Xie, 1990).

Galvanic interactions between sulfide mineral and steel grinding media lead to the formation of iron (Fe) hydroxides by consuming the dissolved oxygen (DO) content and increasing iron levels in the slurry (Bruckard et al., 2011). Galvanic interactions lead to a change in the pulp chemistry and surface properties of ground minerals leading to a reduction in the amount of DO present and a change in the pulp potential, which depending on the impact of galvanic interactions, has a severe impact on the practical control of the redox conditions in the flotation slurry (Bruckard et al., 2011). Galvanic interactions can be impacted by the change in the gaseous atmosphere in the mill. Rao & Finch, (1988b) found that interactions are weakened in nitrogenated water due to lower activity of DO. In a closed mill, DO is consumed in the oxidation of the mineral and hence strongly affects the rate of xanthate adsorption on mineral surfaces by impacting active surface area (Corin et al., 2013; Napier-Munn and Wills, 2005).

Galvanic interactions have shown impacts in the froth phase in complex sulfide ore flotation, where interactions caused by the presence of iron yielded a stable, well-drained froth with a low ratio of solids/ water recovery and large bubbles in the froth (Van Deventer et al., 1993). However, Bruckard et al (2011) note that although reagent addition, such as collectors, lime, or cyanide during milling can alter pulp chemistry, they do not show a strong influence on the subsequent flotation performance. Although the effects of changes in grinding pulp chemistry and environment on the flotation of complex sulfide ores have been studied, impact of water recirculation and residual reagents has not found consensus with Bruckard et al (2011) postulating that it has no impact on subsequent flotation efficiency, while others (Bleiwas, 2012; Levay et al., 2001; Slatter et al., 2009) are optimistic on the impact of residual reagents in flotation. This conflict motivates the relevance of this project. Oxidation of mineral on the mineral surface leads to the formation of hydroxides and sulfur-oxy species, either absorbed in thin layers or precipitated from solution as colloidal particles in acidic and alkaline oxidation respectively (Buckley and Woods, 1984).

In alkaline conditions a layer of the metal hydroxide forms above the sulfur-rich mineral surface creating a metal-deficient sulfide lattice, polysulfide or elemental sulfide (Buckley and Woods, 1984).

2.5 Impact of Water Quality and Scarcity on Flotation

Mineral processing plants utilize varying water qualities throughout their operations, blue water, greywater (i.e., treated sewage effluent), municipal water, and internally recycled water (short and long recycles) (Boujounoui et al., 2015; Liu et al., 2013; Slatter et al., 2009).

Haggard et al., (2015) developed water footprint terminologies across the processing plants stating that "*Blue-water footprint of a process is the volume of ground and surface water that is consumed in the process…The green-water footprint is the volume of rainwater that is stored on or in the soil and is used by plants for evapotranspiration…The grey-water footprint for a process is the volume of clean water required to dilute pollutants in the wastewater to such an extent that the wastewater does not disturb the ambient water quality of the catchment it is released to...Consumption is defined as water that is not returned to the same water resource or is not returned during the same period (lost return flow), is lost through evaporation or integrated to into the product*…" developing the footprint calculation formulas for blue-green and greywater Eq. (2-13), Eq. (2-14) and Eq. (2-15).

$$WF_{proc,blue} = Blue\ water\ evaoration + Blue\ water\ incopoeration + lost\ return\ flow\ (volume/time) \quad \text{Eq. (2-13)}$$

$$WF_{proc,green} = Green\ water\ evaoration + Green\ water\ incopoeration + Incoperation\ (volume/time) \quad \text{Eq. (2-14)}$$

$$WF_{proc,grey} = \frac{L}{C_{max} - C_{nat}} \quad \text{Eq. (2-15)}$$

Where: L is pollutant load (mass/time), C_{max} is ambient water quality for the pollutant (mass/volume), C_{nat} is the natural concentration in the catchment (mass/volume). These waters differ significantly in chemistry and inadvertently affect the flotation chemistry as they differ in species present in solution (biotic and abiotic) and therefore in total dissolved solids (TDS). This has motivated extensive research in the impact of

varying water quality and the species at play on the flotation efficiency (Biçak et al., 2012a; Boujounoui et al., 2015; Finkelstein, 1999; Haran et al., 2008; Ikumapayi et al., 2012; Slatter et al., 2009).

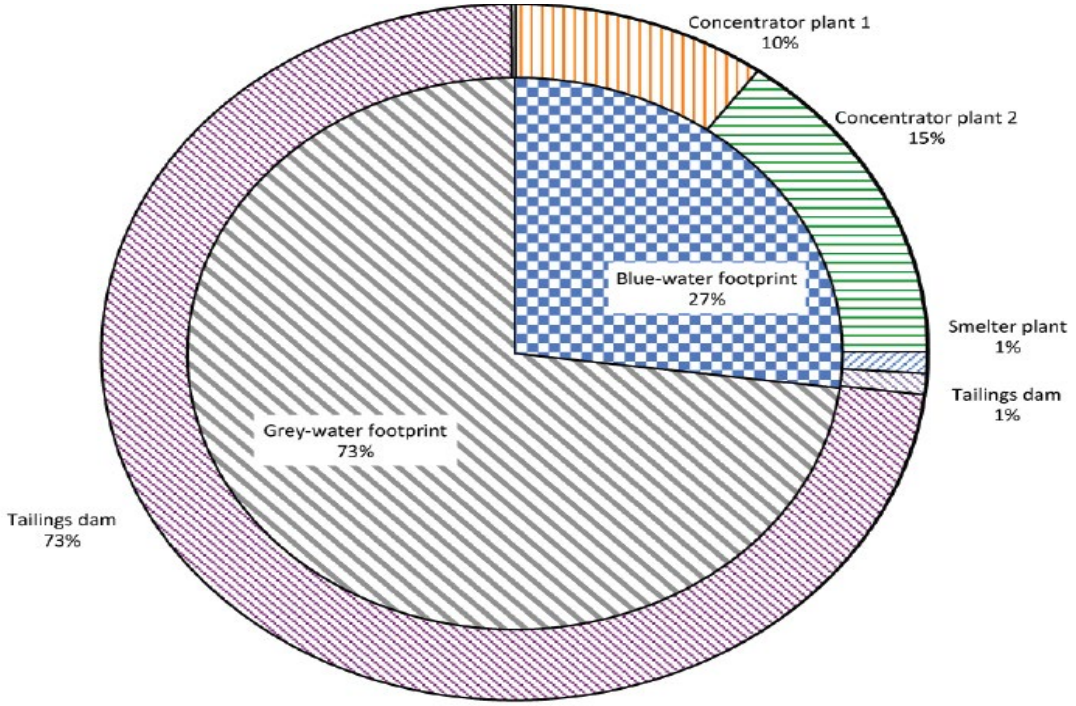

Fig 2-6. Total water footprint for platinum processing plant adapted from (Haggard et al., 2015)

The concentrators represent the froth flotation stages which account for 93% of freshwater withdrawal consumption as shown in Fig 2-6 (Haggard et al., 2015). Deionised water has been shown to achieve superior flotation performance citing reduced reagent adsorption and lower grade and recovery in other water samples in the flotation of copper (Haran et al., 2008); galena and complex polymetallic sulfide ores (Boujounoui et al., 2015; Haran et al., 2008; Ikumapayi et al., 2012).

However, water recycling leads to stabilized flotation rates, residual reagents in the first recycle improved the flotation kinetics however there was no difference whether recycled to the mill or the flotation cell (Boujounoui et al., 2015; Haran et al., 2008). Slatter et al (2009) found that underground water provided comparable results to potable water. The grey water footprint shows the potential water loss of water in the treatment of wastewater and long water recycle from the platinum processing industry, which accounts for 73% of water consumption in the industry as shown in Fig 2-6 (Haggard et al., 2015). Hence water recirculation leads to a higher pollutive impact of the effluent water, and higher water treatment costs.

2.5.1 The Ionic Strength, Total dissolved solids, and Electrical Conductivity

Garrels & Christ (1990) define the ionic strength (IS) of a solution by the average electrostatic interactions of the ions as depicted in Eq. (2-16) where m_i is the molality and z_i is the charge of the ith ion in solution, with a summation done over all the ions present in solution.

This relationship will allow investigation of the impact of water recirculation on IS as determined by the measured EC. EC or specific conductance is the degree to which a substance can conduct electricity (Alva et al., 1991). It is a collectively measures of the dissolved ions in solution with the capability to determine the contribution of individual ions on solution chemistry (McCleskey et al., 2012; Viani and Pettracco, 2016). This is an integral property used to assess properties of natural waters and soil extracts such as the salinity (Dey et al., 2012; Lewis, 1980; Visconti et al., 2010), IS (Lind, 1970; Pintro and Inoue, 1999; Polemio et al., 1980; Ponnaperuma et al., 1966); major solute concentrations (McNeil and Cox, 2000; Pollak, 1954) and TDS (Day and Nightingale, 1984; Gustafson and Behrman, 1939; Lystrom et al., 1978; Singh and Kalra, 1975). Alva et al., (1991) reported a linear relationship between IS and EC with EC is related to IS through Eq. (2-17) adapted from Aqion, (2015).

The EC of the solution provides information on the chemical behavior of dissolved solute, the accuracy of chemical analysis (Clifford et al., 1974; Laxen, 1977; McCleskey, 2011; Miller et al., 1988; Rossum, 1949) and an estimation of the transference (or transport) number of ions that substantially contribute to the conductivity. Allowing us to track the flow of ions throughout the circuit both quantitatively and qualitatively. The EC of a solution can also be estimated from the chemical composition of the ions present (Laxen, 1977; McCleskey et al., 2012; McNeil and Cox, 2000; Rossum, 1949; Visconti et al., 2010). The methods differ in approach by differing in estimation of ionic molar conductivities, ions included in the estimation method, temperature compensation and treatment of ion pairs, with methods differing in ion contribution to the methods summaries in Fig 2-7 (McCleskey et al., 2012). TDS is difficult to measure and is often related to EC using Eq. (2-18) with a suitable K factor of 0.7, in an applicable range between 0.50 to 0.75 used for increasing saline waters, and hence waters with high ion concentration (Walton, 1989).

$$Ionic\ strength\ (M) = \frac{1}{2}\sum_i m_i * z_i^2 \qquad \text{Eq. (2-16)}$$

$$EC\ \left(\frac{\mu S}{cm}\right) = 6.2x10^4 *\ Ionic\ strength\ (IS) \qquad \text{Eq. (2-17)}$$

$$TDS\left(\frac{mg}{l}\right) = K * EC\ \left(\frac{\mu S}{cm}\right) \qquad \text{Eq. (2-18)}$$

Ion	Rossum (1949)	McNeal et al. (1970)	Tanji and Biggar (1972)	Rossum (1975)	Marion and Babcock (1976)	Laxen (1977)	Wüest et al. (1996)	Pawlowicz (2008)	Appelo (2010)	Visconti et al. (2010)	McCleskey et al. (2012)
Major											
H^+				x				x	x	x	x
Na^+	x	x	x	x	x	x	x	x	x	x	x
Ca^{2+}	x	x	x	x	x	x	x	x	x	x	x
Mg^{2+}	x	x	x	x	x	x	x	x	x	x	x
NH_4^+							x	x			x
K^+		x	x	x		x	x	x	x	x	x
Cl^-	x	x	x	x	x	x	x	x	x	x	x
SO_4^{2-}	x	x	x	x	x	x	x	x	x	x	x
HCO_3^-	x	x	x	x	x	x	x	x	x	x	x
CO_3^{2-}	x	x	x	x	x		x	x	x	x	x
F^-								x	x		x
NO_3^-	x	x	x	x	x	x	x	x	x	x	x
Al^{3+}									x		x
Fe^{2+}									x		x
HSO_4^-									x		x
Moderate											
Li^+								x	x		x
OH^-				x				x	x	x	x
Fe^{3+}									x		x
Cu^{2+}								x	x		x
Mn^{2+}									x		x
Zn^{2+}								x	x		x
$NaSO_4^-$					x				x		x
$NaCO_3^-$									x		x
Minor											
Ba^{2+}								x	x		x
Br^-								x	x		x
Cs^+											x
Sr^{2+}								x	x		x
KSO_4^-									x		x
Unknown											
Ag^+								x			
I^-								x			
ClO_4^-								x			
La^{3+}								x			
$MgHCO_3^+$					x				x		
$H_2PO_4^-$					x				x		
HPO_4^{2-}					x				x		

Fig 2-7: Summary of ions included in EC methods adapted from (McCleskey et al., 2012). Ions are grouped in terms of contribution to the conductivity of natural waters, into major (t>0.1), moderate (0.1>t<0.02), minor (t<0.02) ions.

2.5.2 Dissolved Oxygen Concentration (%) and Oxidative Redox Potential

Redox potential (ORP) is an essential indicator of the properties of natural and waste waters (Goncharuk et al., 2010). The Redox potential (ORP value) of is the measure of the relationship between the oxidized and reduced forms of a ions present in solution (Goncharuk et al., 2010). Hydrogen type elements (metal ions) readily donate electrons and have low electrical potential while oxygen in water accepts electrons, and have a higher electrical potential (Goncharuk et al., 2010). ORP values of that are less that <0 mV are typical of waters with containing metal ions with low grade of valence such as Fe^{2+} and are considered to be reduction situations (Goncharuk et al., 2010).

2.5.3 Water Recirculation in Mining Operations: Benefits, Challenges, and Water Quality Variations

With the enactment of stringent laws and policy on water with additional restrictions on mine water discharge and minimizing fresh water feed from municipal sources across the manufacturing industry, water recirculation has risen as a water management strategy (Peters and Meybeck, 2000). Water recirculation as a water management strategy has been favored for the following reason (Carlson et al., 2002; Johnson, 2003; Slatter et al., 2009):

1. Water recirculation prevents environmental pollution from mine water discharge or effluent.

2. It promises to be the best alternative to meet the zero-wastewater effluent from mining operations.

3. And it minimizes freshwater withdrawal.

However: Water recycling does come with disadvantages, Forssberg & Hallin (1989) and Rao & Finch (1989) postulated that water recycling may harm raw material beneficiation with delayed impacts. It has also been suggested that water re-circulation leads to a decrease in reagent efficiency as a result of contaminants, an increase in suspended solids within the recycle water and secondary effects of increased pollutant levels in the recycle water such as chemical and microbiological oxidation products (Slatter et al., 2009).

Internal water recycling has been utilized as an attempt to reduce water withdrawal and effluent from mineral processing plants (Ikumapayi et al., 2012; Liu et al., 2013; Slatter et al., 2009). Recycled water differs due to the point of abstraction in the mineral processing cycle. Abstracted water from tailing dams and clarification ponds are regarded as long recycle waters. These waters contain sulfate, sulfite, chloride, fluoride, magnesium, calcium, sodium, potassium, sulfide, thiosalts, base metals, residual reagents and colloidal materials (i.e., silicate clays, iron hydroxides and natural organic material) (Slatter et al., 2009). Due to the long residence time before reuse, long recycle waters are at a low redox potentials, higher conductivity and low oxygen content (Slatter et al., 2009).

The quality of long recycled water may vary due to evaporation or dilution by green water leading to seasonal variation in its electrical conductivity. Problems associated with long recycle water use are due to residual reagents, reaction products and different types of oils accumulating in the dams. (Slatter et al., 2009). Recycled water abstracted from thickener, concentrator, dewatering and filtration units are regarded as short recycle waters (Liu et al., 2013; Slatter et al., 2009). The water is considered to be in an active state, with shifting chemistry due to reactions occurring in the water with residual ions and reagents in solution (Liu et al., 2013; Slatter et al., 2009). These waters have increased levels of TDS, and the ions and residual reagents are still in an active state, hence reducing fresh reagent requirements (Biçak et al., 2012a; Liu et al., 2013; Slatter et al., 2009). Water recycling has become a significant input to the overall plant water use, accounting for between 60-65% of available water in 2015 (Buchspies et al., 2017).

2.5.4 Causes of Water Quality Variation

Metallurgical operations use process water in concentrator units containing high amounts of dissolved ions which contribute to the complexity of the flotation process, adversely affecting the flotation efficiency (Slatter et al., 2009). Water quality variation in flotation is attributed to both internal and external factors with reference to the concentrator as shown in Fig 2-8. Internal factors include the ore being processed in the concentrator, reagent added into the concentrator and water internal reuse (Liu et al., 2013). External factors are divided into external to concentrator and external to the site. External to concentrator is defined as factors that are within the site boundary including raw water streams and water external reuse (from tailing storage facilities and other site water tasks (Liu et al., 2013).

Raw water and worked water stores are open to systems and hence interact with the surrounding environment and climate leading to mass and energy transfer across site boundaries. This is defined as external to site factors. Of key importance is the impact of internal factors on water quality variation as this will be the focus of the study. Ore oxidation and dissolution during mineral beneficiation introduces various substances into solution impacting water chemistry of the solution (Liu et al., 2013). Reagent addition introduces various organic and inorganic substances into flotation in the form of residual reagents, reaction by-products, and impurities (Liu et al., 2013). Water internal reuse leads to accumulation of species in solution. The impact of inorganic species present in solution has been the subject of a lot of research in water quality (Boujounoui et al., 2015; Ikumapayi et al., 2012; Liu et al., 2013; Slatter et al., 2009). The following discussion sites some of their findings.

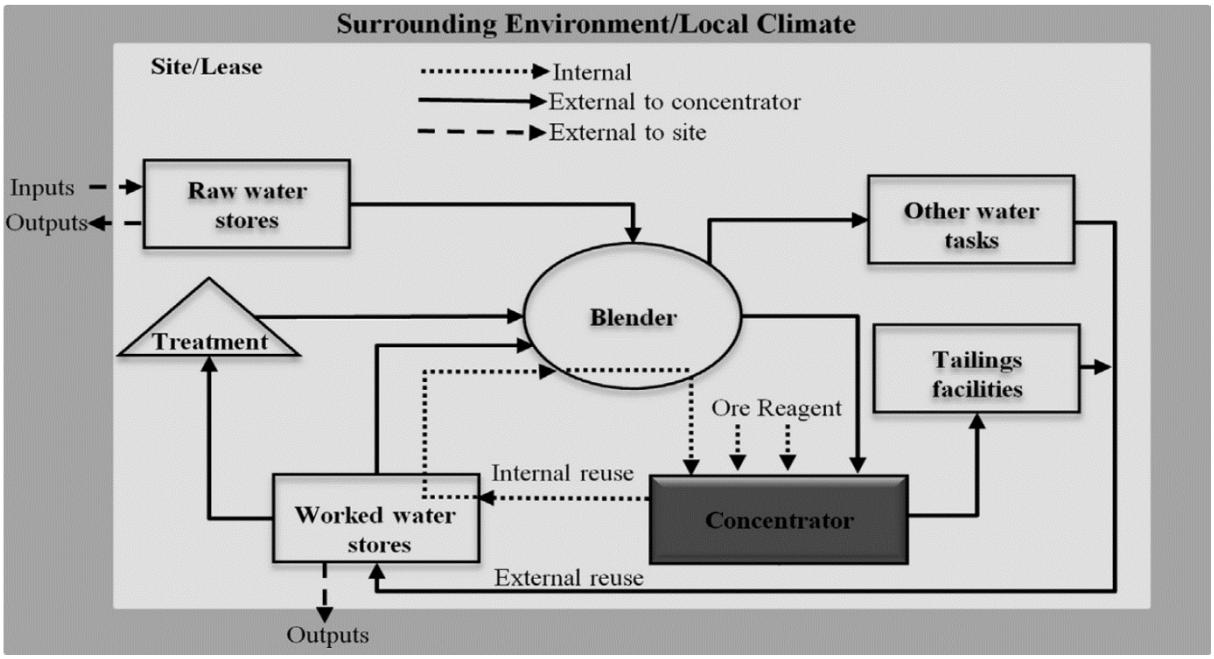

Fig 2-8. A conceptual view of a site water system showing the internal and external factors causing water quality variation in a flotation plant from (Liu et al., 2013).

2.5.5 Consequences of Water Quality Variation on Flotation.

Water quality variation impacts the water chemistry; reaction pathways and species present in solution. Both organic and inorganic constituents have an impact on flotation performance. These constituents interact with and can, therefore, change the properties of the mineral particle, air bubbles and aqueous solution (Liu et al., 2013). These changes affect sub-processes of flotation such as bubble to mineral particle collision, attachment and flotation of stable particle-bubble aggregates which are

buoyant (Liu et al., 2013). Water constituents can also react with reagents added to flotation circuits, changing reagent properties and impacting the reagent performance (Liu et al., 2013).

2.5.5.1 Metal Ions in Solution

Metal ions in solution affect flotation performance. Some metal cations have been shown to activate minerals to be susceptible to reactions with collectors (Finkelstein, 1999). Metal ions in solution raise the critical pH for reaction with thiol collectors, change responses of minerals to particular depressants, and reduce selectivity in flotation (Finkelstein, 1999). Metal ions also show collaborative and predatory impacts on flotation performance.

Metal ions interact with mineral surfaces by adsorption of the metal ions or their hydroxide that adsorb on to the mineral surface impacting the surface charge of the mineral and hence impact flotation efficiency (Biçak et al., 2012a; Boujounoui et al., 2015; Ikumapayi et al., 2012; Slatter et al., 2009). Calcium reduces the impact of copper activation by competing for adsorption at active sites on the mineral surface (Ikumapayi et al., 2012). Calcium at high concentrations (1200-2000 mg/L) leads to depression of sphalerite (Boujounoui et al., 2015) and galena (Ikumapayi et al., 2012) at calcium concentrations of (200 to 500 mg/l) in process water. The findings by Ikumapayi et al., (2012) for galena are disputed by Boujounoui et al., (2015) who operated at higher concentrations in batch flotation but had no impact on the galena flotation. Calcium adsorbs on pentlandite and pyrrhotite impacting hydrophilicity of mineral surfaces. Adding calcium and thiosulfates in steel mill grinding enhances galvanic interactions enhancing thiosulfate adsorption improving copper and nickel sulfide floatability. (Finkelstein, 1999; Martinovic et al., 2005). Calcium and thiosalts improved the grade of Cu in Cu flotation due to calcium's ability to enhance the depression of pyrite (Biçak et al., 2012b).

2.5.5.2 Impact of pH of the Solution

The pH of water has been shown to have a significant impact on metal ion concentrations and the pulp chemistry, affecting the mineral surface and thus the flotation performance (Boujounoui et al., 2015; Ikumapayi et al., 2012). The impact of metal ions and mineral activation in alkaline solutions is more complex (Martinovic et al., 2005). This is seen in the inhibition of activation of high copper concentrations below pH 5 and above pH 12 as the copper forms stable species (Boujounoui et al., 2015; Ikumapayi et al., 2012; Mailula et al., 2003). Change in pH affects the

composition of the surface hydroxyl, sulphoxyl and carbonate species (Ikumapayi et al., 2012). The natural pH of the ore slurry is always alkaline of a pH around 9, owing to the self-buffering capacity of the gangue, hence most sulfide flotation operations run in the pH range of 7-9 (Becker et al., 2006; Khraisheh et al., 2005; Mailula et al., 2003). The addition of ions at pH 9 has been shown to result in the significant depression of talc (Khraisheh et al., 2005).

2.5.5.3 Electrolyte / Ion Concentration in Solution.

Water re-circulation leads to an increase in IS (Corin and Wiese, 2014). The IS of a solution is a useful tool that is used in comparing solutions of diverse compositions because the specific electrical effects of the interactions of the various charged ions present in solution are taken into account, producing a better criterion of solution behaviour than the concentration (Garrels and Christ, 1990). Thus, the IS of an electrolyte solution is a measure of the average electrostatic interactions as shown in (Eq. 2-4) adapted from (Garrels and Christ, 1990).

Froth stability is affected by the type and the concentration of the frother, nature and ionic concentration (inorganic electrolytes e.g. Na^{+}, Ca^{2+} and Mg^{2+}) present, process water quality, suspended particles, gas dispersion angle and particle contact angle (Farrokhpay, 2011). Increase in dissolved ion concentration brought about by water recycling affects the pulp phase properties, impacting the froth stability (Biçak et al., 2012a; Boujounoui et al., 2015; Haran et al., 2008; Slatter et al., 2009), by affecting the water-air interface reducing the rate of coalescence and reducing bubble rupture making the froth stable (Biçak et al., 2012a). Inorganic electrolytes reduce the zeta potential of bubbles and particles, compress the electrical double layers, and hence reduce the repulsive interaction, leading to a dominant hydrophobic force (Kurniawan et al., 2011). However, the impact of electrolytes on froth stability is not only limited to the impact on mineral surface chemistry as shown by the similar contact angles in different water quality for coal flotation (Kurniawan et al., 2011) The presence of electrolytes in aqueous solutions leads to a decrease bubble coalescence and leads to a bubble size reduction depending on the valency of the electrolytes and the surface tension gradient with respect to concentration (Kurniawan et al., 2011). At a transition concentration the bubble size is reduced by 50 % and bubble coalescence is inhibited (Quinn et al., 2007).

Inorganic electrolytes attach to the surface of minerals naturally hydrophobic minerals, and their adsorption disrupts the hydration layer of the surrounding mineral particles and specific adsorption of cations changes the surface charge of the mineral, leading

to a stronger attraction between particles (Kurniawan et al., 2011) . An increase in froth stability is linked to an increase in recovery of all minerals and water at high dissolved ion concentrations in water (Biçak et al., 2012a; Boujounoui et al., 2015). The recovery of chromite flotation is considered to be through entrainment, hence increased recovery of chromite is linked to higher water recovery and increases with the ionic strength of the water (Mailula et al., 2003). Water quality, in terms of ion concentration, impacts depressant efficiency. The presence of potassium, calcium and magnesium ions leads to a favorable effect on the efficiency of depressant adsorption on talc with increasing concentration of ions (Khraisheh et al., 2005). The IS has also been shown to have a significant impact on CMC adsorption on to talc (Khraisheh et al., 2005). Ca^{2+} and Mg^{2+} enhanced depression activity of CMC (Burdukova et al., 2008).

Coagulation tests considering the impact of IS on CMC and flotation performance showed adsorption of CMC onto gangue is enhanced in the presence of inorganic electrolytes (Manono, 2018). Increasing IS leads to the coagulation of gangue particles due to CMC action whilst indirectly removing naturally floatable gangue (NFG) which stabilizes the froth and retarding action of electrolytes on froth stability (Burdukova, 2007; Laskowski et al., 2007). Residual reagents in recycled water affect flotation performance. Residual SIBX in recycled water increased recovery of pentlandite however decreased recoveries and grade of other sulfide minerals (Gray et al., 2016). Bruckard et al (2011) however, states that the presence of reagents like depressants, lime and cyanide in the grinding pulp showed no impact on the subsequent flotation efficiency. An increase in IS has been shown to lead to an increase in froth height and froth collapse time due to inorganic electrolytes inhibiting the coalescence of bubbles. The literature is summarized and grouped into factors, range, parameter affected and the impact of the mineral or the parameter in Table 2-1.

2.6 Bushveld Igneous Complex

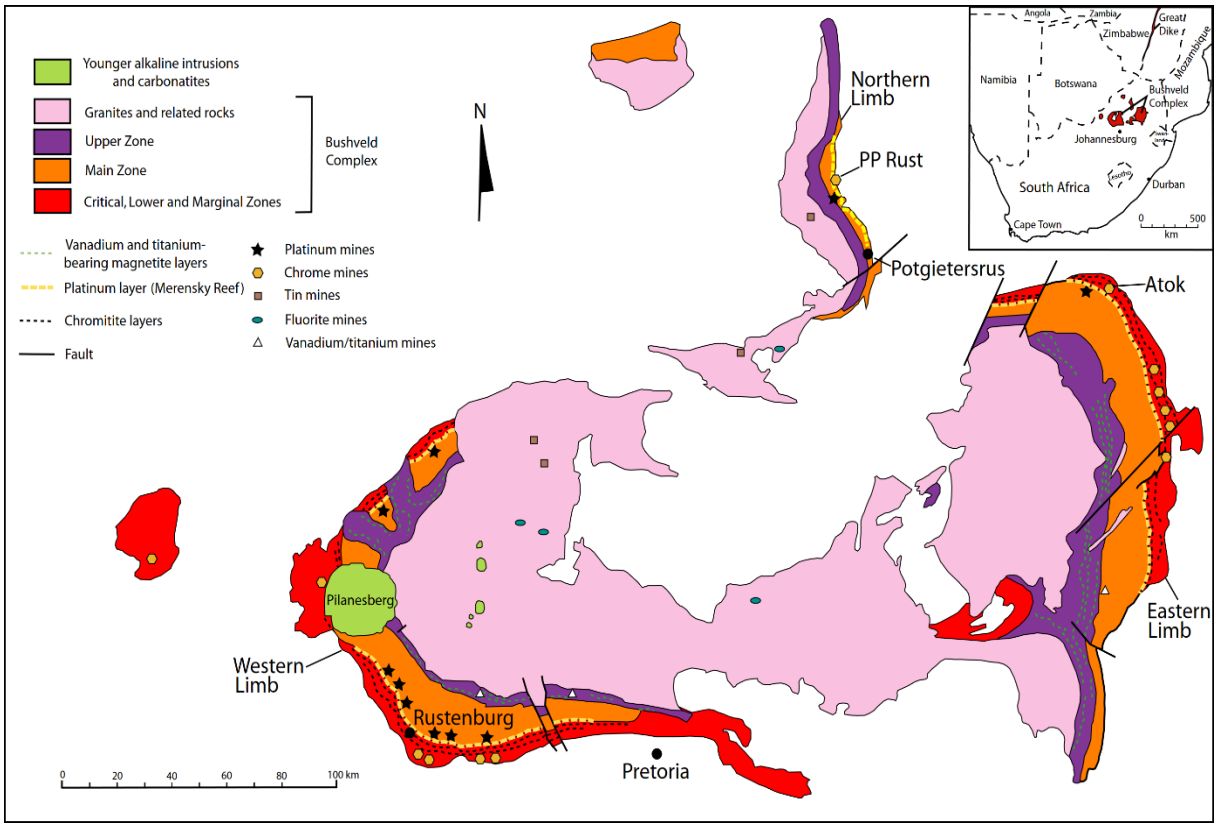

Fig 2-9. Geological Map of the Bushveld Ingenuous Complex adapted from (Mudd et al., 2018)

Platinum Group Minerals (PGM) are mined for their Platinum Group Element (PGE) content. The production of PGE has been dominated by South Africa since the 1950's, accounting for half of the world production in 2015, competing primarily with Russia, producing a third, with the deficit falling to Canada, USA and Zimbabwe (Ek et al., 2004; Mudd et al., 2018). These are mainly mined from the South African Bushveld Igneous Complex (BIC) shown in Fig 2-9 which holds 92 % of PGE reserves containing 204 and 166 million ounces of platinum and palladium respectively, making it one of world largest economic platinum group element (PGE) reserves (USGS, 2020). The BIC produced 72 % of the world's PGE resources in 2019 (USGS, 2020). PGM mining falls under the economic category known as hard rock mining. Mining is an important contributor to South Africa's present and future economic security and income (Gumede, 2018). A combination of economic, social and environmental challenges has had a negative influence on the South African mining sector. This has led to significant losses in net profit margins, return on investments and return on expenditure in the period between 2008 and 2012 (Genc and Jerome, 2014). This has led to the

development of innovative environmentally and economically conscious methods through optimization of PGM extraction and separation from non-sulfide gangue by complementing or improving existing techniques (Slatter et al., 2009).

The Bushveld Igneous Complex (BIC) is one of the world's largest economic platinum group elements (PGE) resources with proven reserves of 204 and 166 million ounces of platinum and palladium respectively (Becker, 2009). The economic horizon of the Complex known as the Rustenburg Layered Suite has critical zones known as Merensky reef, Upper Group 2 (UG2) reef and the Platreef ore bodies that are exploited for their PGM's and base metal sulfides (BMS) (McLaren and De Villiers, 1982; Mudd, 2012). These reefs form the Western, Eastern and Northern limbs of the Complex (Becker, 2009). The UG2 reef is situated between 20 and 400 m below the Merensky reef and can be traced along the surface for nearly the entire 400 km strike length of the Eastern and Western limbs of the Bushveld Complex (Mccall, 2016; McLaren and De Villiers, 1982). The UG2 reef is a major source of PGE with typical grades of 4.5 g/t (Ekmekçi et al., 2003) The UG2 reefs are fond within the Eastern and Western Bushveld complex, containing ores with high PGE attributed values of 85.2 – 91.7% (Mudd et al., 2018).The UG2 reef layer is the uppermost of the more important chromite layers in the upper critical zone of the situated between the UG-1 chromite and the Merensky reef of the Bushveld Complex along the Eastern and Western portions (McLaren and De Villiers, 1982). The UG2 chromite layer varies in thickness between 0.8 – 1.5 m with a grain size in the order of 1.7 mm.

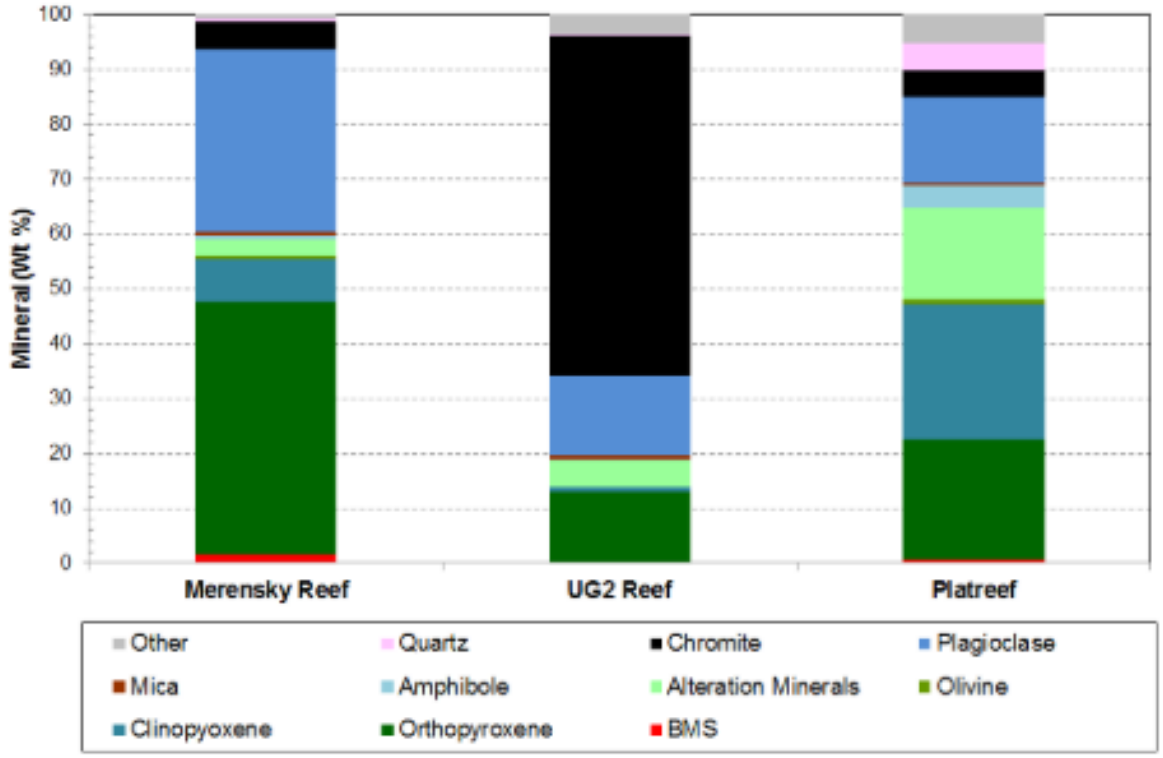

Fig 2-10. Minerals contained in the different Bushveld Ore Bodies (O'connor and Alexandrova, 2021).

The size distribution of base metal sulfides in UG2 reefs is more refined as compared to Merensky reef however achieves lower liberation of the BMS as is visible from the mineral concentrations of the different ore bodies in Fig 2-10 (Dzvinamurungu et al., 2013). The UG2 reef is generally associated by a pegatoidal footwall, with a main layer of a combination of two or more (up to nine) chromite layers overlain by melanotic host rock that contain a thin chromite leader (Mccall, 2016). The eastern limb is often associated with pyroxenite hanging wall whereas the UG2 reef of the western limb is overlain-enriched pyroxenite (Cawthorn, 2011). Samples from the UG2 reef (Impala Platinum UG2 reef) will be used in the experiment.

Table 2-1: UG2 reef Mineral Modal Abundances from UG2 Marikana reef (Dzvinamurungu et al., 2013).

Mineral	Abundance
Chalcopyrite	0.01%
Pentlandite	0.02%
Pyrrhotite	0.00%
Epidote	0.08%
K-Feldspar	0.20%
Phlogopite	1.34%

Quartz	0.07%
Termolite	0.46%
Serpentine and Talc	0.27%
Augite	1.15%
Orthopyroxene (Enstatite)	15.79%
Plagioclase (Anorthite)	25.00%*
Chromite	49%
Other	3.32%

The general mineralogical composition of the ore is given in Table 2-1. UG-2 ore is the second most mined source of PGE in the Bushveld Complex (Nel et al., 2004). UG-2 ore contains two dominant suites of mineralization: chromite and aluminum silicate-based mineralization. The major component of the mineral is the chromite mineral which is a characteristic property of the UG2 reef ore whose physical properties are described in Section 4.2. The aluminium silicate mineralization includes primary magnesium alumino-silicates such as feldspars, pyroxene and chlorite, and hydrothermally altered silicate minerals such as amphiboles and talc (Nel et al., 2004). The aim of UG2 flotation is to recover the sulfides in solid solution as well as liberated PGM or attached to or locked in sulfides (Dzvinamurungu et al., 2013).

It is therefore integral to understand the physical and chemical properties of the sulfide minerals that constitute 0.1 to 0.2% of the UG2 Ore in the base metal suphides (Nel et al., 2004; Wiese and Harris, 2012). The sulfides present composed of chalcopyrite (roughly 10%), pentlandite (roughly 35%) and pyrrhotite (roughly 50% of all sulfides) (Dzvinamurungu et al., 2013; Nel et al., 2004). The valuable PGM's present in the ore and are present in are roughly 45% platinum (Pt), 10% rhodium (Rh), 25 % palladium (Pd), 15% ruthenium (Ru), iridium (Ir) and osmium (Os), and together with gold (Au) and Silver (Ag) are known as precious metals (Nel et al., 2004). Gangue minerals of interest in the UG2 ore are chromite (70%), pyroxene (15-20%), feldspar (3-5%) and talc (1-3%) (Ekmekçi et al., 2003). The flotation behaviour of the sulfides differs as the flotation rate of chalcopyrite is rapid, followed by pentlandite, and lastly pyrrhotite which is considered to be a slow floating sulfide (Becker et al., 2007).

Complete analysis of the ore with the conjunction of experimental tests when studying range of process operations have yielded better metallurgical performance (Becker, 2009). Therefore, in order to successfully stabilize/ control the behaviour of the ore during flotation, a comprehensive understanding of its mineralogy and relationship to flotation is needed (Becker, 2009; Becker et al., 2008). The general formula of the sulfides is given as X_mZ_n with X_m referring to the metallic element and Z_n the non-metallic element with n,m being integers based on the ionic charge (Mhlanga, 2011).

Pyrrhotite $Fe_{(1-x)}S$ with x values ranging from $0 \leq x \leq 0.125$ is one of the most commonly occurring metal sulfide minerals found in ore deposits for nickel-copper, lead-zinc, and platinum group elements (PGE) (Becker, 2009). Due to its coexistence with pentlandite, the understating of the behaviour of pyrrhotite during flotation is of fundamental interest (Mhlanga, 2011). In platinum group element processing pyrrhotite is targeted for its association with the PGE minerals unlike in nickel processing operations where the mineral is rejected to the tailings (Becker, 2009). The reactivity of the pyrrhotite ores leads to its oxidation, acid mine drainage, high concentration of dissolved iron, aluminium and nickel in drainage reduced floatability due to formation of hydrophilic iron hydroxides that render surfaces of pyrrhotite less floatable (Becker et al., 2008). Chalcopyrite is a sulfide mineral containing iron and copper with a chemical formula of $CuFeS_2$ (Lotter et al., 2008) It is the most widespread copper mineral and its structure can be derived from the sphalerite mineral (Zn,Fe)S (Klein et al., 2002). Pentlandite $(Fe,Ni)_9S_8$ is exploited as a source of nickel and is always associated with pyrrhotite (Mhlanga, 2011). Hayes et al., (1987) arranges the floatability of sulfide minerals in descending order as chalcopyrite, galena, pyrrhotite, pentlandite, covellite, bornite, chalcocite, sphalerite, pyrite and arsenopyrite with the first four considered floatable in the absence of collector or oxygen free environments while the last four minerals are sparingly floatable and are recovered increasingly with increasing frother dosage.

The unwanted minerals/ gangue present in the PGM flotation are in the form of silicates which are the most abundant mineral on the earth's crust (Manono, 2012). They differ in structural complexity forming minerals with great physical and chemical complexity. This leads to the minerals having a range from hydroscopic surfaces, to fixed surface charge, and extensive metal surface sites; to having broken Si-O bonds that control the surface behaviour (Manono, 2012). These gangue minerals vary in floatability due to crystal structure, with Talc, a complex structured silicate, taking responsibility for most of the naturally floatable gangue mineral (Manono, 2012).

2.6.1 PGM Mineralogy

The sulfides in the UG2 reef constitute 1% of the ore. Studies on the mineral composition of the UG-2 ore have revealed that between 70 and 80 % of the PGM minerals are linked to base-metal sulfides, with the remaining 10 to 20 % found in the silicate gangue and 5 % in the chromite (Liddel et al., 1985). PGM's grinding produces active sites for interaction by breaking the covalent bonds of their lattice crystal to form fresh surfaces from wetting and grinding which are highly reactive and oxidise readily

in the presence of oxygen (Manono, 2012). UG2 contains minor quantities of copper and nickel sulfides. PGE sulfides comprise roughly 70 % of the PGM with the UG-2 plant feed, with the remainder largely being alloy of iron, lead, arsenic and antimony, or tellurides (Nel et al., 2004). Although PGM mineralisation may be complex, it does not tend to dictate floatability (Nel et al., 2004). PGM are finely disseminated, with an average grain size being about 10 microns so that grain size, liberation and association tend to dictate mineral floatability. The grain size and association can be split into four categories (Nel et al., 2004):Coarse PGM (roughly 5 % of all PGE),PGM associated with base metal and iron sulfides (40 %),PGM occurring on host mineral grain boundaries (30 %), and PGM locked in silicates

PGM's attached to sulfide minerals can be recovered by the flotation of the base metal and iron sulfide minerals while those on the grain boundaries are preferentially released (Nel et al., 2004). PGM locked in silicate minerals require finer and longer liberation in a secondary milling step, ensuring rougher and cleaner flotation times (Nel et al., 2004).

Table 2-2. Summary of literature on the impact of water quality variation on froth flotation chemistry.

Consequences of Water Quality Variation					
Source	**Range**		**Flotation Parameter Affected**	**Impacts on (Mineral / Property.)**	**Source**
	High (mg/L)	Low (mg/L)			
Copper	7-14	0-7	Recovery	A	B, C
			Activator	S, C, P, F	A, B, N, L
			Entrainment	G, PR	A, B
			Reagent	X	C
			Depressant	S	B
			Pulp Chemistry	Activation of chromite (true flotation)	H, L
Lead	-	-	Activator	Less than Copper	B
			Reagent	X	C
Zinc	20-40	< 20	Recovery	C, S, C, PR	B
			Depressant	S	B
Iron	-	-	Activator	PR	D
Calcium	1200-2000		Depressant	S	B
			Depressant	G	F
			Depressant	G	B
			Pulp Chemistry	PR, PY	
			Comminution Chemistry	Copper and Sulfide floatability	D, L
Sulfate ions			Recovery	A	B, C
			Recovery	A	F
pH			Pulp Chemistry	Metal ions	F
			Activator	A	L
	5	12	Inhibits High Copper Effects	Formation of stable species	B, F, H
			Mineral Chemistry	Surface composition	
		9	Depressant	T	G
Ionic Strength			Froth Chemistry	Froth Stability	A, B, E, N
			Recovery	A	A, B
			Reagent activity	depressant efficiency	
			Depressant Adsorption	T	G, K
	Residual SIBX		Recovery	PE	I

Residual reagents			Recovery	other sulfide minerals	I
potassium, calcium and magnesium			Depressant Adsorption	T	G
Calcium and magnesium			Reagent activity	Depression activity of CMC	M

Table 2-3. Key for the summary of literature on the impact of water quality variation on flotation.

Key, Variables and Reference List.			
	Impact of High Concentration	(Biak et al., 2012)	A
	Impact of Low Concentration	(Boujounoui et al., 2015)	B
	Disputed results	(Corin et al., 2011)	C
	Impact of presence	(Finkelstein, 1999)	D
		(Haran et al., 2008)	E
All minerals	A	(Ikumapayi et al., 2012)	F
Sphalerite	S	(Khraisheh et al., 2005)	G
Chalcopyrite	C	(Mailula et al., 2003)	H
Pyroxene	P	(Manenzhe, 2018)	I
Galena	G	(Manono, 2012)	K
Collector sequestration	X	(Martinovic et al., 2005)	L
Pyrite	PR	(Mhlanga, 2011)	M
Pentlandite	PE	(Slatter et al., 2009)	N
Talc	T		
Feldspar	F		
Pyrite	PR		
Pyrrhotite	PY		

3 Research Approach

3.1 Research Key Questions, Hypotheses and Objectives.

3.1.1 Aim and Key Questions.

In line with the ongoing research discussion and the literature gap identified in Section 1.2, the impact of short water recirculation on the flotation chemistry and its impact on the flotation performance became the focal point of the study.

The project monitored the impact of change in water quality through water recycling on the flotation chemistry and the properties of pulp by observing and recording the EC, TDS, DO% and ORP readings during the experiment as well as residual reagent concentration in the tailing's slurry with multimeter probes and analytical spectroscopy, respectively.

Beyond the water recovery, the froth stability of the tailings pulp and recovered water samples was analyzed using 2 & 3 phase dynamic froth stability tests. Gallery discrete automated colorimetric analysis of tailings water samples was performed to determine the ionic concentration of selected ions in the tailings water samples. The project then analyzed the impact of the change in water quality through water recycling on the flotation performance through the analysis of the solids, water and sulfide mineral recoveries and grades.

Finally, the project analyzed the impact of water recycling on the post flotation thickeners efficiency, by performing coagulation tests to determine settling rates after flotation at different water quality developed due to water recycling. The investigation simulated the primary rougher flotation step of UG2 ore as it is the first processing step for the fine ground ore from the crushers.

Experimental results were utilized to develop efficiency indicators, kinetic and first order response models, water and solids recoveries, and sulfide minerals grades and recoveries, which were then compared to established mechanisms in literature as well as baseline tests performed as discussed in Chapter 2 and Chapter 4.1. The objectives of the proposed work were structured in the from key questions developed to identify the impact of water re-circulation on the froth and pulp properties and how these impacted the flotation performance.

- ✓ *What is the impact of a change in water quality on the settling rate of the tailings from UG2 ore froth flotation?*

- ✓ *What is the impact of a change in Water Quality through Water Recycling, and point of addition of recycled water, on the flotation performance of a UG2 ore?*
- ✓ *What is the impact of a change in Water Quality through Water Recycling, and the point of addition of Recycled Water, on Froth Stability?*
- ✓ *What is the impact of a change in Water Quality through Water Recycling on the Electrical Conductivity (EC), Oxidative Redox Potential (ORP), Dissolved Oxygen Concentration (DO %) of the Batch Flotation Feed Slurry, Tailings Slurry and Recovered Water Samples?*
- ✓ *What is the impact of a change in Water Quality through Water Recycling on the Residual Reagent Concentration and Reagent Efficiency (%)?*
- ✓ *What is the impact of Water Recycling on the Concentration of Ca^{2+}, Mg^{2+}, SO_4^{2-} and Cl^- present in the tailings water?*

The main objective of this study was to investigate the impact of short water recirculation to different units of operation (mill or float cell) on the flotation performance of a UG2 sulfide ore in comparison to performance at a constant baseline water quality. The second **objective** was to determine whether experimental methods applied can be adequately used to monitor changes in water quality and develop inferences on flotation performance.

3.1.2 Hypotheses

Water Recirculation leads to an increase in the EC, and TDS concentration, through accumulation of ions (cations e.g., Ca^{2+} and Mg^{2+}, and anions e.g., SO_4^{2-} and Cl^-).

This occurs by ore dissolution which is based on the rest potential (ORP) of the system.

Hence an overall higher IS that leads to higher froth stability and therefore higher solids and water recoveries.

In turn, the grade of the concentrate decreases due to the higher froth stability and a higher degree of gangue entrainment.

Water recirculation leads to slower transparency rates of tailings due to the presence and accumulation of small particles (d < 25 µm), and accumulation of

ions through ore dissolution which leads to a increase in the system charge leading to an increase in repulsion between particles.

Water recirculation leads to a buildup in residual reagent concentration for both collector and depressant, due to accumulation of unused reagent remaining in the water.

In addition to the hypotheses developed, the experimental methodology allows for the project to test another hypothesis based on the impact of change in depressant dosage on the solids and water recovery, sulfide minerals grade and recovery, and the degree of entrainment. Although the impact of depressant dosage on flotation performance is well developed in literature as studied by Dhliwayo (2005); Morris et al (2002); Wiese et al (2007) and Wiese and Harris (2012) amongst others, test work on different ore bodies improves on the strength of the developed relationships, thus it was hypothesized that:

Increase in depressant dosage at a constant water quality, collector and frother dosage during flotation of a UG2 ore leads to a decrease in the solids, water, and gangue recovery, improving the grade of Cu and Ni in the concentrate due to the depression of NFG, reducing the total solids recovery and the froth stability of the froth, with all NFG depressed at a dosage of 300 g/t.

4 Experimental Plan

4.1 Experimental Plan

The experimental program was divided into 2 phases. Phase 1 constituted a series of baseline tests to establish the relationship between depressant dosage and solids recovery and establish the entrainment factor and quantity of NFG in the UG2 ore. Phase 2 was conducted to evaluate the impact of water recirculation at different points of addition (i.e., water recirculation to the mill vs. the flotation cell) on flotation performance. The materials and methods utilized in the study are described in Sections 4.2 to 4.13. An outline of the two phases and design of the experiment is illustrated in Fig 4-1. All measurements were conducted in triplicate to allow for statistical analysis of the results. Subsequent error analysis was found to be within 5 % for solids and 10 % for water recovered. The flow of materials and measurement points are illustrated in the schematic diagram in Fig 4-2. It is important to note that Water Quality in this project is defined by the quantity of inorganic ions present in the water and is not similar to the water quality terminology used in environmental studies.

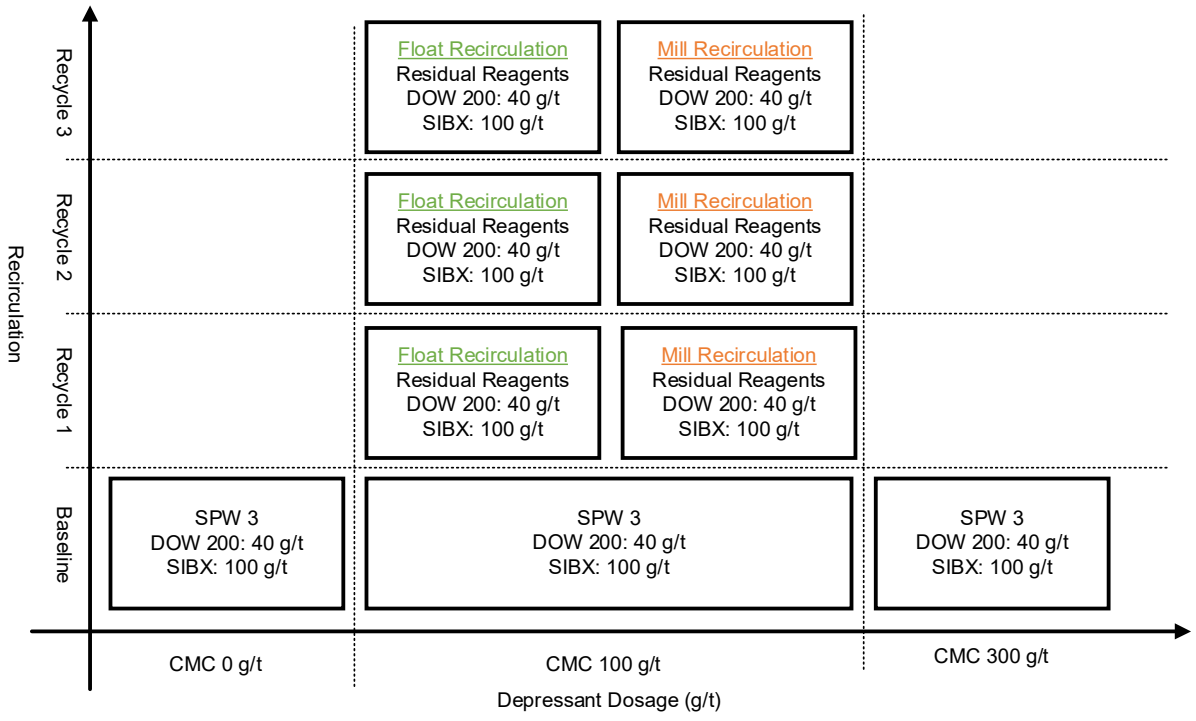

Fig 4-1. One factor at a time design for the experimental conditions tested on the UG2 ore.

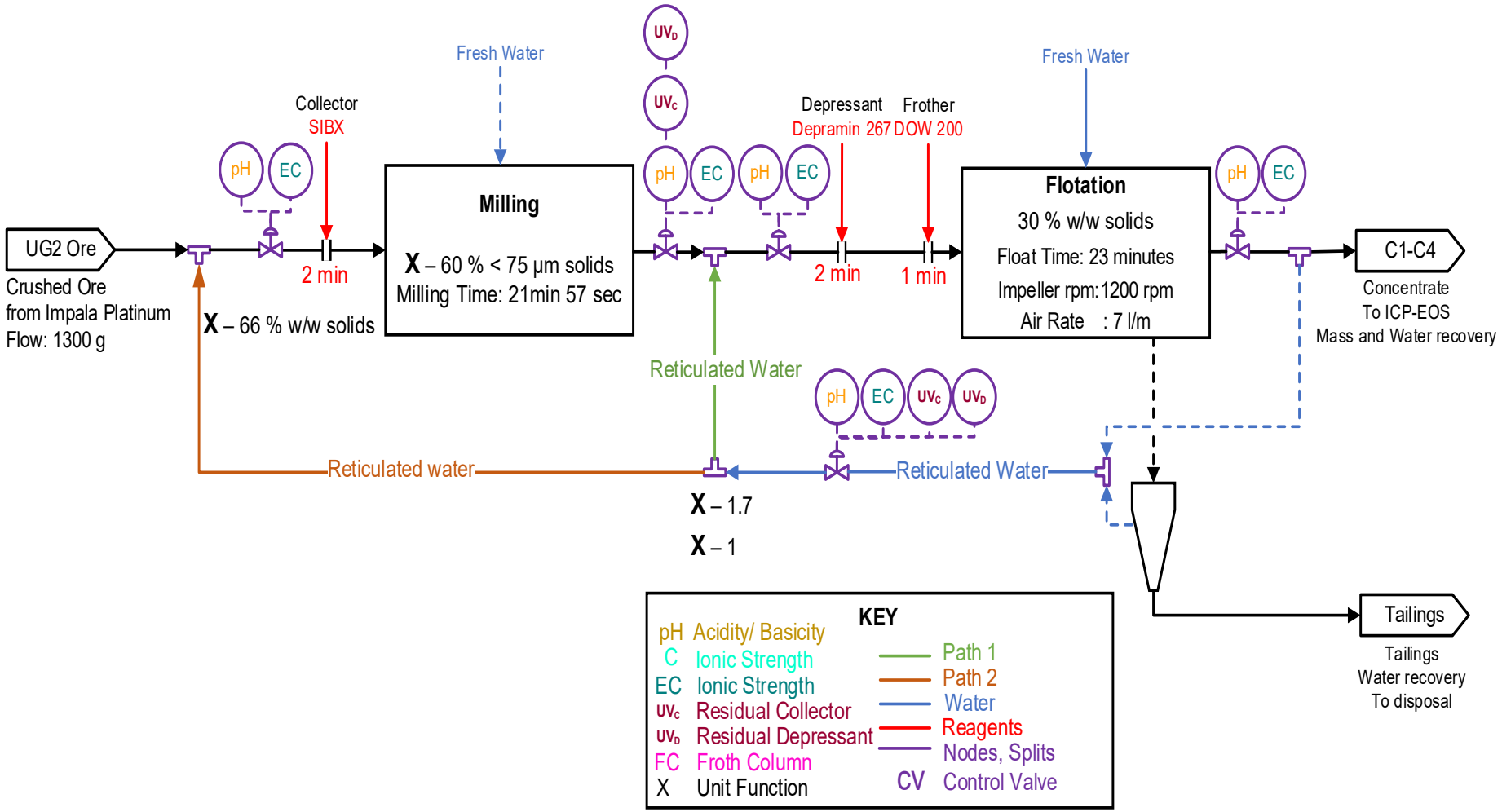

Fig 4-2. Schematic summary of procedures in water recirculation.

4.2 UG2 Ore Mineralogy

The UG2 ore sample was obtained from Impala Platinum, situated within the Bushveld Igneous Complex (BIC) in South Africa. The ore is a low-grade Cu-Ni PGM ore and is the second most mined source of Base Metal Sulfides (BMS) in the Bushveld Complex (Nel et al., 2004). The sulfide minerals present are <1% of the ore and are composed of chalcopyrite (roughly 10% of all sulfides), pentlandite (roughly 35 % of all sulfides) and pyrrhotite (roughly 50% of all sulfides) (Dzvinamurungu et al., 2013; Nel et al., 2004). The valuable PGM's present in the ore are roughly 45% platinum (Pt), 10 % rhodium (Rh), 25 % palladium (Pd), 15 % ruthenium (Ru), iridium (Ir) and osmium (Os), and together with gold (Au) and silver (Ag) are known as precious metals (Nel et al., 2004). A sample of UG2 ore (OD 1390) head assay was determined to contain 27.33 % Cr_2O_3, 22.25 % Fe_2O_3, 19.53 %, SiO_2 14.19 % MgO, 1.81 %, CaO, 0.028 % S, 101 ppm Cu, 1300 ppm Ni, and Pd< 100 ppm (Jasieniak et al., 2010). Gangue minerals of interest in the UG2 ore are chromite (70%), pyroxene (15-20%), feldspar (3-5%) and talc (1-3%) and are important to consider owing to their possible impact on both the grade and recovery due to their natural flotation and entrainment in the flotation concentrates (Ekmekçi et al., 2003). The bulk UG2 ore was supplied in 2019 by Impala Platinum mines in 220 L clamp sealed drums as blended, crushed in four 15 kg ore bags. 13 kg of the ore was riffled and split into 1.3 kg portions using a vibrating rotary splitter developed by Dikie and Stockler (Allen, 1965). This approach produces a consistent composition between the test charges, as the riffler reduced the group and segregation error, hence reducing the relative standard deviation of the sample mean pay-metal grade.

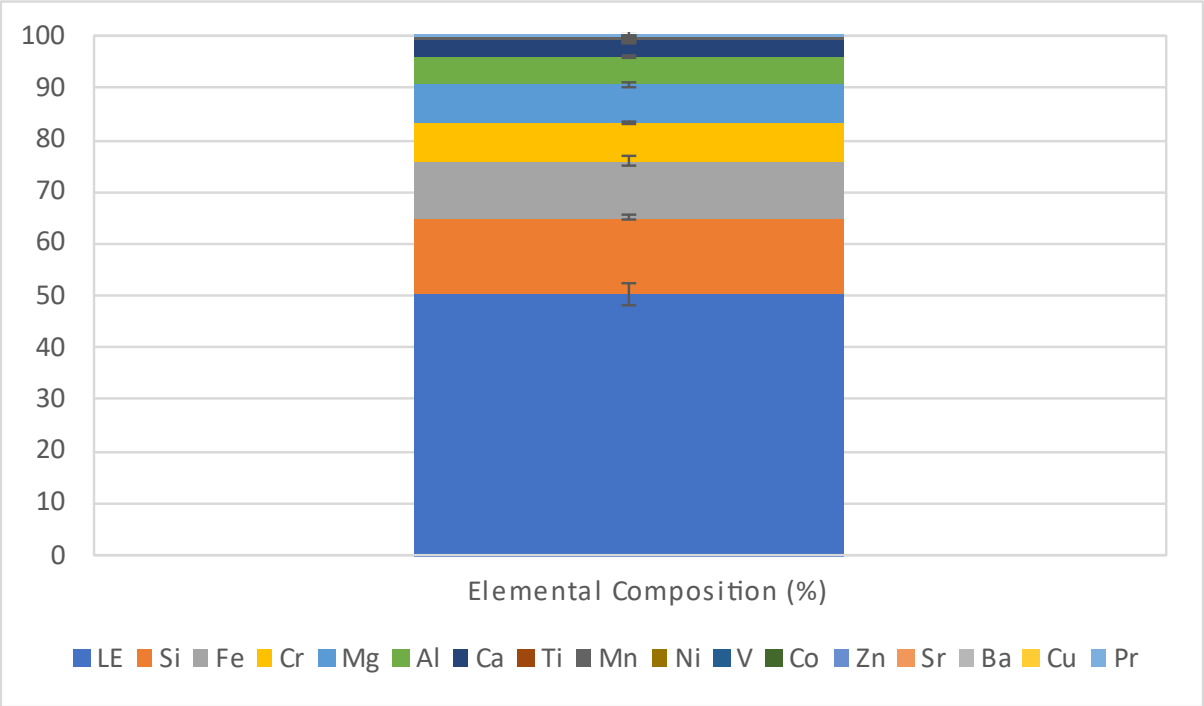

Fig 4-3. Individual elemental composition of the UG-2 Ore feed analyzed using an X-Ray Florence (XRF).

It is clear from the XRF analyses of the feed samples shown in Fig 4-3 that the light elements (LE), e.g., Li, Be and Na, form the bulk of the ore, with Mg, Al, Ca, and Cr has other elements in significant quantities. All elements above 10^4 ppm are shown in Fig 4-3, S, Mo, Ce, La, Zr, P are all below 10^4 ppm but above 10^3 ppm, Pb, Rb are all below 10^3 ppm and above 10^2 ppm, As, Se and Ag are all below 10^2 ppm. The mean copper and nickel values shown in Table 4-1 for the UG-2 Reef were calculated from the concentrate and tailings data developed from all the batch flotation tests.

Table 4-1. Mean calculated feed values for the UG-2 ores received in 2019.

	Copper, wt%	**Nickel, wt%**
UG-Ore Sample	0.011 ± 0.0002%	0.129 ± 0.003%

4.3 Electrical Conductivity, Dissolved Oxygen, pH, and Redox Potential Measurements

Key chemical properties of the solution (slurry and or water) were monitored and sampled at different points of the experimental program as shown by the valves in Fig 4-2. The Electrical Conductivity (EC), Potential of Hydrogen (pH), Oxidation Reduction Potential (ORP), Total Dissolved Solids (TDS) and Dissolved Oxygen Concentration (DO%) of the flotation feed, flotation tailings and the recovered tailings and concentrate

water were measured. The measurements for EC, DO%, pH, TDS and ORP were measured using a HANNA Instruments' multiprobe HI9298194 probe number S/N K3595444 (Hanna Instrument Inc., 2021).

Electrical Conductivity (EC) or specific conductance is the degree to which a substance can conduct electricity and is a measure of the collective charge of the dissolved ions in solution (Alva et al., 1991; McCleskey et al., 2012; Viani and Pettracco, 2016). This is an integral property used to assess properties of natural waters and soil extracts such as the salinity (Dey et al., 2012; Lewis, 1980; Visconti et al., 2010), Ionic Strength (IS) (Lind, 1970; Pintro and Inoue, 1999; Polemio et al., 1980; Ponnaperuma et al., 1966), major solute concentrations (McNeil and Cox, 2000; Pollak, 1954) and Total Dissolved Solids (TDS) (Day and Nightingale, 1984; Gustafson and Behrman, 1939; Lystrom et al., 1978; Singh and Kalra, 1975) The Redox potential (ORP value) is the measure of the relationship between the oxidized and reduced forms of ions present in solution (Goncharuk et al., 2010). The potential of hydrogen (pH) of a solution is a quantitative measure of the acidity or basicity of liquids or other aqueous solutions and is an important quality of a substance with an impact on the nature of interactions with other substances (Encyclopaedia Britannica, 2012). Dissolved Oxygen Concentration (DO %) refers to the concentration of oxygen gas incorporated in an aqueous solution or a liquid, which has an impact on reactions that oxygen dependent (Encyclopaedia Britannica, 2012). Table 4-2 displays the EC, DO %, pH, ORP and TDS properties of the 3 SPW as measured by the multiprobe as described in Section 4.3.

Table 4-2. EC, DO%, pH, ORP and TDS readings of 3 SPW from the Multiprobe.

Variable	**3 SPW**
EC [µS/cm]	5623
D.O. [%]	57.6
pH	8.82
TDS [ppt]	2.811
ORP [mV]	147.7

4.4 Synthetic Plant Water Preparation

The Centre for Minerals Research (CMR) at the University of Cape Town (UCT) developed a synthetic plant water (1 SPW) recipe to mimic typical water quality determined at several PGM concentrators across the BIC (Wiese et al., 2005). At the time, this water comprised of a total dissolved solids content (TDS) of 1023 mg/L and an ionic strength (IS) of 0.0242 mol.dm^{-3} (Corin et al., 2011; Wiese et al., 2005). However steady increases in dissolved ion concentrations in process, recycled and

tailings water has rendered water of TDS of 1023 mg/L atypical of most PGM concentrators today (Corin et al., 2011). Therefore, synthetic plant water of higher TDS content was proposed to better represent typical water concentrations in PGM concentrators.

Individual salts of general reagent grade were dissolved in tap water to prepare synthetic plant waters 3 and 5 SPW recipes were adapted from 1 SPW by multiplying the concentration of respective ions by three and five, respectively, to represent the increase in ion concentration on-site over time. All salts were supplied by Merck in powder form and are displayed in Table 4-3 and material safety data sheets can be found in Appendix C.

Table 4-3. The individual salts used to prepare synthetic plant water and their purity.

Magnesium Sulphate	Magnesium Nitrate	Calcium Nitrate	Calcium Chloride	Sodium Chloride	Sodium Carbonate
99%	99%	99%	99.99%	99.50%	99.50%
$MgSO_4.7H_2O$	$Mg(NO_3)_2.6H_2O$	$Ca(NO_3)_2.4H_2O$	$CaCl_2.H_2O$	NaCl	Na_2CO_3

The salts were dissolved in tap water with and stirred with an impeller in two 3 L buckets. 3 SPW was considered to represent the current on-site feed process water quality and was used as the baseline water quality. Standards ionic concentrations contained in 1, 3 and 5 SPW are shown in Table 4-4.

Table 4-4. The concentration of ions presents in synthetic plant water in mg/L (adapted from Wiese et al., 2005; Corin et al., 2011; Manono et al., 2018).

	Ca^{2+}	Mg^{2+}	Na^{+}	Cl^{1-}	SO_4^{2-}	NO_3^{-}	CO_3^{2-}	TDS (mg/L)	IS (M)
1 SPW	80	70	153	287	240	176	17	1023	0.0241
3 SPW	240	212	459	861	719	527	51	3069	0.0721
5 SPW	400	350	765	1435	1200	880	85	5115	0.1205

4.5 Reagents Preparation, Storage and Disposal.

There were five reagents utilized in the experiments, namely, collectors, frother and depressants were utilized during the flotation procedure, while phenol and sulfuric acid were utilized during the colorimetric analysis for residual depressant in the tailings and

concentrate water. The properties and suppliers of these reagents are outlined in Sections 4.5.1 to 4.5.5.

4.5.1 Collector

The ionic thiol collector utilized in all the batch flotation tests was sodium isobutyl xanthate (SIBX), with a 90 % active content with a molecular weight of 172 g/mol supplied by AECI Senmin in pellet form. Due to the rapid decomposition of xanthates at elevated temperature, a 1% (w/v) solution of SIBX was prepared daily, with active content considered, by crushing the pellets in a crucible and motor, and dissolving the solid in distilled water before experiments. The collector was dosed into the mill at 150 g/t for all the runs. When the reagent was not in use it was stored in a refrigerator at 9 ^{o}C. The unused SIBX solution was discarded daily in a safe and environmentally responsible manner as outlined by the product material and data safety sheet and laboratory guidelines availed in Fig 9-11 in Appendix C.

4.5.2 Depressant

The polysaccharide depressant utilized in the batch flotation tests was Depramin 267, a Carboxy Methyl Cellulose (CMC) of a molecular weight of 325 000 g/t. This was supplied at a purity of 72% by Akzo Nobel Functional Chemicals in powder form. A 1% (w/v) solution of the depressant was prepared daily for use by hydrating the required amount, considering the active content, of dry depressant powder in distilled water, agitated using a magnetic stirrer for two hours to prevent the formation of lumps. The depressant was dosed at 0 g/t, 100 g/t and 300 g/t as prescribed in the experimental design. The high and low depressant dosage of 300 g/t and 0 g/t were used to develop the entrainment factor under the assumption that at an extremely high dosage, all-natural floating gangue is depressed and that the only source of gangue is through entrainment in the froth. The 100 g/t dosage was the normal dosage for all the standard conditions and the recirculation experiments as described in Section 4.12 and 4.13. When the reagent was not in use it was stored in a refrigerator at 9 ^{o}C. The unused Depramin 267 solution was discarded in a safe and environmentally responsible manner as outlined in the product material data safety sheet and laboratory rules Fig 9-12. MSDS for CMC adapted from (USK, 2007) in Appendix C.

.

4.5.3 Frother

The polyglycol frother utilized in the batch flotation tests was DOW 200, supplied by the DOW Chemical Company, of a molecular weight of 220 g/mol supplied at a purity of 100% in liquid form. The frother was dosed in the flotation cell at 40 g/t for all runs using a P200 Gilson Air displacement pipette. After use the reagent was stored at room temperature in the reagent cupboard. The product safety data sheet is available in Fig 9-10 in Appendix C.

4.5.4 Phenol

The phenol indicator used in the absorbance tests for the determination of residual CMC present in water samples prepared in Section 4.4 was prepared from phenol crystals of analytical grade of 99.5 % purity supplied by Sigma-Aldrich. A 5% (w/v) solution was prepared by dissolving the required amount of phenol in distilled water. The preparation and use of phenol were done in a fume cupboard due to the high toxicity of the phenol solution. 1 mL of the phenol solution was added to 1 ml of the sample solution in a test tube using a P3000 Gilson air displacement pipette. The prepared phenol solution was used for a week stored at room temperature in the toxic reagent cupboard and was discarded as outlined in the product material data safety sheet and laboratory guidelines availed in Fig 9-13 in Appendix C.

4.5.5 Sulfuric Acid

The sulfuric acid utilized in the absorption studies for the determination of residual CMC present in the water obtained from the batch flotation tests in Section 4.12 was suppled in liquid form as reagent grade of a purity of 95-97% supplied by Merck Laboratories. 5 mLl of Sulfuric Acid was pipetted using a P5000 Gilson air displacement pipette carefully into the test tube containing phenol and sample solution. The residual reagent mixture was discarded as outlined in the product material safety sheet and laboratory guideline available in Fig 9-14 Appendix C.

Table 4-5. Summary of the properties of flotation reagents utilized in the experiments.

Collector	**Type**	**SIBX**	
	Dosage	150	g/t
	Molecular Weight	172	g/mol
	Chemical Formula	$(CH_3)CHCH_2OCS_2Na$	
	Purity	90%	
	Supplier	AECI Senmin	

Frother	**Type**	**DOW 200**	
	Dosage	40	g/t
	Molecular weight	220	g/mol
	Chemical Formula	$CH_3(C_3H_6O)_3OH$	
	Purity	100%	
	Supplier	DOW Chemical Company	
Depressant	**Type**	**CMC (Depramin 267)**	
	Dosage	0, 100, 500	
	Molecular weight	325 000	g/t
	Chemical Formula	$C_8H_{15}NaO_8$	
	Purity	72%	
	Supplier	AKZO Nobel Functional Chemicals	

4.6 Adsorption Kinetic Studies

To determine the residual concentrations of reagents, present in the tailings and concentrate product, adsorption kinetic studies were utilized. Absorption is utilized as an analytical technique to characterize and quantify a substance, as each substance uniquely adsorbs light, and the amount of light absorbed is a function of the amount of substance present (Swinehart, 1962). With the path length constant, the absorbance is directly proportional to the concentration of the substance (Paul Yates, 2012; Swinehart, 1962). This allows for quantification of organic molecules, inorganic ions or complexes in solution through Ultraviolet or Visible light Spectroscopy (Caro, 2017). The absorbance/optical density of a solution is a measure of the quantity of light absorbed by the solution (ISO Comittee, 2009). Absorbance is the ratio of radiant flux transmitted by a material Φ_e^i and the radant flux received by a material Φ_e^t as shown in Eq. (4-1) adapted from (Swinehart, 1962).

$$A = \log_{10} \frac{\Phi_e^i}{\Phi_e^t} = \varepsilon l c \qquad \text{Eq. (4-1)}$$

Absorbance is related to concentration of a solution through the Beer-Lambert Law developed in 1852 which relates the radiant power (intensity) (A) in a beam of electromagnetic radiation (usually ordinary light), to the length of the path (l) of the beam in an absorbing medium (path length) of a particular molar absorbance coefficient (ε) at a particular concentration of the substance (c) at a as shown in Eq. (

4-1) (Swinehart, 1962). Residual xanthate (SIBX) in residual water samples was tested from the prepared samples in Section 4.13. 3 mL of the sample was pipetted using a P5000 Gilson air displacement pipette into a transparent plastic cuvette with 3.5 mL capacity and a light path of 10 mm. The sample absorbance was measured against a blank solution of distilled water for a SIBX absorbance peak of 301 nm in a Biochrom Ltd. Ultrospec 2100 Pro Scanning, UV/Visible Spectrometer (Tornell, 1967, 1966a, 1966b). To develop a relationship between the absorbance and concentration of xanthates, a calibration curve of absorbance values of samples of known SIBX concentrations was developed as shown in Fig 4-4. A linear regression of the plot produced an equation relating the absorbance to concentration which was utilized to estimate the concentration of residual xanthates in the water from their measured absorbance.

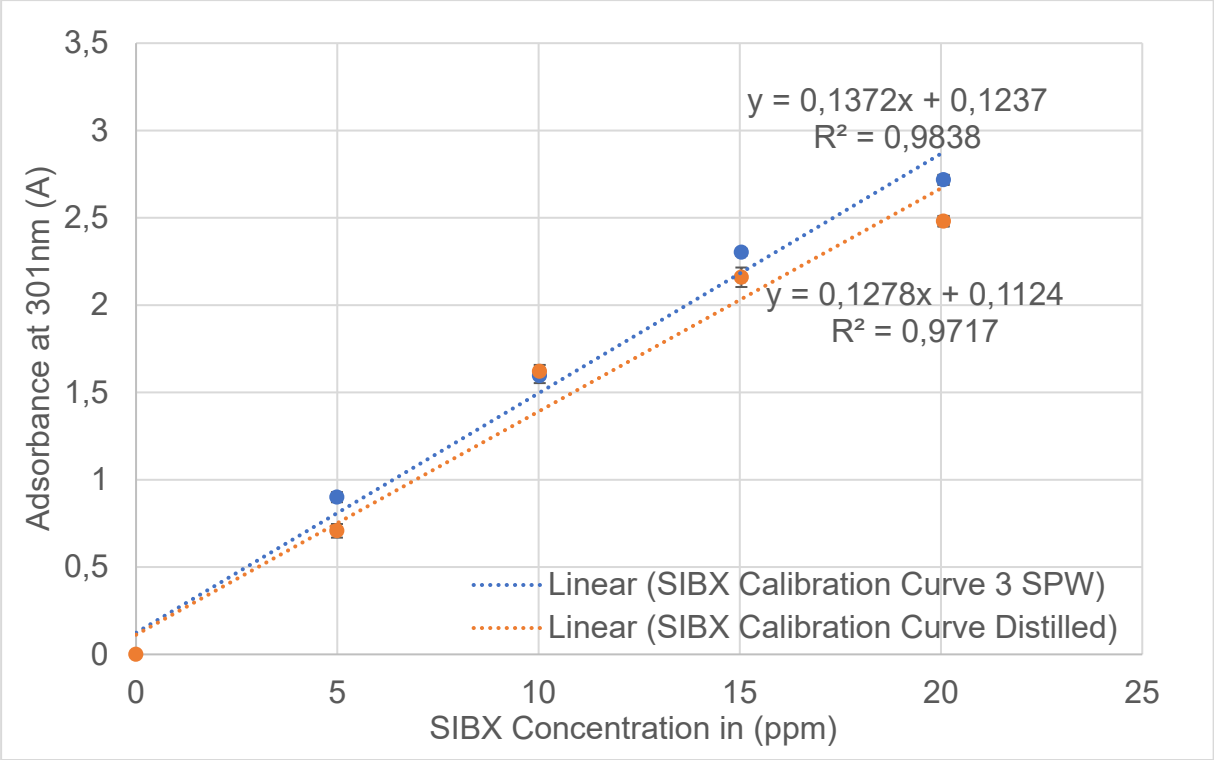

Fig 4-4. Absorbance of SIBX as a function of its concentration.

Residual depressant (CMC) in water samples was tested from the prepared samples in Section 4.13 using the Dubois method (Dubois et al., 1956) developed for the determination of the presence of reducing sugars through colorimetric treatment with phenol and sulfuric acid. The treated solution produces an orange yellow color sample with an absorbance peak at a wavelength of 490 nm. 1 mL of the tested sample pipetted using a P3000 Gilson air displacement pipette into a test tube. For both

samples, 1 mL of phenol solution prepared in Section 4.5.4 is added to a sample test tube followed by 5 mL of the sulfuric acid prepared in Section 4.5.5. A blank is also prepared from 3 SPW water, with the addition of 1mL sulfuric acid and 5 mL phenol in a separate test tube. The sample is allowed to stand for 10 min, then it is stirred for 40 min on a vortex stirrer. After the reaction time is complete, 3 mL of the sample was pipetted using a P5000 Gilson air displacement pipette into a transparent plastic cuvette with a capacity of 3.5 mL and a light path length of 10 mm. The sample absorbance was measured against a blank solution at 490 nm in a Biochrom Ltd. Ultrospec 2100 Pro Scanning, UV/Visible Spectrometer. To develop a relationship between the absorbance and concentration of CMC, a calibration curve of absorbance values of samples of known CMC concentrations was developed as shown in Fig 4-5. A linear regression of the plot produced an equation relating the absorbance to concentration which was utilized to estimate the concentration of CMC in the water sample from their measured absorbance.

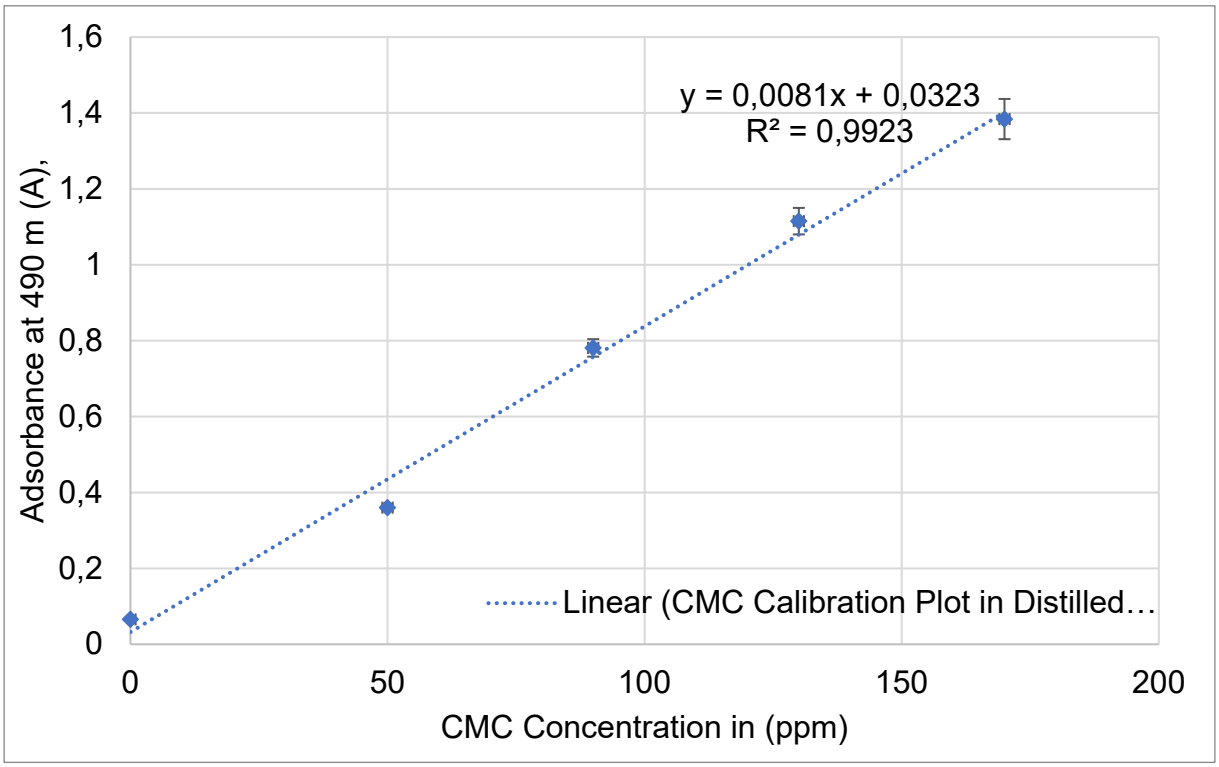

Fig 4-5. Absorbance of CMC as a function of its concentration.

The Reagent Efficiency (RE) was calculated based on the assumption that unused reagent was only present in the water as free reagent therefore the difference between Residual Reagent Concentration (RRC) in a sample and Reagent Feed Concentration (RFC) (which considers the RRC in the recycled water was used as a feed to the

process) could be termed as the reagent consumption, and its ratio to the RFC become the RE% as shown in Eq. (4-2).

$$RE_{(i)}\ (\%) = \frac{\left(RFC + RRC_{(i-1)}\right) - RRC_i}{RFC} \qquad \text{Eq. (4-2)}$$

4.7 Froth Stability

The effect of water re-circulation on froth stability was investigated using a stability column test rig shown in Fig 4-6. This was done to develop insights on the impact of recirculation on residual frother concentration and frothing ability. The procedure detailed was adapted from Sheni (2016). The Perspex column had a diameter of 10 cm and a height of 1 m. The airflow rate of the column was maintained at 7 L/min. A pore-2 frit was used to regulate the bubble size. The procedure was applied on the tailings pulp (3 phase) and recirculated water (2 phase) prepared in Section 4.13, which were pumped into the column through the bottom inlet to a height of 200 mm while the impeller is off. The inlet valve was closed. The agitator was switched on once the fluid had reached the level of the impeller and remained on until the end of the experiment. Air was sparged into the column and the rotameter was used to maintain the air flow rate. Each test was run recording the height of the froth at 10 seconds intervals until the equilibrium height (H_{max}) was achieved. These heights were measured from the ruler attached to the equipment. Once the froth stopped rising, the air was turned off and the slurry recovered.

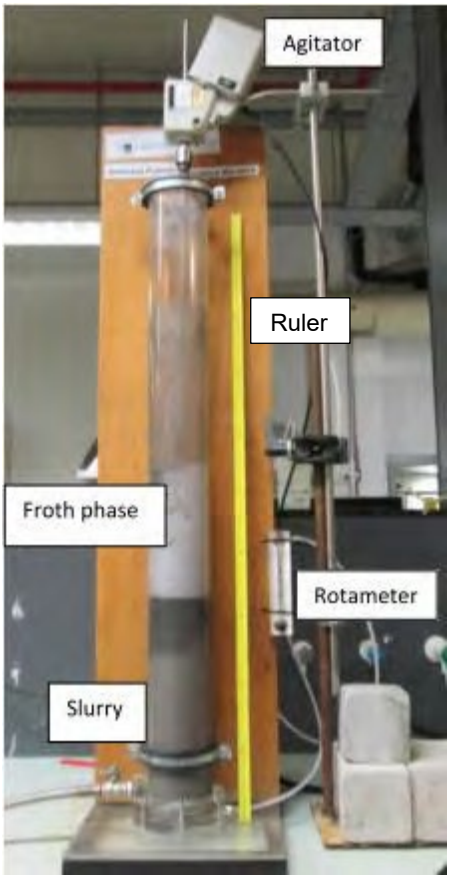

Fig 4-6. Stability column with an agitator, ruler, and rotameter. The in slurry and froth phases are indicated on the image adapted from (Sheni, 2016)

2 phase and 3 phase dynamic stability tests for the second phase of experiments were fit to a kinetic model relating the froth height, $H\ (t)$, to an exponential function of time (t) as shown in Eq. (4-3). The equilibrium maximum height (H_{max}) and the characteristic bubble lifetime (τ) are inferred from data obtained in the experiments as the model has been shown to be an excellent fit to experimental data and industrial scale date as shown in (Barbian et al., 2006, 2005b, 2003)

$$H(t) = H_{max}(1 - e^{-\frac{t}{\tau}}) \qquad \text{Eq. (4-3)}$$

A chi squared test was used to fit the model data and establish whether a relationship exists between the experimental variables under the null hypothesis that no relationship exists. A chi squared value (x^2) was calculated using Eq. (4-4) where the experimental value is (O_i) is subtracted from the predicted value is (E_i). A GRG non-linear solver minimizes the x^2 value by changing the R_∞ and k values. A P value is developed for (n (number of readings)-1) from a chi table for an alpha value of 0.05,

hence a 95 % confidence interval. Models with x^2 within the confidence interval were accepted and considered an adequate representation of the experimental values.

$$x^2 = \sum_{i=0}^{n} \frac{(O_i - E_i)^2}{E_i} \qquad \text{Eq. (4-4)}$$

4.8 Coagulation Tests

The project utilizes spectroscopy to investigate the settling rate of solids in the tailings, utilizing the methodology developed from Thierie (2018) who used a Short Wavelength Near Infrared light beam to investigate hindered settling of solids in wastewater. The project adopted the method and utilized a real time visible light spectrometer to monitor the change in absorbance over time to indicate the settling rate of the solid phase. Fig 4-7 shows the absorbance spectrum of air, distilled water and 3 SPW at wavelengths between 200 and 1000 nm. The maximum absorbance for 3 SPW water was achieved at 850 ± 1.63 nm wavelength, and this was chosen to be the operating wavelength for the coagulation tests.

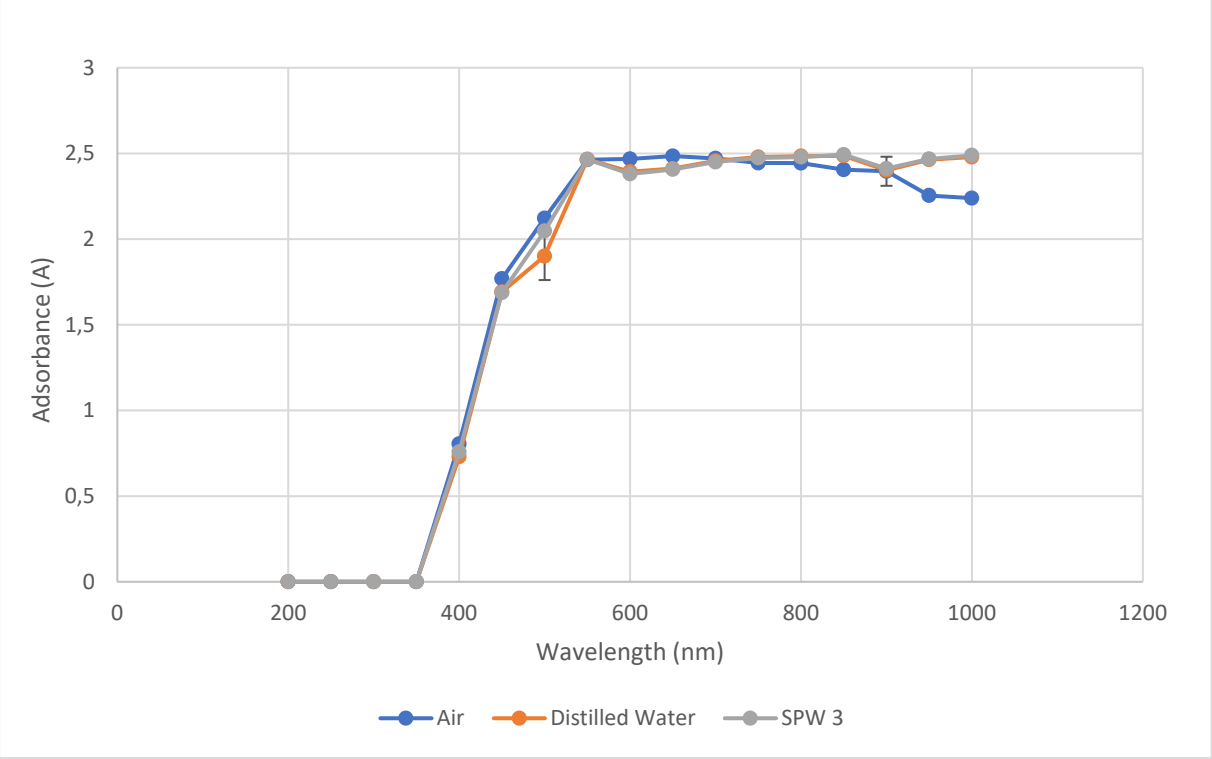

Fig 4-7. Absorbance spectrum of Air, Distilled Water and 3 SPW between 200 – 1000 nm at 50 nm intervals.

The settling time was determined immediately after each run to prevent the residual reagents present from reacting or interactions to occur that could impact the settling time. The impeller in the float cell was kept on while a sample was drained to ensure consistent pulp concentration in the sample. A tailing sample was tapped from the tailings outflow pipe. The sample was weighed. A P5000 Gilson air displacement pipette with a sliced tip was set to 3 ± 0.01 mL and used to extract and place the sample in a transparent plastic cuvette with 3.50 mL capacity and a light path of 10 mm. The UV / Vis spectrometer was set to 850 nm blanked with a 3 SPW sample. The sample was thoroughly shaken and placed in the spectrometer with a timer switched on simultaneously. The absorbance of the sample was recorded for two hours. Eq. (4-5) adapted from Thierie, (2018) was used to calculate transparency $(T(t)\%)$ of the sample as a function of time where A_b is the dark current obtained by cutting the power supply (i.e., maximum absorbance 2.500 A), A_o is the absorbance of the blank 3 SPW sample and A_m(t) is the absorbance of the sample at the measured time.

$$T(t)\% = \frac{A_b - A_{m(t)}}{A_b - A_o}\% \qquad \text{Eq. (4-5)}$$

$$T(t)\% = \frac{T_\infty^2 * k * t}{1 + T_\infty * k * t}\% \qquad \text{Eq. (4-6)}$$

Eq. (4-6) is a second order kinetic model of the transparency $(T(t)\%)$ where time is denoted as (t), with a maximum transparency (T_∞) and a transparency rate (k) as constants. The T_∞ and k were model fit to a second order kinetic model from using a chi squared test was used to establish whether a relationship exists between the experimental variables under the null hypothesis that no relationship exists. A chi squared value (x^2) was calculated using Eq. (4-7) where the experimental value is (O_i) is subtracted from the predicted value is (E_i). A GRG non-linear solver minimizes the x^2 value be changing the R_∞ and k values. A P value is developed for (n (number of readings)-1) from a chi table for an alpha value of 0.05, hence a 95 % confidence interval. Models with x^2 within the confidence interval were accepted and considered to be an adequate representation of the experimental values.

$$x^2 = \sum_{i=0}^{n} \frac{(O_i - E_i)^2}{E_i} \qquad \text{Eq. (4-7)}$$

4.9 Thermo Scientific Gallery Discrete Automated Photometric (Colorimetric) Analyzer (GDAPA)

The project also focused on monitoring the ionic species present in the water to be recycled using a Gallery Discrete Automated Photometric (Colorimetric) Analyzer (GDAPA). The ions chosen are ions that are of significant quantities in the ore body as indicated from the XRF analysis of the ore in Section 4.2 in Fig 4-3. GDAPAs have been used by water quality analysts and regulators to develop an understanding of complex water matrices. Primarily to monitor increased inputs of Total Dissolved Solids (TDS) and specific ions present in water resulting from; mining activities, wastewater effluent discharge, agricultural practice, irrigation runoff, and rising/brackish groundwater, estuarine water and nutrient cycling in hypersaline environments (Anning and Flynn, 2014; Cañedo-Argüelles et al., 2013; Corsi et al., 2015; Evans et al., 2014; Johnson et al., 2010; Kaushal et al., 2018, 2005; Naftz, 2017; Novotny et al., 2008; Schraga and Cloern, 2017; Stanton et al., 2017; Williams et al., 2000). GDAPAs are fast, flexible and precise for complex samples of variable matrixes, test parameter and low volume samples achieving a high throughput with minimal supervision (Rastetter et al., 2000; ThermoFisher Scientific, 2020, 2018a, 2018b, 2003). All analyses were performed on a Thermo Fisher Scientific Automated Gallery Discrete Colorimetric Analyzer. The instrument is calibrated using stock calibration samples stored on the analyzer as shown in Table 4-6 with reagent compositions that are all in compliance with the ISO 15923-1 standard.

Table 4-6. Analytes, reagents and reference standards for analytes sourced from (Rastetter et al., 2000; ThermoFisher Scientific, 2018a)

Product/ Analyte	Composition of System Reagent	Reference Standard
Chloride R1 (984264)	Methanol, iron (3) nitrate, mercury di-thiocyanate, nitric acid	ISO 15923-1 ISO 15682
Sulfate R1 (984648)	Barium chloride, hydrochloric acid, stabilizers	ISO 15923-1 SM4500 $SO4^{2}$-E
Magnesium R1 (984358)	Xylidyl blue I	Tietz Fundamentals of Clinical Chemistry, 5th Edition
Calcium R1 (984361)	Arsenazo III	Tietz Fundamentals of Clinical Chemistry, 5th Edition

Stetson et al., (2019) summarizes the operations in the analyser as follows; The incubator hub aligns the cuvette segment along the sample and reagent discharge paths. The cell segments are then aligned one after another with the dosing needle of the robot arm. The samples are then mixed using an ancillary stirrer and then returned to the washing station where the needle and stirrer blades are washed with deionized water. During the dosing process, the cuvette segment returns to the incubator, where a programmed reaction time of up to 3600 sec occurs. Reagent blanks are measured after the sample and its first reagent are combined and mixed. The incubation program finalizes in the photometric module. The modules sequentially measure the absorbance of chromophores in each cell of the cuvette segment. The absorbance of the reagent blanks is converted to concentrations from on-line calibration parameters using regression parameters. The parameters are sourced from the instrument's operating system database memory.

4.10 XRF Analysis of Solids Samples

The metal ion content in the concentrate, feed and tailings was determined using an Olympus Vanta Handheld-XRF Analyzer (Olympus, 2021). All solid samples were analyzed for their copper and nickel concentrations, which were utilized to develop the mass balance over the flotation cell. Appreciating that XRF analysis may not be perfectly accurate with regards to the mineralogy of the sample, the gangue mineral concentration was determined from the difference between the total valuable mineral and the total mass of the concentrates.

4.11 Ore Comminution

The 1.3 kg ore samples prepared in Section 4.2 were ground in a laboratory-scale stainless steel rod mill (10 L Eriez MACSALAB Rod Vessel Mill of Grade 304 driven by a double roller 120 mm diameter by 1200 mm length powered by a 0.37 kW 220 Volt Motor (Eriez Manufacturing Co., 2021) to 60% passing 75 µm at 66 % solid mass content by adding 681 $\pm$ 3 g of feed water (3 SPW or the recycled water). The Eriez stainless steel mill, milling media and dimensions are shown in Table 4-7. The ionic thiol collector described in Section 4.5.1 was added to the mill followed by the addition of 3 SPW plant water or recycled water as described in Section 4.4 and Section 4.13 respectively. Finally, the 1.3 kg ore samples prepared in Section 4.2 are added to the mill followed by the addition of the rods as described in the mill specifications summary in Table 4-7. The mill lid was placed on and screwed shut to prevent spillages. The mill was then placed on a double roller which was turned on at 62 rpm and a timer was started simultaneously. The mill was stopped after the milling time needed to achieve

the required grind size had lapsed, and the pulp was recovered and sieved through a 1 mm sieve and transferred to the float cell.

Table 4-7. Characteristics for the 10 L Stainless Steel Laboratory Scale Mill

Rods	**Diameter**	**Length**	**Number of Rods**
	25 mm	285 mm	6
	20 mm	285 mm	8
	16 mm	285 mm	6
Mill	**Internal Diameter**	**Internal Length**	**Rotation Speed**
	210 mm	295 mm	62 rpm
Calculated Milling Time	1317 sec		

The grind size chosen matched the rougher grind used in mining operations processing UG2 ores similar to the one used in this study. Milling was conducted for pre-determined time intervals of 5, 15, 21 and 25 min. The milling time targeting 60% passing 75 μm was derived from the milling curve in Fig 4-8 from the linearized equation fitted to the data points and was found to be 21 min and 57 sec (1317 sec). Wet screening was performed on the milled ore to determine the particle size distribution of the milled ore as shown in Fig 4-9. Screening showed that 62 % of the solids were below 75 μm.

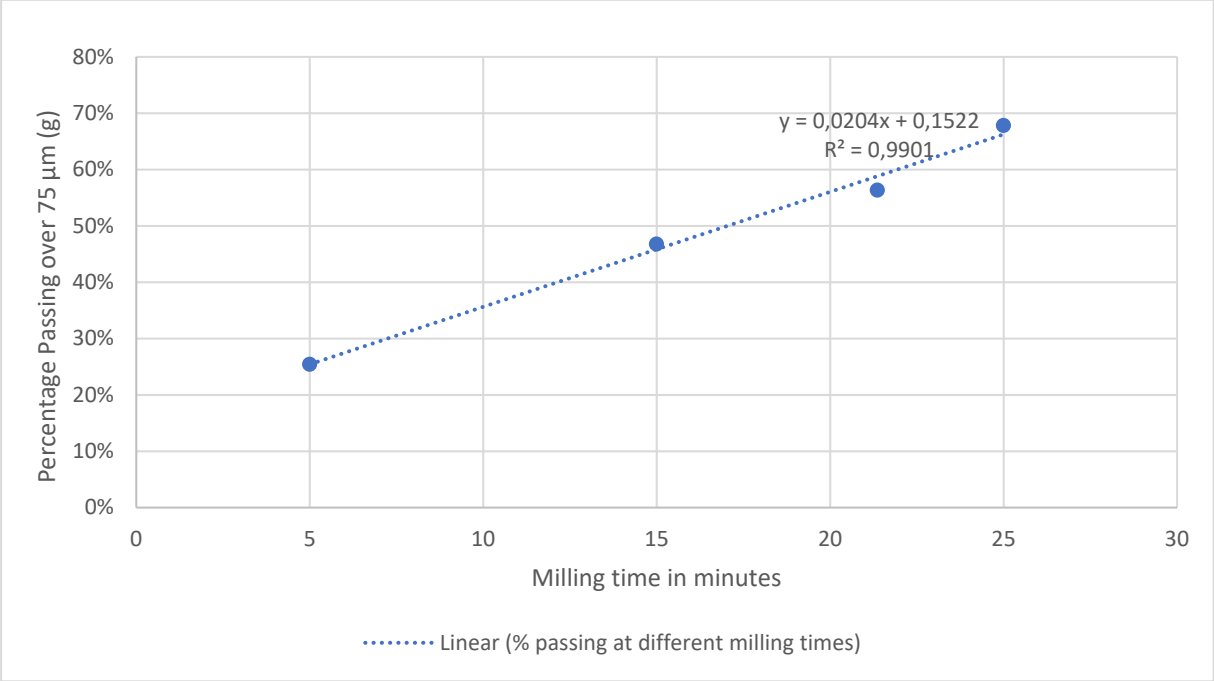

Fig 4-8. % Mass of UG-2 Ore passing a 75 µm screen size against the milling time of the sample.

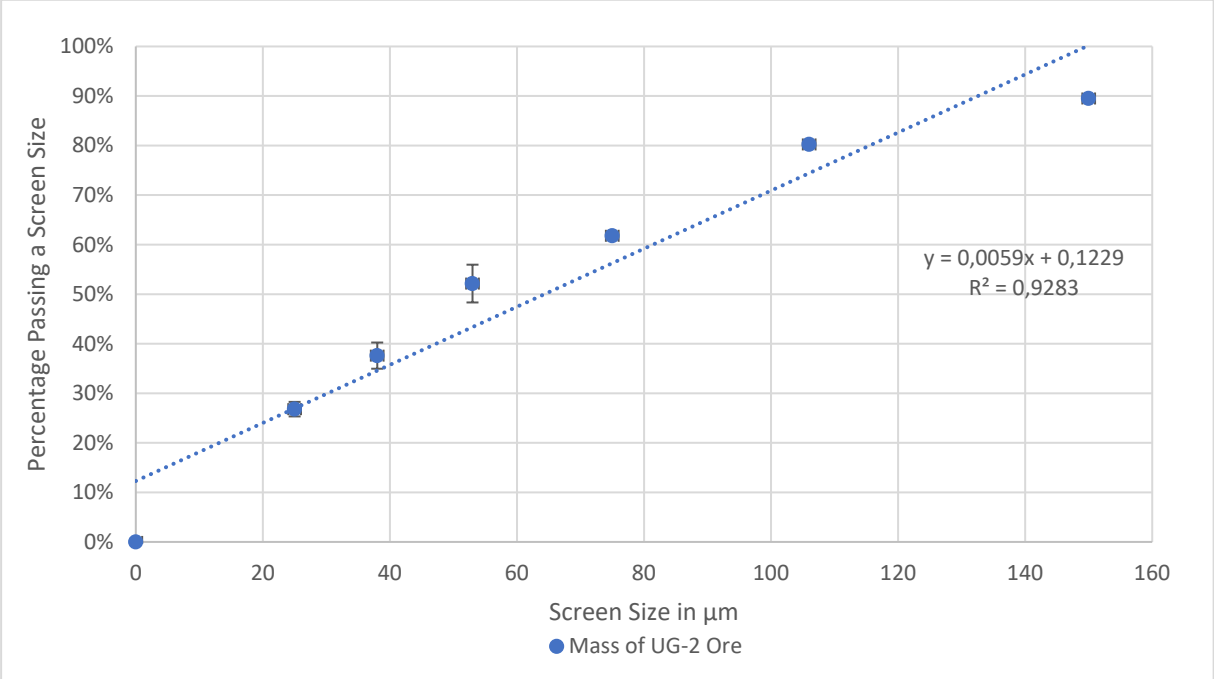

Fig 4-9.Cumulative Particle Size Distribution of Milled UG2 ore developed through wet screening.

4.12 Batch Flotation Test

The bench-scale flotation tests were conducted in a 3 L Barker laboratory batch flotation cell as seen in Fig 4-5 accompanied by the wash bottles and concentrate trays C1, C2, C3, and C4, top up water bottles 1 and 2 and volumetric flasks for reagent preparation. The flotation standard conditions and variables of the cell are shown in Table 4-8.

Fig 4-10. 3 L Barker Flotation Cell.

The milled slurry was transferred to a 3 L Barker flotation cell with a top-driven impeller, and a Wilkerson ¼ inch 0-8 bar air regulator to control the air flow rate. The impeller speed was set to 1200 rpm. The flotation cell containing the slurry was topped up to 3 L with the necessary water to achieve a pulp density of 33 % solids. A 40 mL feed sample was taken before the addition of the flotation reagents to the float cell using a syringe. The slurry was conditioned for 2 min with the CMC depressant, Depramin 267, at the required dosage followed by 1 minute with the polyglycol frother, DOW 200, at a dosage of 40 g/t prepared and handled as described in Sections 4.5.2 and 4.5.3, respectively. For the experiments with varying depressant dosage (0 g/t CMC, 100 g/t

CMC and 300 g/t CMC), freshly prepared 3 SPW was used, whereas for those experiments with simulated short water recirculation (to the mill or to the float cell), CMC depressant was dosed at a fixed dosage of 100 g/t with water recovered as prescribed in Section 4.13. After reagent conditioning, the air valve was opened and a constant airflow rate of 7 L/min was maintained for all tests. Four concentrates, denoted as C1 to C4, were collected through the scraping of the froth phase at 15 sec intervals, for 2, 4, 6 and 8 min respectively while maintaining a 2 cm froth height throughout by the manual addition of plant water at 3 SPW. Two 40 mL tailings samples were taken after the flotation process using a syringe. The general experimental sequence is summarized schematically in Fig 4-11 and the procedures are summarized in Table 4-8.

Table 4-8. Summary of the batch flotation procedure

Action	**Conditioning**	**Cumulative Time (min)**
Milling	As determined from the milling curve	As determined from milling curve
Collector	Added to the mill	Added to the mill
Depressants	2	0
Frother	1	2
Air fed	0	3
C1	2	5
C2	4	9
C3	6	15
C4	8	23

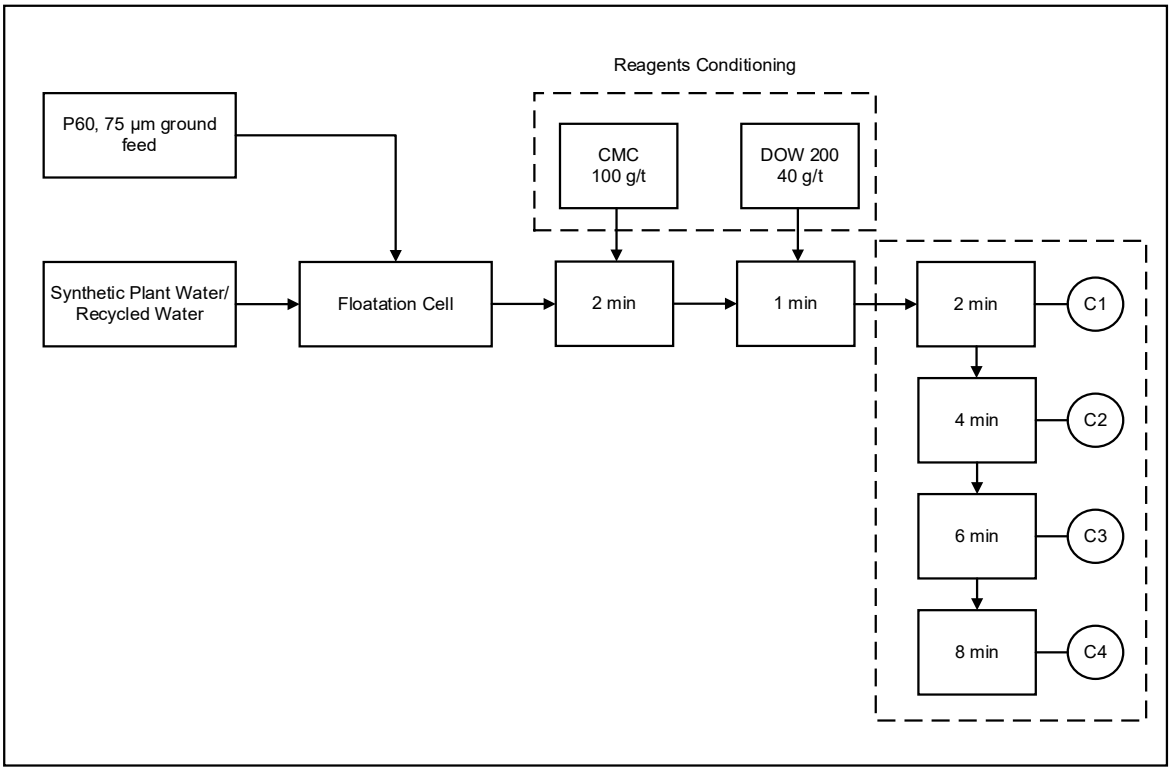

Fig 4-11. A summary of the experimental sequence adopted for the flotation of UG2 Ore

The water recovered with the feed, concentrates and tailings samples was measured and recorded. The feed sample, concentrates and tailings samples were filtered using a Buchner funnel. The solids were dried in an oven overnight and weighed before performing elemental analysis of ions present through XRF analysis as described in Section 4.10. The residual water from the concentrate samples was recovered from the Buchner flask. The tailings were filtered using a filter press through a filter paper. The tailing water was recovered from the water disposal pipe of the filter press to be used in the recirculation experiments as described in Section 4.13. A 40 mL sample of the tailings and concentrate water was syringed and filtered through a 0.45 µm polyvinylidene fluoride syringe filter and stored in a 50 mL sample vial. These samples were used for the chemical analyses to determine the ion concentration of selected ions present in the solution through GDACA as described in Sections 4.9. Water samples were analyzed for residual reagents and ion concentration using a spectrometer and a gallery discrete colorimetric analyzer.

No reagents were utilized for pH maintenance, however the pH over all the experiments was basic at 8.23 $\pm$ 0.03, typical of a low-grade Cu-Ni-PGM sulfide ore flotation (Dzingai et al., 2020). Entrainment (ε) is the non-selective recovery of both

valuable and gangue particles carried up by the flow of water and air into the concentrate (Napier-Munn and Wills, 2005). Water recovery has been associated with the degree of entrainment as it is the medium of froth stability and is related through Eq. (4-8) from (Subrahmanyam and Forssberg, 1988; Vos et al., 2014).

$$R_{gangue} = \varepsilon R_{water} \qquad \text{Eq. (4-8)}$$

Flotation kinetic models were developed based on a first order rate model adapted from Klimpel model as shown in Eq. (4-9) for rectangular distributions which adequately modes metallic ore flotation with low recoveries, similar to the ore used in this study (Dowling et al., 1985; Sahoo et al., 2020; Yuan et al., 1996). The model is given by:

$$R = R_{\infty}(1 - e^{-kt}) \qquad \text{Eq. (4-9)}$$

Where R is the accumulated recovery at time t, R_{∞} is the maximum (or equilibrium) recovery that might be reached at infinite time, and k is the first order rate constant (s^{-1}) determines the rate at which recovery attains equilibrium recovery value. For rate models against water recovery, k units are (g^{-1}) (Chaves and Ruiz, 2009). A chi squared test was used to fit the model data and establish whether a relationship exists between the experimental variables under the null hypothesis that no relationship exists. A chi squared value (x^2) was calculated using Eq (4-1) where the experimental value is (O_i) is subtracted from the predicted value is (E_i). A GRG non-linear solver minimizes the OBJ value by changing the R_{∞} and k values. A P value is developed for (n (number of readings)-1) from a chi table for an alpha value of 0.05, hence a 95 % confidence interval. Models with x^2 within the confidence interval were accepted and considered to well relate experimental values to the model.

$$x^2 = \sum_{i=0}^{n} \frac{(O_i - E_i)^2}{E_i} \qquad \text{Eq (4-1)}$$

4.13 Simulating Water Recirculation

When simulating short term recycle runs, following initial batch flotation, the tailings filtrate was recovered using a filter press and used as part of the feed water for subsequent flotation. The total volume of tailings water recovered and used in subsequent flotation was 2200 ± 34 g. There were two routes in which the water was

utilized. The first route is called mill recirculation (denoted by a prefix “M”), and as shown in Fig 4-12, and requires the recirculation of 681 ± 3 g of the tailings water being fed to the mill to be used as the process water for milling. The rest of the recirculated water, 1519 ± 34 g, was utilized in washing the mill and transferring the slurry to the float cell. An additional 438 ± 34 g of 3 SPW was used to top up the float cell to the 3 L mark (33 % pulp density). The second route is called float cell recirculation (denoted by a prefix “F”), and as shown in Fig 4-13, requires 681 ± 3 g of 3 SPW water to be fed to the mill to be used as process water for milling. Of the 2200 ± 34 g of recirculated water recovered, 1920 ± 34 g was then used to transfer the slurry to the float cell and the rest of the recirculated water, 280 ± 34 g, was used as top up water during the flotation experiment to its completion. The water recirculation procedure was repeated three times for both points of addition to create round 1, 2 and 3.

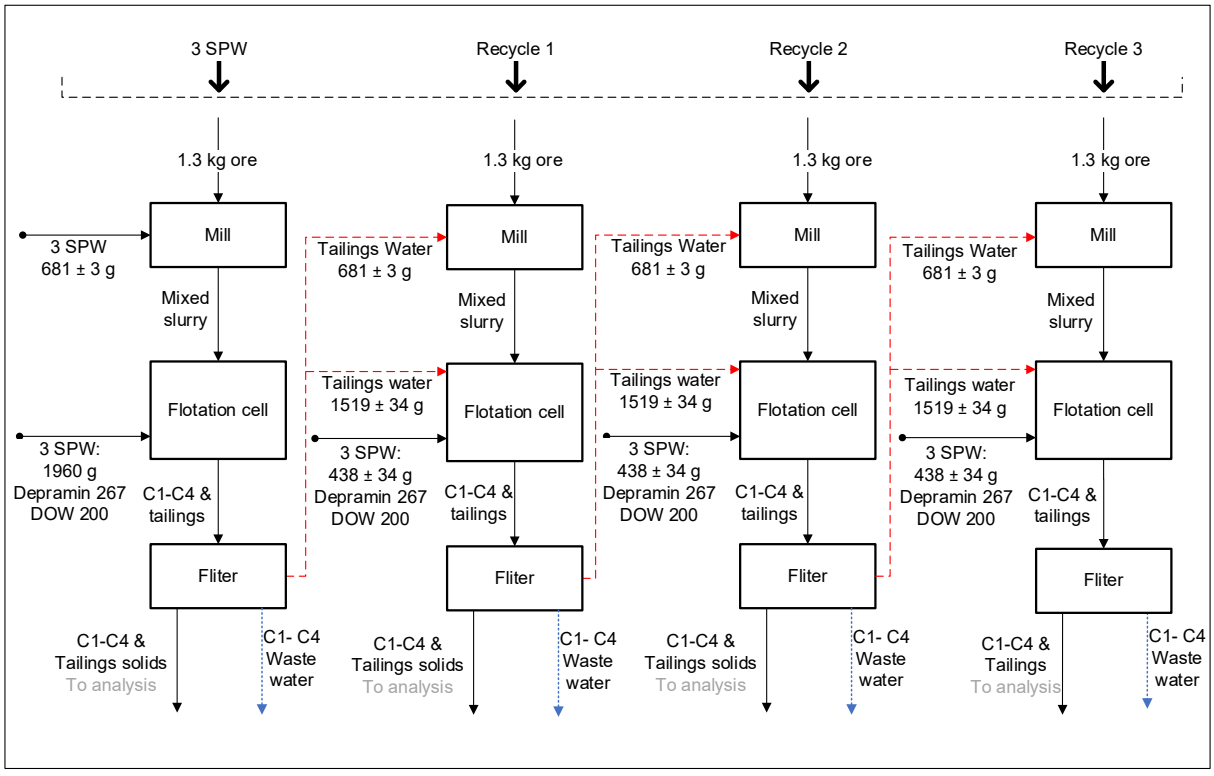

Fig 4-12. Simulation of the mill recirculation procedure.

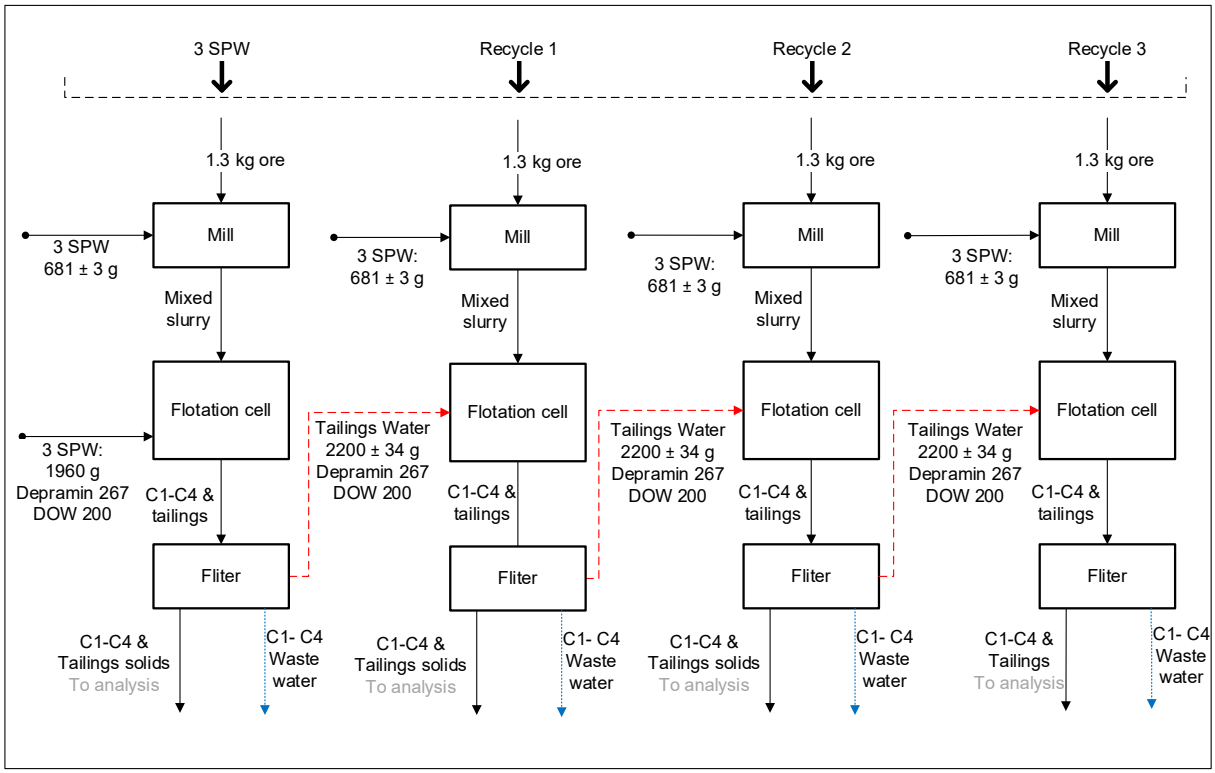

Fig 4-13. Simulation of the float cell recirculation procedure.

5 Results

5.1 Electrical Conductivity (EC), Total Dissolved Solids (TDS), Dissolved Oxygen (DO %) and Oxidative Redox Potential (ORP) Measurements in the Flotation Cell and for Recovered Water from the Tailings and Concentrates.

5.1.1 Electrical Conductivity (EC) Measurements.

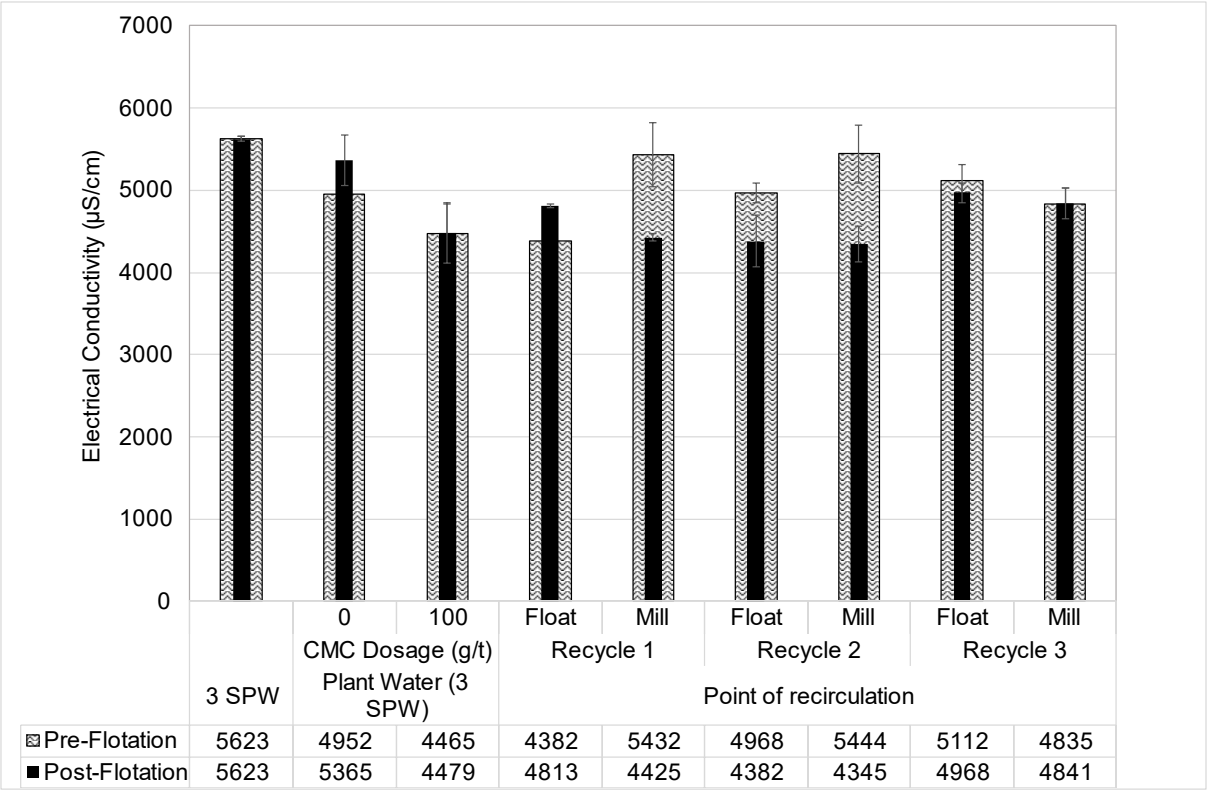

Fig 5-1. EC (µS/cm) measurements at the flotation cell before and after flotation from the second phase of the experiments.

Fig 5-1 shows the electrical conductivity (EC) measured at the start and end of the batch froth flotation tests for all the experiments conducted. Pre-flotation electrical conductivity measurements show the impact of milling on the electrical conductivity of the feed slurry. Post flotation shows the impact of froth flotation on the electrical conductivity of the tailing's slurry in the flotation cell. The electrical conductivity at the start of froth flotation is higher at 4950 µS/cm for the feed slurry at 0 g/t depressant dosage as compared to 100 g/t depressant dosage whose EC was at 4470 µS/cm. After flotation the electrical conductivity of the tailing's slurry is also higher at 5370 µS/cm for 0 g/t depressant dosage as compared to 100 g/t depressant dosage at 4480 µS/cm.

Comparing the electrical conductivity measurements for the second phase of experiments considers the impact of the point of addition of recycled water on the electrical conductivity of the mill product / feed slurry (pre-flotation). At the first recycle, recycling water through the mill produced a feed slurry at a higher EC, at 5430 µS/cm, as compared to recycling water through the float cell whose feed slurry was at 4380 µS/cm. At the second recycle, the feed slurry produced when recycling water through the mill a has a higher EC of 5440 µS/cm, as compared to when recycling water through the float cell, at a feed slurry EC of 4970 µS/cm. At the third recycle, the electrical conductivity of the feed slurry when recycling water to the mill was lower at an EC of 4835 µS/cm, as compared to 5112 µS/cm which was achieved with recycling to the float cell.

Finally, the EC measurements of the tailings pulp for the second phase of experiments were considered for the impact of the point of addition of recycled water on the electrical conductivity of the flotation product (post-flotation). At the first recycle, the tailings slurry had a slightly higher EC when recycling water through the float cell, at 4813 µS/cm, as compared to when recycling water through the mill, at 4425 µS/cm. At the second recycle, the tailings slurry had a higher EC when recycling water through the float cell, at 4382 µS/cm, as compared to when recycling water through the mill, at 4345 µS/cm. At the third recycle, the tailings slurry had a higher EC when recycling water through the float cell, at 4968 µS/cm, as compared to when recycling water through the mill, at 4841 µS/cm.

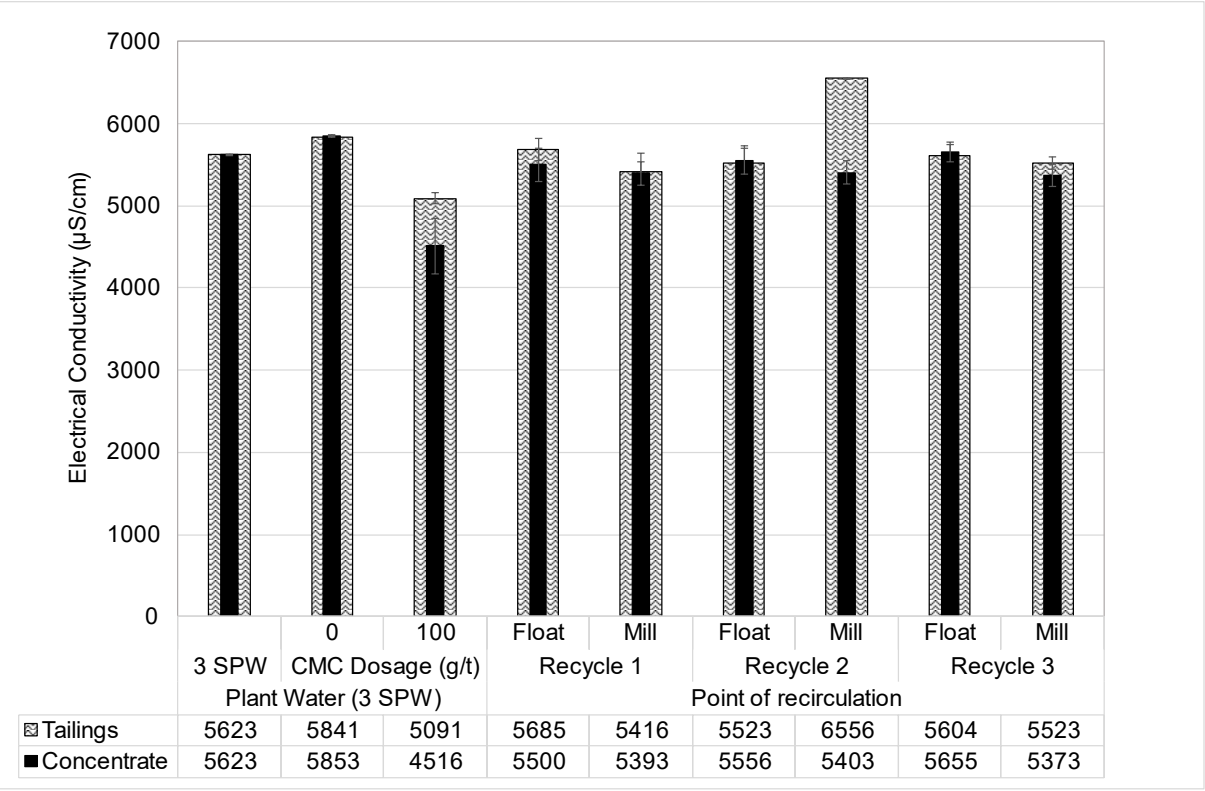

	3 SPW	0	100	Float	Mill	Float	Mill	Float	Mill
	Plant Water (3 SPW)	CMC Dosage (g/t)		Recycle 1		Recycle 2		Recycle 3	
				Point of recirculation					
Tailings	5623	5841	5091	5685	5416	5523	6556	5604	5523
Concentrate	5623	5853	4516	5500	5393	5556	5403	5655	5373

Fig 5-2. EC (µS/cm) measurements of recovered water from the Tailings (RWT) and recovered water from the Concentrates (RWC) from the second phase of the experiments.

Fig 5-2 shows the electrical conductivity (EC) of the recovered water from tailings and concentrates slurries post-flotation. For the tailing water produced at different depressant dosages, the tailings from flotation at 0 g/t depressant dosage had a higher EC, at 5840 µS/cm, as compared to the tailings water at 100 g/t depressant dosage with an EC of 5090 µS/cm. For the concentrate water produced at different depressant dosages, the tailings from flotation at 0 g/t depressant dosage had a higher EC, at 5850 µS/cm, as compared to the tailings water at 100 g/t depressant dosage, at 4520 µS/cm.

A comparison of the electrical conductivity of the tailing water produced in the second phase of experiments was performed. At the first recycle, the tailings water produced from froth flotation with recycled water fed to the float cell and the mill had an electrical conductivity, at 5690 and 5420 µS/cm, respectively, higher for float cell recirculation. At the second recycle, the tailings water produced from froth flotation with recycled water fed to the mill had a higher EC, at 6560 µS/cm, as compared to when recycling water through the float cell which produced a feed slurry at an EC of 5520 µS/cm. At the third recycle, the tailings water produced from froth flotation with recycled water fed

to the float cell had an EC of 5604 µS/cm compared to an EC of 5523 µS/cm for tailing water recirculated through the mill.

A comparison of the electrical conductivity of the concentrate water produced in the second phase of experiments was performed. At the first recycle, the concentrate water produced from froth flotation with recycled water fed to the mill had an EC of 5393 µS/cm which was lower than the EC of the from recirculation through the float cell whose EC was at 5500 µS/cm. At the second recycle, the concentrate water produced from froth flotation with recycled water fed to the mill had an EC of 5403 µS/cm which was lower than the EC of the concentrate water from recirculation through the float cell whose EC was at 5556 µS/cm. At the third recycle, the concentrate water produced from froth flotation with recycled water fed to the mill had an EC of 5373 µS/cm which was lower than the EC of the concentrate water from float cell recirculation whose EC was at 5655 µS/cm.

Overall, results Fig 5-2 showed that the EC was higher for both RWT and RWC from water recirculation through the float cell compared to the mill except for recycle 2 where it was seen that for RWT from water recirculation through the float cell resulted in a lower EC compared to the recirculation through the mill.

5.1.2 Total Dissolved Solids (TDS) Measurements.

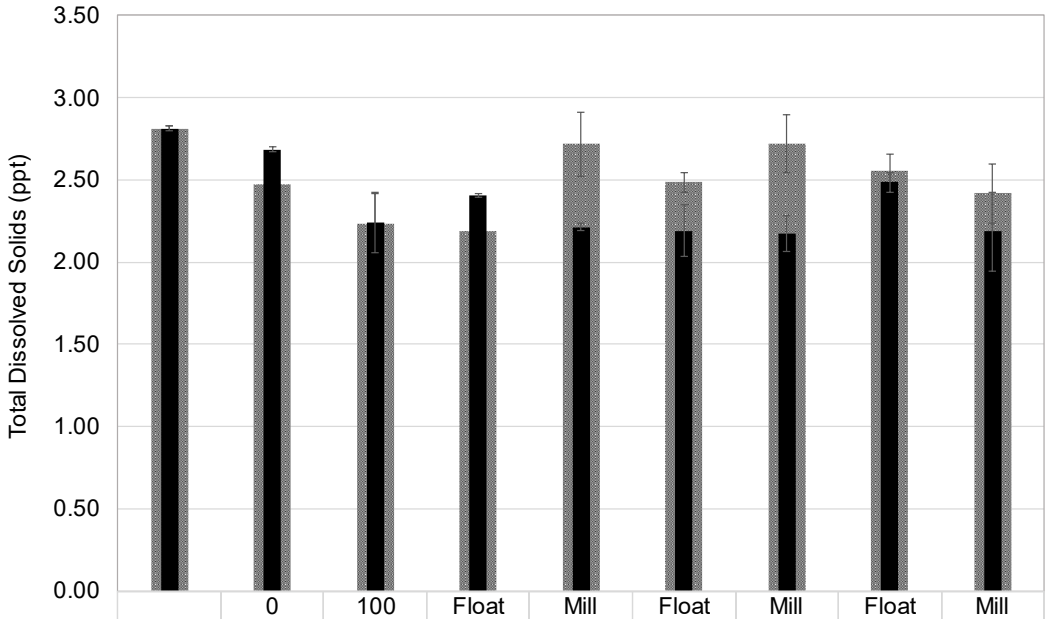

	3 SPW	0	100	Float	Mill	Float	Mill	Float	Mill
	Plant Water (3 SPW)	CMC Dosage (g/t)		Recycle 1		Recycle 2		Recycle 3	
				Point of recirculation					
Pre-Flotation	2.81	2.48	2.23	2.19	2.72	2.48	2.72	2.56	2.42
Post-Flotation	2.81	2.68	2.24	2.41	2.21	2.19	2.17	2.48	2.18

Fig 5-3. TDS (ppt) measurements at the flotation cell before and after flotation from the second phase of the experiments.

Fig 5-3 shows the total dissolved solids (TDS) measured at the start and end of the batch froth flotation test for all the second phase of experiments, as well as for the froth flotation tests conducted at different depressant dosages and for 3 SPW. Pre flotation total dissolved solids measurements show the impact of milling on the dissolved solids concentrations of the feed slurry. Post flotation shows the impact of froth flotation on the total dissolved solids of the tailing slurry in the flotation cell. The total dissolved solids at the start of froth flotation were higher at 0 g/t depressant dosage, at 2.48 ppt, as compared to 100 g/t depressant dosage, at a TDS of 2.23 ppt. After flotation the total dissolved solids of the tailing's slurry are higher at 0 g/t depressant dosages, at 2.68 ppt, as compared to the tailing slurry at 100 g/t depressant dosage with a TDS of 2.24 g/t.

Comparing the total dissolved solids measurements for the second phase of experiments considers the impact of the point of addition of recycled water on the total dissolved solids concentration of the mill product, i.e., pre-flotation.

At the first recycle, recycling water through the mill produced a feed slurry with a higher TDS at 2.73 ppt, as compared to recycling water through the float cell with a feed slurry at a TDS of 2.48 ppt. At the second recycle, recycling water through the mill produced a feed slurry at a higher TDS of 2.72 ppt, as compared to when recycling water through the float cell which produced a feed slurry with a TDS of 2.48 ppt. At the third recycle, recycling water through the mill produced a feed slurry with a lower TDS at 2.42 ppt, as compared to when recycling water through the float cell which produced a feed slurry at 2.56 ppt.

Finally, we compare the TDS of the tailings pulp for the second phase of experiments. At the first recycle, recycling water through the float cell has a tailings slurry with a higher TDS at 2.41 ppt, as compared to when recycling water through the mill which produced a tailing slurry at a TDS of 2.21 ppt. At the second recycle, TDS of the tailings water is slightly higher in float cell recirculation, at 2.19 ppt as compared to water recycling water through the mill, at a TDS of 2.17 ppt. At the third recycle, the TDS of the tailing's slurry is higher when recycling water through the float cell, at 2.48 ppt, as compared to recycling water to the mill which produced a tailing slurry at a TDS of 2.18 ppt.

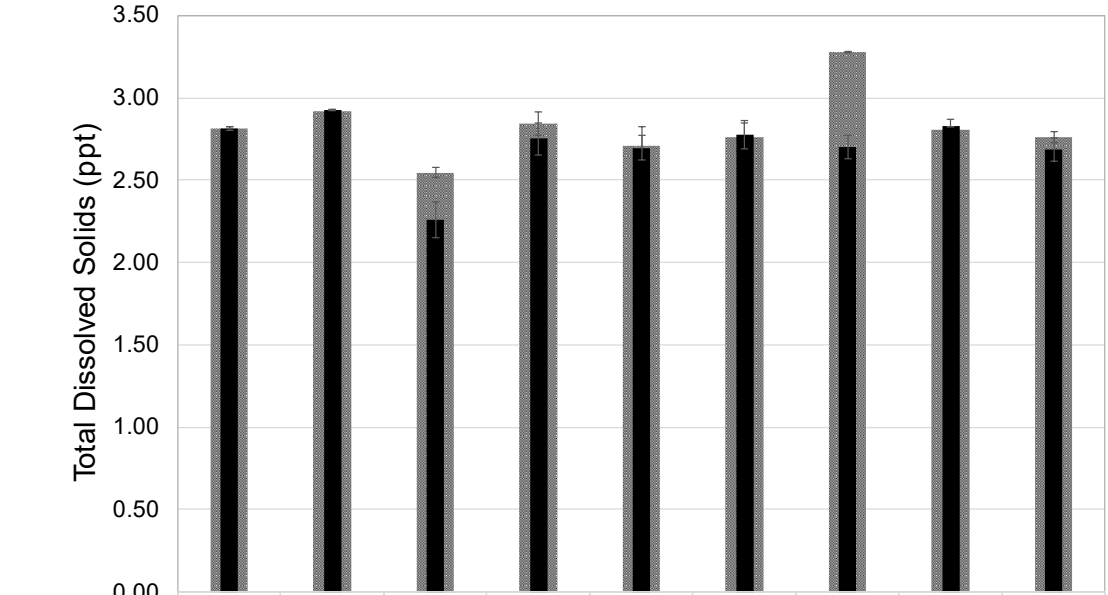

Tailings	2.81	2.92	2.55	2.84	2.71	2.76	3.28	2.80	2.76
Concentrate	2.81	2.93	2.26	2.75	2.70	2.78	2.70	2.83	2.69

Fig 5-4. TDS (ppt) measurements of recovered tailings (RWT) and concentrate (RWC) water from the second phase of the experiments.

Fig 5-4 shows the total dissolved solids (TDS) of the recovered tailings and concentrate water post froth flotation. For the tailing water (RWT) produced at different depressant dosages, the tailings from flotation at 0 g/t depressant dosage had a higher TDS, at 2.92 ppt, as compared to the tailings water at 100 g/t depressant dosage, at 2.55 ppt. The concentrate water (RWC) produced at different depressant dosages, the concentrate from flotation at 0 g/t depressant dosage had a higher TDS at 2.93 ppt, as compared to the concentrate water at 100 g/t depressant dosage, at 2.26 ppt.

A comparison of the TDS of the tailing water (RWT) produced in the second phase of experiments was performed. At the first recycle, the tailings water produced from froth flotation with recycled water fed to the mill has a lower TDS at 2.72 ppt as compared to 2.84 ppt for float cell recirculation tailing water. At the second recycle, the tailings water produced from froth flotation with recycled water fed to the mill resulted in a TDS at 3.30 ppt, which is higher when compared to tailings water produced recycling water through the float cell, at a TDS of 2.76 ppt. At the third recycle, the tailings water produced from froth flotation with recycled water fed to the mill resulted in a TDS, at 2.76 ppt, as compared to when recycling water through the float cell with a higher TDS, at 2.80 ppt.

A comparison of the total dissolved solids of the concentrate water (RWC) produced in the second phase of experiments was also performed. At the first recycle, the concentrate water produced from froth flotation with recycled water fed to the mill and has a lower TDS, at 2.70 ppt, as compared to recycling water through the float cell that produced a concentrate water product with a TDS of 2.75 ppt. At the second recycle, the concentrate water produced from froth flotation with recycled water fed to the mill had a lower TDS at 2.70 ppt as compared to RWC produced when water is recycled through the float cell at a TDS of 2.78 ppt. Finally at the third recycle, the concentrate water produced from froth flotation with recycled water fed to the mill has a lower TDS, at 2.69 ppt as compared to the product when water is recycled through the float cell at a TDS if 2.83 ppt.

5.1.3 Oxidative Redox Potential (ORP) Measurements.

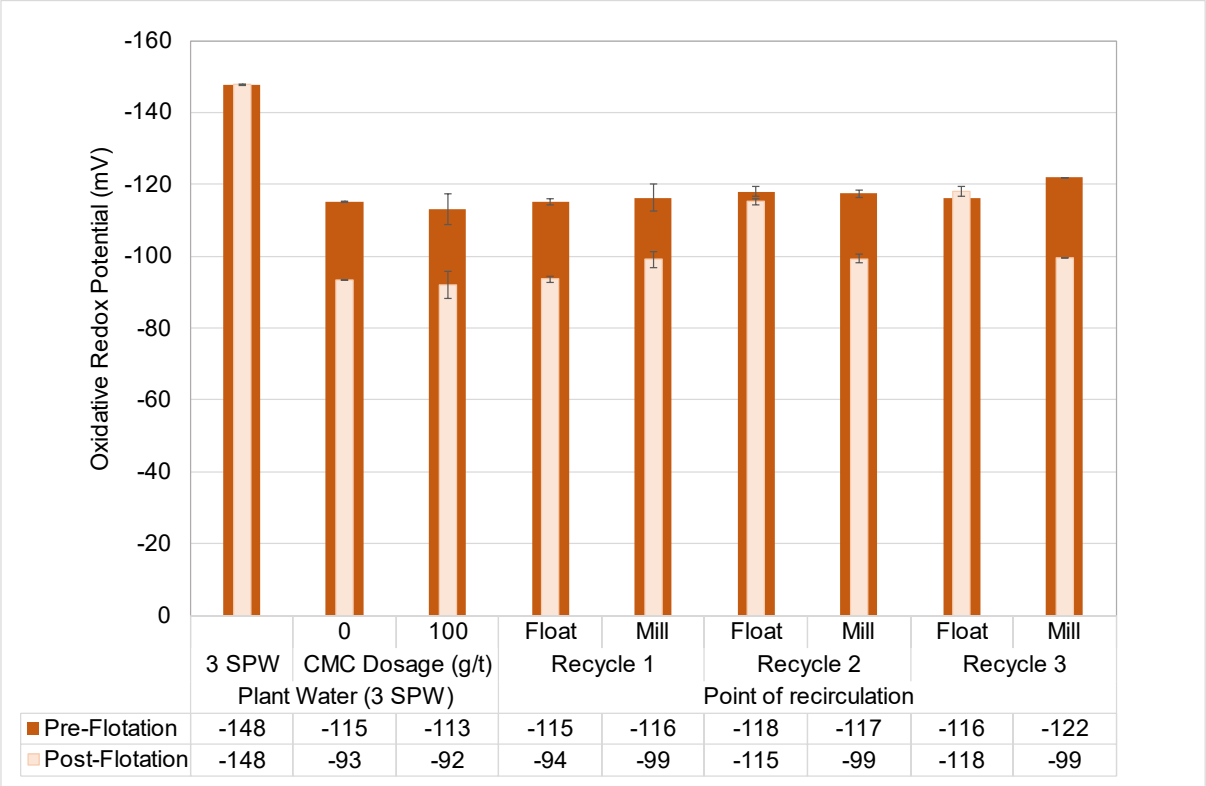

	3 SPW	0	100	Float	Mill	Float	Mill	Float	Mill
	Plant Water (3 SPW)	CMC Dosage (g/t)		Recycle 1		Recycle 2		Recycle 3	
				Point of recirculation					
Pre-Flotation	-148	-115	-113	-115	-116	-118	-117	-116	-122
Post-Flotation	-148	-93	-92	-94	-99	-115	-99	-118	-99

Fig 5-5. ORP (mV) measurements at the flotation cell before and after flotation from the second phase of the experiments.

Fig 5-5 shows the Oxidative Redox Potential (ORP) measured at the start and end of the batch froth flotation test for all the second phase of experiments, as well froth flotation tests at different depressant dosages and for 3 SPW. Pre-flotation oxidative redox potentials measurements showed the impact of milling on the feed slurry oxidative redox potential. Post flotation shows the impact of froth flotation on the oxidative redox potential of the tailing's slurry in the flotation cell. Oxidative redox potential at the start of and end of froth flotation are higher for the feed slurry and tailings slurry from flotation at0 g/t depressant dosages, at -115 mV and -93 mV for pre and post flotation as compared to at 100 g/t depressant dosages, whose pre and post flotation ORP are at -113 mV and -92 mV.

Comparing the oxidative redox potential measurements for the second phase of experiments considers the impact of the point of addition of recycled water on the oxidative redox potential of the mill product, i.e., pre-flotation. At the first recycle, recycling water through the mill had a higher oxidative redox potential in the feed slurry in the float cell, at -116 mV, as compared to recycling water through the float cell that

produced a float feed with at a redox potential of, -115 mV. At the second recycle, recycling water through the float cell had a higher ORP in the feed slurry in the float cell, at -118 mV, as compared to recycling water through the mill at a redox potential of, -117 mV. At the third recycle, recycling water through the mill had a higher ORP in the feed slurry in the float cell, at -122 mV, as compared to recycling water through the float cell at a redox potential of, -116 mV, respectively.

Finally, a comparison of the oxidative redox potential of the tailings pulp for the second phase of experiments was made. At the first recycle, recycling water through the mill had a higher ORP in the feed slurry, at -99 mV, as compared to recycling water through the float cell, at -94 mV. At the second recycle, recycling water through the float cell had a higher ORP in the feed slurry, at -115 mV, as compared to recycling water through the mill, at -99 mV. Finally, at the third recycle, recycling water through the float cell had a higher ORP in the feed slurry, at -118 mV, as compared to recycling water through the mill, at -99 mV.

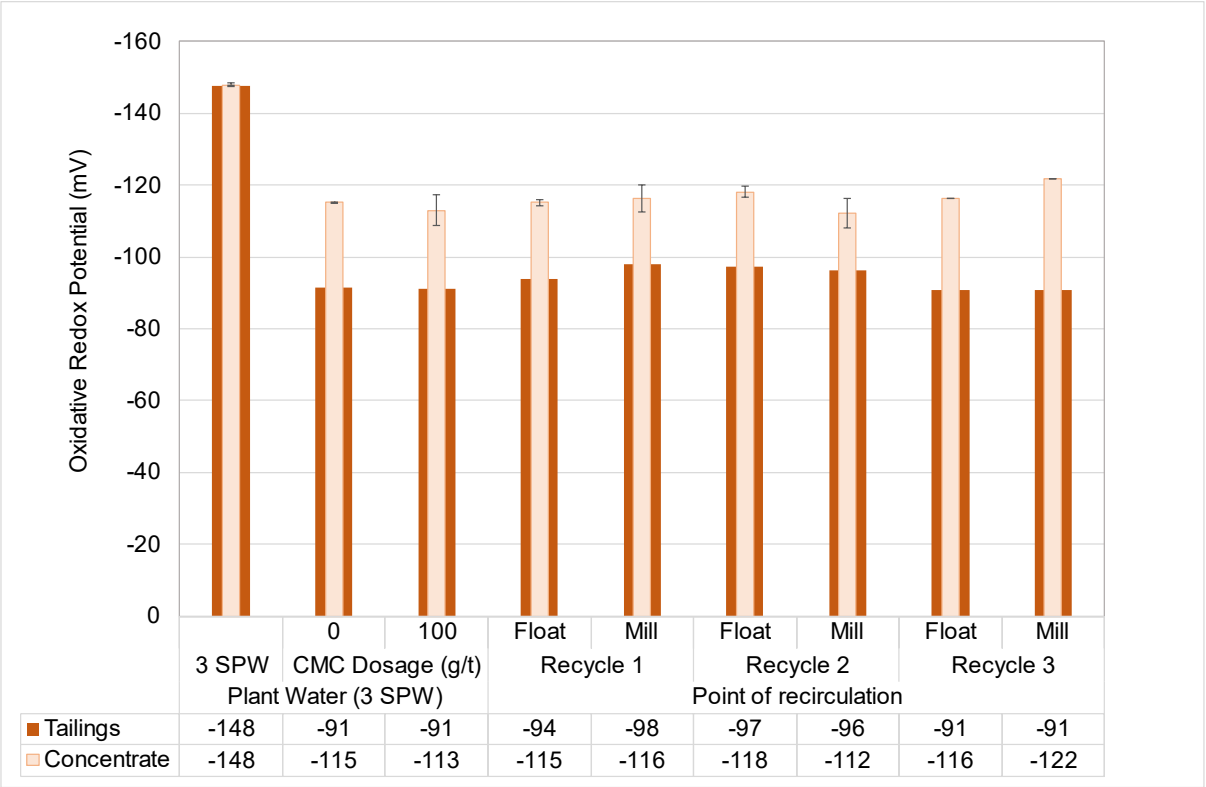

Fig 5-6. ORP (mV) of recovered water from tailings (RWT) and recovered water from concentrates (RWC) from the second phase of the experiments.

Fig 5-6 shows the Oxidative Redox Potential (ORP) of the recovered tailings and concentrate water post froth flotation. For the tailing water (RWT) produced at different depressant dosages, the tailings water from flotation at 0 and 100 g/t depressant dosages resulted in similar Oxidative Redox Potentials, at -91 mV. The concentrate water (RWC) produced at 0 g/t depressant dosages has higher ORP at -115 mV as compared to -113 mV produced at a depressant dosage of 100 g/t.

A comparison of the Oxidative Redox Potential of the tailing water (RWT) produced in the second phase of experiments was performed. At the first recycle, the tailings water produced from froth flotation with recycled water fed to the mill had a higher ORP at –98 mV as compared to the tailing water produced when recycling water through the float cell at an ORP at -94 mV. At the second recycle, the tailings water produced from froth flotation with recycled water fed to the float cell had a slightly higher ORP at – 97 mV as compared to the tailing water produced when recycling water through the mill at an ORP of -96 mV. At the third recycle, the tailings water produced from froth flotation with recycled water fed to the mill and the float cell had similar Oxidative Redox Potentials, at ≈ -91 mV.

A comparison of the total dissolved solids of the concentrate water (RWC) produced in the second phase of experiments was performed. At the first recycle, the concentrate water produced from froth flotation with recycled water fed to the float cell had a slightly higher ORP at –116 mV as compared to the concentrate water produced when recycling water through the mill at an ORP of -115 mV. At the second recycle, the concentrate water produced from froth flotation with recycled water fed to the float cell had a higher ORP, at -118 mV, as compared to mill recirculation RWC, at an ORP of -112 mV. At the third recycle, the concentrate water produced from froth flotation with recycled water fed to the mill had a higher ORP, at -122 mV, as compared to float cell recirculation RWC, at an ORP of -116 mV.

5.1.4 Dissolved Oxygen (DO%) Measurements.

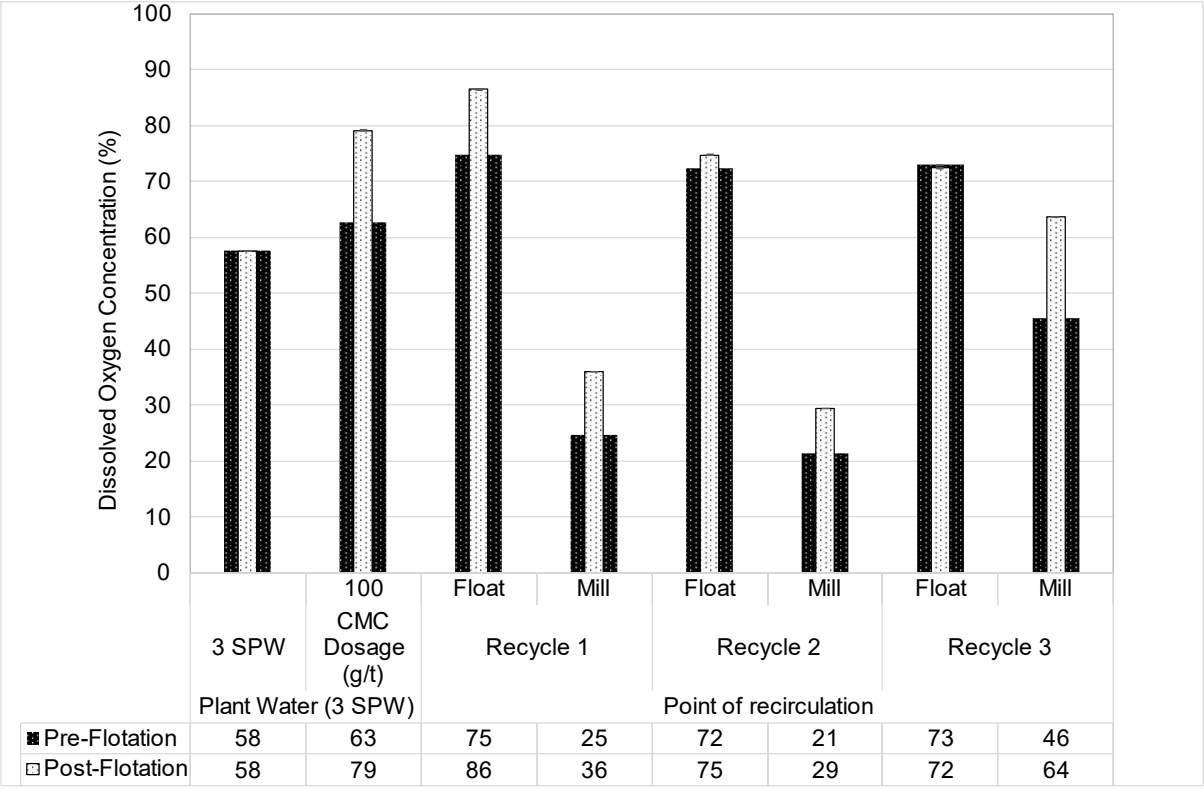

	3 SPW	100 CMC Dosage (g/t)	Float	Mill	Float	Mill	Float	Mill
	Plant Water (3 SPW)		Recycle 1		Recycle 2		Recycle 3	
			Point of recirculation					
Pre-Flotation	58	63	75	25	72	21	73	46
Post-Flotation	58	79	86	36	75	29	72	64

Fig 5-7. DO (%) measurements at the flotation cell before and after flotation from the second phase of the experiments.

Fig 5-7 shows the dissolved oxygen concentration (%) measured at the start and end of the batch froth flotation test for all the second phase of experiments, as well froth flotation at different depressant dosages and for 3 SPW. Pre-flotation dissolved oxygen measurements show the impact of milling with recycled water on the dissolved oxygen concentration. Post flotation shows the impact of froth flotation on the total dissolved oxygen concentration in the tailing's slurry in the flotation cell.

A comparison of the dissolved oxygen concentration in the feed slurry from the second phase of experiments was performed. At the first recycle, recycling water through the float cell had a produced a float feed with a DO %, at 75 %, as compared to when recycling water through the mill with a float feed DO% at 25 %. At the second recycle, recycling water through the float cell had a produced a float feed with a DO %, at 72 %, as compared to when recycling water through the mill with a float feed at DO % at 21 %. At the third recycle, recycling water through the float cell had produced a float feed with a DO %, at 73 %, as compared to when recycling water through the mill with a float feed at DO % at 46 %.

Finally, comparing the DO % of the tailings pulp for the second phase of experiments; at the first recycle, recycling water through the float cell resulted in a DO % of 86 %, as compared to when recycling water through the mill, at a DO % of 36 %. At the second recycle recycling water through the float cell had a dissolved oxygen concentration, at 75 %, as compared to when recycling water through the mill, at a DO % of 29 %. At the third recycle, recycling water through the float cell had a dissolved oxygen concentration, at 72 %, as compared to when recycling water through the mill, at DO % at 64 %.

5.2 Concentration of Selected Anions and Cations in Tailings Water.

Table 5-1. Concentration (mg/L) of dissolved Ca^{2+}, Mg^{2+} SO_4^{2-} and Cl^- present in tailings water recovered post flotation in phase 2 of the experimental program.

	3 SPW	Recycle 0	Recycle 1		Recycle 2		Recycle 3	
			Mill	Float	Mill	Float	Mill	Float
Ca^{2+}	240	240 ± 3	237 ± 6	248 ± 1	234 ± 6	254 ± 2	241 ± 6	258 ± 6
Mg^{2+}	212	207 ± 3	207 ± 12	242 ± 7	193 ± 1	198 ± 3	164 ± 12	191 ± 12
SO_4^{2-}	719	792 ± 10	708 ± 14	804 ± 57	740 ± 9	805 ± 17	783 ± 14	813 ± 14
Cl^-	861	1247 ± 127	1057 ± 15	999 ± 120	1032 ± 12	1027 ± 128	1054 ± 15	1021 ± 15

Table 5-1 illustrates the concentration of magnesium (Mg^{2+}), calcium (Ca^{2+}), sulfate (SO_4^{2-}), and chloride (Cl^-) in the tailings water recovered after filtering tailings pulp prepared in Section 4.13 from Phase 2 of the experimental program. The gallery discrete colorimetric analyser provides concentrations of ions in the tailings water in mg/L from the water samples described in Section 4.9. The concentrations of cations in the tailings water from flotation under baseline conditions (Recycle 0) were at 240 mg/L and 207 mg/L for Ca^{2+} and Mg^{2+} respectively, which were close to the concentration of these ions in feed water (3 SPW) shown in Table 5-1, thus this method could be deemed appropriate in estimating approximate cation concentration in the tailings water. The tailings water from the first recycle (Recycle 1) had Ca^{2+} concentrations higher when recycling water through the float, at 248 mg/L, than when recycling water through the mill, at 237 mg/L. The tailings water from the second recycles (Recycle 2) Ca^{2+} concentrations were higher when recycling water through the float cell, at 254 mg/L, than when recycling water through the mill, at 234 mg/L. Finally, the tailings water from the third recycle (Recycle 3) had higher Ca^{2+} concentrations when water was recycled through the float, at 258 mg/L, than when recycling water through the mill, at 241 mg/L. A consistent trend for Ca^{2+} was that for a particular recirculation, the concentration was similar in all the tailings samples.

Tailings water samples were also compared based on their Mg^{2+} concentrations. Tailings water from the first recycles (Recycle 1) consisted of Mg^{2+} concentrations that were higher when recycling through the float cell, at 242 mg/L, than when recycling through the mill, at 208 mg/L. The tailings water from the second recycle (Recycle 2) had Mg^{2+} concentrations higher when recycling through the float cell, at 198 mg/L, than when recycling through the mill, at 193 mg/L. Finally, the tailings water from the third recycles Mg^{2+} concentrations were higher when recycling through the float cell, at 191 mg/L, than when recycling through the mill, at 164 mg/L. Overall, the concentration of Ca^{2+} and Mg^{2+} in tailings water was higher in float cell recirculation than in mill recirculation. Also of note, all the Ca^{2+} in mill recirculation were close to the ion's concentrations in the feed water (3 SPW). Mg^{2+} in the tailings in mill recirculation, and float recirculation, with exemption of the first recycle through the float cell, were lower than Mg^{2+} concentration in the feed water (3 SPW).

Table 5-1 shows the concentrations of anions in the tailings water, sulfate (SO_4^{2-}) and chloride (Cl^-), concentrations in the tailings water recovered after filtering tailing pulp prepared in Section 4.13 from Phase 2 of the experimental program. The tailings water concentrations in the tailings water from flotation under baseline conditions (Recycle 0) were at 792 mg/L and 1250 mg/L, for SO_4^{2-} and Cl^- respectively, which were slightly higher than the concentration of these ions in 3 SPW as shown in Table 5-1. The tailings water from the first recirculation had SO_4^{2-} concentrations higher when water was recycled through the float cell, at 804 mg/L, compared to recycling water through the mill, at 708 mg/L. The tailings water from the second recycle (recycle 2) had SO_4^{2-} concentrations higher when recycling water through the float cell, at 805 mg/L than when recycling water through the mill, at 740 mg/L. Finally, the tailings water from the third recycle had SO_4^{2-} concentrations higher in float cell recirculation, at 813 mg/L than in mill recirculation, at 783 mg/L. SO_4^{2-} concentrations are higher in float cell recirculation as compared to mill recirculation overall.

The tailings water from the first recirculation had Cl^- concentrations higher when water was recycled through the mill, at 1057 mg/L, compared to recycling water through the float cell, at 999 mg/L. The tailings water from the second recycle (recycle 2) had Cl^- concentrations higher when recycling water through the mill, at 1032 mg/L than when recycling water through the float cell, at 1027 mg/L. Finally, the tailings water from the third recycle had Cl^- concentrations higher in mill recirculation, at 1054 mg/L than in float cell recirculation, at 1021 mg/L. Cl^- concentrations are higher in mill recirculation as compared to float cell recirculation overall.

5.3 Concentration of Residual Reagents in Water Recovered from the Tailings and Concentrates and Overall Reagent Efficiency.

Calibration curves developed for the collector and depressant in the reagent suite and absorbance of the samples in the second phase of experiments were utilized to find the concentration of reagents present as shown in Section 4.6 and Fig 4-4 and for SIBX and CMC respectively.

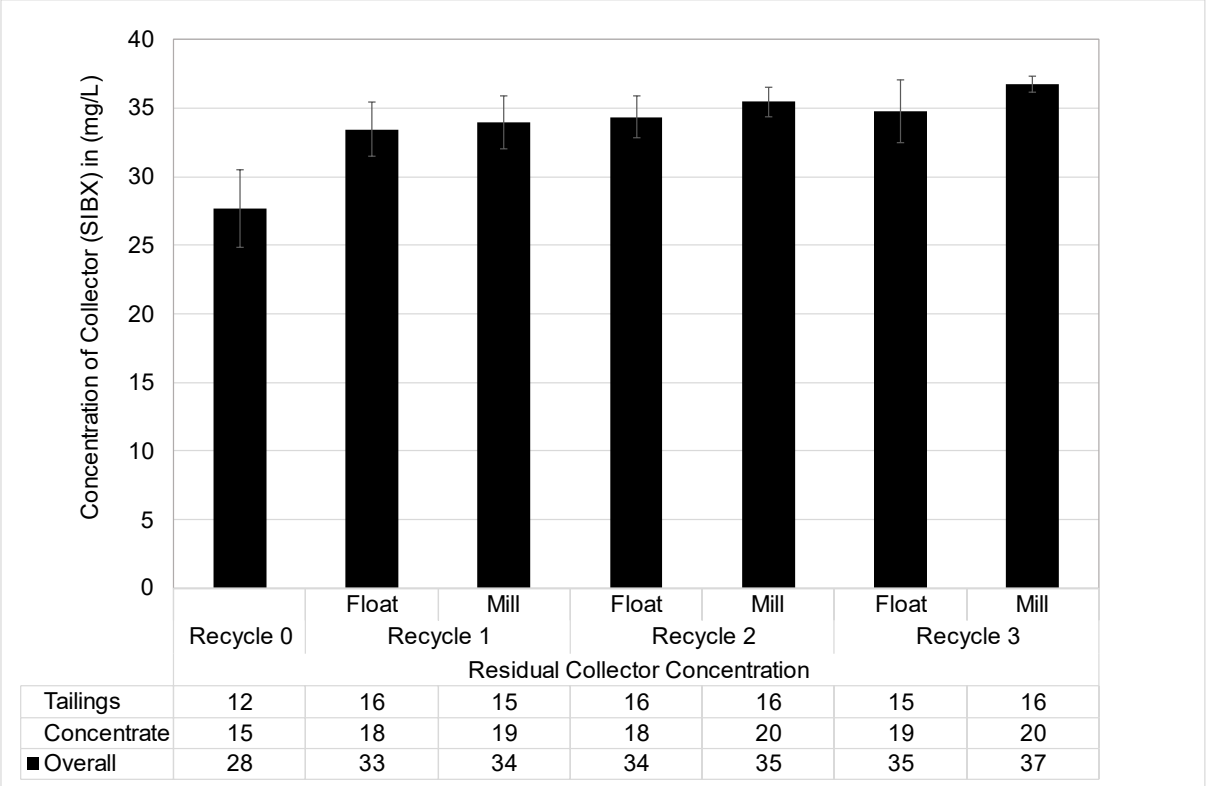

Tailings	12	16	15	16	16	15	16
Concentrate	15	18	19	18	20	19	20
Overall	28	33	34	34	35	35	37

Fig 5-8. Bar graph showing the overall concentration of Sodium Iso-Butyl Xanthate (collector) present in the recovered tailings and concentrate water, as well as the concentration in each sample, from all the tests in the second phase of experiments.

Fig 5-8 shows the overall concentration of Sodium Iso-Butyl Xanthate present in the recovered tailings and concentrate water, as well as the concentration in each sample, from all the tests in the second phase of experiments. The base line float had 28 mg/L of residual collector and was the lowest residual collector concentration in all of the tested conditions. At the first recycle, the overall concentration of collector in the flotation product (tailings and concentrate) was lower for the product of float cell recirculation, at 33 mg/L, at a concentration of 16 and 18 mg/L in the tailings and concentrate water respectively, as compared to the product of the mill recirculation, at 34 mg/L, at a concentration of 15 and 19 mg/L in the tailings and concentrate water respectively. At the second recycle, the overall concentration of collector in the flotation

product was also lower for the product of float cell recirculation, at 34 mg/L, at a concentration of 16 and 18 mg/L in the tailings and concentrate water respectively, as compared to the product of the mill recirculation, at 35 mg/L, at a concentration of 16 and 20 mg/L in the tailings and concentrate water respectively. At the third recycle, the overall concentration of collector in the flotation product was lower for the product of float cell recirculation, at 35 mg/L, at a concentration of 15 and 19 mg/L in the tailings and concentrate water respectively, as compared to the product of the mill recirculation, at 37 mg/L, at a concentration of 16 and 20 mg/L in the tailings and concentrate water respectively.

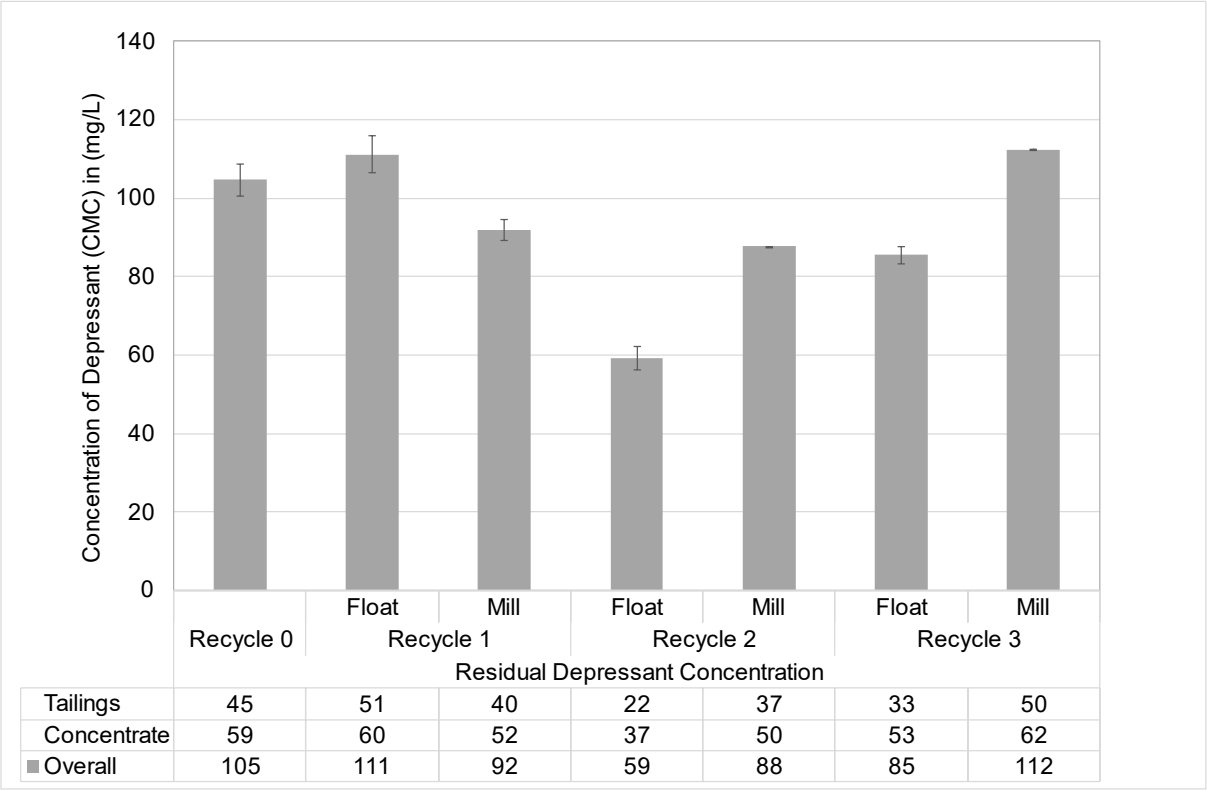

Tailings	45	51	40	22	37	33	50
Concentrate	59	60	52	37	50	53	62
Overall	105	111	92	59	88	85	112

Fig 5-9. Bar graph showing the overall concentration of Carboxyl Methyl Cellulose (depressant) present in the recovered tailings and concentrate water, as well as the concentration in each sample, from all the tests in the second phase of experiments.

Fig 5-9 shows the overall concentration of Carboxyl Methyl Cellulose present in the recovered tailings and concentrate water, as well as the concentration in each sample, from all the tests in the second phase of experiments. The base line float has 105 mg/L of residual depressant. At the first recycle, the overall concentration of collector in the flotation product (tailings and concentrate) was higher in float cell recirculation, by 19 mg/L overall, and 8 mg/L and 11 mg/L in the tailings and concentrate water respectively, as compared to mill recirculation, at an overall concentration of 92 mg/L,

20 mg/L and 52 mg/L in the tailings and concentrate water, respectively. At the second recycle, the overall concentration of collector in the flotation product (tailings and concentrate) was higher in mill recirculation, by 29 mg/L overall and at 8 mg/L and 15 mg/L in the tailings and concentrate water respectively, as compared to float cell recirculation, at an overall concentration of 59 mg/L with 22 mg/L and 37 mg/L in the tailings and concentrate water, respectively. Finally at the third recycle, the overall concentration of collector in the flotation product (tailings and concentrate) was higher in mill recirculation, by 27 mg/L overall, 7 mg/L and 9 mg/L in the tailings and concentrate respectively, as compared to float cell recirculation, at an overall concentration of 85 mg/L, 33 mg/L and 53 mg/L in the tailings and concentrate water, respectively.

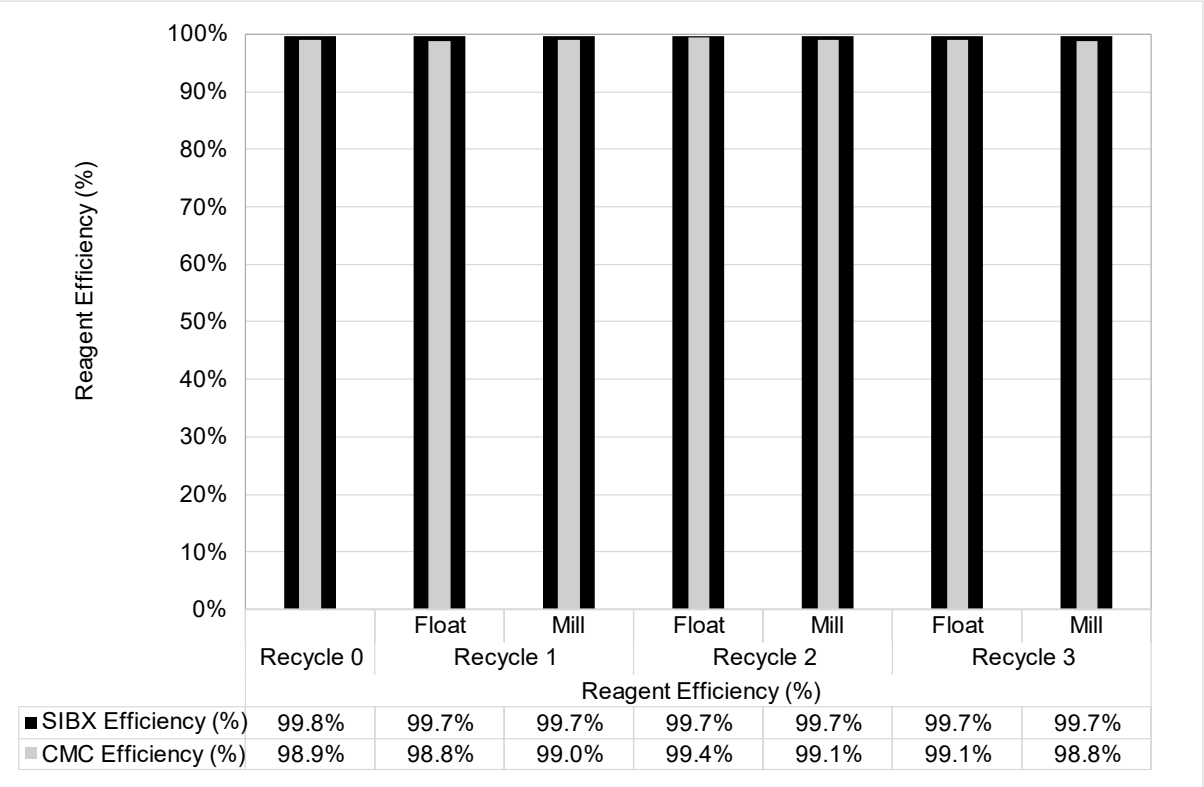

Fig 5-10 Bar graph showing the overall reagent efficiency for the collector and depressant for the all the tests in the second phase of experiments.

Fig 5-10 shows the overall reagent efficiency for the collector and depressant for all the tests in the second phase of experiments. The overall reagent efficiency for both reagents is high and similar at 99.7 % and 99 % for collector and depressant respectively, for all the baseline and all recycle conditions, irrespective of the point of addition. Consecutive recirculation led to a slight increase in the quantity of residual collector present in the flotation product, at 1 mg/L per recycle, therefore the residual

collector is consumed as if not, the concentration would be increasing by about 26 mg/l. Overall, concentrate product contains higher concentrations of residual reagents.

5.4 Settling Rate of Solids in Tailings.

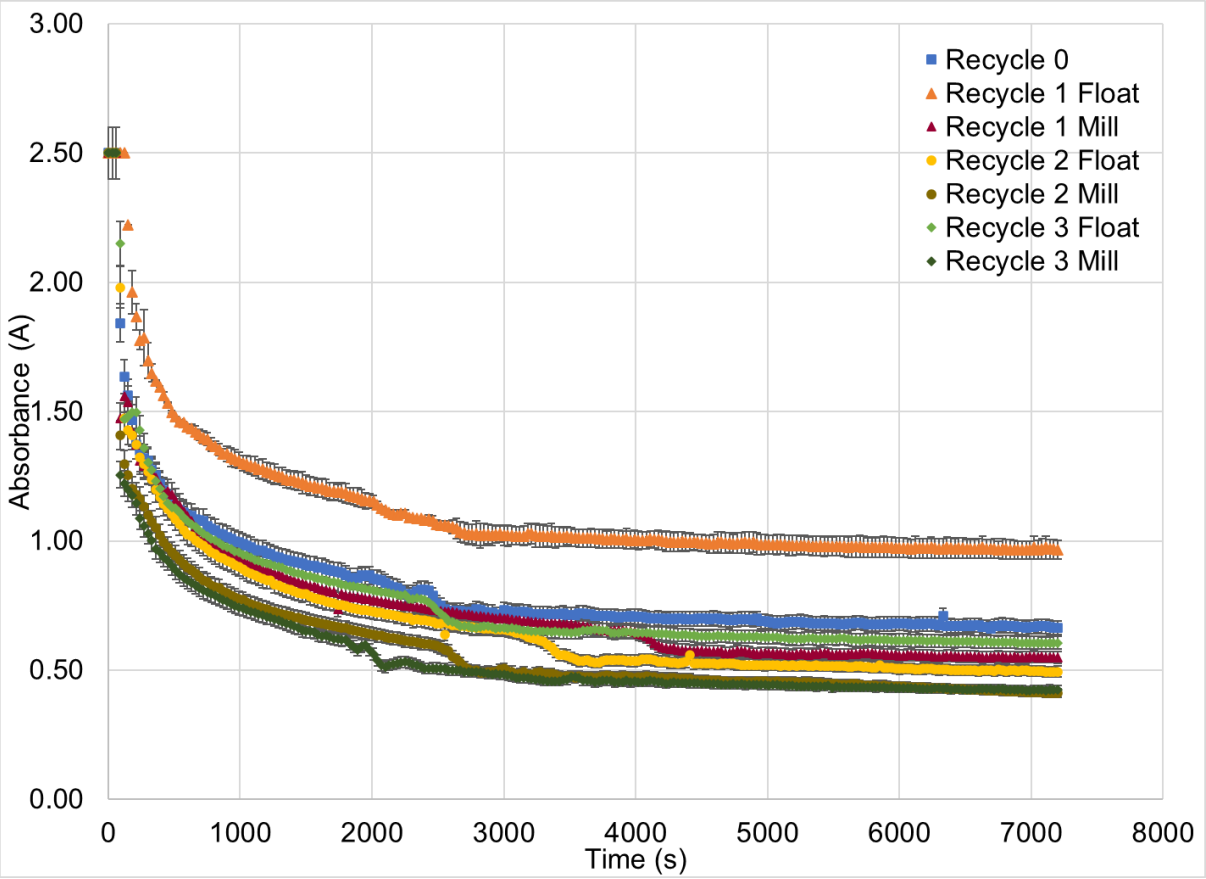

Fig 5-11. Absorbance (A) of 3 mL tailings water sample as a function of time (s) for all tested conditions in the second phase of experiments.

Fig 5-11 displays the Absorbance (A) of 3 mL tailings water samples measured in a spectrometer as a function of time (s) for all the second phase of experiments. It is assumed that the concentration of solids is similar in all samples and represents the solids fraction present in the flotation cell. All samples displayed a maximum absorbance at the start of the experiments. Majority of the settling occurred in the first 3000 s (≈ 1 hour), with a rapid decrease in absorbance in the first 500 s, followed by a steady decrease in absorbance between 500 and 3000 s. The minimum absorbance value achieved at the maximum test time, 7200 s, differed in each sample, with the lowest absorbance in Recycle 2 and 3 in Mill recirculation, followed by Recycle 2 Float Cell, Recycle 1 Mill, Recycle 3 Float Cell, Recycle 0 and Recycle 1 Float Cell, in that order.

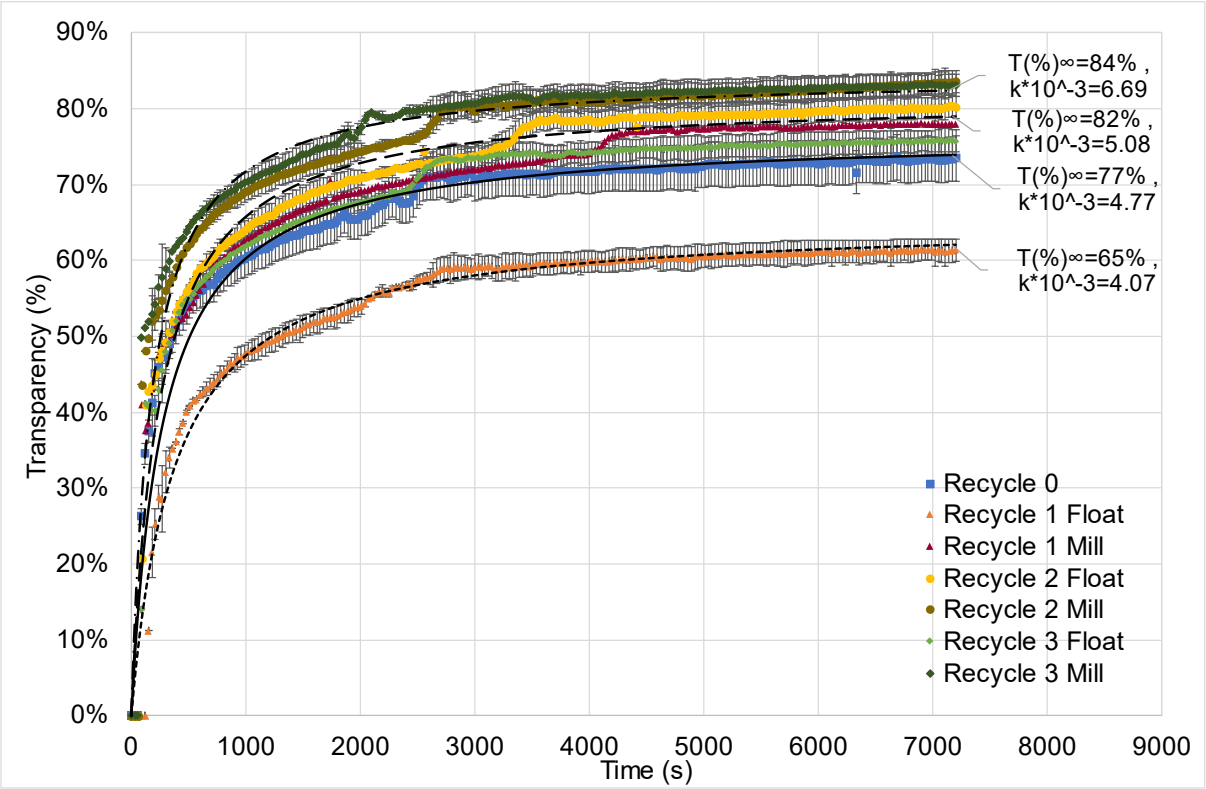

Fig 5-12. Second order kinetic models fitted to the sample transparency T (%) as a function of time (t) for the second phase of experiments.

Fig 5-12 shows second order kinetic models fit to the transparency T (%) of the tailing samples across all the tests for the second phase of experiments as a function of time. The first 500 s are marked by a rapid increase in transparency, the transparency was 50 % in most samples excluding Recycle 1 when recycling to the float cell that had a transparency of 40 %. From 500 to 3000 s, the transparency improved moderately from 50 % to between 70 and 80 % for all recirculated conditions, except Recycle 1 in float cell recirculation which increased to 60 %. Second order kinetic models developed four distinct models, all with different T_∞, with a spread of 20 %, and k, with a spread of 2.7*10^{-3} s^{-1}. The lower model achieved a theoretical maximum transparency T (%) at 65 % at a rate of 4.07*10^{-3} s^{-1} and best fits Recycle 1 in float cell recirculation. The third upper model achieved a theoretical maximum transparency T (%) at 77 % at a rate of 4.77*10^{-3} s^{-1},and well fits Recycle 0 and Recycle 3 in float cell recirculation. The second upper model achieved a theoretical maximum transparency T (%) at 82 % at a rate of 5.08*10^{-3} s^{-1}, and was a good model fit for Recycle 2 in float cell recirculation and recycle 1 in Mill recirculation. Finally, the first model achieved a theoretical maximum transparency T (%) at 82 % at a rate of 6.69*10^{-3} s^{-1} and was a good model fit for Recycle 2 and 3 in Mill recirculation. Overall recycled water, except for Recycle 1 in float cell recirculation, achieved maximum transparency at a higher transparency rate

in recycled water as compared to Recycle 0. Overall, recycling water through the mill achieved higher maximum transparency T (%) at a higher transparency rate compared to recycling through the mill.

5.5 Froth and Foam Responses in Varying Depressant Concentration and Water Quality.

All the values in this section are model fit values calculated as described in 4.7, and were chi tested for a P value of 0.05, hence have a 95 % confidence interval, motivating that the models display the relationship between froth height and time. This section covers the froth stability parameters developed from 2 and 3 phase foam and froth dynamic stability tests as described in Section 4.7.

5.5.1 3-Phase Dynamic Froth Stability

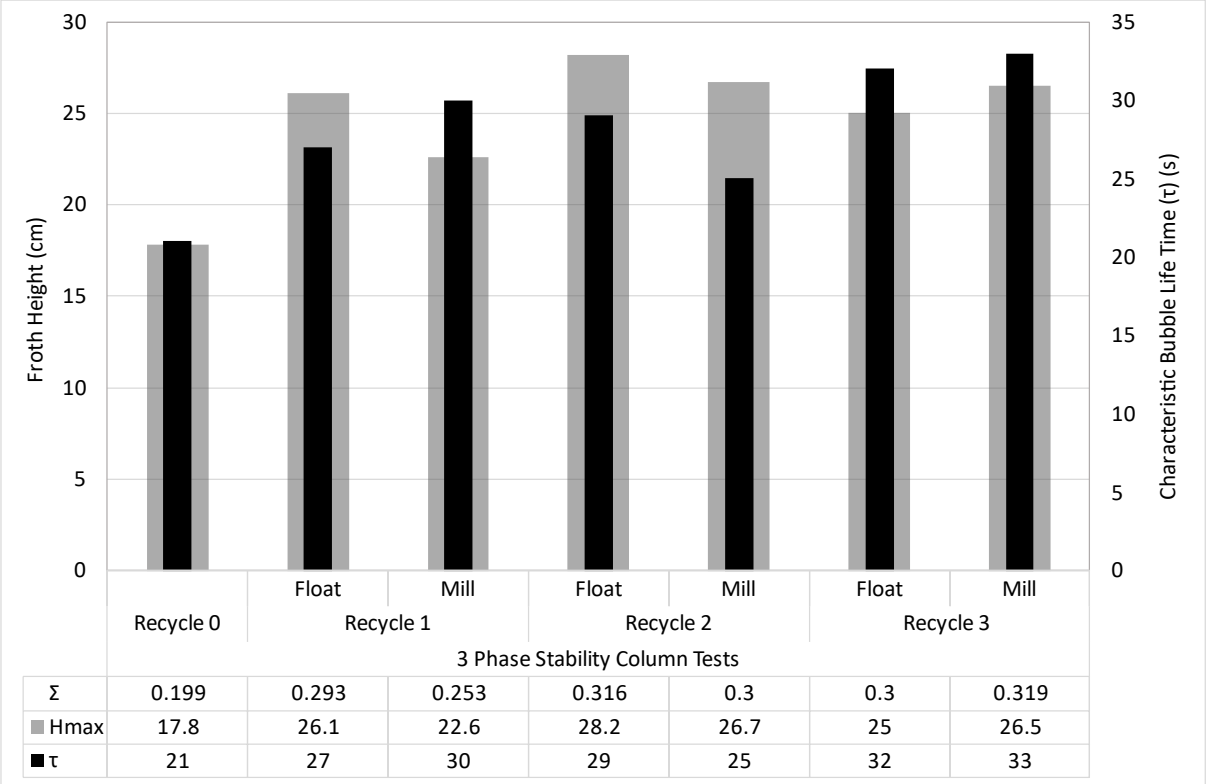

Σ	0.199	0.293	0.253	0.316	0.3	0.3	0.319
Hmax	17.8	26.1	22.6	28.2	26.7	25	26.5
τ	21	27	30	29	25	32	33

Fig 5-13. Equilibrium froth height (H_{max}), Characteristic Bubble Lifetime (τ) and dynamic froth stability factor (∑) developed form kinetic models of three phase dynamic tests of tailings slurry for the second phase of experiments.

Fig 5-13 shows the equilibrium froth height (H_{max}) and characteristic bubble lifetime (τ) develop from froth stability kinetic model Eq. (4-3) as bar and tabulated values, and dynamic froth stability factor (∑) tabulated for the 3 phase tests of the tailing's samples

in the second phase of experiments. Dynamic tests of the tailing's samples form the second phase of experiments is a direct measure of the froth stability (Liu et al., 2013). Comparing the stability parameters developed for the second phase of experiments can be utilized to deduce the influence of changing water quality on froth stability. Tailings from Recycle 0 (baseline float) achieved an equilibrium froth height of 18 cm, with a characteristic bubble lifetime of 21 s and a froth stability factor of 0.2. The tailings from the first recycle through the float cell achieved a higher equilibrium froth height by 4 cm, at a froth height of 26 cm, compared to the tailings of the first recycle to the mill. The tailings for Recycle 1 through the mill have a shorter characteristic bubble lifetime by 3 s, at a bubble lifetime of 30 s, compared to the tailings of the first recycle to the float cell. The froth stability factor (∑) of the tailings from the first recycle through the float cell had a higher froth stability factor, at 0.29, as compared to the tailings from the first recycle through the mill at 0.25. Overall, the higher equilibrium froth height and hence froth stability factor show that the froth was more stable in recycle 1 in the float cell recirculation compared to mill recirculation.

The tailings from the second recycle through the float cell achieved a higher equilibrium froth height at 28 cm for float cell recirculation as compared to mill recirculation at a froth height of 27 cm. The characteristic bubble lifetime between the two points of addition was higher when water was recycled through the float cell by 4 s, at a bubble lifetime of 29 s, compared to the tailings of the first recycle to the mill. The froth stability factor (∑) of the tailings from the first recycle through the float cell had a higher froth stability factor, at 0.32, as compared to the tailings from the first recycle through the mill at 0.30. Overall, the higher froth height, and longer bubble lifetime, hence less bursting, show that the froth was more stable in Recycle 2 in float cell recirculation compared to mill recirculation.

The tailings from the third recycle through the float cell achieved a higher equilibrium froth height at 27 cm for mill recirculation as compared to float cell recirculation at a froth height of 25 cm. The bubble lifetime between the two points of addition was also higher in mill recirculation at 33 s as compared to float cell recirculation at 32 s. The froth stability (∑) of the tailings from the third recycle through the mill had a higher froth stability, at 0.32, as compared the tailings from the first recycle through the float cell at 0.30. Overall, the similar equilibrium froth height and hence froth stability and the similar bubble lifetime, hence less bursting, between the two points of additions, show that the froth stabilities at the third recycle were similar, if not slightly higher in mill recirculation, however, would achieve a maximum froth height faster in float recirculation.

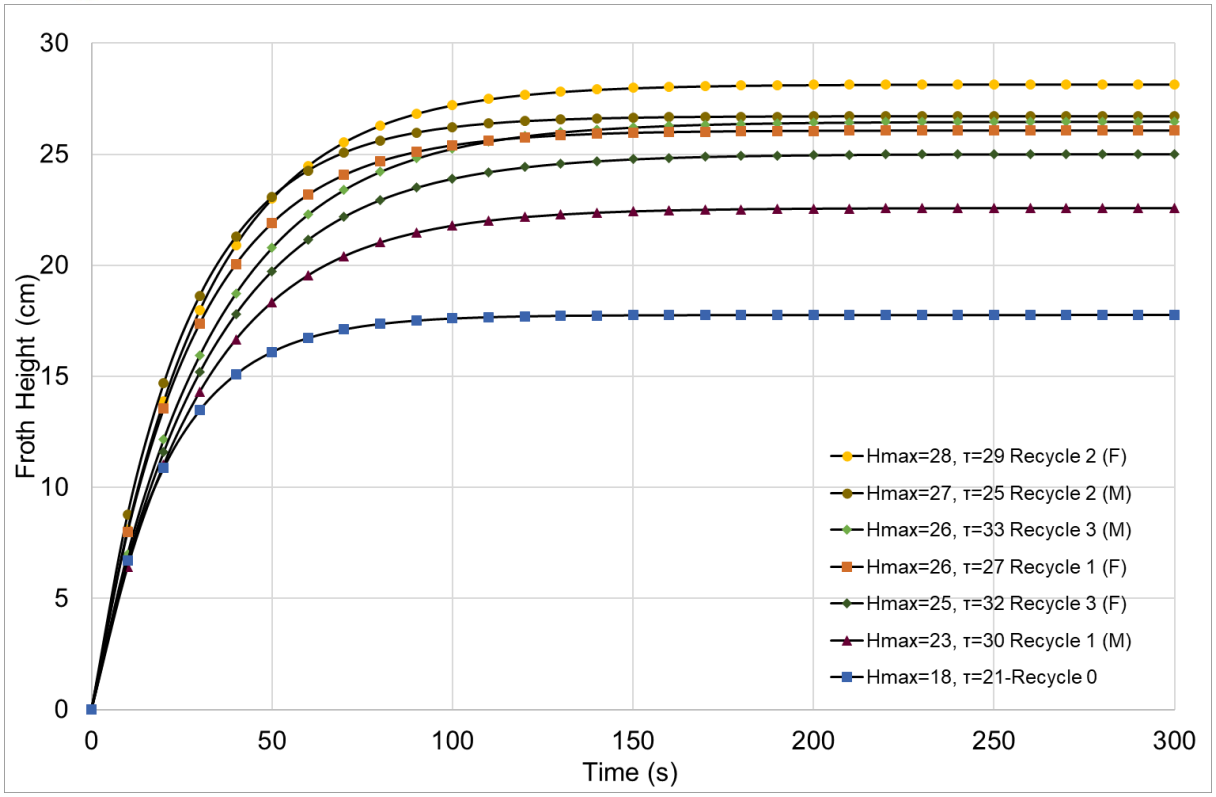

Fig 5-14. Kinetic models (lines) of froth height (cm) of the tailings pulp data set, shown by data points, for all conditions in the second phase of experiments.

Fig 5-14 shows the kinetic models of froth height of the tailings pulp across all the tests for the second phase of experiments as a function of time. The kinetic models developed show that froth from all the tested conditions achieved an equilibrium froth height within the first 160 seconds (≈3.5 minutes). The maximum equilibrium froth height led to significant differences between all of model, with Recycle 2 for the float cell recirculation being the upper model, recycles 2 and 3 in mill recirculation, and Recycle 2 in float cell recirculation being the second upper model, Recycle 3 in float cell recirculation being the third upper model, Recycle 1 in mill recirculation being the fourth upper model, and finally Recycle 0 being the lower model. The impact of bubble lifetime can be observed between the Recycle 2 and 3 in mill recirculation, as Recycle 2, at a bubble lifetime of 25 s, achieved equilibrium froth height faster as compared to Recycle 3, at a bubble lifetime of 33 s. Therefore, for froths at similar height, a longer bubble lifetime led to a slower froth build up and would in turn led to a lower mineral recovery. Float cell recirculation produced froths with either higher equilibrium froth heights, or lower bubble lifetimes, overall producing more efficient froths that led to overall higher solids recovery as compared to mill recirculation's.

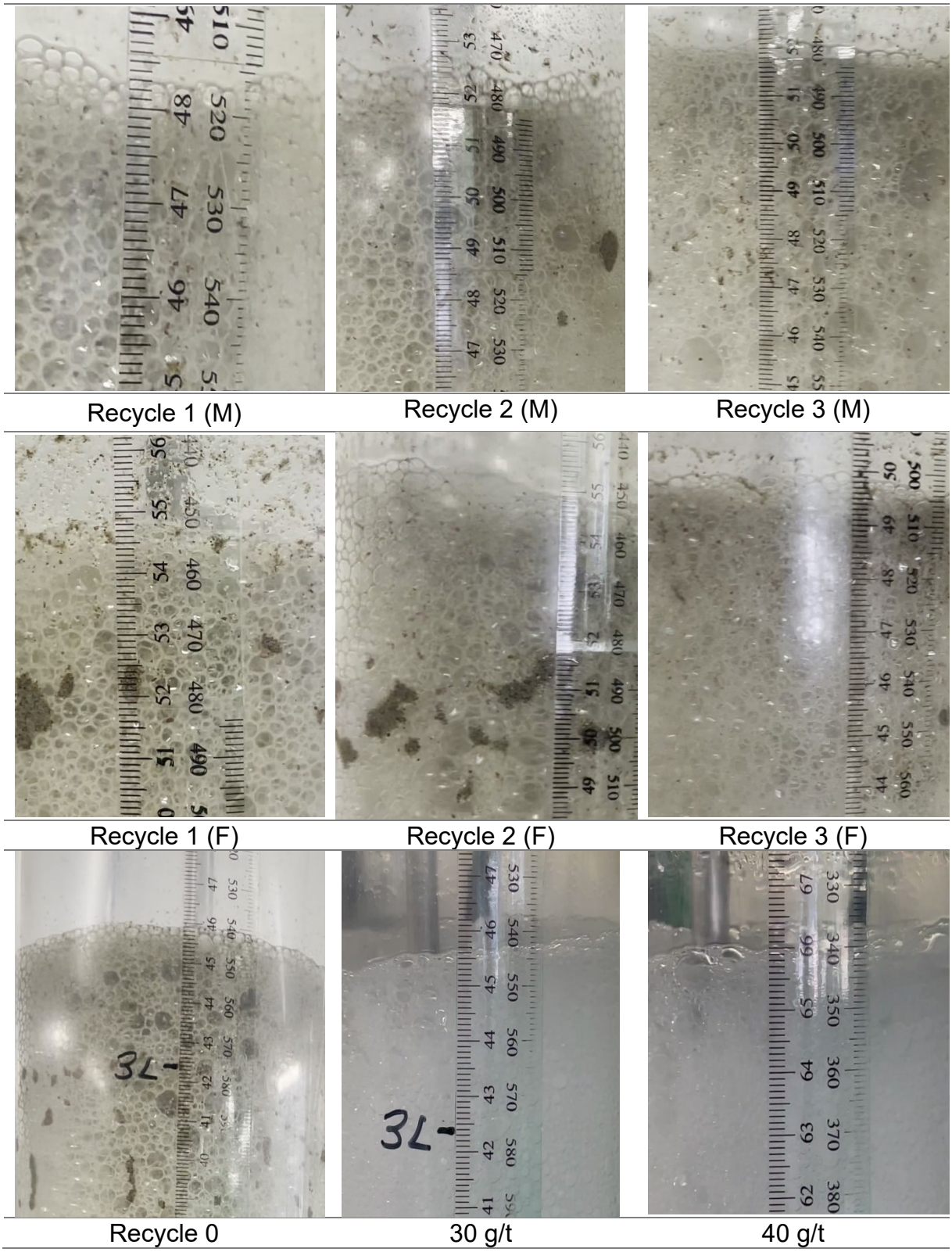

Fig 5-15. The frothing photos of tailings pulps from the second phase of experiments, and 3 SPW water at 30 g/t and 40 g/t frother dosages, at the same air flowrate of 7 L/min.

Fig 5-15 shows the images taken in the frothing process of tailings pulps from all the tests in the second phase of experiments at the same air flowrate. Mill recirculation experiments showed larger bubble sizes in all the photos compared to float cell recirculation, therefore, froth recirculation led to the formation of smaller bubbles. Recycle 0 visually displays significantly larger bubble sizes in terms of diameter.

5.5.2 2-Phase Recovered Tailings Water Dynamic Foam Stability

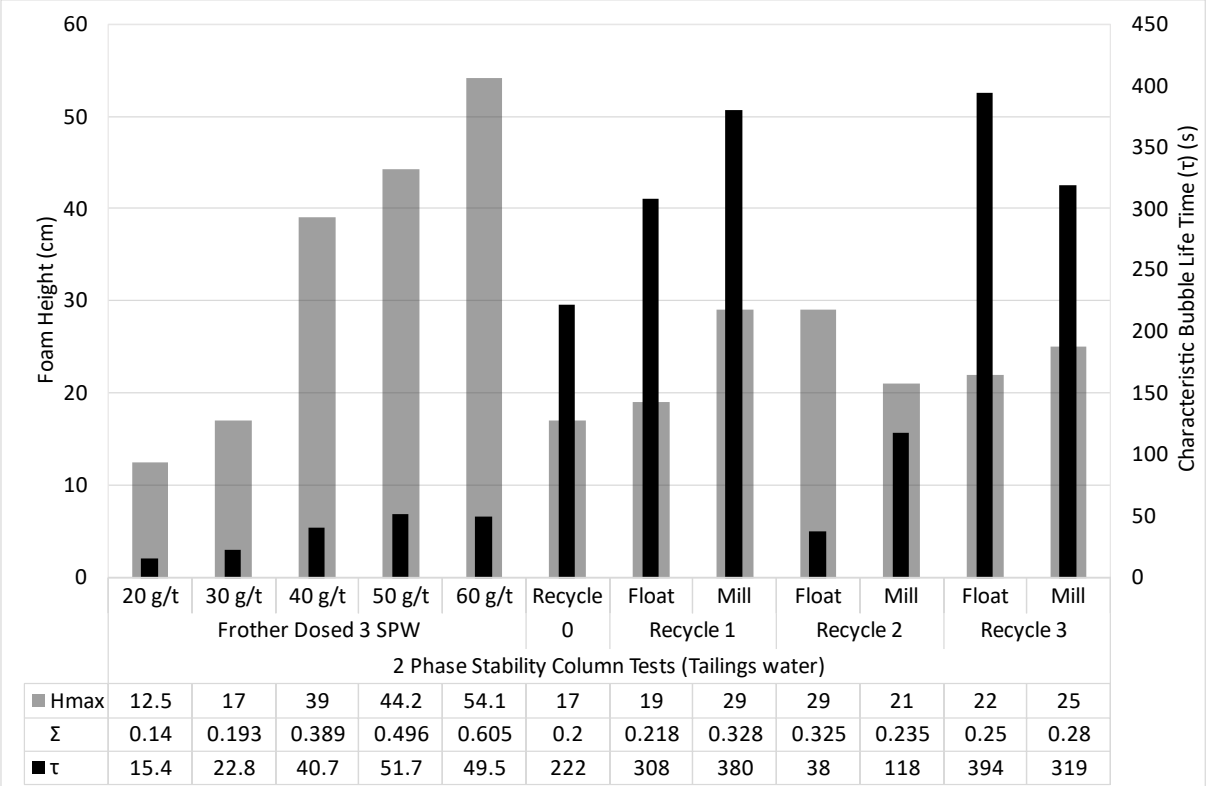

	20 g/t	30 g/t	40 g/t	50 g/t	60 g/t	Recycle 0	Float Recycle 1	Mill Recycle 1	Float Recycle 2	Mill Recycle 2	Float Recycle 3	Mill Recycle 3
	Frother Dosed 3 SPW											
	2 Phase Stability Column Tests (Tailings water)											
Hmax	12.5	17	39	44.2	54.1	17	19	29	29	21	22	25
Σ	0.14	0.193	0.389	0.496	0.605	0.2	0.218	0.328	0.325	0.235	0.25	0.28
τ	15.4	22.8	40.7	51.7	49.5	222	308	380	38	118	394	319

Fig 5-16. Equilibrium foam height (H_{max}), Characteristic Bubble Lifetime (τ) and dynamic foam stability ($\sum$) developed from kinetic models of two-phase dynamic tests of 3 SPW water at different concentration of frother and for recovered tailings water from the second phase of experiments.

Fig 5-16 shows the equilibrium foam height (H_{max}) and characteristic bubble lifetime (τ) developed from foam stability kinetic model Eq. (4-3) as bar and tabulated values and dynamic foam stability ($\sum$) tabulated for the 2 phase tests for 3 SPW water at different frother concentrations and for recovered tailings water from the second phase of experiments at a fixed frother dosage of 40 g/t. Increasing the concentration of frother from 20 to 60 g/t led to an increase in the equilibrium foam height by nearly four times, at heights of 12.5, 17, 39, 44 and 54 cm, at 20, 30, 40, 50 and 60 g/t frother dosages, respectively. Similarly, the bubble lifetime also increased with an increase in the frother dosage from 20 g/t to 50 g/t by nearly three and a half times, from 15, 23,41,

and ≈50 cm, for 20 g/t, 30 g/t, 40 g/t and 50-60 g/t frother dosages. An increase in the frother dosage led to an increase in the foam stability by about 6 times between 20 and 60 g/t, at 0.1, 0.2, 0.4, 0.5 and 0.6 for 20 g/t,30 g/t, 40 g/t, 50 g/t and 60 g/t frother dosages, respectively.

Foam stability tests from the second phase of experiments showed the impact of water recycling on the water on the foam stability of the tailings water. Tailings water from Recycle 0 had the lowest foam height of all the tests in the second phase of experiments, at a foam height of 17 cm. At the first recycle, recycling water through the mill led to a high foam, by 10 cm, with a longer bubble lifetime, by 72 s, and a more stable foam, by 0.1, at a height of 29 cm, bubble lifetime of 380 s, and a foam stability of 0.33, as compared to tailings water recycled through the float cell. At the second recycle, recycling water through the float cell led to a higher foam, by 9 cm, with a shorter bubble lifetime, by 70 s, and a more stable foam, by 0.1, at a height of 29 cm, bubble lifetime of 38 s, and a foam stability of 0.33, as compared to tailings water recycled through the float cell. Finally at the third recycle, recycling water through the mill led to a slightly higher foam, by 3 cm, with a longer bubble lifetime, by 50 s, and a slightly more stable foam, by 0.03, at a height of 25 cm, bubble lifetime of 390 s, and a foam stability of 0.25, as compared to tailings water recycled through the float cell.

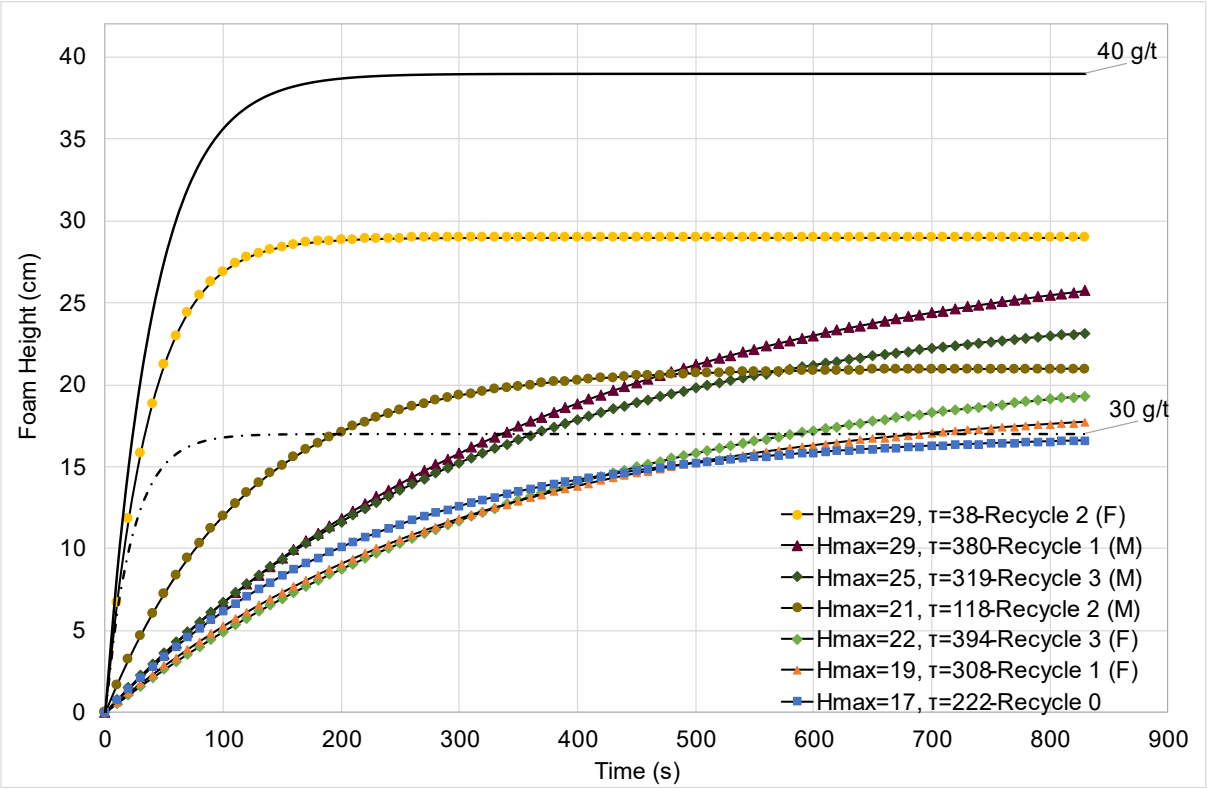

Fig 5-17. Kinetic models (lines) of foam height (cm) of recovered tailings water data set, shown by data points, for all conditions in the second phase of experiments.

Fig 5-17 shows the kinetic models of foam height (cm) of recovered tailings water across all the tests for the second phase of experiments as a function of time (s). Foam build-up differed in build-up time and height, with fast build up foams being seen in recycle 2 in float cell and mill recirculation as well as at 30 and 40 g/t in 3 SPW water, and slow foams build ups for Recycle 1 and 3 for float cell and mill recirculation. In comparison to the buildup of foam in 3 SPW at 30 and 40 g/t, that have a short build up time, the slow build up time in Recycle 1 and 3 for float cell and mill recirculation is a negative impact of water recirculation, due to the formation of over-stabilized froths. While in terms of foam heights, each condition displayed a distinct foam height descending in the following order, recycle 2 (F), recycle 1(M), recycle 3 (M), recycle 2 (M), recycle 3 (F), recycle 1 (F) and recycle 0 in that order. Therefore, recycle 0 had the lowest foam height and a longer bubble lifetime.

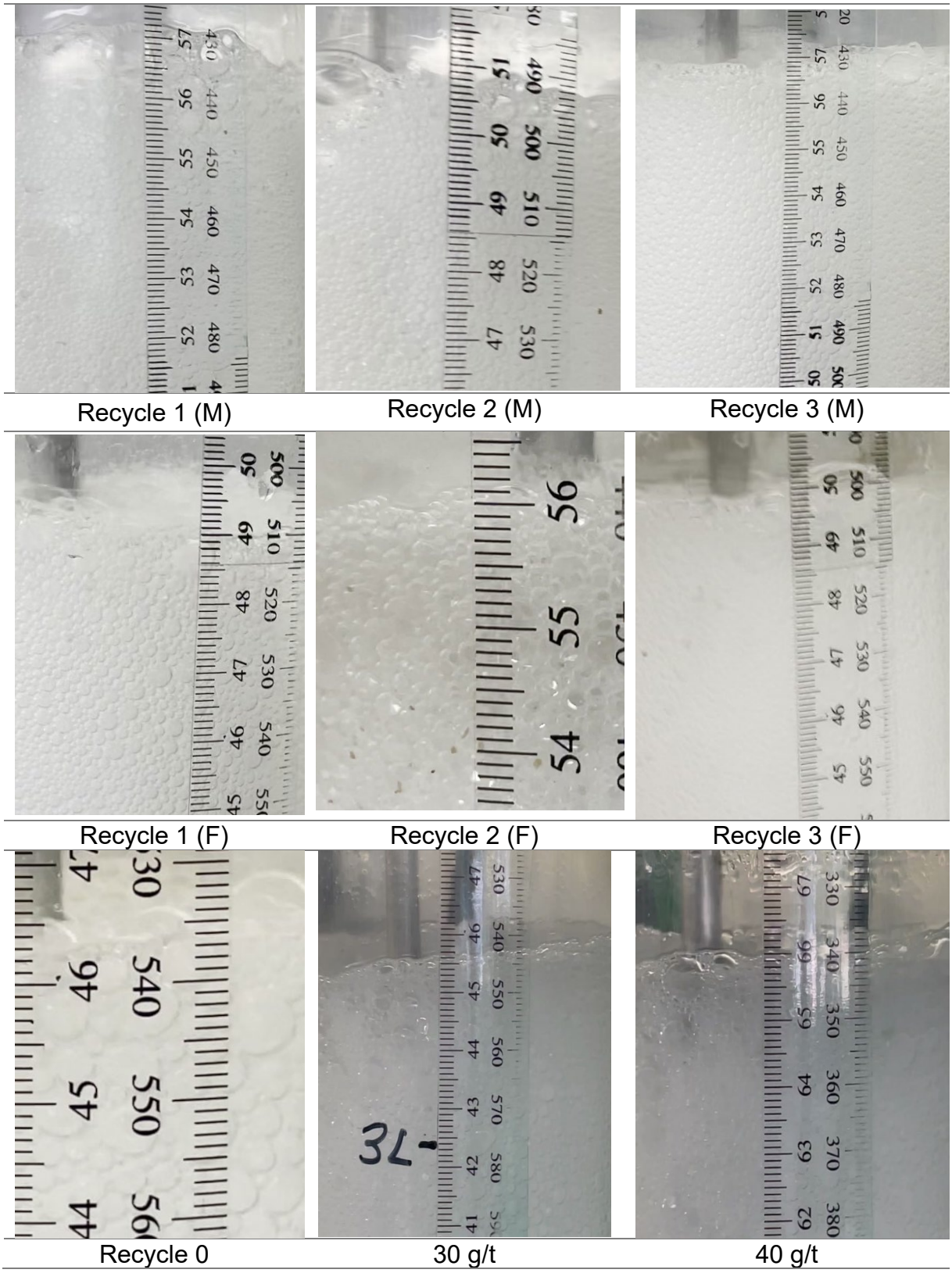

Fig 5-18. The foaming photos of recovered tailing water from the second phase of experiments, and 3 SPW water at 30 g/t and 40 g/t frother dosages, at the same air flowrate of 7 L/min.

Fig 5-18 shows the images taken in the foaming process of tailings water from all the tests in the second phase of experiments at the same air flowrate. The majority of foams have visually similar bubble characteristics, similar to the foams from 30 and 40 g/t, except for Recycle 0, which has the largest bubble sizes for all the tested conditions.

5.5.3 2-Phase Recovered Concentrate Water Dynamic Foam Stability

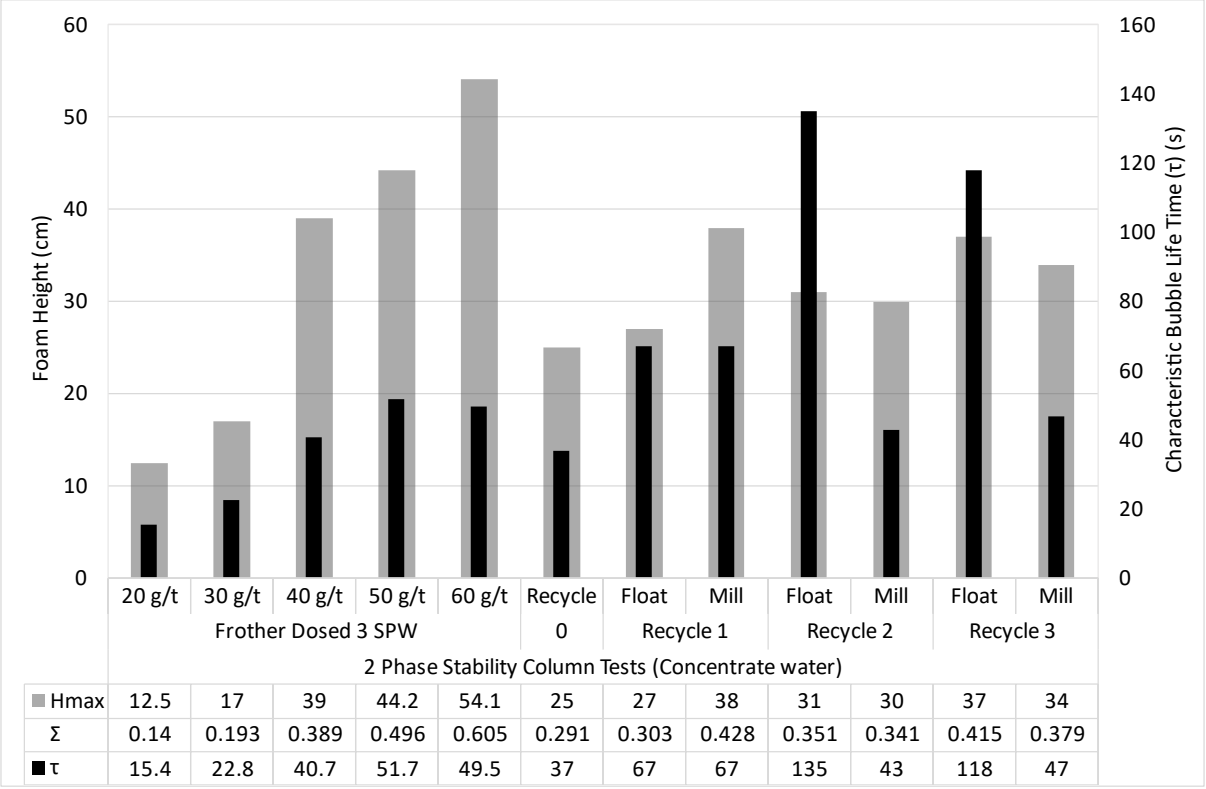

Fig 5-19. Equilibrium foam height (H_{max}), Characteristic Bubble Lifetime (τ) and dynamic foam stability ($\sum$) developed form kinetic models of two-phase dynamic tests of 3 SPW water at different concentration of frother and for the water recovered from the concentrate samples from the second phase of experiments.

Fig 5-19 shows the equilibrium foam height (H_{max}) and characteristic bubble lifetime (τ) developed from the foam stability kinetic model Eq. (4-3) as bar and tabulated values and dynamic foam stability ($\sum$) tabulated for the 2 phase tests for 3 SPW water at different concentrations of the frother and for recovered water from the concentrates of second phase of experiments. Foam stability tests from the second phase of experiments show the impact of water recycling on the water on the foam stability of the concentrate. Concentrate water from Recycle 0 had the lowest foam height of all the tests in the second phase of experiments, at a foam height of 25 cm. At the first recycle, recycling water through the mill led to a higher foam height, by 10 cm, with a

similar bubble lifetime and a more stable foam, by 0.13, at a height of 38 cm, bubble lifetime of 67 s, and a foam stability of 0.43, as compared to tailings water recycled through the float cell. At the second recycle, recycling water through the float cell led to a slightly higher foam height, by 1 cm, with a longer bubble lifetime, by 100 s, and a similar foam stability factor, at a height of 31 cm, bubble lifetime of 135 s, and a foam stability of 0.35, as compared to tailings water recycled through the mill. Finally at the third recycle recycling water through the float cell led to a slightly higher foam height, by 4 cm, with a longer bubble lifetime, by 70 s, and a slightly more stable foam, by 0.04, at a height of 37 cm, bubble lifetime of 120 s, and a foam stability of 0.42, as compared to tailings water recycled through the mill.

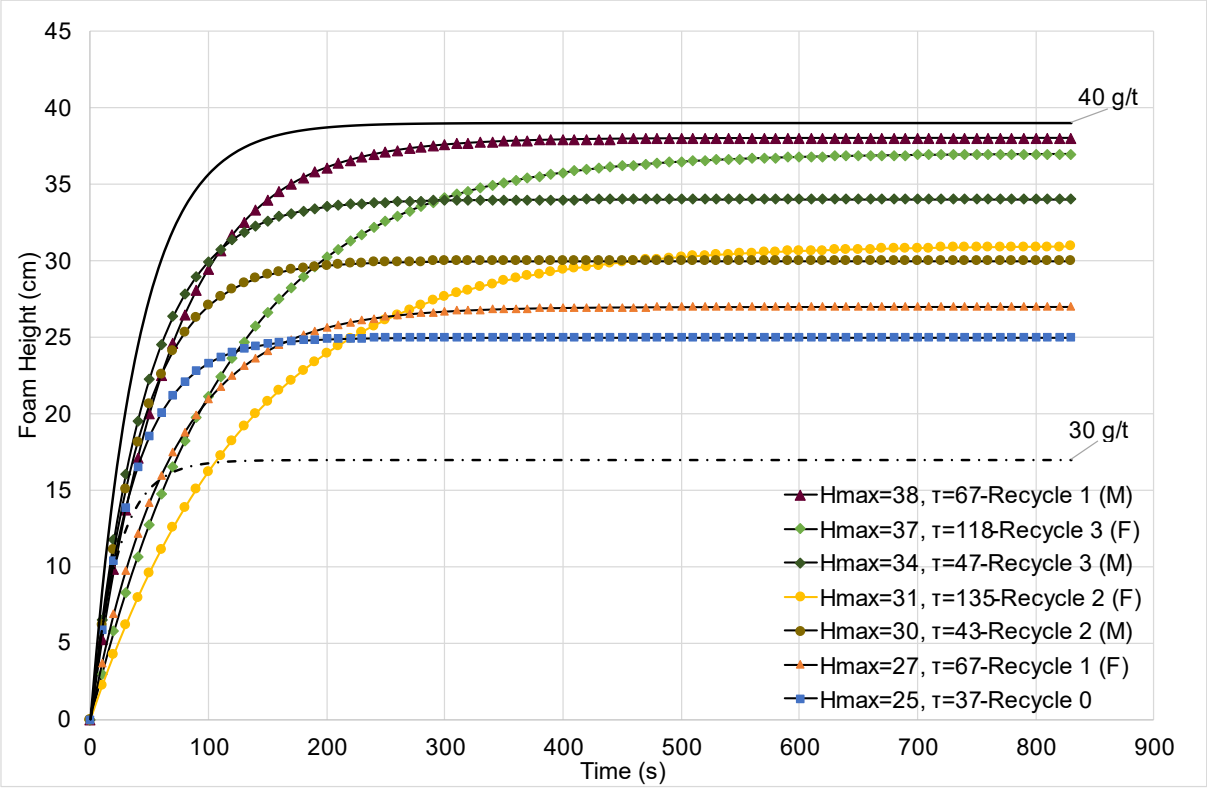

Fig 5-20. Kinetic models (lines) of foam height (cm) of recovered concentrate water data set, shown by data points, for all conditions in the second phase of experiments.

Fig 5-20 shows the kinetic models of foam height (cm) of recovered concentrate water across all the tests for the second phase of experiments as a function of time (s). Foam builds up differed in build-up time and height, with fast build up foams being recycle 1 to 3 for mill recirculation as well as at Recycle 1 in float cell recirculation, and slow foams build ups for Recycle 2 and 3 for float cell recirculation. The difference in equilibrium foam height time for the fast and slow floats was 500 seconds (about 8 minutes). The slow foam build-ups of Recycle 2 and 3 in float recirculation and the low

foam height for Recycle 1 were contrary to the solids and water recoveries observed and the 3 phase tailings tests.

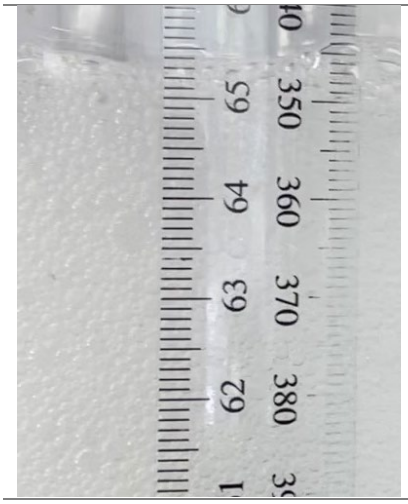

Recycle 1 (M)

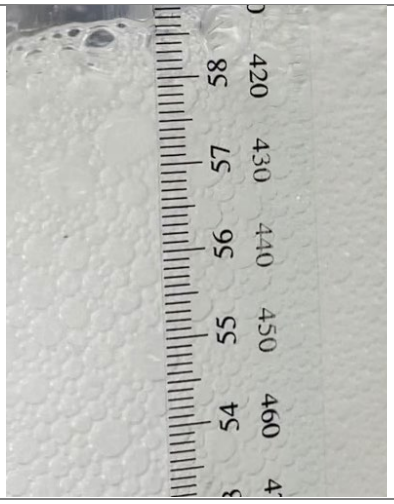

Recycle 2 (M)

Recycle 3 (M)

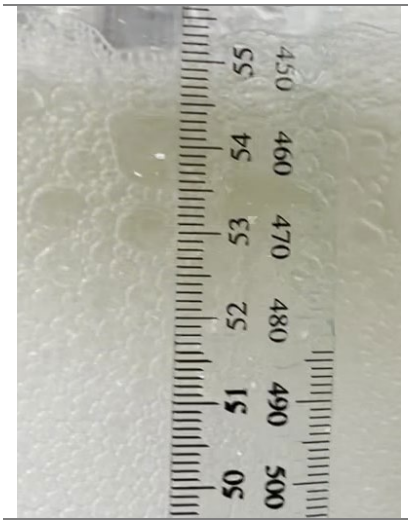

Recycle 1 (F)

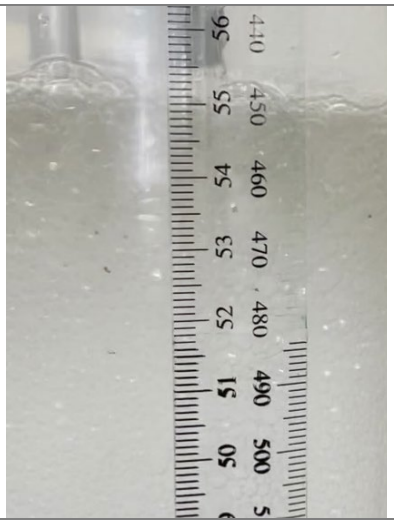

Recycle 2 (F)

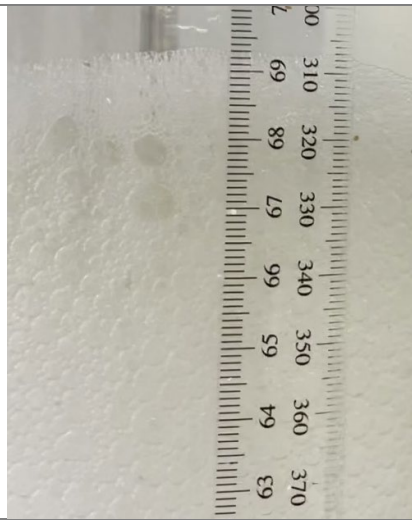

Recycle 3 (F)

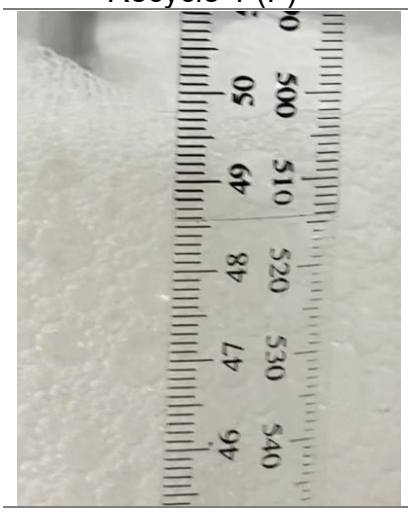

Recycle 0

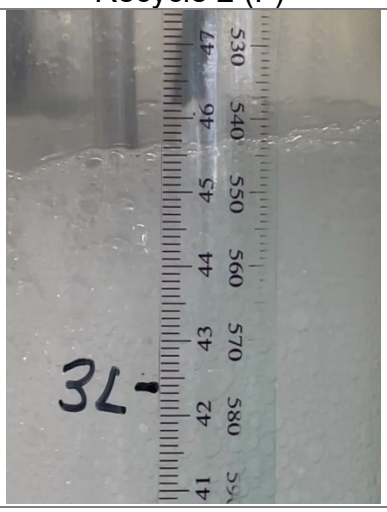

30 g/t

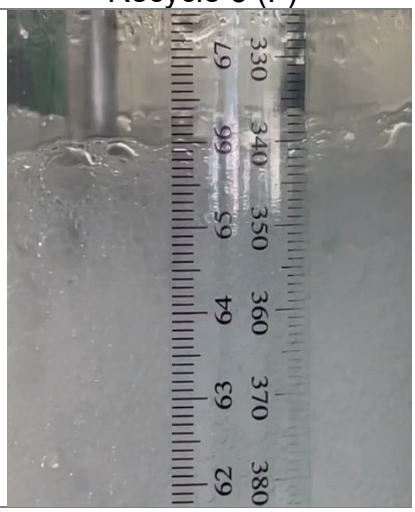

40 g/t

Fig 5-21. The foaming photos of concentrate water from the second phase of experiments, and 3 SPW water at 30 g/t and 40 g/t frother dosages, at the same air flowrate of 7 L/min.

Fig 5-21 shows the images taken in the foaming process of tailings water from all the tests in the second phase of experiments at the same air flowrate. Visually, two distinct bubble regimes are available, with large bubbles being in Recycle 0 as well as all Recycle 1 to 3 in float cell recirculation, as compared to small bubbles observed in Recycle 1 to 3 in mill recirculation.

5.6 Flotation Response in Varying Depressant Concentration and Water Quality.

5.6.1 Solid and Water Recoveries in Varying Depressant Concentrations and Water Quality.

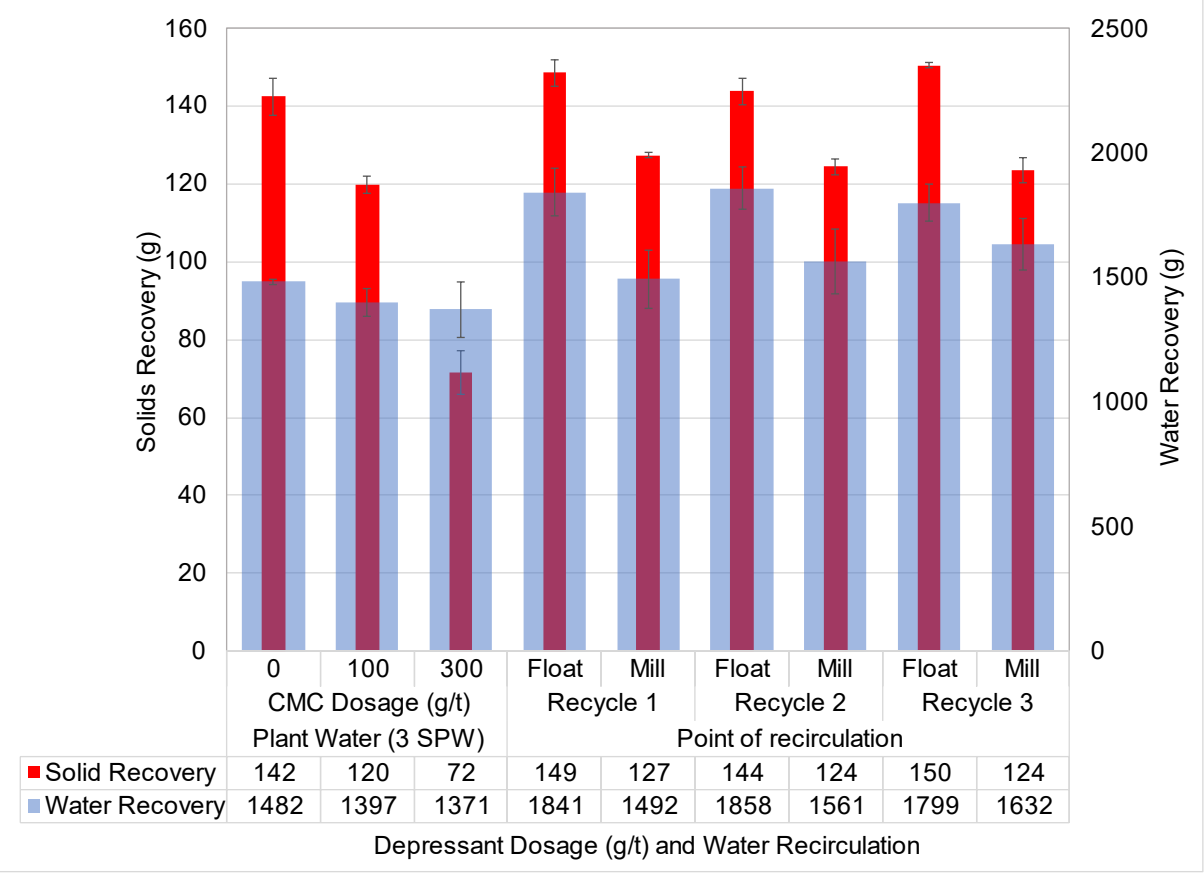

Fig 5-22 The quantity of solids and water reporting to the concentrate for all conditions tested.

Table 5-2. Entrained gangue (Ent) and solid to water ratio for all the conditions tested.

	Plant Water (3 SPW)			Point of recirculation					
	CMC Dosage (g/t)			Recycle 1		Recycle 2		Recycle 3	
	0	100	300	Float	Mill	Float	Mill	Float	Mill
Ent (g)	77.4	72.9	71.6	96.1	77.9	97	81.5	92.2	85.2
S/W (%)	10	9	5	8	8	9	8	8	8

Fig 5-22 shows the overall recovery of solids and process water reporting to the concentrates while Table 5-2 displays the entrainment factors (ε) and ratio of solids to water recovery (S/L) for all the conditions tested.

The first phase evaluates the impact of changing the depressant dosage for a fixed ionic strength of synthetic plant water (3 SPW). The quantity of solids recovered across the first phase descends from 142 g to 120 g to 71.6 g at depressant dosages of 0 g/t, 100 g/t, and 300 g/t, respectively, decreasing with increasing depressant dosage. The quantity of water recovered across the first phase is significantly lower from 1480 g to 1400 g for floats at depressant dosages of 0 g/t and 100 g/t, respectively, much more than the water recoveries between 100 g/t and 300 g/t with a difference of only 26 g with 100 g/t being higher. The decrease in water recovery accompanied by the reduction in entrained gangue from 77.4 g to 72.9 g between floats at 0 and 100 g/t depressant dosages aligns well with the observed decline in solids recoveries. The decrease in solids recoveries observed between floats at 100, and 300 g/t also ties nicely with the reduction in entrainment from 72.9 g to 71.6 g.

Flotation at 100 g/t depressant, 40 g/t frother, and 150 g/t collector dosages was a benchmark to assess the deviation caused by the recycling of process water to flotation performance and is the baseline (Recycle 0) for the recycles. Comparing the solids recovery over the first recycle at the two recycling points; a higher solids recovery at the first mill recycles is seen, recovering 149 g, than at the first float recycles, recovering 127 g. Overall, solids recoveries with recycled water are higher than those observed at a 100 g/t depressant dosage at a recovery of 120 g. The increase in solids recovery with water recirculation is accompanied with an increase in entrained gangue from 72.9 g, with float cell recirculation higher at 96.1 g as compared to 77.9 g in mill recirculation. At the second recycle, the quantity of solids recovered in the second float recycle is higher than that observed at 100 g/t depressant dosage, recovering 144 g. Concurrently the entrained gangue recoveries were higher for float cell recirculation, at 97.0 g as compared to mill recirculation, at 81.5 g. Finally, at the third recycle, the third recycle to the float recovers more solids than that observed at 100 g/t, recovering

150 g. Concurrently the entrained gangue recoveries were higher for float cell recirculation, at 92.2 g as compared to mill recirculation, at 85.2 g. The second and third recycles of water through the mill, yielded 124 g of solids each, comparable to the recovery at a depressant dosage of 100 g/t. Recycling water through the float cell achieved similar solids recoveries from all the recycles (Recycle 1, 2, and 3). It can be seen that the same pattern when recycling water through the mill was observed.

Overall, the total quantity of solids recovered is higher by 20 % in float recirculation, recovering 443 g, than in mill recirculation, recovering 375 g. Analyzing the water recovery when floating with once recycled water, it can be noted that the quantity of water recovered when recycling to the float cell is higher, with a water recovery of 1840 g than that observed at 100 g/t depressant dosage, recovering 1400 g.

Comparing the quantity of water recovered at all the recycles against each other and against the water recovery achieved when floating at a depressant dosage of 100 g/t. For the first recycle, what is of note is that the quantity of water recovered when recycling through the float is higher than that observed when floating at 100 g/t depressant dosage, recovering 1841 g of water, which is 350 g more than mill recirculation. For the second recycle, of note that the quantity of water recovered when recycling through the float is also higher than that observed when floating at 100 g/t depressant dosage, recovering 1858 g of water which is 300 g more than mill recirculation. Finally, in the third recycle, the water when floating with recycled water, at both recycling points, is more than that recovered when floating at 100 g/t depressant dosage, recovering 1800 g and 1630 g when recycling through the float and mill, respectively. Overall, the quantity of water recovered is higher when recycled water is introduced into the flotation cell than floating with 3 SPW at the same depressant, frother, and collector dosages. Conversely, recycling through the mill achieves slightly higher water recoveries to floating with 3 SPW at the same depressant, frother, and collector dosages. When recycling to the float cell, the total quantity of water is higher by 17 % than when recycling to the mill. The comparable water recoveries achieved in mill recirculation agree with the similar entrainment factors across all the mill recirculation's at 0.084 ≈ 0.079 ≈ 0.075 for Recycle 1, 2, and 3, respectively. Equally, the water recovery across the float recirculation remains comparable across all recycles when recycling to the float cell, agreeing with the comparable entrainment factors across the recycles at 0.08 ≈ 0.077 ≈ 0.084 for Recycle 1, 2, and 3, respectively.

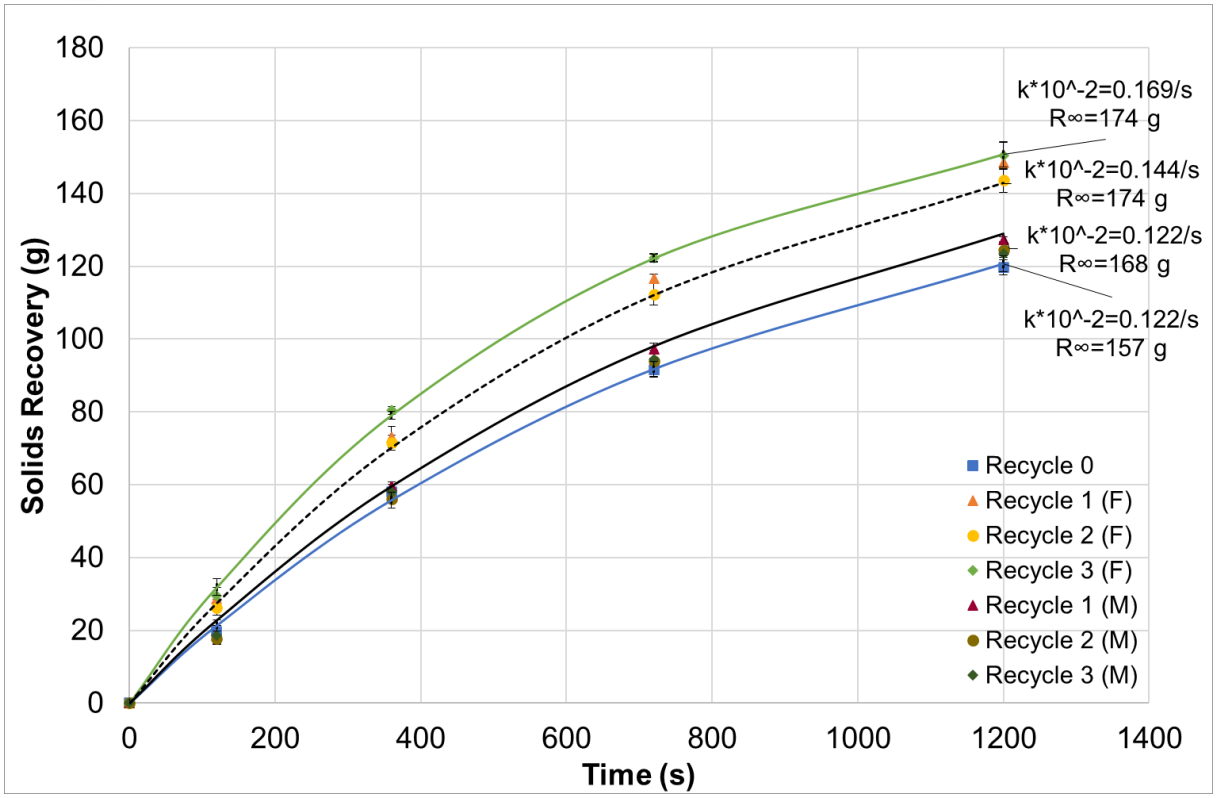

Fig 5-23. First order kinetic models (lines) fitted to cumulative solids recoveries data set, shown by data points, for all conditions in the second phase of experiments.

Fig 5-23 shows the first order kinetic models for cumulative solids recovered across all the tests conducted at 100 g/t depressant, 40 g/t frother and 150 g/t collector dosage at varying water quality as a function of time. First order kinetic models fit to the data, developing four distinct rate relationships between floating time and solids recovery. R_∞ represents the maximum possible solids recovery while k represents the rate constant. A higher rate constant therefore means, the process approaches its maximum quicker, hence a lower residence time. The highest rate of recovery is observed during the final recycle to the float cell and has the highest possible solids recovery and the largest k value of $0.169*10^{-2}$ s^{-1}. The second-rate model has a lower k value of $0.144*10^{-2}$ s^{-1}, and well fits recycle 1 and 2 through the float cell. This is as expected, as recycling through the float cell recovered more solids overall. The third model achieves a maximum solids recovery of 168 g, at a k value of $0.122*10^{-2}$ s^{-1}. This model best described mill recirculation tests which achieved overall had lower solids recoveries when compared to float cell recirculation. The last model has the lowest maximum solids recovery of 157 g, and visually models experimental data using 3 SPW water at the standard reagent dosages. From the first order rate models, water recirculation leads to a change in flotation performance, leading to an increase in solids recovery, more important when recycling through the float cell than the mill.

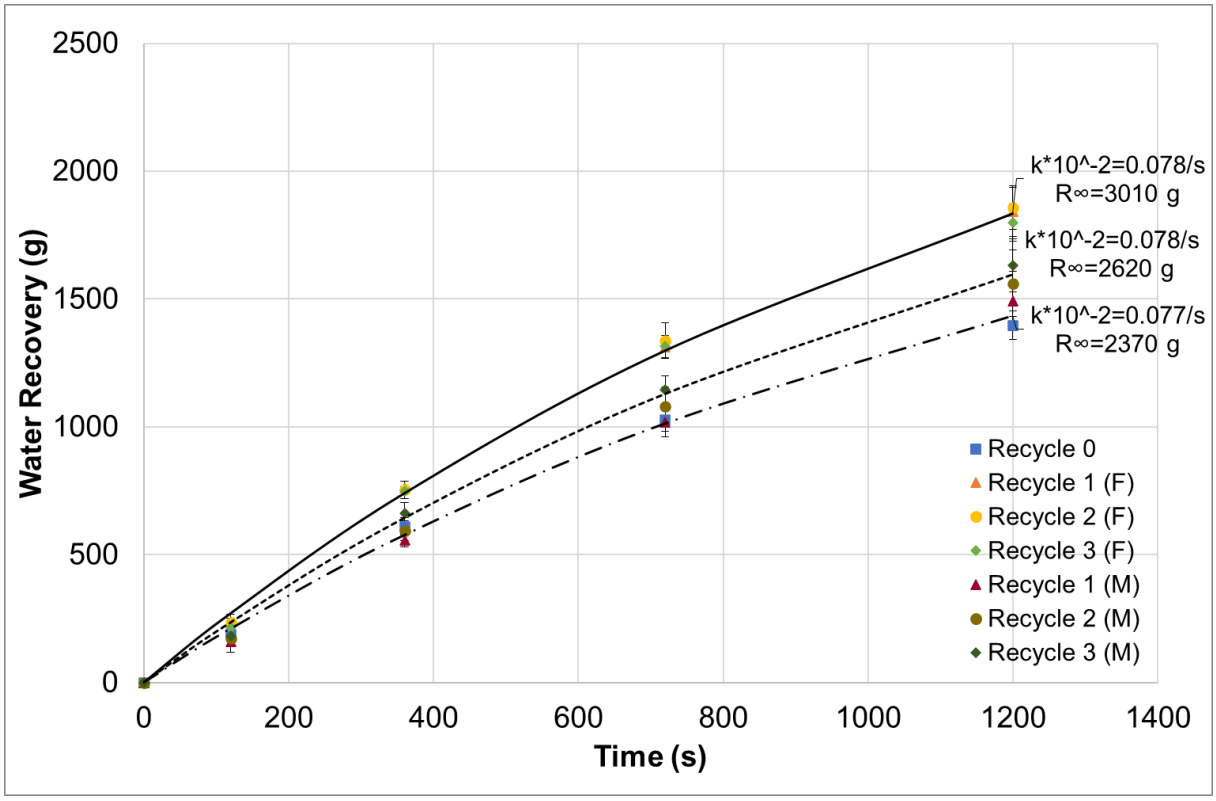

Fig 5-24. Kinetic models (lines) fitted to cumulative water recoveries data set, shown by data points, for all conditions in the second phase of experiments.

Fig 5-24 shows the first order kinetic models for cumulative water recovery across all the tests from the second phase of experiments as a function of time. From these trends developed three distinct rate relationships. The higher rate model has a higher maximum water recovery at 3010 g with a k value of $0.078*10^{-2}$ s^{-1} and fits cumulative water recoveries from all the recycles to through the float cell. The second model differs from the faster model by the R_∞ achieved recovering 2620 g and fits well the cumulative water recoveries achieved from recycles 2 and 3 when recycling through the mill. The slowest model has the lowest R_∞ of 2370 g of water at a k value of $0.077*10^{-2}$ s^{-1} and fits well the cumulative water recoveries experimental data obtained from using 3 SPW (baseline test) and the first recycle through the mill.

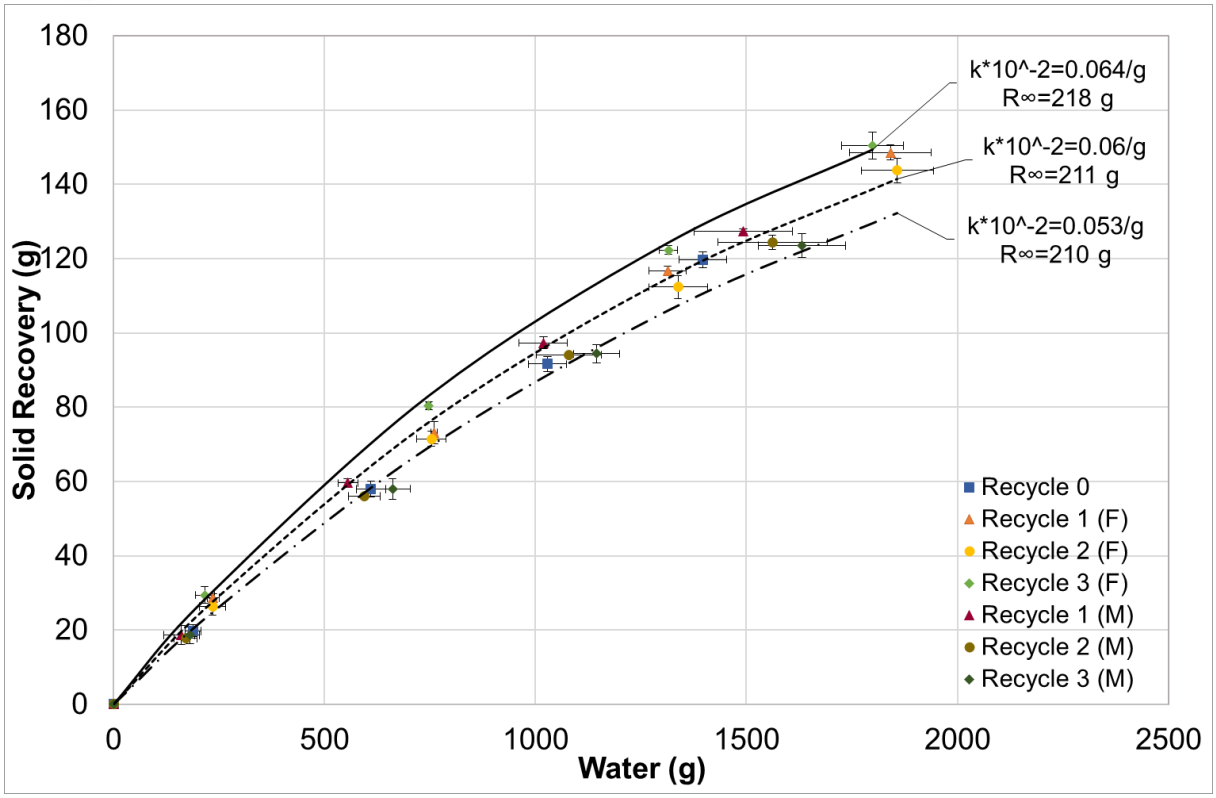

Fig 5-25 First order response (lines) fitted to cumulative solids recoveries data set, shown by data points, for all conditions in the second phase of experiments.

Fig 5-25 shows the first order response models for the cumulative solid's recoveries across all the tests from the second phase of experiments as a function of water recovery. From these experimental data, three response relationships were developed using the first order model, representing the upper, middle, and lower rate relationships per unit mass of water. The upper bound has the highest maximum solids recovery of 218 g for a k value of $0.064*10^{-2}$ g^{-1} which visually fits the experimental data for the third recycle to the float cell. The second response model has a maximum solids recovery of 211 g at a growth of $0.06*10^{-2}$ g^{-1} recovering less solids per unit mass of water. This trend models majority of the experimental results, with recycles 1 and 2 for both float cell and mill recirculation's and baseline test data visually fitting the model. The lower model achieves the lowest solids recovery of 210 g at a growth of $0.053*10^{-2}$ g^{-1}, and visually fits experimental data from the third recycle through the mill. The higher growth model achieves a higher water efficiency, recovering more solids per gram of water. Conversely the lower growth model has a lower water efficiency, recovering less solids per gram of water. The equilibrium maximum recovery changes by 8 g between the lower and higher model, showing the relative flexibility between the different floats.

5.6.2 Copper Recoveries and Grades in Varying Depressant Concentrations and Water Quality.

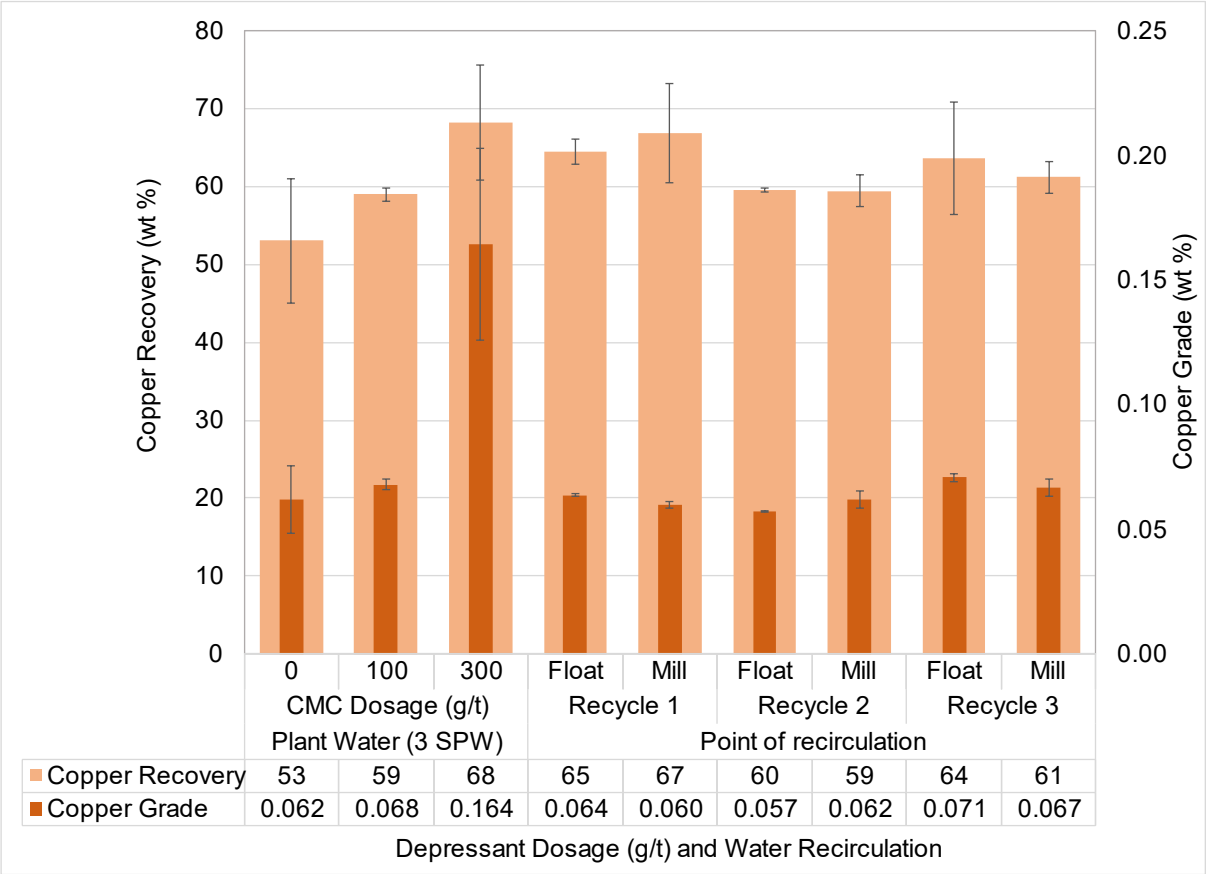

Fig 5-26. The final cumulative recoveries and grades of copper in the solids reporting to the concentrates for all conditions.

Fig 5-26 shows the cumulative final copper recovery and grade for all tested conditions. Across the first phase of experiments, increasing depressant concentration of between 100 and 300 g/t led to a significant three-fold increase in the grade from 0.062 % to 0.164 %. The similar recovery of copper between 100 to 300 g/t dosage and the 58 % increase in grade motivates that depressant enhances the selectivity of the froth flotation process, through increasing the hydrophilicity of the gangue. Floating at 0 g/t achieved comparable copper recoveries to flotation with 100 and 300 g/t. A slight increase in recovery is also observed when increasing the depressant from 100 to 300 g/t from 60 % to 68 %, respectively. It is affirmative that at a constant collector and frother dosage, an increase in the depressant dosage led to an increase in the grade of copper as compared to flotation in the absence of a depressant with a minimal impact on the recovery, showing the interaction between depressant and gangue.

In the second phase of experiments the water quality was varied using recycled water consecutively recycled through the mill for three recycles. The results shown Fig 5-26 in compare the copper grades and recoveries against each other and against flotation at 100 g/t depressant dosage, 40 g/t frother, and 150 g/t collector dosage (Recycle 0). At the first recycle stage, recycle 1, recycling through the float cell achieved a higher copper grade of 0.064 %, as compared to recycling through the mill with a grade of 0.060 %. Conversely, at the second recycle, recycling through the mill achieved a higher grade of 0.062 % as compared to 0.057 % when recycling through the float cell. In the third recycle, recycling through the float cell achieved a higher grade of 0.071 % as compared to 0.067 % when recycling through the mill. Overall, recycling through the float cell achieved higher grades of copper as compared to recycling to the mill. The fluctuation in copper recovery between the different flotation conditions could be due to changes in froth stability, reagent concentration due to residual reagents, or changes in water chemistry.

Conversely, at a particular recycle, flotation with recycled water achieves slight differences in the copper recoveries, where at the first recycle the recovery is higher in mill recirculation by 2 % and is lower by 1 % and 3% in recycle 2 and 3 when compared to float recirculation. In fact, only two changes in copper recoveries are of note; Firstly, it can be seen that the recovery of copper in the first recycle for both points of addition surpass the copper recovery at 100 g/t depressant dosage of 59 %, recovering 65 % and 67 % in float cell and mill recirculation, respectively. Secondly, it can also be observed that a change in recovery occurs in float cell recirculation between Recycle 1 and Recycle 2 in float cell recirculation dropping from 64.5 % to 59.6 %, respectively.

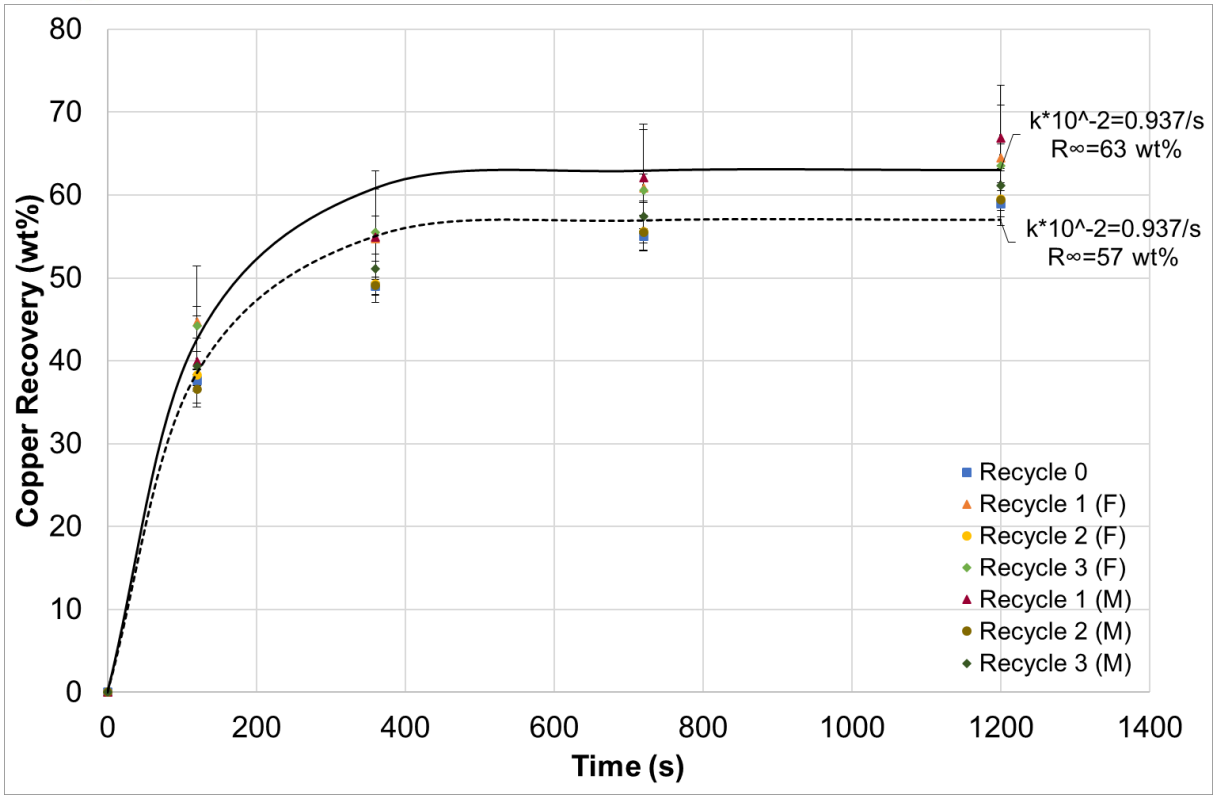

Fig 5-27. Kinetic models (lines) fitted to cumulative copper recoveries, shown by data points, for all conditions in the second phase of experiments.

Fig 5-27 shows the first order kinetic models fitted to the experimental data on the cumulative copper recovery across all the tests for the second phase of experiments as a function of time. From the cumulative copper recoveries, two distinct kinetic models were developed, showing the upper and lower bounds. Both models have similar rate constants, at $0.937*10^{-2}\ s^{-1}$, and differ in R_∞ recovering 63 % for copper in the upper model as compared to 57 % in the lower bound. The upper kinetic model best represents the recoveries for recycle 1 in both float cell and mill recirculation. The second model best fits Recycle 0, Recycle 2 for both float cell and mill recirculation and Recycle 3 in mill recirculation. Recycle 3 in float cell recirculation fits in both models due to large deviation observed in the recovery. In both models, majority of the copper is recovered in the first 200 seconds and reaches an equilibrium recovery at 400 seconds. Kinetic and first response models of copper recovery prove that copper is a fast-floating mineral, hence the similar rate and growth constants of recoveries are expected, portraying an independence of the residence time for chalcopyrite recovery from the influence of the change in water quality. Therefore, the impact of changing water quality can be linked directly to the equilibrium recovery achieved, hence the production volumes achieved. Kinetic models of copper recovery differ in equilibrium copper recovery achieved, with float cell recirculation achieving a higher recovery as

compared to mill recirculation, apart from Recycle 2 in the latter and Recycle 1 in the former.

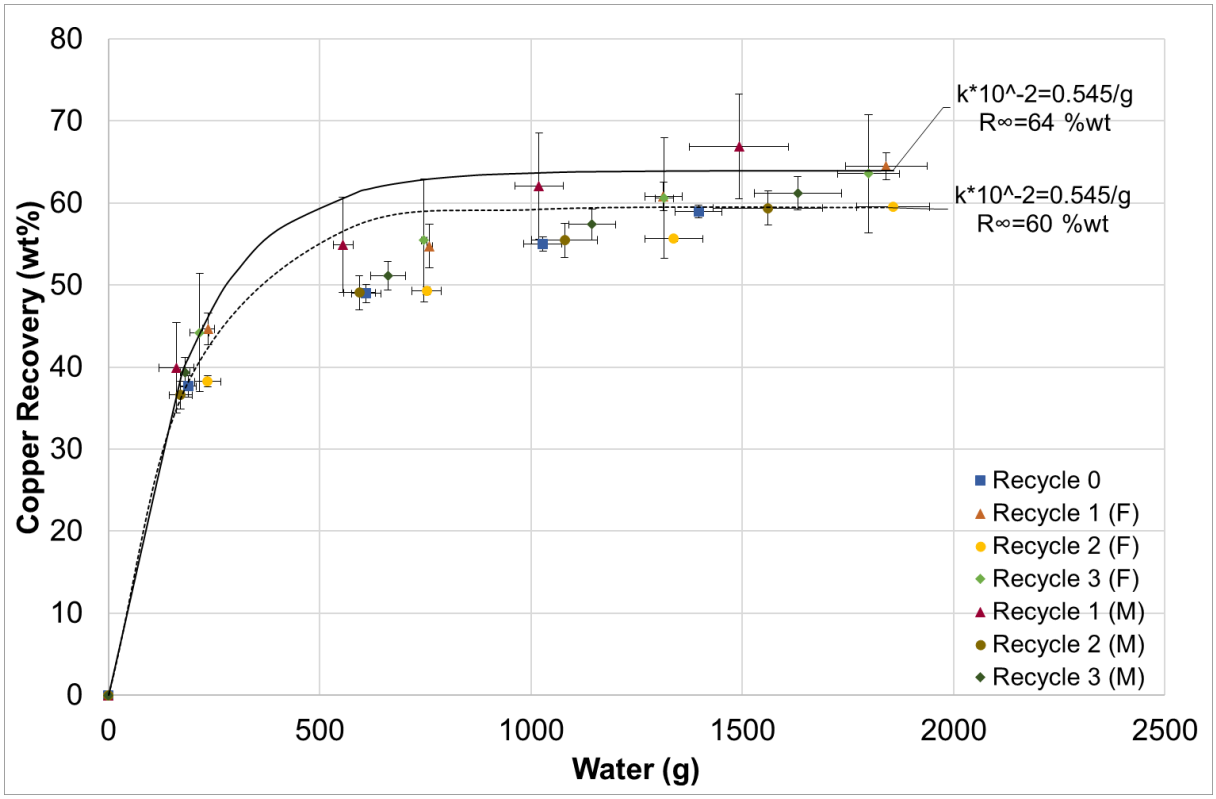

Fig 5-28. First order response (lines) fitted to cumulative copper vs water recoveries, shown by data points, for all conditions in the second phase of experiments.

Fig 5-28 shows the first order response models fit to the cumulative copper recovery across all the tests for the second phase of experiments as a function of water. From the cumulative copper recoveries, two distinct models were developed, the upper and lower bounds. Both models have similar growths, at $0.545*10^{-2}\ g^{-1}$, and differ in R_∞ at 64 % and 60 % for the upper and lower models, respectively. The upper model best fits recycle 1 in mill recirculation, and the final recovery of recycle 1 and recycle 3 in float cell recirculation. The lower model fits Recycle 0, Recycle 2 for both float cell and mill recirculation and Recycle 3 in mill recirculation. The deviation of copper recoveries from their kinetic and first response models after the first concentrate (200 seconds) shows that cumulative copper recoveries are better represented by a piecewise combination of models, with first order for the initial rates ($0 \leq t \leq 200$ s: $0 \leq g \leq 500$ g). The use of piecewise models has also been motivated by studies by Imaizumi, (1963) for modelling kinetics in coal flotation.

5.6.3 Nickel Recoveries and Grades in Varying Depressant Concentrations and Water Quality.

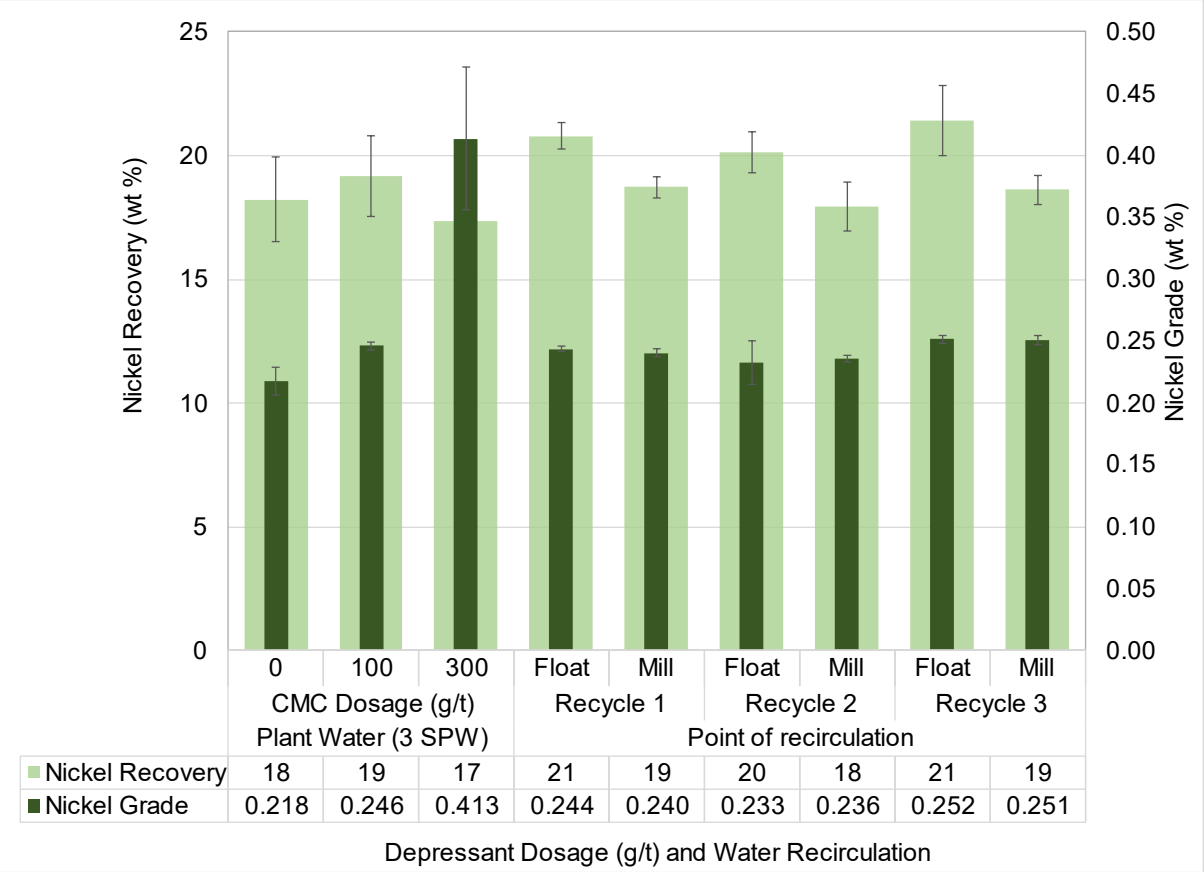

Fig 5-29. The cumulative recoveries and grades of nickel in the solids reporting to the concentrates for all conditions.

Fig 5-29 shows the cumulative final nickel recovery and grade for all tested conditions. With a constant collector dosage of 150 g/t and a frother dosage of 40 g/t, increasing the depressant dosage between 0 and 300 g/t resulted in a 40–50% increase in cumulative nickel grade, from 0.218 % and 0.246 % at 0 and 100 g/t, respectively, to 0.412% at 300 g/t. Conversely, the nickel recoveries between the first phase experiments differ slightly at 18.2 %, 19.2 %, and 17.4 % for 0, 100, and 300 g/t, respectively. Thus, at a constant collector and frother dosage, an increase in depressant dosage leads to improved selectivity of the flotation process and a significant increase in the nickel grade with little or no impact on the nickel recoveries.

The second phase of experiments investigated the effect of change in water quality by using recycled water from preceding tests starting from a baseline test (Recycle 0) at a frother dosage of 40 g/t, collector dosage of 150 g/t, and depressant dosage of 100 g/t. Comparing the nickel recoveries achieved at first recycle (Recycle 1) for the two

recycling points, it can be seen that higher cumulative nickel recoveries were achieved when water was recycled through the float cell, recovering 21 %, compared to recycling through the mill which recovered 19% nickel. For the second recycle (Recycle 2), the cumulative nickel recovery is also higher when floating using recycled water through the float cell, recovering 20 %, while recycling water through the mill recovered 18 %. Finally, the third recycle (Recycle 3) confirms that recycling water through the float cell achieves higher nickel recoveries, recovering 21 %, compared to recycling through the mill at a recovery of 19 %.

In other words, a bank of concentrators recycling water to the float cell would have a 2.3 % higher nickel recovery than recycling through the mill. However, it would still achieve a similar recovery as floating with 3 SPW water due to the range in nickel recovery observed from the tests under these conditions. The higher recovery of nickel observed in float cell recirculation further motivates that changing the point of addition of recycled water leads to a change in the flotation performance. Conversely, the addition point of recycled water did not lead to any meaningful change in the grade achieved at similar recycle stages. The cumulative nickel grades in the second phase of the experiments changes slightly and is higher for float cell recirculation's 1 and 3 by 0.004 and 0.001 respectively and is higher in mill recirculation by 0.003 in recycle 2. The only distinct result is the low grade achieved at Recycle 2 in float cell recirculation. Nickel grades also differ when Recycle 1 and Recycle 3 are compared, with Recycle 3 having a higher grade of 0.252 % and 0.251 % in float cell and mill recirculation, respectively, than Recycle 1, which has 0.244 % and 0.240 % in float cell and mill recirculation, respectively.

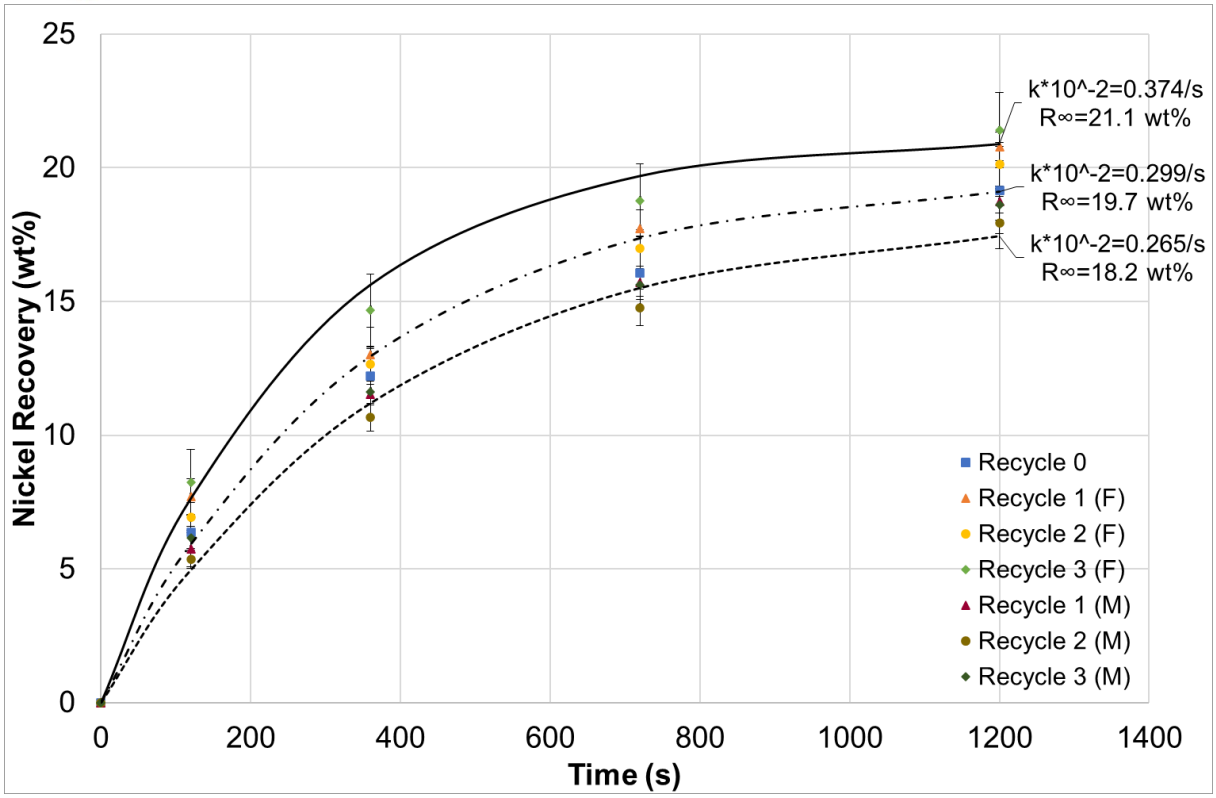

Fig 5-30. Kinetic models (lines) fitted to cumulative nickel recoveries, shown by data points, for all conditions in the second phase of experiments.

Fig 5-30 shows the kinetic models fit to the cumulative nickel recovery across all the tests for the second phase of experiments as a function of time. From the cumulative recoveries, three distinct models were developed at different R_∞ and rate constant (k). The upper kinetic model has an R_∞ of 21 % nickel recovery at a rate of $0.37*10^{-2}$ s^{-1} and fits well to the cumulative nickel recoveries observed in recycle 3 for float cell recirculation, as well as being the initial rate and equilibrium recovery for Recycle 1 and 2. The middle model has an $R_\infty$of 20 % at a rate of $0.30*10^{-2}$ s^{-1} and visually is a good fit for cumulative recoveries observed in Recycle 1 and 2 in float cell recirculation, as well as being the initial rate for Recycle 0 and the equilibrium recovery for Recycle 0 and Recycle 1 and 3 in mill recirculation. Finally, the lower model has an R_∞ of 18 % at a rate of $0.27*10^{-2}$ s^{-1} and visually fits well with the cumulative recoveries observed in all mill recirculation, and the equilibrium recovery for Recycle 3 in mill recirculation. Kinetic modelling shows that a change in water quality through point of addition and water recycling lead to a change in the equilibrium recovery and rate of recovery, and hence the performance of the concentrator. Float cell recirculation overall achieved a higher equilibrium nickel recovery at a higher rate, hence would require a lower residence time for the concentrator, performing better than floating at baseline conditions (Recycle 0). Mill recirculation overall shows a lower equilibrium nickel

recovery at a slower rate and would therefore require a higher residence time in the concentrator.

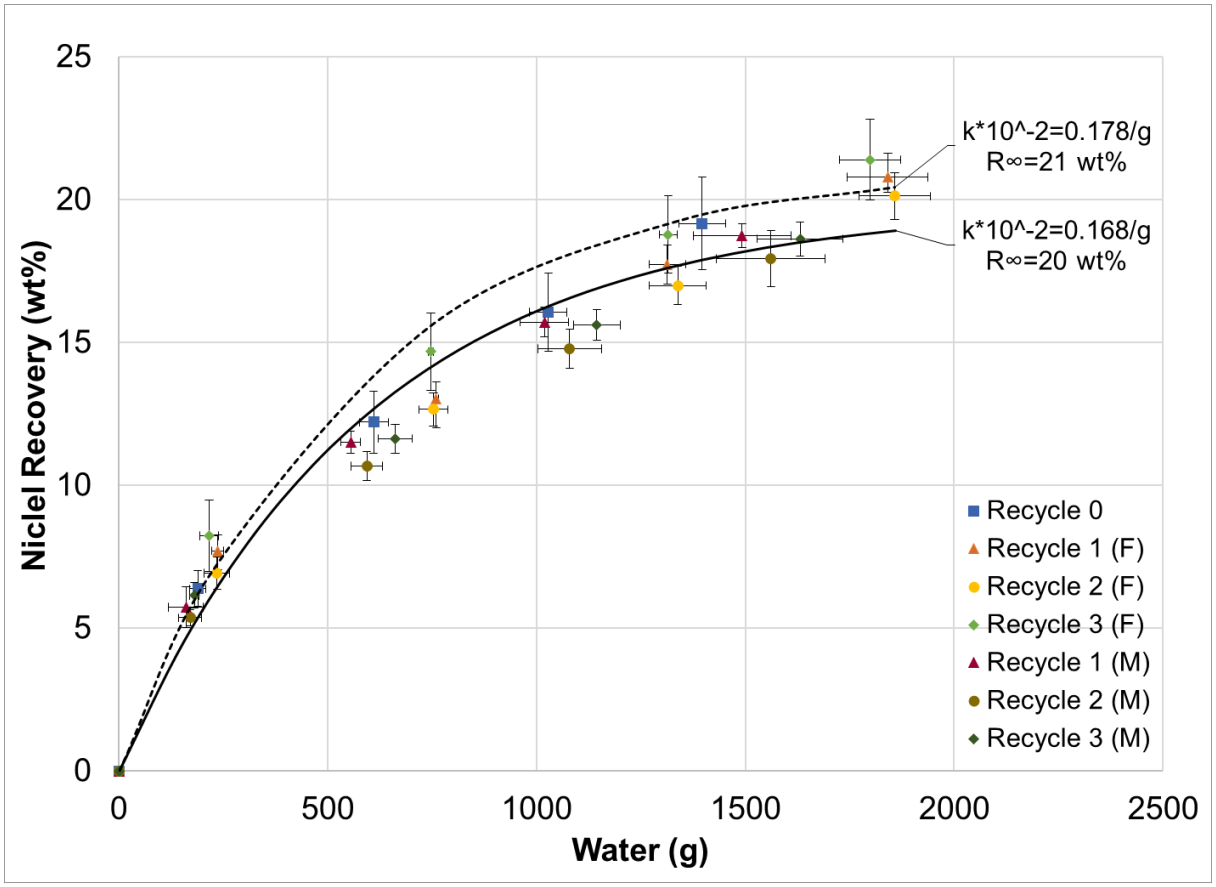

Fig 5-31. First order response (lines) fitted to cumulative nickel vs water recoveries, shown by data points, for all conditions in the second phase of experiments.

Fig 5-31 shows the first order response models fit to the cumulative nickel recovery across all the tests for the second phase of experiments as a function of water. Two distinct response models were developed to represent the relationship between nickel and water recovery. The higher model has an R_∞ of 21 % at a growth of $0.178*10^{-2}$ g^{-1} of water and fit well to the initial nickel recoveries (below 500 g of water) as well as general trend of cumulative nickel recoveries for Recycle 3 in float cell recirculation and the equilibrium recovery for float cell recirculation and Recycle 0 (Baseline). The second model has a lower R_∞ of 20 % at a growth of $0.168*10^{-2}$ g^{-1} and represents majority of the nickel recovery observed between 500 and 1500 g of water for conditions in the second phase of experiments and the equilibrium recoveries of all mill recirculation. These results suggest that a change in water quality through water recycling led to a change in the nickel recovery per unit gram of water, with water

recycling through the float cell recovering more nickel as compared to recycling water through the mill.

Overall, first order kinetic models of the second phase of experiments show a change in the flotation performance caused by the point of addition of recycled water as well as an impact on nickel recovery. Recycling water through the float cell had an overall higher equilibrium recovery of nickel at a higher recovery rate, hence a lower residence time at a higher flotation performance compared to recycling water through the mill. Similarly, float cell recirculation also had an overall higher equilibrium nickel recovery at a higher nickel load per g of water as compared to mill recirculation.

6 Discussion

The aim of this project was to investigate how short cycle water recirculation affects the flotation performance of a specific Cu-Ni-PGM ore. The understanding of the impact could provide solutions by which to use short recirculation of water and the potential impact that a change in water quality can have on downstream processes such as dewatering prior to the water recovered from the being fed back into milling and flotation. Two points of recirculation for recycled tailings water, viz. to the mill and to the float cell, were utilized in the batch flotation tests in the presence of SIBX, CMC and DOW 200 as the collector, depressant and frother respectively. This section of the thesis focuses on the synthesis of the key findings from the results developed from the experimental program described in Chapter 4.1 and presented in Chapter 4 to discuss the hypotheses of the study presented in Chapter 3.1.2.

6.1 Determining the Entrainment Factor, NFG Ore Content using CMC.

The first phase of the study focused on determining the quantity of naturally floating gangue (NFG), by determining an entrainment factor (Wiese et al., 2007). Due to the linear relationship between gangue recovery and depressant dosage, the study increased the depressant dosage from 0 g/t to 100 g/t and finally to 300 g/t to ensure complete depression of all NFG (Wiese, 2009). Similar to the established literature (Dhliwayo, (2005); Morris et al., (2002); Wiese et al., (2007) and Wiese and Harris, (2012), this study agrees with the following hypothesis in the context of a UG2 ore:

An increase in depressant dosage at a constant water quality, collector and frother dosage during flotation of a UG2 ore leads to a decrease in the solids, water, and gangue recovery, improving the grade of Cu and Ni in the concentrate due the depression of NFG, reducing the total solids recovery and the froth stability of the froth, with all NFG depressed at a dosage of 300 g/t.

The findings of this study showed that at 100 g/t the entrainment factor was 0.085 g solids per g of water. In this study, increasing the depressant dosage led to an overall decrease in the quantity of solids recovered and the degree of entrainment also decreased accordingly as shown by the entrained gangue reported in Fig 5-22. This shows that the selective impact of the depressant on gangue was improved in increasing depressant dosages, improving gangue hydrophilicity, and thus leading to lower solid recoveries in agreement with the hypothesis tested.

Established literature, Dhliwayo, (2005); Morris et al., (2002); Wiese et al., (2007) and Wiese and Harris, (2012), also observed a decrease in solids and water recovery with an increase in CMC depressant dosage on sulfide ores. The decrease in NFG in the froth phase led to a decrease in the froth stability due to a decrease in the amount of hydrophobic particles in the froth phase that are imperative for froth stabilization (Ekmekçi et al., 2003; Farrokhpay, 2011). This leads to a decrease in the water recovery (Wiese, 2009). The decrease in froth stability means that there is higher bubble coalescence and bubble rupture in the froth, reducing the carrying capacity and drainage of solids out of the froth as bubbles rupture, thus reducing the solids recovery (Farrokhpay, 2011; Farrokhpay and Zanin, 2012; Quinn et al., 2007). For the given ore, the concentration of NFG was determined to be about 4-6 % based on mass balance analysis from solids, water, and entrainment factor available in Fig 5-22 and Table 5-2. Although the recovery of gangue by entrainment between 0 g/t and 100 g/t depressant dosage decreased, the water recoveries did not change significantly, implying that the depressant acted primarily on the gangue mineral surface, inducing hydrophilicity, but not to the detriment of the water carrying capacity of the bubbles which reported to the froth phase, supporting a depressant dosage of 100 g/t as the baseline and suitable depressant concentration.

Increasing the depressant dosage led to an increase in the grade of the sulfide minerals as shown by the grades of Ni and Cu in the concentrates improving by 2 to 3 times from the grade at 0 g/t depressant dosage as shown in Fig 5-26 and Fig 5-29. This result is attributed to the depression of NFG which is known to dilute the grade of the concentrate when not sufficiently depressed (Wiese et al., 2007). This significant improvement in grades, motivates the use of CMC as a talc depressant in the flotation of UG2 ore, due to the strong negative charge density of CMC which can disperse the pulp (Becker et al., 2007; Manono et al., 2012; Wiese and Harris, 2012). As expected, the improvement in grade of sulfide minerals did not lead to a change in the recovery achieved as depressant selectively interacts with gangue. However unliberated sulfides were depressed at high depressant dosages of 300 g/t leading to a detrimental decrease in Ni recovery (Wiese, 2009).

6.2 Effect of Water Recirculation on the Pulp Chemistry

The main focus on the second phase of the study was on the impact of changing water quality through water recycling at different points of addition (mill vs float cell) on the pulp chemistry as described in Section 5.1, 5.2 and 5.3. Measurement of the change in pulp chemistry considered the EC, TDS, ORP and DO% as well as concentrations of residual reagents and specific inorganic ions and are reported in Sections 5.1.1 to 5.1.4. As expected, the observed trends in EC measurements from all the samples in the second phase mimic the observations made from TDS measurements, further showing that EC is a good measure of the TDS and vice versa as described in literature (Day and Nightingale, 1984; Gustafson and Behrman, 1939; Lystrom et al., 1978; Singh and Kalra, 1975). It was therefore hypothesized that:

Water Recirculation leads to an increase in the EC, and TDS concentration, through accumulation of ions (cations e.g., Ca^{2+} and Mg^{2+}, and anions e.g., SO_4^{2-} and Cl^-);

> *… occurs by ore dissolution which is based on the rest potential (ORP) of the system.*

EC, TDS and ORP readings were at their highest for 3 SPW, decreasing after contact with the ore in the comminution due to ore oxidation and dissolution which led to change in the species of ions in solution and the subsequent precipitation of ions out of solution in the form of colloidal species such as metal oxy-hydroxides, an indication of the impact galvanic interactions occurring in the milling environment (Bruckard et al., 2011; Górniak et al., 2009; Levay et al., 2001; Liu et al., 2013). In addition to the change in EC, the feed and tailings slurry all had a negative ORP in all recovered water samples, due to the presence of cations (i.e. Fe^{2+}, Ca^{2+}, Mg^{2+}) and thus the pulp was in a reductive state overall (Goncharuk et al., 2010). Water recirculation led to an increase in ORP above the base line conditions, possibly due to the galvanic interactions between minerals and grinding media.

Milling using recycled water (mill recirculation), in comparison to milling with 3 SPW, enhances the impact of the galvanic interaction of the ore due to the longer contact time with the ore as shown in Fig 5-1 and Fig 5-3, producing feed slurries at higher EC, TDS and ORP than those milled with process water (Goncharuk et al., 2010; Le et al., 2020). The higher extent of galvanic interactions, as shown by depletion in the DO %

from mill recirculation; produces a float feed slurry with a lower DO % as shown in Fig 5-7 (Bruckard et al., 2011).

The trends in EC, TDS, ORP and DO % show that comminution of the ore affects the pulp chemistry, the surface properties and the floatability of sulfide minerals mainly through electrochemical interactions, surface morphology and mechano-chemical reactions (Rao and Finch, 1988b; Wang and Xie, 1990).

Post flotation, the EC and TDS concentration of the tailings slurry was generally lower than the pre flotation value due to the dilution and the flow of ions that were present in the froth to the concentrate as shown in Fig 5-1 and Fig 5-3 (Goncharuk et al., 2010; Le et al., 2020). Therefore, both milling and flotation led to a change in the ionic concentration and hence the ionic strength of the pulp. Tailings and concentrate water samples all had similar EC and TDS concentrations as well as ORP readings for a particular recycle, apart from Recycle 2 and 3 in mill recirculation and the baseline tests, therefore the change in water quality during flotation produced water of a similar ionic strength in the concentrate and tailings, and thus downstream effects would be expected to be similar irrespective of the point of addition of recycled water. This provides the opportunity to recover and recycle from both concentrate and tailings dewatering units, i.e., thickeners and cyclones. The higher ionic concentration observed post milling in mill recirculation flows out of the pulp into the concentrate (playing a role in froth stabilization), leading to a decrease in IS of the tailing's product and a higher concentrate EC as observed in Recycle 2 and 3 in mill recirculation. Float cell recirculated water on the other hand had similar ORP readings in both the tailings water and the concentrate water, corresponding to the similar trends in EC values. Therefore, the change in water chemistry differs by point of addition. In addition, the EC and TDS of the tailings slurry and recovered water samples were higher than the feed slurry reading in float cell (Recycle 1 and 3), showing an increase in dissolved ion concentration during flotation. In addition, the higher ORP observed in float cell recirculation tailings slurries point to a higher concentration of cations present in the slurry due to continued ore dissolution during flotation.

The cations and anions present in the tailings slurry were monitored and shown in Section 5.2 for Ca^{2+}, Mg^{2+}, SO_4^{2-} and Cl^- which are typically found in PGM flotation circuits, owing to gangue dissolution (Jasieniak et al., 2010). Ca^{2+}, Mg^{2+} and SO_4^{2-} concentrations are higher in tailings water in float cell recirculation than in mill recirculation due to continuous dissolution of ore during froth flotation. Conversely the flow of ions in mill recirculation is further justified by the decrease in Ca^{2+}, Mg^{2+} and

SO_4^{2-} ions observed as they fell below base line test conditions the ions are utilized in the stabilization of the froth.

Conversely, for Cl^- concentrations in tailings water, mill recirculation had higher concentration than float cell recirculation. However, all Cl^- concentrations in the experiments with recycled water are lower than the Cl^- concentrations in the tailings water from the baseline float showing possible Cl^- precipitation.

Overall, as float cell recirculated water has higher Ca^{2+}, Mg^{2+}, and SO_4^{2-} at a higher EC and TDS, it can be considered to have higher ionic strength hence leading to higher solids and water recoveries due to improved froth stability similar to the observations of Dzingai et al. (2020) who showed an increase in water recoveries when moving from 3 SPW to 10 SPW. Therefore, in line with previous research, it could be said that ore dissolution and oxidation occurred during froth flotation leads to changes in water chemistry (Le et al., 2020). The higher ionic strength at the end of float cell recycles is a result of the availability of DO % in feed slurry promoting redox reactions between Fe^{3+} and other more reductive cations such as Ca^{2+} and Mg^{2+} (Bruckard et al., 2011). Water recycling through the mill produced a feed slurry with a significantly lower oxygen concentration, due to the continuous consumption of the available oxygen in galvanic interactions in the mill (Bruckard et al., 2011). The lower DO concentration observed in mill recirculation creates a low potential solution which could prevent the oxidation of the collector to form dithiolate which in turn may lead to lower flotation performance through reduced recoveries and grades of the desired minerals (Bradshaw et al., 2006; Yoon and Basilio, 1993).

6.3 Effect of Water Recirculation on Residual Reagent Concentration.

In addition to pulp chemistry measurements, the concentration of residual collector and depressant present in the tailings and concentrate water was measured, to determine the impact of changes in water quality on reagent concentration and consumption as a measure of reagent efficiency. It was therefore hypothesised that;

Water recirculation leads to a buildup in residual reagent concentration for both the collector, depressant and frother, due to accumulation of unused reagent remaining in the water.

Overall, the concentration of residual collector as shown in Fig 5-8 is lower (ppm range) compared to the collector feed of 150 g/t (11 g/L). Similarly, the concentration of

residual depressant as shown in Fig 5-9 is lower (ppm range) as compared to the feed of 100 g/t (9 g/L).

Therefore, as expected, changes in water quality through water recirculation did not hinder collector or depressant interaction with the valuable and non-valuable mineral surfaces leading to the high consumptions observed in the reagent efficiency and residual reagent concentrations in Fig 5-10 (Le et al., 2020; Wiese et al., 2007). The residual collector concentrations at a particular recycle were higher than the baseline conditions and their preceding recycles, but the increase is in smaller concentrations than the overall residual concentration showing the consumption of residual reagents during the milling and flotation operations. It is thus clear that the hypothesis holds for residual collector concentration. In addition, residual collector concentrations were higher in mill recirculation as compared to float cell recirculation due to the lower DO % in mill recirculation which hindered collector ore interactions, reducing its consumption (Garrels and Christ, 1990; King, 1982; Lovell, 1982). According to Gray et al., (2016), an increase in the solids recovery with a decrease in Cu grade and recovery is expected as the concentration of residual collector increases. However, this is not similar to the trends observed in the mineral recoveries and grades achieved in this study. Therefore, adding to the contention on the role of residual reagent on flotation performance as described in Slatter et al., (2009).

Residual depressant dosages displayed utilization of residual reagents present with reagent concentrations falling below their baseline dosed concentrations in Recycles 2, Recycle 1 (M) and Recycle 3 (F), and only slightly above in Recycle 1 (F) and Recycle 3 (M), where (M) denotes mill recirculation, and (F) denotes float cell recirculation. Therefore, for depressant dosages, the hypothesis does not hold. This is an added benefit of short water recirculation through utilization of residual reagents that would have otherwise gone to waste (Slatter et al., 2009). Overall, the concentration of residual depressant is higher in mill recirculation as compared to float cell recirculation, leading to the higher grades of Cu and Ni as observed in float cell recirculation (Bruckard et al., 2011). The presence of residual reagents motivates that short water recycling can have a detrimental impact on the effluent water chemistry and would require further treatment as prescribed by Slatter et al., (2009). Additionally, the concentrate water contains higher concentrations of residual reagents, due to the dilution of the tailings water in the float cell as the top up water is added. Therefore, concentrates water from cyclones and dewatering units are a valuable water source for water recirculation.

To investigate residual frothability of recovered water samples, 2 phase tests on the tailings and concentrate water samples were performed and compared to the calibration flotation tests.

The differences in froth stability observed in the 2-phase froth tests showed that a change in frothability occurred due to a change in the water chemistry and presence of residual frother. Foam stability of recycled water achieved foam heights within the froth heights observed at 30 and 40 g/t frother dosages, therefore displaying significant frothing properties. What is uncharacteristic is the longer bubble lifetime observed in the foam stability. Tailings water and concentrate from recirculated floats achieved higher foam heights and or had longer bubble lifetimes (exception of Recycle 2) due to the improved compression of the electrical double layer leading to the formation of smaller longer lasting bubbles, a characteristic of more stable foams as shown by the calibration plots in Fig 5-16 and Fig 5-19. The longer bubble lifetimes suggest a change in bubble rupture and bubble coalescence, and the formation of smaller bubbles. Inorganic electrolytes have been said to reduce the zeta potential of bubbles and particles, compressing the electrical double layers, and thus reducing the repulsive interaction, leading to a dominant hydrophobic force (Kurniawan et al., 2011). As for the point of recirculation, float cell reticulated more often, Recycle 1 and 3 for tailings water and Recycle 2 and 3 for concentrate water, had longer bubble lifetimes as compared to mill recirculated water, due to the higher ionic strength observed in these recycled water sources. The impact of the longer bubble lifetimes is well displayed in the kinetic models in Fig 5-20, where longer bubble lifetimes lead to slower froth build ups that achieved maximum froth height much later. In addition, due to the compression of the electrical double layer, the bubbles formed at longer bubble lifetimes are larger due to the larger volume of air carried as shown in Fig 5-17 and Fig 5-21.

Although there is no correlation between the bubble lifetimes and the height of the froth, and hence overall froth stability, these changes in froth stability could lead to variations in performance in downstream processes post flotation in industrial scale concentrator circuits.

6.4 Effect of Water Recirculation on Tailings Settling Rate

The tailings from flotation concentrators are fed to thickeners to dewater them (Mwale et al., 2005). The settling rate is an important operating parameter due to its influence on the operating time. The absorbance and transparency rates of the tailings from the

experiments performed were displayed in Fig 5-11and Fig 5-12, respectively. Initially it was hypothesized that;

Water recirculation leads to slower transparency rates of tailings due to the presence and accumulation of small particles (d < 25 µm), and accumulation of ions through ore dissolution which leads to an increase in the system charge leading to an increase in repulsion between particles.

Transparency rates and absorbance plots of all the tested conditions investigated the coagulation of tailings pulp. The tailings slurry in the settling tests was found to contain a solids concentration of 43 %, due to the flow of solids to the concentrate. The particle size distribution was also an important factor, however as expected majority of the small particles below 38 µm are better recovered, accounting for 67 % of the solids recovered to the concentrate during flotation as shown by the PSD of the tailings in Fig 6-1 and the feed in Fig 4-9 (Mwale et al., 2005). Therefore, while the hypothesis implies the accumulation of small particles in the tailings, there are in fact less fine (<25 µm) particles in the tailings than the feed, hence the smaller particles were recovered to the concentrate.

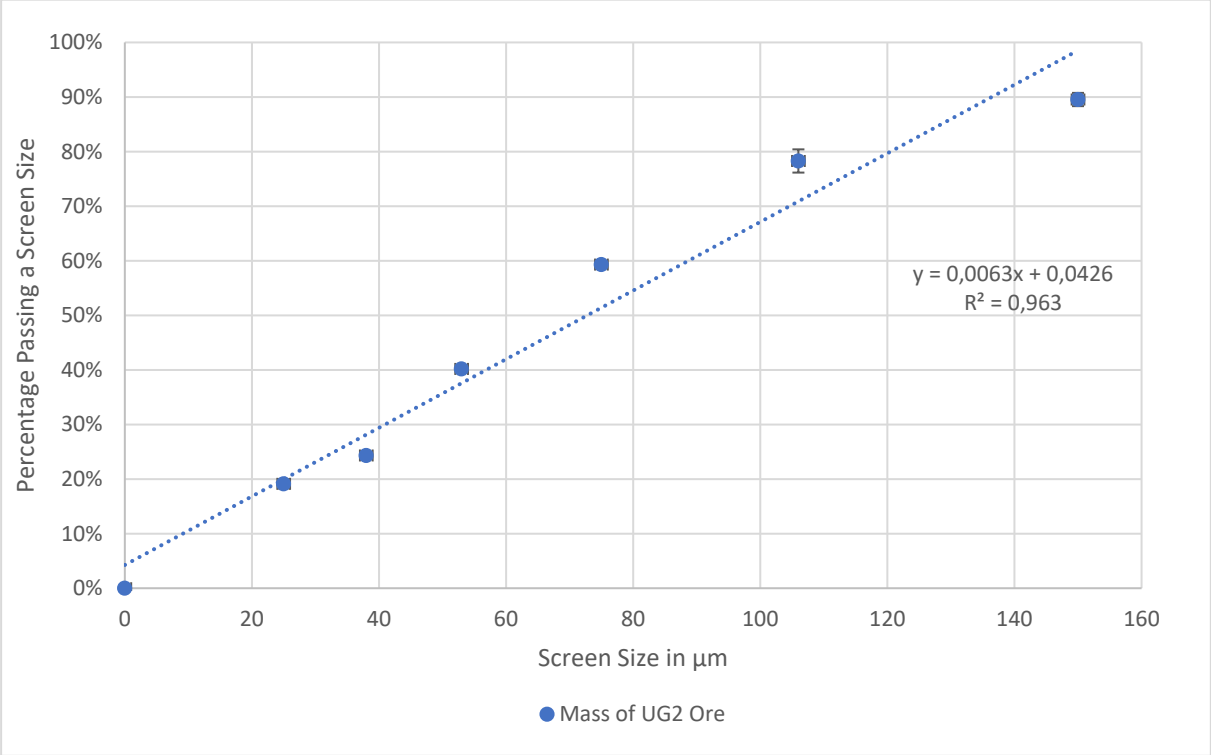

Fig 6-1. Cumulative Particle Size Distribution of Tailings from UG2 ore developed through wet screening

In fact, the tailings are mostly concentrated with larger sized particles (d> 38 µm), as compared to the feed, and for the significantly large particle sizes, the settling rate is a factor of the density of the particles (Mwale et al., 2005). This leads to fast transparency rates at the start of settling, which is similar in all the conditions in the first 60 seconds. After which the transparency rates begin to differ, between recirculated and non-recirculated and the point of addition of recirculated water, at this point the transparency rate constant (k) had an impact on how fast the maximum transparency would be achieved. Overall, 50 % transparency was achieved within the first 500 seconds in most conditions. Furthermore, for all the tested conditions, a maximum recovery was achieved within 3000 s (≈ 1 hour). Therefore, the maximum transparency became an important yardstick when comparing the change in transparency at the different tested conditions. The fast increase in transparency due to the initial settling of large particle followed by a slow build in transparency up to its maximum motivates and led to the use of second order kinetics as shown in Eq. (4-6) to model the trends observed. Settling rates for particles were modeled based on Stokes law for particles with Reynolds Number (Re) <0.2 as shown Eq. (6-1) where (g) represents the acceleration due to gravity (m/s), (d) diameter of spherical particle (m), (ρ_s), (ρ) density of the solid and liquid respectively, (K) Kozeny constant and (ε) cake voidage (Mwale et al., 2005).

$$u_p = \frac{d^2(\rho_s - \rho)g\varepsilon^3}{36K\mu(1-\varepsilon)} \qquad \text{Eq. (6-2)}$$

From Eq. (6-3) it is clear that for large particle sizes the settling rate is defined by the top part of the equation while as the particle size decreases, the viscosity of the fluid plays a role in the settling velocity. The ionic concentration of the fluid has an impact on the slurry viscosity (Slatter et al., 2009). Therefore, the initial rapid increase in transparency is due to the large particle sizes settling, however the settling rates begin to differ due to the increase in the denominator of Eq. (4-6) increasing, where if compared to the settling rate formula is a factor of the viscosity of the fluid. Thus, an increase in the electrolyte concentration in recycled water increased the slurry viscosity.

In recirculated water the coagulation of tailings was generally more rapid and produced a more transparent supernatant as compared to the base line conditions for most of the tests.

Therefore, the presence and accumulation of inorganic species (Ca^{2+} and Mg^{2}) and residual reagents influenced coagulation by adsorbing on to the gangue surface enhancing flocculation by improving the specific gravity of the pulp. In addition, the compression of the electrical double layer due to the presence of Ca^{2+} and Mg^{2+} improved the coagulation of particles by improving particle contact and hence overall flocculation (Boshrouyeh Ghandashtani et al., 2022). Mill recirculation achieved higher transparency and transparency rates as compared to float cell recirculation, due to the lower concentrations of charged ions present in the tailings water reducing the impact of particle repulsion in the slurry slowing down settling rates.

6.5 Effect of Water Recirculation on the Dynamic Froth Stability and Flotation Performance.

The change in water quality due to an increase in the ionic concentration can be observed through water recovery during froth flotation and from froth stability tests (Corin et al., 2011; Farrokhpay, 2011). However, the increase in frothability with an increase in ionic strength is not expected as the frother utilized is a poly glycol ether, Dow 200, which is a non-ionic frother and such, it would not be affected by the ionic concentration (Corin et al., 2011). Film stability in the presence of hydrophobic particles has been shown to increase with a decrease in contact angle and is at a maximum between contact angles of 66^{o} and 0^{o}, and is at a minimum when hydrophilic particles are present (Farrokhpay, 2011). The increase in froth stability is compounded during froth flotation, as the presence of hydrophobic materials in the froth lead do a more stable froth as observed by Farrokhpay, (2011), hence the significant difference observed in solids and water recoveries observed in float cell and mill recirculation. With this in mind, 3-phase froth stability tests on the tailings showed the minimum froth stability due to the high concentration of naturally hydrophobic gangue. The foam and froth stability results differ significantly, and this is as expected due to the impact of solid particles on the froth stability as the particles impact the froth stability as they form coherent shells around the bubbles and stabilize the liquid films forming a three-dimensional network in the bulk aqueous phase (Farrokhpay, 2011; Farrokhpay and Zanin, 2012; Kurniawan et al., 2011; Wiese and Harris, 2012). The initial hypothesis was that:

“Water recirculation increases solids and water recoveries, increasing the recovery of gangue, in turn, the grade of the concentrate decreases due to the higher froth stability and a higher degree of gangue entrainment.”

3-phase dynamic froth stability tests showed that for all recirculated floats had froths that developed with higher equilibrium froth height (H_{max}), longer bubble lifetimes and higher dynamic stability factors, and hence a higher froth stability than baseline conditions, Recycle 0, similar to findings on the impact of degrading water quality (Corin et al., 2011; Mccall, 2016; O'Connor and Mills, 1995). The higher froth stability observed in recycled water can be attributed to an increase in the ionic strength of its slurry which improves the gas hold up (volume % of air on the froth phase) by compressing the electrical double layers between the bubbles leading to the formation of more stable, high froths with short build up time, leading to higher water and solids recoveries as observed in Fig 5-22 (Corin et al., 2011; Kurniawan et al., 2011; Manono et al., 2012; Quinn et al., 2007; Slatter et al., 2009).

This is due to a reduction of the zeta potential between particles and bubbles and a higher surface tension leading to stronger liquid film around the bubbles (Kurniawan et al., 2011).

Recycling water through the float cell achieved the highest equilibrium froth height, and longest bubble lifetime in most of the tested conditions, suggesting that recycling water through the float achieved a higher froth stability. This further confirms the impact of additional redox reactions occurring during froth flotation due to the presence of DO %. The lower froth stability observed when recycling water through the mill could also be due to the destruction of residual frother at high temperatures achieved in the mill (Farrokhpay, 2011; Farrokhpay and Zanin, 2012). The increased froth stability leads to a non-selective increase in solids recovery, leading to more entrained gangue recovery and this is more significant in float cell recirculation observed in Table 5-2. The higher froth stability due to water recycling affects the performance of the batch flotation tests as observed in the solids, water, Cu and Ni recoveries and grades Fig 5-8 to Fig 5-31. Therefore, the change in water quality, through short recirculation led to a change in water quality, and this change had an effect on the flotation performance, increasing the solids and water recoveries due to an increase in ionic strength of recirculated process water.

The point of addition of recycled water led to a difference in the flotation performance at similar recycle stages. Recycling water led to an increase in solids and water recoveries above the baseline conditions, with the increase observed being more significant in float cell recirculation. Higher water recoveries led to higher solids recoveries due to both entrainment, entrapment and reduced drainage from bubble

ruptures, however it is non-selective thereby, reducing the grades of the concentrate, as observed (Corin et al., 2011; Manono et al., 2018).

Kinetic models of solids and water recoveries further qualify the observed difference both in the rate constants and equilibrium recovery between the tested conditions. The rate constants for solids and water recoveries being highest in float cell recirculation, with a less notable difference between mill recirculation and baseline models, therefore water reticulation led to an improved flotation performance as per the maximum recovery of solids and water and the rate constants of recovery (Boujounoui et al., 2015; Haran et al., 2008). The higher ionic strength in float cell recirculation led to an increase in gangue entrainment, increasing the solids per gram of water recovered due to the increased froth stability with reduced drainage and bubble coalescence (Barbian et al., 2006, 2005a).

Overall, the similar gangue entrainment and water and solid recoveries observed across floats for a particular point of addition can be attributed to the slow build-up of ionic strength through consecutive recycles due to a short residence time. Significant deviations in the foam/froth height and the bubble lifetime observed as an impact of water recirculation can lead to two outlier conditions one of fast floating height foams/froths, similar to process water foam development, or slow developing foams (large bubble lifetime) with a low foam/froth height, with significant implications on the overall flotation performance (Farrokhpay, 2011; Farrokhpay and Zanin, 2012; Kurniawan et al., 2011; Wiese and Harris, 2012).

The change in water quality impacts the sulfide mineral recoveries and grades, significantly, influencing the flotation performance. Sulfide recovery and grade respond differently to changes in water quality. Cu and Ni recoveries and grade were used to introspect on the flotation performance of other PGE's. Recoveries and grade of fast-floating mineral like chalcopyrite (Cu), showed different performance to slower floating mineral like pentlandite (Ni) (Becker et al., 2007). Flotation of Cu achieved a higher maximum recovery when using recycled water due to the higher mass pull, and due to the fast-floating nature of chalcopyrite, both points of addition were at a similar flotation rate constant. Flotation using recycled water achieved a higher Ni and Cu recovery per unit mass of water as compared to the baseline floats, with the highest recoveries observed in float cell recirculation, suggesting a higher carrying capacity of recycled water (Boujounoui et al., 2015; Haran et al., 2008). The increase in Cu grades at higher Ca^{2+} concentrations was also observed by Dzingai et al. (2020), who noted increased grades at higher concentrations of Ca^{2+} up to 400 mg/L in 3 SPW water.

Ca^{2+} forms $CaCO_3$ and $Ca(OH)_2$ that can interact and form precipitates on the mineral surface, with its effect suggested to be more effective on Ni bearing minerals, leading to lower Ni recoveries observed in float cell recirculation (Kirjavainen et al., 2002). Due to the higher prevalence of Mg^{2+} in the ore, at 7 %, than Ca^{2+} at 3 %, it is oxidised more, having a significant impact on flotation performance where at its highest concentrations in Recycle 2 in float cell and mill recirculation and Recycle 3 in mill recirculation, the lowest Cu recoveries were achieved similar to findings by Dzingai et al. (2020). Therefore, the non-selective increase in mass pull due to increased ionic strength and the impact of selected ions improved the recoveries of Cu and Ni, and float cell recirculation achieving the highest mass pull, similar to observations by Manono et al.(2018).

Cu and Ni grades and recoveries were lower compared to other studies due to the choice of reagent suite selection, the presence of particular ions (Ca^{2+} and Mg^{2+}) and the operating pH of 8.23 ± 0.03 in the flotation of UG2 ores, allowing the observations observed that would not be possible under optimized conditions in Fig 5-26 and Fig 5-29 (Afolabi et al., 2013; Dzingai et al., 2020). There is no association between SO_4^{2-} concentrations and changes in the Cu and Ni grades and recoveries; as they fell within concentration boundaries of between 720 to 1200 mg/L previously attributed to being threshold concentrations that have no impact on the grades and recoveries (Dzingai et al., 2021). The increase in mineral recoveries with mass pull showed that ions present did not inhibit the hydrophobic nature of the minerals, ensuring that the recirculated water was still fit for purpose.

However, the change in water quality can lead to unprecedented changes in performance, for example Recycle 2 in float recirculation resulted in lower Cu recovery per mass of water. This could be attributed to the short bubble lifetime observed in both foam and froth stability of the tailings, similar to 3 SPW froths and foams, hence a lower Cu recovery as a result of an increased in drainage and bubble rupture (Farrokhpay, 2011). The second anomaly observed was the higher equilibrium recovery of Cu observed in the first recycle through the mill in both kinetic and water response models. High froth heights for both the concentrate and tailing water foam stability tests were also observed and these correlated well with the improvement in Cu recoveries. These two situations show distinct changes in the water quality that led to outlier performance, and that the reactions still occurring and in the presence of complex chemical lead to an active and dynamic state of recirculated water that have an impact on flotation performance.

7 Conclusions

This study did not directly change the water quality; however, water recirculation was simulated through a benchscale set-up as described in Chapter 4. Through the methodology developed in Chapter 4, it was possible to both monitor and link observations to studies that controlled the variables monitored. Therefore, changes in water quality were monitored by a number of methods, already available and compared to available trends to predict and control the performance of mineral concentrators. Although this study performed a small number of short recycles, the change in water quality was observed in flotation performance as well as in the solids, water, sulfide mineral recoveries and grades. The properties of the froth and foam as well as the mineral characteristics were determined including the determination of residual collectors, depressants and frothers in the recirculated process water.

7.1 What is the impact of a change in Water Quality through Water Recycling on the Electrical Conductivity (EC), Oxidative Redox Potential (ORP), Dissolved Oxygen Concentration (DO %) of the Batch Flotation Feed Slurry, Tailings Slurry and Recovered Water Samples?

EC and TDS measurements of all the samples showed similar trends as expected showing that EC is a good measure of TDS and vice versa. The interaction of the ore with 3 SPW water led to a decrease in the EC, TDS, ORP due to a decrease in ionic concentration through precipitation of salts and these reactions consume the DO %. Galvanic interactions occurring in the mill led to an increase in the ionic concentrations as shown in the higher EC, TDS and ORP measurements, and consecutive milling with recycled water led to accumulation of ions due to the longer contact period. Galvanic interactions consume the available DO %, leading to significantly lower DO % when milling with recycled water. The concentration of DO % controls further ore dissolution as observed in float cell recirculation which had continuous ore dissolution leading to a higher ionic concentration as shown by the EC, TDS, and ORP readings.

Ions present post milling are utilized in froth stabilization as observed in mill recirculation leading to a decrease in the ionic concentration. The higher EC, TDS, and ORP observed in the tailings from float cell recirculation is further confirmed by the higher ionic concentration of Ca^{2+}, Mg^{2+}, and SO_4^{2-}. Monitoring the EC, TDS and ORP pre and post flotation informed on the flow of ions during flotation, where in mill recirculation the ion concentration decreases due to the role of ions in froth stabilization and hence are carried away in the froth as shown by the decrease in EC.

The impact of addition of top up water led to dilution of the tailing's slurry at a lower EC, TDS and ORP reading. What is clear from pulp chemistry measurements is that continuous water recycling leads to an accumulation of ions present in solutions. These ions are common to the ore and play a role in the flotation performance by impacting froth stability. The choice of point of addition of recycled water plays a significant impact on the availability of dissolved oxygen and the chemical interactions that can occur during froth flotation.

The similar chemical properties of the tailings and concentrate waters, justifies recycling of water recovered from both the cyclones and thickeners to other unit operations in a typical sulfide ore concentrator. The benefit of monitoring EC, TDS, ORP and DO % allowed for the monitoring of galvanic interactions and ore dissolution occurring during froth flotation and the impact of these changes on the flotation performance.

Furthermore, short water recirculation leads to changes in the water chemistry and can affect flotation performance based on how the change in water chemistry affects both the pulp phase and froth phase phenomena.

7.2 What is the impact of Water Recycling on the Concentration of Ca^{2+}, Mg^{2+}, $SO_4^{2-}$and Cl^- present in the tailings water?

GDACA of tailings water samples showed the concentrations of Ca^{2+}, Mg^{2+}, SO_4^{2-} and Cl^- present in the tailings water. The concentration of Ca^{2+}, Mg^{2+} and SO_4^{2-} were at their highest in float cell recirculated water as compared to base line test conditions and mill recirculated water samples.

Mill recirculated tailings water concentrations of Ca^{2+}, Mg^{2+} and SO_4^{2-} were below baseline conditions. Cl^- concentrations were at their highest in the tailings of the baseline tests, and for all the recirculated water, mill recirculated water had higher Cl^- concentrations as compared to float cell recirculated water. Significant Mg^{2+}concentrations reduced the flotation performance of Cu due to its ability to coat on to the mineral surface preventing collector interaction.

The higher concentration of ions in recirculated tailings water further justified the higher ionic strength as observed in 3 and 2 phase froth stability and EC, TDS and ORP measurements and the difference in ionic strength between the two points of addition.

7.3 What is the impact of a change in water quality on the settling rate of the tailings from UG2 ore froth flotation?

The settling of the tailing's slurry was monitored through the transmission measurement of the supernatant solution. Transparency and transparency rate constants calculated informed on the rate of change in settling of particles. The transparency rates are all similar within the first 50 seconds due to the rapid settling of large particles, after which the repulsion owing to the presence of ions impacts the rate of particle collisions and coagulation of the tailings.

Recirculation to the float cell resulted in leads to a faster rate of settling as observed in the rate constant above the settling rate observed in the baseline test leading to a transparency of the supernatant above 70 %. Recirculation to the mill cell resulted in the highest settling rate observed above float cell recirculation as observed in the rate constant and achieve the highest transparency above 80 %. Water recirculation improved the rate of settling of the particles present in the tailings due to the higher ionic strength which causes a higher system charge, leading to higher repulsions, causing more collisions of particles which in the presence of CMC aided the flocculation of particles.

7.4 What is the impact of a change in Water Quality through Water Recycling, and the point of addition of Recycled Water, on Froth Stability?

The increase in froth stability brought about by water recirculation was monitored through 3 phase, 2 phase stability column flotation tests and the overall water recovery. The increase in ionic strength due to water recycling led to an increase in the froth height, dynamic stability factor and bubble lifetime of the tailings slurry and recovered water samples in all samples tested above the baseline conditions and were at their highest in float cell recirculation.

The improved ionic concentration reduced the zeta potential of bubbles and particles, compressed the electrical double layers, and hence reduced the repulsive interaction, leading to a dominant hydrophobic force. The increase in bubble lifetime led to a slow development of froths which is detrimental to flotation performance due to an increase in the residence time before the recovery of value.

Water recirculation leads to a change in the ionic concentration of the water that significantly increases the strength of the electrical double layer leading to significantly longer bubble lifetime observed in 2 phase as compared to 3 phase tests. The 3 phase tests show the impact of the presence particles on the froth stability as they form coherent shells around the bubbles and stabilize the liquid films forming a three-dimensional network in the bulk aqueous phase.

The nature of particles is also important as froth stability is at its highest in the presence of hydrophilic particles which at a high contact angle of 66^{o} reduce the zeta potential of bubbles, compressing the electrical double layers, and hence reduce the repulsive interaction, leading to a dominant hydrophobic force.

The relatability of the 3-phase tailing froth stability and flotation performance allows for the feedback analysis of flotation performance through 3 phase dynamic stability tests. In addition, a significant increase or decrease in froth stability of foams (2 phase tests) due to the change in the ionic concentration leads to a significantly high and low Cu recoveries respectively as shown in the study.

All recovered water samples had a froth stability higher than at a frother dosage at 30 g/t, due to the improved ionic strength and the residual frother present. However, addition of frother in subsequent tests is advised as the increase in bubble lifetime is a demerit of the higher ionic strength and can be mitigated by addition of fresh frother. Recycling to the mill can lead to residual frother destruction due to the high temperatures achieved in the mill, thereby denaturing, or lowering the activity of the residual frother molecules.

7.5 What is the effect of a change in Water Quality through Water Recycling, and point of addition of recycled water, on the flotation performance of a UG2 ore?

The change in water quality increased the ionic strength, increasing the solids, water, Cu and Ni recoveries, maximum recoveries, and rate constants, however due to the non-selective increase in entrainment which is increased by increased water recoveries/froth stabilities, the recirculation of water leads to a dilution of the concentrate grade.

The higher ionic strength observed in the float cell recirculated water led to higher solids, water, Cu and Ni recoveries, maximum recoveries and rate constants as compared to mill recirculation. Furthermore, the particle size analysis of the feed and tailings samples from the baseline tests showed that majority of the particles recovered in the concentrate were well below 38 μm, further justifying the importance of comminution in froth flotation. Short water recycling led to an improved flotation performance in terms of solids, water and sulfide recovery and addition of recycled water to the float cell achieved the highest performance in leu of a slight decrease in sulfide grade as observed in both points of additions.

Recovery kinetics of slow floating minerals are affected by a change in water quality as the increase in ionic concentrations and froth stability leads to an increase in the recovery of sulfide minerals. Accumulation of ions brought about by water recirculation may lead to an increase in solids, water, sulfide mineral and gangue recoveries in a concentrator and downstream when a series of concentrator are in use. Monitoring and control of the change in water quality is imperative to ensure that the product grade is not adversely affected.

7.6 Concluding Remarks

This study successfully showed that water recycling leads to an increase in ionic concentrations due to ore dissolution in the mill and during froth flotation. The dissolved ions are primarily from the common gangue minerals found in the ore such as Ca^{2+}, Mg^{2+}, SO_4^{2-} and Cl^-. The choice of point of addition leads to a significant difference in performance and pulp chemistry; recycling water to comminution operations may lead to a depletion of DO % present while recycling water to the float cell may allow for the highest froth stability achievable as per the tests.

The higher ionic strength in the water quality improves the solids, water, and sulfide recovery, with a higher solids load per unit water. However, as entrainment is non-selective, an increase in the amount of entrained gangue as seen in this study may have a detrimental impact on the concentrate grade. The study has also shown that EC, ORP, DO %, 2 and 3 phase froth stability tests are good indicators of pulp chemistry and froth stability and can be utilized to inform decisions on water recirculation during the flotation of low-grade Cu-Ni-PGM ores such as the one used in this study.

Short water recirculation contains residual reagents which may be present in minimal concentrations; hence additional dosing of reagents is necessary to achieve the desired flotation performance. Furthermore, the settling rate in tailings thickeners may initially be controlled by the flow of large particle sizes but is aided by the presence of ions that improve the flocculation in the pulp hence thickener operations will benefit from water recycling. The improved ionic strength can be detrimental due to the longer bubble lifetime leading to slow developing froths that require longer residence times in the concentrator to achieve a suitable froth recovery.

8 Recommendations

After consideration of the results and conclusions developed from this study, the following recommendations have been made:

- Similar tests must be performed on different ore bodies and assess if the observations can be translated to other ores.
- The strong initial dependence of settling rate on particle size motivates for an analysis of settling rate as a function of particle size to develop information on settling rates.
- First order kinetic models of Cu and Ni recoveries and water response did not perfectly model the trends suggesting a need for an application of more complex models.
- pH control should be considered in the test procedure as a maintained variable to remove any variations that may have an impact on flotation performance.
- The higher ionic strength observed post milling motivate GDACA of the feed water samples to further inform on the impact of galvanic interactions.
- The increase in froth stability observed in response to water recycling motivates that zeta potential and bubble size tests must be considered to further interrogate the impact of water quality change.
- Quantitative analysis of residual frother to decouple the impact of residual ionic strength and residual frother on froth stability must be conducted.
- Factorial Design of experiment accompanied by statistical analysis to develop relationships of the different factors to consider must be included in future studies.
- The significant difference in EC between SPW water and slurry motivates that test work on the impact of ore contact time on the water quality must be considered.
- The slow change in performance for consecutive recycles per point of addition motivates for a study with more recycles with controlled interval times or the implementation of longer residence times per recycle run.

9 References

Afolabi, A.S., Muzenda, E., Abdulkareem, S.A., 2013. Effect of pH on the floatability of base metal sulphides PGMs. Lect. Notes Electr. Eng. 170 LNEE, 239–248. https://doi.org/10.1007/978-94-007-4786-9_19

Allen, T., 1965. Particle size measurement. Powder Technol. Ser. 2, 529. https://doi.org/10.1038/208529b0

Alva, A.K., Sumner, M.E., Miler, W.P., 1991. Relationship between ionic strength and electrical conductivity for soil solutions. Soil Sci. 152.

Anning, D.W., Flynn, M.E., 2014. Dissolved-solids sources, loads, yields, and concentrations in streams of the conterminous United States, Scientific Investigations Report. Reston, VA. https://doi.org/10.3133/sir20145012

Aqion, 2015. Electrical conductivity [WWW Document]. URL https://www.aqion.de/site/130 (accessed 7.13.20).

Barbian, N., Hadler, K., Cilliers, J.J., 2006. The froth stability column: Measuring froth stability at an industrial scale. Miner. Eng. 19, 713–718. https://doi.org/10.1016/j.mineng.2005.09.021

Barbian, N., Hadler, K., Ventura-Medina, E., Cilliers, J.J., 2005a. The froth stability column: Linking froth stability and flotation performance. Miner. Eng. 18, 317–324. https://doi.org/10.1016/j.mineng.2004.06.010

Barbian, N., Hadler, K., Ventura-Medina, E., Cilliers, J.J., Jokinen, M., Jokinen, M., Suoniemi-kähärä, A., Barbian, N., Hadler, K., Ventura-Medina, E., Cilliers, J.J., 2005b. The froth stability column: Linking froth stability and flotation performance. Miner. Eng. 18, 317–324. https://doi.org/10.1016/j.mineng.2004.06.010

Barbian, N., Ventura-Medina, E., Cilliers, J.J., 2003. Dynamic froth stability in froth flotation. Miner. Eng. 16, 1111–1116. https://doi.org/10.1016/j.mineng.2003.06.010

Becker, M., 2009. The mineralogy and crystallography of pyrrhotite from selected nickel and PGE ore deposits and its effect on flotation performance. Dep. Mater. Sci. Metall. Eng. University of Pretoria.

Becker, M., Bradshaw, D.J., Harris, P.J., Wiese, J.G., Becker, M., Bradshaw, D.J., Harris, P.J., 2007. Interpreting the role of reagents in the flotation of platinum-bearing Merensky ores. J. South. African Inst. Min. Metall. 107, 29–36.

Becker, M., De Villiers, J.R.R., Bradshaw, D., 2008. Evaluation of pyrrhotite from selected Ni and platinum group element (PGE) ore deposits and the influence of its mineralogy on flotation performance. Australas. Inst. Min. Metall. Publ. Ser. 401–409.

Becker, M., Harris, P., Wiese, J., Bradshaw, D.J., 2006. The use of quantitative

mineralogical data to interpret the behaviour of gangue minerals in the flotation of Merensky ores, in: MEI Conference on Automated Mineralogy, Brisbane.

Biçak, Ö., Ekmekçi, Z., Can, M., Öztürk, Y., 2012a. The effect of water chemistry on froth stability and surface chemistry of the flotation of a Cu-Zn sulfide ore. Int. J. Miner. Process. 102–103, 32–37. https://doi.org/10.1016/j.minpro.2011.09.005

Biçak, Ö., Ekmekçi, Z., Can, M., Öztürk, Y., Bıçak, Ö., Ekmekçi, Z., Can, M., Öztürk, Y., Biçak, Ö., Ekmekçi, Z., Can, M., Öztürk, Y., Bıçak, Ö., Ekmekçi, Z., Can, M., Öztürk, Y., 2012b. The effect of water chemistry on froth stability and surface chemistry of the flotation of a Cu–Zn sulfide ore. Int. J. Miner. Process. 102–103, 32–37. https://doi.org/https://doi.org/10.1016/j.minpro.2011.09.005

Bickerman, J.J., 1973. Foam films. Foams.

Bleiwas, D.I., 2012. Estimated Water Requirements for the Conventional Flotation of Copper Ores. USGS Open-File Rep. 2012–1089, 1–13.

Boshrouyeh Ghandashtani, M., Costine, A., Edraki, M., Baumgartl, T., 2022. The impacts of high salinity and polymer properties on dewatering and structural characteristics of flocculated high-solids tailings. J. Clean. Prod. 342, 130726. https://doi.org/10.1016/j.jclepro.2022.130726

Boujounoui, K., Abidi, A., Bacaoui, A., El Amari, K., Yaacoubi, A., 2015. The influence of water quality on the flotation performance of complex sulphide ores: case study at Hajar Mine, Morocco. J. South. African Inst. Min. Metall. 115, 1243–1251. https://doi.org/10.17159/2411-9717/2015/v115n12a14

Bradshaw, D.J., 1997. Synergistic effects between thiol collectors used in the flotation of pyrite 220.

Bradshaw, D.J., Buswell, A.M., Harris, P.J., Ekmekci, Z., 2006. Interactive effects of the type of milling media and copper sulphate addition on the flotation performance of sulphide minerals from Merensky ore Part I: Pulp chemistry. Int. J. Miner. Process. 78, 153–163. https://doi.org/10.1016/j.minpro.2005.10.004

Bruckard, W.J., Sparrow, G.J., Woodcock, J.T., 2011. A review of the effects of the grinding environment on the flotation of copper sulphides. Int. J. Miner. Process. 100, 1–13. https://doi.org/10.1016/j.minpro.2011.04.001

Buchspies, B., Thormann, L., Mbohwa, C., Kaltschmitt, M., 2017. Environmental Aspects. https://doi.org/10.3390/min7110225

Buckley, A.N., Woods, R., 1984. An X-ray photoelectron spectroscopic study of the oxidation of chalcopyrite. Aust. J. Chem. 37, 2403–2413.

Bulatovic, S.M., 2007. Handbook of Flotation Reagents, 1st ed, Flotation of Sulphide Ores. Elsevier Science Publishers Ltd, Petersborough. https://doi.org/10.1016/b978-0-444-53029-5.x5009-6

Bunyak, D., 2000. To Float or Sink: A Brief History of Flotation Milling. Min. Hist. Assoc. 7, 35–44.

Burdukova, E., 2007. Surface Properties of New York Talc as a Function of pH, Polymer Adsorption and Electrolyte Concentration. Univeristy Cape T. 140.

Burdukova, E., Leerdam, G.C. Van, Prins, F.E., Smeink, R.G., Bradshaw, D.J., Laskowski, J.S., 2008. Effect of calcium ions on the adsorption of CMC onto the basal planes of New York talc – A ToF-SIMS study 21, 1020–1025. https://doi.org/10.1016/j.mineng.2008.03.017

Cañedo-Argüelles, M., Kefford, B.J., Piscart, C., Prat, N., Schäfer, R.B., Schulz, C.-J., 2013. Salinisation of rivers: An urgent ecological issue. Environ. Pollut. 173, 157–167. https://doi.org/https://doi.org/10.1016/j.envpol.2012.10.011

Carlson, L., Bigham, J.M., Schwertmann, U., Kyek, A., Wagner, F., 2002. Scavenging of As from acid mine drainage by schwertmannite and ferrihydrite: A comparison with synthetic analogues. Environ. Sci. Technol. 36, 1712–1719. https://doi.org/10.1021/es0110271

Caro, C.A. De, 2017. UV / VIS Spectrophotometry.

Cawthorn, R.G., 2011. Geological interpretations from the PGE distribution in the Bushveld Merensky and UG2 chromitite reefs 111, 11–14.

Celik, M.S., Somasundaran, P., 1980. Wettability Of Reservoir Minerals By Flotation And Correlation With Surfactant Adsorption. SPE Oilf. Geotherm. Chem. Symp. https://doi.org/10.2118/9002-MS

Chau, T.T., 2009. A review of techniques for measurement of contact angles and their applicability on mineral surfaces. Miner. Eng. 22, 213–219. https://doi.org/10.1016/j.mineng.2008.07.009

Chaves, A.P., Ruiz, A.S., 2009. Considerations on the kinetics of froth flotation of ultrafine coal contained in tailings. Int. J. Coal Prep. Util. 29, 289–297. https://doi.org/10.1080/19392690903558371

Clifford, R.K., Purdy, K.L., Miller, J.D., 1974. in Proc. Appl. Interfaciai Phenomena in Flotation Research, null.

Corin, K.C., Mishra, J., O'Connor, C.T., 2013. Investigating the role of pulp chemistry on the floatability of a Cu–Ni sulfide ore. Int. J. Miner. Process. 120, 8–14.

Corin, K.C., Reddy, A., Miyen, L., Wiese, J.G., Harris, P.J., 2011. The effect of ionic strength of plant water on valuable mineral and gangue recovery in a platinum bearing ore from the Merensky reef. Miner. Eng. 24, 131–137. https://doi.org/10.1016/j.mineng.2010.10.015

Corin, K.C., Wiese, J.G., 2014. Investigating froth stability : A comparative study of ionic strength and frother dosage. Miner. Eng. 66–68, 130–134.

https://doi.org/10.1016/j.mineng.2014.03.001

Corsi, S.R., De Cicco, L.A., Lutz, M.A., Hirsch, R.M., 2015. River chloride trends in snow-affected urban watersheds: Increasing concentrations outpace urban growth rate and are common among all seasons. Sci. Total Environ. 508, 488–497. https://doi.org/10.1016/j.scitotenv.2014.12.012

Couper, J.R., Penney, W.R., Fair, J.R., Walas, S.M.B.T.-C.P.E. (Second E. (Eds.), 2005. Chapter 10 - Mixing and Agitation. Gulf Professional Publishing, Burlington, pp. 277–328. https://doi.org/https://doi.org/10.1016/B978-075067510-9/50042-5

Crozier, R.D., 1992. Flotation: theory, reagents and ore testing. Pergamon Oxford.

Dautzenberg, H., Kowal, A., Kowal, J., Dietzel, W., 1984. Decomposition of xanthates in flotation solutions, in: Reagents in Mineral Industry. IMM London, pp. 47–51.

Day, B.A., Nightingale, H.I., 1984. Relationships Between Ground-Water Silica, Total Dissolved Solids, and Specific Electrical Conductivity. Groundwater 22, 80–85.

Desa, U.N., 2016. Transforming our world: The 2030 agenda for sustainable development.

Dey, S., Parolis, L.A.S., Yorath, G., 2012. Quantification of sulphydryl collector-mixture used in sulphide ore flotation. Trans. Indian Inst. Met. 65, 387–392. https://doi.org/10.1007/s12666-012-0142-9

Dhliwayo, E.C., 2005. The interactive effect of depressant type and dosage with frother dosagein the flotation of a PGE ore.

DOW CORING, 2015. MSDS DOW CORING 200 [WWW Document]. URL http://webcache.googleusercontent.com/search?q=cache:9LbFSuuSAT8J:download.flukecal.com/pub/literature/SDS_dw200-05.pdf+&cd=2&hl=en&ct=clnk&gl=za (accessed 7.18.20).

Dowling, E.C., Klimpel, R.R., Aplan, F.F., 1985. Model Discrimination in the Flotation of a Porphyry Copper Ore. Mining, Metall. Explor. 2, 87–101. https://doi.org/10.1007/BF03402602

Dubois, M., Gilles, K.A., Hamilton, J.K., Rebers, P.A., Smith, F., 1956. Colorimetric Method for Determination of Sugars and Related Substances. Anal. Chem. 28, 350–356. https://doi.org/10.1021/ac60111a017

Dzingai, M., Manono, M., Corin, K., 2020. Simulating the Effect of Water Recirculation on Flotation through Ion_Spiking: Effect of Ca2+ and Mg2+. Minerals 13. https://doi.org/https://doi.org/10.3390/min10111033

Dzingai, M., Manono, M.S., Corin, K.C., 2021. Probing the effect of water recycling on flotation through anion spiking using a low-grade Cu–Ni–PGM ore: The effect of NO3−, SO42− and S2O32−. Minerals 11. https://doi.org/10.3390/min11040340

Dzvinamurungu, T., Viljoen, K.S., Knoper, M.W., Mulaba-Bafubiandi, A., 2013. Geometallurgical characterisation of Merensky Reef and UG2 at the Marikana Mine, Bushveld Complex, South Africa. Miner. Eng. 52, 74–81. https://doi.org/10.1016/j.mineng.2013.04.010

Ek, K.H., Morrison, G.M., Rauch, S., 2004. Environmental routes for platinum group elements to biological materials — a review 335, 21–38. https://doi.org/10.1016/j.scitotenv.2004.04.027

Ekmekçi, Z., Bradshaw, D.J., Allison, S.A., Harris, P.J., 2003. Effects of frother type and froth height on the flotation behaviour of chromite in UG2 ore. Miner. Eng. 16, 941–949. https://doi.org/10.1016/j.mineng.2003.08.001

Encyclopaedia Britannica, 2012. Encyclopaedia Britannica [WWW Document]. Encycl. Br. URL https://www.britannica.com/technology/flotation-ore-dressing (accessed 6.29.20).

Eriez Manufacturing Co., 2021. Rod/Ball Mill| Eriez Lab Equipment.

Evans, D.M., Zipper, C.E., Donovan, P.F., Daniels, W.L., 2014. Long-Term Trends of Specific Conductance in Waters Discharged by Coal-Mine Valley Fills in Central Appalachia, USA. J. Am. Water Resour. Assoc. https://doi.org/10.1111/jawr.12198

Farrokhpay, S., 2011. The significance of froth stability in mineral flotation - A review. Adv. Colloid Interface Sci. 166, 1–7. https://doi.org/10.1016/j.cis.2011.03.001

Farrokhpay, S., Zanin, M., 2012. An investigation into the effect of water quality on froth stability. Adv. Powder Technol. 23, 493–497. https://doi.org/10.1016/j.apt.2012.04.012

Finch, J.A., 1995a. Pergamon Column flotation : A selected review part IV :novel flotation devices * Froth washing. Science (80-.). 8, 587–602.

Finch, J.A., 1995b. Column flotation: a selected review—part IV: novel flotation devices. Miner. Eng. 8, 587–602.

Finkelstein, N.P., 1999. Addendum to: The activation of sulphide minerals for flotation: A review. Int. J. Miner. Process. 55, 283–286. https://doi.org/10.1016/S0301-7516(98)00052-0

Flottec, L., n.d. SIBX MSDS [WWW Document]. URL http://webcache.googleusercontent.com/search?q=cache:Mwsz5immzF8J:flottec.s3-us-west-1.amazonaws.com/uploads/9fffdccd-23d9-442f-ab9e-be146ae07f95/Flottec%2520SIBX%2520Collector%2520SDS%2520r00%2520EN%25202015-12-31.pdf+&cd=1&hl=en&ct=clnk&gl=za (accessed 7.18.20).

Forssberg, K.S.E., Hallin, M.I., 1989. Process Water Reticulation in a Lead-Zinc Plant and other Sulphide Flotation Plants, in: Proc, Symp. Challenges in Mineral Processing. Society of Mining Engineers.

Fuerstenau, M.C., 1982. Sulphide mineral flotation: in Principles of Flotation. SAIMM Monogr. Ser. 3, 159–182.

Garrels, R.M., Christ, C.L., 1990. Solutions, minerals and equilibria. Carbonate equilibria, 77-131.

Genc, B., Jerome, J., 2014. Challenges in the South African Platinum Sector. Mine Plan. Equip. Sel. 1–9. https://doi.org/10.1007/978-3-319-02678-7

Goncharuk, V. V., Bagrii, V.A., Mel'nik, L.A., Chebotareva, R.D., Bashtan, S.Y., 2010. The use of redox potential in water treatment processes. J. Water Chem. Technol. 32, 1–9. https://doi.org/10.3103/S1063455X10010017

Górniak, A., Wojakowska, A., Plińska, S., Krzyżak, E., 2009. Electrical conductivity in solid solutions and in two-phase regions of the silver halide-bivalent metal (cadmium, cobalt, zinc) halide systems. J. Therm. Anal. Calorim. 96, 133–140. https://doi.org/10.1007/s10973-008-9292-8

Gray, D., Cameron, T., Briggs, A., 2016. Kevitsa Nickel Copper Mine, Lapland, Finland.

Gumede, H., 2018. The socio-economic effects of mechanising and/or modernising hard rock mines in South Africa. South African J. Econ. Manag. Sci. 21, 1–11. https://doi.org/10.4102/sajems.v21i1.1848

Gustafson, H., Behrman, A.S., 1939. Determination of total dissolved solids in water by electrical conductivity. Ind. Eng. Chem. Anal. Ed. 11, 355–357.

Haggard, E.L., Sheridan, C.M., Harding, K.G., 2015. Quantification of water usage at a South African platinum processing plant. Water SA 41, 279–286. https://doi.org/10.4314/wsa.v41i2.14

Hanna Instrument Inc., 2021. Multiparameter Bluetooth ® Portable pH / EC / opdo ® Meter.

Haran, N.P., Boyapati, E.R., Boontanjai, C., Swaminathan, C., 2008. Kinetics Studies on Effect of Recycled Water on Flotation of Copper Tailings from Benambra Mines, Victoria. Dev. Chem. Eng. Miner. Process. 4, 197–211. https://doi.org/10.1002/apj.5500040305

Harris, P.J., 1982. Frothing phenomena and frothers. South African Inst. Min. Metall. Princ. Flot. 237–250.

Hayes, R.A., Price, D.M., Ralston, J., Smith, R.W., 1987. Collectorless Flotation of Sulphide Minerals. Miner. Process. Extr. Metall. Rev. 2, 203–234. https://doi.org/10.1080/08827508708952606

Hintikka, V. V., Leppinen, J.O., 1995. Potential control in the flotation of sulphide minerals and precious metals. Miner. Eng. 8, 1151–1158. https://doi.org/10.1016/0892-6875(95)00080-A

Hu, W., 2014. Flotation Circuit Optimisation and Design 1–150.

Ikumapayi, F., Makitalo, M., Johansson, B., Rao, K.H., 2012. Recycling of process water in sulphide flotation: Effect of calcium and sulphate ions on flotation of galena. Miner. Eng. 39, 77–88. https://doi.org/10.1016/j.mineng.2012.07.016

Ikumapayi, F., Rao, K.H., 2015a. Recycling Process Water in Complex Sulfide Ore Flotation: Effect of Calcium and Sulfate on Sulfide Minerals Recovery. Miner. Process. Extr. Metall. Rev. 36, 45–64. https://doi.org/10.1080/08827508.2013.868346

Ikumapayi, F., Rao, K.H., 2015b. Recycling Process Water in Complex Sulfide Ore Flotation : Effect of Calcium and Sulfate on Sulfide Minerals Recovery Recycling Process Water in Complex Sulfide Ore Flotation : Effect of Calcium and Sulfate on Sulfide Minerals Recovery 7508. https://doi.org/10.1080/08827508.2013.868346

Imaizumi, T., 1963. Kinetic consideration of froth flotation, in: Proceedings of the Sixth International Mineral Processing Congress, 1963. Pergamon Press, pp. 581–593.

Intergovernmental Panel on Climate Change (Ed.), 2014. Summary for Policymakers, in: Climate Change 2013 – The Physical Science Basis: Working Group I Contribution to the Fifth Assessment Report of the Intergovernmental Panel on Climate Change. Cambridge University Press, Cambridge, pp. 1–30. https://doi.org/DOI: 10.1017/CBO9781107415324.004

ISO Comittee, 2009. AS/NZS ISO 31000: 2009 Risk Management–Principles and Guidelines. Stand. Aust. New Zeal. Stand. Committee, Sidney.

Jacques, S., 2017. Effect of Grinding Chemistry on the Sulphidisation and Flotation Performances of Transitional Oxide-Sulphide Copper Ore 0–100.

Jameson, G.J., 1984. Physical aspects of fine particle flotation. Princ. Miner. Flotat. 215.

Jasieniak, M., St, R., Smart, C., 2010. Surface chemical mechanisms of inadvertent recovery of chromite in UG2 ore flotation: Residual layer identification using statistical ToF-SIMS analysis. Int. J. Miner. Process. 94, 72–82. https://doi.org/10.1016/j.minpro.2009.12.003

Johnson, B.N.W., 2003. Issues in maximisation of recylcing of water in a mineral processing plant.

Johnson, B.R., Haas, A., Fritz, K.M., 2010. Use of spatially explicit physicochemical data to measure downstream impacts of headwater stream disturbance. Water Resour. Res. 46, 1–15. https://doi.org/10.1029/2009WR008417

Kaushal, S.S., Groffman, P.M., Likens, G.E., Belt, K.T., Stack, W.P., Kelly, V.R., Band, L.E., Fisher, G.T., 2005. Increased salinization of fresh water in the northeastern United States. Proc. Natl. Acad. Sci. 102, 13517–13520. https://doi.org/10.1073/pnas.0506414102

Kaushal, S.S., Likens, G.E., Pace, M.L., Utz, R.M., Haq, S., Gorman, J., Grese, M., 2018. Freshwater salinization syndrome on a continental scale. Proc. Natl. Acad. Sci. 115, E574 LP-E583. https://doi.org/10.1073/pnas.1711234115

Kawatra, S.K., Darling, P., 2011. Fundamental principles of froth flotation. SME Min. Eng. Handb. 2, 1517–1531.

Khraisheh, M., Holland, C., Creany, C., Harris, P., Parolis, L., 2005. Effect of molecular weight and concentration on the adsorption of CMC onto talc at different ionic strengths. Int. J. Miner. Process. 75, 197–206. https://doi.org/10.1016/j.minpro.2004.08.012

King, R.P., 1982. Principles of flotation. South African Inst. Min. Metall. Kelvin House, 2 Holl. St, Johannesburg, South Africa, 1982. 268.

Klein, C., Dutrow, B., Dana, J.D., Klein, C., 2002. Manual of mineral science. Wiley New York.

Klimpel, R.R., 1984. Froth Flotation: The Kinetic Approach.

Klimpel, R.R., Isherwood, S., 1991. Some industrial implications of changing frother chemical structure. Int. J. Miner. Process. 33, 369–381. https://doi.org/https://doi.org/10.1016/0301-7516(91)90064-P

Kurniawan, A.U., Ozdemir, O., Nguyen, A. V., Ofori, P., Firth, B., 2011. Flotation of coal particles in MgCl2, NaCl, and NaClO 3 solutions in the absence and presence of Dowfroth 250. Int. J. Miner. Process. 98, 137–144. https://doi.org/10.1016/j.minpro.2010.11.003

Laskowski, J.S., Liu, Q., O'Connor, C.T., 2007. Current understanding of the mechanism of polysaccharide adsorption at the mineral/aqueous solution interface. Int. J. Miner. Process. 84, 59–68. https://doi.org/10.1016/j.minpro.2007.03.006

Laxen, D.P.H., 1977. A specific conductance method for quality control in water analysis. Water Res. 11, 91–94.

Le, T., Schreithofer, N., Dahl, O., 2020. Dissolution Test Protocol for Estimating Water Quality Changes in Minerals Processing Plants Operating With Closed Water Circulation. Minerals 10, 653. https://doi.org/10.3390/min10080653

Leja, J., Schulman, J.H., 1954. Flotation theory: molecular interactions between frothers and collectors at solid–liquid–air interfaces. Trans. AIME 199, 221–228.

Levay, G., Smart, R.S.C., Skinner, W.M., 2001. The impact of water quality on flotation performance. J. South African Inst. Min. Metall. 101, 69–75.

Lewis, E., 1980. The practical salinity scale 1978 and its antecedents. IEEE J. Ocean. Eng. 5, 3–8. https://doi.org/10.1109/JOE.1980.1145448

Liddel, K.S., McRae, L.B., Dunne, R.C., Liddell, K.S., Dunne, R.C., McRae, L.B., Liddel, K.S., McRae, L.B., Dunne, R.C., 1985. Process routes for beneficiation of noble metals from Merensky and UG-2 ores. Mintek, pp. 789–816.

Lind, C.J., 1970. Specific conductance as a means of estimating ionic strength.

Liu, W., Moran, C.J., Vink, S., 2013. A review of the effect of water quality on flotation. Miner. Eng. 53, 91–100. https://doi.org/10.1016/j.mineng.2013.07.011

Lotter, N.O., Bradshaw, D.J., Becker, M., Parolis, L.A.S., Kormos, L.J., 2008. A discussion of the occurrence and undesirable flotation behaviour of orthopyroxene and talc in the processing of mafic deposits. Miner. Eng. 21, 905–912. https://doi.org/10.1016/j.mineng.2008.02.023

Lovell, V.M., 1982. Industrial flotation reagents. South African Inst. Min. Metall. Princ. Flot. 73–89.

Lystrom, D.G., Rinella, R.A., Knox, W.D., 1978. Definition of regional relationships between dissolved solids and specific conductance, Susquehanna river basin, Pennsylvania and New York. J. Res. US Geol. Surv 6, 541–545.

Mailula, T.., Bradshaw, D.J., Harris, P.J., 2003. The effect of copper sulphate addition on the recovery of chromite in the flotation of UG2 ore. South African J. Econ. Manag. Sci. https://doi.org/10.1016/j.mineng.2003.08.001

Manenzhe, R.R.M., 2018. The, Investigating the Effect of Water Quality on Adsorption of a Xanthate Collector in the Flotation of a Sulphide Ore, Univeristy of Cape Town. Cape Town. https://doi.org/10.1007/s10008-007-0419-9

Manono, M., 2018. Investigating Electrolyte-Reagent-Mineral Interactions in Response to Water Quality Challenges in the Flotation of a PGM Ore. Cape Town.

Manono, M., 2012. An investigation into the effect of ionic strength of plant water on valuable mineral and gangue recovery of a platinum bearing ore from the merensky reef. Cape Town.

Manono, M., Corin, K., Wiese, J., 2018. Water quality effects on a sulfidic PGM ore: Implications for froth stability and gangue management. Physicochem. Probl. Miner. Process. 54, 1253–1265. https://doi.org/10.5277/ppmp18181

Manono, M.S., Corin, K.C., Wiese, J.G., 2013. The effect of ionic strength of plant water on foam stability: A 2-phase flotation study. Miner. Eng. 40, 42–47. https://doi.org/https://doi.org/10.1016/j.mineng.2012.09.009

Manono, M.S., Corin, K.C., Wiese, J.G., 2012. An investigation into the effect of various ions and their ionic strength on the flotation performance of a platinum bearing ore from the Merensky reef. Miner. Eng. 36–38, 231–236. https://doi.org/https://doi.org/10.1016/j.mineng.2012.03.035

Martinovic, J., Bradshaw, D.J., Harris, P.J., 2005. Investigation of surface properties of

gangue minerals in platinum bearing ores. J. South African Inst. Min. Metall. 105, 349–356.

Mccall, M.-J., 2016. Mineralogical and geochemical variations in the UG2 reef at Booysendal and Zondereinde mines , with implications for beneficiation of PGM. (MSc Thesis) 140.

McCleskey, B.B., Nordstrom, K.K., Ryan, J.N., 2012. Comparison of electrical conductivity calculation methods for natural waters. Limnol. Oceanogr. Methods 10, 952–967. https://doi.org/10.4319/lom.2012.10.952

McCleskey, R.B., 2011. Electrical conductivity of electrolytes found in natural waters from (5 to 90) C. J. Chem. Eng. Data 56, 317–327.

McLaren, C.H., De Villiers, J.P.R., 1982. The platinum-group chemistry and mineralogy of the UG-2 chromitite layer of the Bushveld complex. Econ. Geol. 77, 1348–1366. https://doi.org/10.2113/gsecongeo.77.6.1348

McNeil, V.H., Cox, M.E., 2000. Relationship between conductivity and analysed composition in a large set of natural surface-water samples, Queensland, Australia. Environ. Geol. 39, 1325–1333. https://doi.org/10.1007/s002549900033

Merck, 2020. Poly(ethylene glycol) dimethyl ether [WWW Document]. Prod. Coparison Guid. URL https://www.sigmaaldrich.com/catalog/substance/polyethyleneglycoldimethylether123452499155711?lang=en&region=ZA (accessed 6.7.20).

Mhlanga, S.S., 2011. Investigating the relative adsorption of polymeric depressants on pure mienerals.

Miller, R.L., Bradford, W.L., Peters, N.E., 1988. Specific conductance: theoretical considerations and application to analytical quality control. US Government Printing Office.

Miranda-Trevino, J.C., Pappoe, M., Hawboldt, K., Bottaro, C., 2013. The Importance of Thiosalts Speciation: Review of Analytical Methods, Kinetics, and Treatment. Crit. Rev. Environ. Sci. Technol. 43, 2013–2070. https://doi.org/10.1080/10643389.2012.672047

Moldoveanu, S.C., David, V., 2017. Chapter 7 - RP-HPLC Analytical Columns, in: Moldoveanu, S.C., David, V. (Eds.), Selection of the HPLC Method in Chemical Analysis. Elsevier, Boston, pp. 279–328. https://doi.org/https://doi.org/10.1016/B978-0-12-803684-6.00007-X

Morris, G.E., Fornasiero, D., Ralston, J., 2002. Polymer depressants at the talc – water interface : adsorption isotherm , microflotation and electrokinetic studies 67, 211–227.

Mudd, G.M., 2012. Key trends in the resource sustainability of platinum group elements. Ore Geol. Rev. 46, 106–117.

https://doi.org/10.1016/j.oregeorev.2012.02.005

Mudd, G.M., Jowitt, S.M., Werner, T.T., 2018. Global platinum group element resources, reserves and mining – A critical assessment. Sci. Total Environ. 622–623, 614–625. https://doi.org/10.1016/j.scitotenv.2017.11.350

Mustafa, S., Hamid, A., Naeem, A., Sultana, Q., 2004. Effect of pH, temperature and time on the stability of potassium ethyl xanthate. J. Chem. Soc. Pakistan.

Muzenda, E., Abdulkareem, A.S., Afolabi, A.S., 2013. Reagent optimization across a UG2 plant. Lect. Notes Eng. Comput. Sci. 1 LNECS, 575–579.

Muzinda, I., Schreithofer, N., 2018. Water quality effects on flotation : Impacts and control of residual xanthates 125, 34–41. https://doi.org/10.1016/j.mineng.2018.03.032

Mwale, A.H., Musonge, P., Fraser, D.M., 2005. The influence of particle size on energy consumption and water recovery in comminution and dewatering systems. Miner. Eng. 18, 915–926. https://doi.org/10.1016/j.mineng.2005.02.014

Naftz, D., 2017. Inputs and Internal Cycling of Nitrogen to a Causeway Influenced, Hypersaline Lake, Great Salt Lake, Utah, USA. Aquat. Geochemistry 23, 199–216. https://doi.org/10.1007/s10498-017-9318-6

Napier-Munn, T., Wills, B.A., 2005. Wills' Mineral Processing Technology, Wills' Mineral Processing Technology. https://doi.org/10.1016/B978-0-7506-4450-1.X5000-0

Nel, E., Theron, J., Martin, C., Raabe, H., 2004. PGM Ore Processing at Impala's UG-2 Concentrator in Rustenburg, South Africa. Sgs Miner. Serv. 1–11.

Novotny, E. V, Murphy, D., Stefan, H.G., 2008. Increase of urban lake salinity by road deicing salt. Sci. Total Environ. 406, 131–144. https://doi.org/https://doi.org/10.1016/j.scitotenv.2008.07.037

O'connor, C., Alexandrova, T., 2021. The geological occurrence, mineralogy, and processing by flotation of platinum group minerals (Pgms) in South Africa and Russia. Minerals 11, 1–15. https://doi.org/10.3390/min11010054

O'Connor, C.T., Mills, P.J.T., 1995. The influence of bubble size on scale-up of column flotation cells. Miner. Eng. 8, 1185–1195. https://doi.org/10.1016/0892-6875(95)00083-3

Olympus, 2021. Vanta Element-S XRF Analyzer Affordable Alloy ID and Light Element Analysis.

Pan, Y., Bournival, G., Ata, S., 2022. Foaming behaviour of frothers in the presence of PAX and salt. Miner. Eng. 178, 107405. https://doi.org/10.1016/j.mineng.2022.107405

Paul Yates, 2012. Using the equation of a straight line | Maths | Education in Chemistry [WWW Document]. URL https://eic.rsc.org/maths/using-the-equation-of-a-straight-line/2000169.article (accessed 4.18.19).

Pearse, M.J., 2005. An overview of the use of chemical reagents in mineral processing. Miner. Eng. 18, 139–149. https://doi.org/10.1016/j.mineng.2004.09.015

Peters, N.E., Meybeck, M., 2000. Water Quality Degradation Effects on Freshwater Availability: Impacts of Human Activities. Water Int. 25, 185–193. https://doi.org/10.1080/02508060008686817

Pintro, J., Inoue, T.T., 1999. A comparative study of determined and calculated values of ionic strength of different nutrient solutions consisting of an ionic pair. J. Plant Nutr. 22, 1223–1231.

Polemio, M., Bufo, S., Paoletti, S., 1980. Evaluation of ionic strength and salinity of groundwaters: effect of the ionic composition. Geochim. Cosmochim. Acta 44, 809–814.

Pollak, M.J., 1954. The use of electrical conductivity measurements for chlorinity determination. Johns Hopkins University, Chesapeake Bay Institute.

Ponnaperuma, F.N., Tianco, E.M., Loy, T.A., 1966. Ionic strengths of the solution of flooded soils and other natural aqueous solutions from specific conductance. Soil Sci. 102.

Qing You, L., Heping, L., Li, Z., 2007. Study of galvanic interactions between pyrite and chalcopyrite in a flowing system: implications for the environment. Environ. Geol. 52, 11–18. https://doi.org/10.1007/s00254-006-0444-5

Quinn, J.J., Kracht, W., Gomez, C.O., Gagnon, C., Finch, J.A., 2007. Comparing the effect of salts and frother (MIBC) on gas dispersion and froth properties. Miner. Eng. 20, 1296–1302. https://doi.org/10.1016/j.mineng.2007.07.007

Ramos, O., Castro, S., Laskowski, J.S., 2013. Copper–molybdenum ores flotation in sea water: Floatability and frothability. Miner. Eng. 53, 108–112.

Rao, M.K.Y., Natarajan, K.A., 1989. Effect of electrochemical interactions among sulfide minerals and grinding medium on chalcopyrite flotation. Mining, Metall. Explor. 6, 146–151.

Rao, S.R., Finch, J.A., 1989. A review of water re-use in flotation. Miner. Eng. 2, 65–85.

Rao, S.R., Finch, J.A., 1988a. No Title. Canad. Met. Quart. 27, 253.

Rao, S.R., Finch, J.A., 1988b. Galvanic Interaction Studies on Sulphide Minerals. Can. Metall. Q. 27, 253–259. https://doi.org/10.1179/cmq.1988.27.4.253

Rao, S.R., Moon, K.S., Leja, J., 1976. Effect of grinding media on the surface reactions

and flotation of heavy metal sulphides. Flot. M. Gaudin Meml.

Rastetter, M., Gawler, J., Kiviluoma, M., Suoniemi-kähärä, A., 2000. Determination of Water Pollutants Using Photometric Analysis 1–6.

Rossum, J.R., 1949. Conductance method for checking accuracy of water analyses. Anal. Chem. 21, 631.

Sahoo, S.K., Suresh, N., Varma, A.K., 2020. Determining the Best Particle Size-Class for Flotation of a High Ash Coal. Int. J. Coal Prep. Util. 40, 755–765. https://doi.org/10.1080/19392699.2017.1409216

Schaschke, Carl, 2014. Oxforad Dictionary of Chemical Engineering. Oxford University Press, Oxford.

Schraga, T.S., Cloern, J.E., 2017. Water quality measurements in San Francisco Bay by the U.S. Geological Survey, 1969-2015. Sci. Data 4, 2021. https://doi.org/10.1038/sdata.2017.98

Shen, Y., Nagaraj, D.R., Farinato, R., Somasundaran, P., 2016. Study of xanthate decomposition in aqueous solutions. Miner. Eng. 93, 10–15. https://doi.org/10.1016/j.mineng.2016.04.004

Sheni, N.R., 2016. Considering the effect of pulp chemistry during flotation on froth stability. Cape Town.

Sigmaalderich, 2019. Material Saftey Data Sheets [WWW Document]. MSDS. URL https://www.sigmaaldrich.com/south-africa.html (accessed 9.12.19).

Singh, T., Kalra, Y.P., 1975. Specific conductance method for in situ estimation of total dissolved solids. Journal-American Water Work. Assoc. 67, 99–100.

Slatter, K.A., Plint, N.D., Cole, M., Dislook, V., Palm, N., De Vaux, D., Oostendorp, B., 2009. Water Management in Anglo Platinum Process Operations : Effects of Water Quality on Process Operations. Abstr. Int. Mine Water Conf. Pretoria, South Africa, 19th – 23rd Oct. 2009 Proc. ISBN Number 978-0-9802623-5-3 46–55.

Spottiswod, D.J., Kelly, E.G., 1982. Mineral Processing: An Introduction to the Principles.

Stanton, J.S., Anning, D.W., Brown, C.J., Moore, R.B., McGuire, V.L., Qi, S.L., Harris, A.C., Dennehy, K.F., McMahon, P.B., Degnan, J.R., Böhlke, J.K., 2017. Brackish groundwater in the United States, Professional Paper. Reston, VA. https://doi.org/10.3133/pp1833

Stetson, S.J., Patton, C.J., Guaglione, N., Chestnut, Z., 2019. Measurement of nutrients in saline and hypersaline waters by discrete analyzer colorimetry without matrix matched calibration standards. Talanta 203, 297–304. https://doi.org/10.1016/j.talanta.2019.05.066

Subrahmanyam, T. V, Forssberg, E., 1988. Froth stability, particle entrainment and drainage in flotation — A review. Int. J. Miner. Process. 23, 33–53. https://doi.org/https://doi.org/10.1016/0301-7516(88)90004-X

Sweet, C., Van Hoogstraten, J., Harris, M., Laskowski, J.S., 1997. The effect of frothers on bubble size and frothability of aqueous solutions, in: Processing of Complex Ores–Proc. 2nd UBC-Mc Gill Int. Symp. Metallurgical Society of CIM, Montreal. pp. 235–245.

Sweet, J.A., 1999. Investigation of a methodology to decouple physical and chemical effects for flotation circuit performance evaluation.

Swinehart, D.F., 1962. The Beer-Lambert Law 39, 333–335. https://doi.org/10.1021/ed039p333

ThermoFisher Scientific, 2020. Solution for routine and comprehensive water analysis 20.

ThermoFisher Scientific, 2018a. Fast and Accurate Thermo Scientific Gallery Discrete Industrial Analyzers - Automated Nutrient Analysis and Water Quality Monitoring.

ThermoFisher Scientific, 2018b. Easy soil testing at a South African fertilizer manufacturer. Gall. Discret. Anal. 3.

ThermoFisher Scientific, 2003. Speed and flexibility. ThermoFisher Sci. 110, 37.

Thierie, J., 2018. Activated sludge settling analysis using a near infrared optoelectronic device: Overview and application to wastewater treatment. Spectrosc. Eur. 30, 16–19.

Tornell, B., 1967. Xanthate Decomposition in Acid Media. 3. Cellulose Xanthate-Experimental Details and Empirical Results. Sven. Papperstidning-Nordisk Cellul. 70, 268.

Tornell, B., 1966a. Xanthate decomposition in acid media. 1. Experimental technique and a study of decomposition of ethyl xanthate. Sven. Papperstidning-Nordisk Cellul. 69, 658.

Tornell, B., 1966b. Xanthate decomposition in acid media. 2. Decomposition of a dixanthate and a study of influence of molecular aggregation. Sven. Papperstidning-Nordisk Cellul. 69, 695.

Usaini, M.N.S., Ali, M., Usman, H.A., 2014. Determination of liberation size of Akiri copper ore , Nasarawa state , north-central Nigeria.

USGS, 2020. Mineral Commodity Summaries 2020.

USK, 2007. MSDS CMC [WWW Document]. MSDS. URL https://www.vento.com.vn/docs/en/CMC-HPMC/MSDS CMC.pdf (accessed 7.18.20).

V.P. Finkelstein, N., 1972. Fundamental studies of the flotation process : the work of the National Institute for Metallurgy. J. South. African Inst. Min. Metall. 72, 328–342.

Van Deventer, J.S.J., Ross, V.E., Dunne, R.C., 1993. The effect of galvanic interaction on the behaviour of the froth phase during the flotation of a complex sulphide ore. Miner. Eng. 6, 1217–1229. https://doi.org/https://doi.org/10.1016/0892-6875(93)90100-2

Viani, R., Pettracco, M., 2016. Coffee. Ullmann's Encycl. Ind. Chem. 43, 153–155. https://doi.org/10.1002/14356007.a07

Visconti, F., J.M., Rubio, J.L., 2010. An empirical equation to calculate soil solution electrical conductivity at 25°C from major ion concentrations. Eur. J. Soil Sci. 61, 980–993. https://doi.org/10.1111/j.1365-2389.2010.01284.x

Vos, C.F., Stange, W., Bradshaw, D.J., 2014. A new small-scale test to determine flotation performance - Part 1: Overall performance. Miner. Eng. 66, 62–67. https://doi.org/10.1016/j.mineng.2014.04.015

Walton, N.R.G., 1989. Electrical Conductivity and Total Dissolved Solids—What is Their Precise Relationship? Desalination 72, 275–292. https://doi.org/10.1016/0011-9164(89)80012-8

Wang, J., Somasundaran, P., 2005. Adsorption and conformation of carboxymethyl cellulose at solid-liquid interfaces using spectroscopic, AFM and allied techniques. J. Colloid Interface Sci. 291, 75–83. https://doi.org/10.1016/j.jcis.2005.04.095

Wang, X.H., Forssberg, E., Bolin, J.J., 1989. No Title. Miner. Process. Extra. Met. Rev. 4, 165.

Wang, X.H., Xie, Y.E.N., 1990. The Effect of Grinding Media and Environment on the Surface Properties and Flotation Behaviour of Sulfide Minerals. Miner. Process. Extr. Metall. Rev. 7, 49–79. https://doi.org/10.1080/08827509008952666

Wasserlauf, M., Dutrizac, J.E., 1984. Canmet's Project on the Chemistry, Generation and Treatment of Thiosalts in Milling Effluents. Can. Metall. Q. 23, 259–269. https://doi.org/10.1179/cmq.1984.23.3.259

Wiese, J., Harris, P., 2012. The effect of frother type and dosage on flotation performance in the presence of high depressant concentrations. Miner. Eng. 36–38, 204–210. https://doi.org/10.1016/j.mineng.2012.03.028

Wiese, J., Harris, P., Bradshaw, D., 2007. The response of sulphide and gangue minerals in selected Merensky ores to increased depressant dosages. Miner. Eng. 20, 986–995. https://doi.org/10.1016/j.mineng.2007.03.008

Wiese, J., Harris, P., Bradshaw, D., 2005. The influence of the reagent suite on the flotation of ores from the Merensky reef. Miner. Eng. 18, 189–198. https://doi.org/10.1016/j.mineng.2004.09.013

Wiese, J.G., 2009. Investigating depressant behavior in the flotation of selected Merensky Ores., Univeristy of Cape Town. Cape Town.

Williams, D.D., Williams, N.E., Cao, Y., 2000. Road salt contamination of groundwater in a major metropolitan area and development of a biological index to monitor its impact. Water Res. 34, 127–138. https://doi.org/https://doi.org/10.1016/S0043-1354(99)00129-3

Wills, B.A., Napier-Munn, T.J., 2006. An introduction to the practical aspects of ore treatment and mineral recovery. Wills' Miner. Process. Technol. 267–352.

Yoon, R.H., Basilio, C.I., 1993. Adsorption of thiol collectors on sulphide minerals and precious metals–a new perspective, in: Proceedings of the XVIII International Mineral Processing Congress. Aus. IMM, p. 611.

Yuan, X.M., Pålsson, B.I., Forssberg, K.S.E., 1996. Flotation of a complex sulphide ore II. Influence of grinding environments on Cu/Fe sulphide selectivity and pulp chemistry. Int. J. Miner. Process. 46, 181–204. https://doi.org/10.1016/0301-7516(95)00095-X

APPENDIXES

Appendix A. Froth Stability Data

Table 9-1. Experimental Data from 2 Phase Stability Column Tests of all recovered Concentrate Water for all Tested Conditions.

	2 Phase Stability Column Tests (Concentrate)											
	Frother Dosed 3 SPW					0	Recycle 1		Recycle 2		Recycle 3	
	20 g/t	30 g/t	40 g/t	50 g/t	60 g/t	Recycle	Float	Mill	Float	Mill	Float	Mill
Hi, max	12.9	18	39.6	46.1	53.9	26	30	39	33	32	39	35
Hi, max error	0.6	0.2	0.2	0.2	0.2	0	3	1	7	2	3	5
H_{max}	12.5	17	39	44.2	54.1	25	27	38	31	30	37	34
Tau	15.4	22.8	40.7	51.7	49.5	37	67	67	135	43	118	47
Σ	0.14	0.193	0.389	0.496	0.605	0.291	0.303	0.428	0.351	0.341	0.415	0.379
P value test	1	1	1	1	1	1	1	1	1	1	1	1
p value from sum (X^2)	1	1	1	1	1	1	1	1	1	1	1	1
X^2 Actual	0.239	0.268	0.389	0.343	2.52	1	16	2	20	3	12	2
X^2 Theoretical	0	0	0	1	2.8	0	0	0	0	0	0	0

CV	45	45	45	45	45	148	148	148	148	148	148	148

Table 9-2. Experimental Data from 2 Phase Stability Column Tests of all recovered Tailing Water Samples of all Tested Conditions.

	2 Phase Stability Column Tests (Tailings water)										
	Frother Dosed 3 SPW					0	Recycle 1		Recycle 2		Recycle 3	
	20 g/t	30 g/t	40 g/t	50 g/t	60 g/t	Recycle	Float	Mill	Float	Mill	Float	Mill
Hi, max	12.9	18	39.6	46.1	53.9	18	20	27	31	23	24	24
Hi, max error	0.6	0.2	0.2	0.2	0.2	1	0	3	3	0	3	6
H_{max}	12.5	17	39	44.2	54.1	17	19	29	29	21	22	25
Tau	15.4	22.8	40.7	51.7	49.5	222	308	380	38	118	394	319
Σ	0.14	0.193	0.389	0.496	0.605	0.2	0.218	0.328	0.325	0.235	0.25	0.28
P value test	1	1	1	1	1	1	1	1	1	1	1	1
p value from sum (X^2)	1	1	1	1	1	1	1	1	1	1	1	1
X^2 Actual	0.239	0.268042	0.389	0.343	2.52	17	24	35	10	39	50	34
X^2 Theoretical	0	0	0	1	2.8	0	0	36	0	40	48	34
CV	45	45	45	45	45	148	148	148	148	148	148	148

Table 9-3. Experimental Data from 3 Phase Stability Column Tests of all recovered Tailing Pulp Samples of all Tested Conditions.

	3 Phase Stability Column Tests						
	Recycle 0	Recycle 1		Recycle 2		Recycle 3	
		Float	Mill	Float	Mill	Float	Mill
Hi, max	19.4	27.8	24.4	30.3	30	26.8	28.5
Hi, max error	0.6	2.5	0.6	3.2	3.2	0.7	0.8
H_{max}	17.8	26.1	22.6	28.2	26.7	25	26.5
τ	21	27	30	29	25	32	33
Σ	0.199	0.293	0.253	0.316	0.3	0.3	0.319
P value test	1	1	1	1	1	1	1
p value from sum (X^2)	1	1	1	1	1	1	1
X^2 Actual	5	5	4	6	9	8	6
X^2 Theoretical	0	0	0	87	0	0	0
CV	147	147	147	147	147	147	147

Appendix B. Mass Balance Data

	Reagents	Sample	Time, min	Mass Pull, g	Water Rec, g	Cum Mass, g	Cum Water, g	Ave cum Mass, g	Std dev	Std error	Ave cum w Rec, g	Std dev	Std error	Copper %	Copper Mass	Cum Copper Mass	Copper Grade %	Copper Rec %	Ave Copper grade %	Std dev	Std error	Ave Copper rec %	Std dev	Std error	Nickel %	Nickel Mass	Cum Nickel Mass	Nickel Grade %	Nickel Rec %	Ave Nickel grade %	Std dev	Std error	Ave Nickel rec %	Std dev	Std error
Recycle 0.1	100 g/t SIBX 150 g/t Depramin 267 40 g/t DOW 200	C1 C2 C3 C4 F T T2 T3 Cc+Tl Mass Bal	2 6 12 20	19.69 36.72 34.48 29.32 1289.44 1135.60 14.94 24.69	168.29 372.77 411.05 419.58	19.69 56.41 90.89 120.21	168.29 541.06 952.11 1371.69	19.77 57.95 91.59 119.75	4.46 6.04 5.97 6.00	1.58 2.14 2.11 2.12	189.31 610.32 1028.41 1396.79	53.24 98.17 127.01 157.28	18.82 34.71 44.90 55.61	0.25 0.05 0.03 0.02 0.01 0.0044 0.00600 0.011	4.93 1.67 0.96 0.57 15.42 0.07 0.15 14.25 92.43	4.93 6.60 7.56 8.14	0.25 0.12 0.08 0.07	34.63 46.33 53.08 57.11	0.27 0.12 0.08 0.07	0.05 0.01 0.01 0.01	0.02 0.00 0.00 0.00	37.67 48.99 55.04 58.96	3.72 3.11 2.43 2.27	1.32 1.10 0.86 0.80	0.48 0.24 0.18 0.17 0.14 0.12 0.12 0.132	9.36 8.74 6.22 5.06 180.20 1.78 3.02 171.53 95.19	9.36 18.10 24.32 29.38	0.48 0.32 0.27 0.24	5.46 10.55 14.18 17.13	0.50 0.32 0.27 0.25	0.05 0.01 0.01 0.01	0.02 0.01 0.00 0.00	6.37 12.21 16.06 19.16	1.76 3.06 3.97 4.59	0.62 1.08 1.37 1.62
Recycle 0.2	100 g/t SIBX 150 g/t Depramin 267 40 g/t DOW 200	C1 C2 C3 C4 F T T2 T3 Cc+Tl Mass Bal		18.70 36.17 32.10 26.49 1254.57 1115.01 12.07 12.03	175.23 454.17 454.76 428.61	18.70 56.87 88.97 115.46	175.23 629.40 1084.16 1512.77				1490.11 65.99			0.30 0.04 0.02 0.02 0.01 0.00570 0.0044 0.011	5.53 1.42 0.73 0.52 16.69 0.07 0.05 13.94 83.54	5.53 6.94 7.67 8.19	0.30 0.12 0.09 0.07	39.64 49.80 55.01 58.73						0.51 0.24 0.18 0.18 0.14 0.12 0.00 0.077	9.58 8.99 5.74 4.74 177.52 1.44 0.00 96.99 54.64	9.58 18.57 24.31 29.05	0.51 0.33 0.27 0.25	9.87 19.14 25.06 29.95						
Recycle 0.3	100 g/t SIBX 150 g/t Depramin 267 40 g/t DOW 200	C1 C2 C3 C4 F T T2 T3 Cc+Tl Mass Bal	2 6 12 20	21.23 40.85 36.76 29.07 1223.69 1065.97 16.48 13.33	258.78 448.47 420.99 357.49	21.23 62.08 98.84 127.91	258.78 707.25 1128.24 1485.73	19.63 60.16 95.91 125.02	2.27 2.72 4.14 4.09	1.61 1.93 2.93 2.90	197.60 614.20 993.54 1324.54	66.53 131.60 190.50 227.96	61.19 93.06 134.71 161.19	0.28 0.04 0.02 0.02 0.01 0.00460 0.00520 0.012	5.87 1.57 0.79 0.56 14.19 0.08 0.07 14.16 99.79	5.87 7.44 8.24 8.80	0.28 0.12 0.08 0.07	41.47 52.55 58.15 62.09	0.28 0.12 0.08 0.07	0.01 0.00 0.00 0.00	0.00 0.00 0.00 0.00	39.29 50.96 56.93 61.21	3.09 2.24 1.72 1.25	2.18 1.59 1.22 0.88	0.53 0.23 0.18 0.17 0.13 0.11 0.12 0.130	11.26 9.20 6.57 4.93 157.73 1.81 1.64 159.47 101.10	11.28 20.49 27.05 31.98	0.53 0.33 0.27 0.25	7.07 12.85 16.96 20.05	0.53 0.33 0.28 0.25	0.00 0.00 0.00 0.00	0.00 0.00 0.00 0.00	6.35 12.15 16.10 19.11	1.03 0.99 1.23 1.33	0.73 0.69 0.87 0.94
Recycle 0.4	100 g/t SIBX 150 g/t Depramin 267 40 g/t DOW 200	C1 C2 C3 C4 F T T2 T3 Cc+Tl Mass Bal		18.02 40.21 34.75 29.14 1248.24 1095.08 15.00 14.04	136.41 384.73 337.69 304.52	18.02 58.23 92.98 122.12	136.41 521.14 858.83 1163.35							0.29 0.04 0.03 0.02 0.01 0.004800 0.005000 0.011	5.15 1.70 0.88 0.64 16.33 0.07 0.07 13.89 85.05	5.15 6.86 7.74 8.38	0.29 0.12 0.08 0.07	37.10 49.38 55.71 60.33						0.53 0.25 0.19 0.17 0.13 0.12 0.13 0.137	9.60 10.00 6.44 5.03 166.37 1.83 1.78 170.96 102.75	9.60 19.60 26.03 31.06	0.53 0.34 0.28 0.25	5.82 11.46 15.23 18.17						
Recycle 0.5	100 g/t SIBX 150 g/t Depramin 267 40 g/t DOW 200	C1 C2 C3 C4 F T T2 T3 Cc+Tl Mass Bal	2 6 12 20	19.30 36.97 35.92 29.18 1258.00 1106.82 14.30 15.51	166.96 406.39 388.49 344.89	19.30 56.27 92.19 121.37	166.96 573.35 961.84 1306.73	16.36 52.55 86.80 114.93	4.16 5.27 7.46 9.11	2.94 3.73 5.29 6.45	173.52 601.76 1031.56 1367.97	9.27 40.18 68.59 86.60	6.56 28.41 69.72 61.24	0.23 0.03 0.02 0.02 0.01 0.005400 0.004100 0.010	4.42 1.23 0.73 0.48 10.44 0.08 0.06 12.25 117.36	4.42 5.65 6.37 6.86	0.23 0.10 0.07 0.06	36.05 46.07 51.99 55.94	0.28 0.12 0.08 0.07	0.08 0.02 0.02 0.01	0.06 0.02 0.01 0.01	33.46 45.15 52.01 56.16	3.66 1.30 0.03 0.30	2.59 0.92 0.02 0.22	0.46 0.22 0.17 0.16 0.13 0.12 0.13 0.137	8.84 8.14 6.05 4.35 166.43 1.78 2.03 172.68 103.75	8.84 16.99 23.03 27.59	0.46 0.30 0.25 0.23	5.12 9.84 13.34 15.98	0.49 0.31 0.26 0.23	0.04 0.02 0.01 0.01	0.03 0.01 0.01 0.01	4.60 9.61 13.08 15.73	0.73 0.31 0.37 0.35	0.52 0.22 0.26 0.25
Recycle 0.6	100 g/t SIBX 150 g/t Depramin 267 40 g/t DOW 200	C1 C2 C3 C4 F T T2 T3 Cc+Tl Mass Bal		13.42 35.40 32.79 26.97 1261.06 1130.20 10.60 11.78	180.07 450.10 471.10 327.93	13.42 48.82 81.61 108.46	180.07 630.17 1101.27 1429.20							0.34 0.06 0.04 0.02 0.01 0.00520 0.00600 0.012	4.57 1.98 1.15 0.64 18.66 0.06 0.07 14.79 79.27	4.57 6.54 7.70 8.34	0.34 0.13 0.09 0.08	30.88 44.23 52.03 56.37						0.52 0.25 0.18 0.17 0.14 0.12 0.13 0.134	6.92 8.97 5.80 4.50 170.37 1.26 1.50 169.23 99.33	6.92 15.89 21.70 26.20	0.52 0.33 0.27 0.24	4.09 9.39 12.82 15.48						
Recycle 0.7	100 g/t SIBX 150 g/t Depramin 267 40 g/t DOW 200	C1 C2 C3 C4 F T T2 T3 Cc+Tl Mass Bal	2 6 12 20	18.54 36.54 32.22 30.24 1212.13 1085.91 17.31 11.37	144.56 351.63 412.96 341.64	18.54 55.08 87.30 117.54	144.56 496.19 909.15 1250.79	20.51 60.97 96.67 126.86	2.79 8.32 13.24 13.18	1.97 5.88 9.36 9.32	124.45 482.51 869.11 1191.90	28.44 19.35 56.63 83.29	20.11 13.69 40.05 58.90	0.29 0.04 0.02 0.02 0.01 0.0043 0.00540 0.011	5.40 1.51 0.78 0.46 13.33 0.07 0.06 13.46 100.96	5.40 6.91 7.70 8.15	0.29 0.13 0.09 0.07	40.12 51.36 57.17 60.56	0.15 0.06 0.04 0.03	0.21 0.09 0.06 0.05	0.15 0.06 0.04 0.03	#DIV/0! #DIV/0! #DIV/0! #DIV/0!	#DIV/0! #DIV/0! #DIV/0! #DIV/0!	#DIV/0! #DIV/0! #DIV/0! #DIV/0!	0.57 0.23 0.17 0.17 0.14 0.12 0.12 0.134	10.56 8.58 5.50 5.01 171.88 2.05 1.41 162.15 94.34	10.56 19.14 24.64 29.65	0.57 0.35 0.28 0.25	6.51 11.81 15.20 18.29	0.28 0.17 0.14 0.13	0.40 0.25 0.20 0.18	0.28 0.17 0.14 0.13	#DIV/0! #DIV/0! #DIV/0! #DIV/0!	#DIV/0! #DIV/0! #DIV/0! #DIV/0!	#DIV/0! #DIV/0! #DIV/0! #DIV/0!
Recycle 0.8	100 g/t SIBX 150 g/t Depramin 267 40 g/t DOW 200	C1 C2 C3 C4 F T T2 T3 Cc+Tl Mass Bal	2 6 12 20	29.29 40.51 30.11 24.97 1239.64 1089.49 12.66 12.61	284.14 499.88 447.62 422.45	29.29 69.80 99.91 124.88	284.14 784.02 1231.64 1654.09	24.00 63.34 94.44 120.17	7.49 9.14 7.74 6.66	5.30 6.47 5.47 4.71 0.04	229.69 706.71 1157.90 1583.43	77.01 109.33 104.28 99.93	54.45 77.31 73.74 70.66 0.04	0.19 0.04 0.02 0.02 0.01 0.0043 0.005200 0.011	5.56 1.44 0.67 0.45 12.52 0.05 0.07 13.41 107.08	5.56 7.00 7.66 8.11	0.19 0.10 0.08 0.06	41.46 52.19 57.15 60.51	0.24 0.11 0.08 0.07	0.07 0.02 0.01 0.00	0.05 0.01 0.00 0.00	40.80 51.31 56.42 59.98	0.94 1.25 1.04 0.74	0.66 0.89 0.73 0.52	0.42 0.23 0.17 0.17 0.14 0.13 0.12 0.137	12.36 9.24 5.20 4.31 175.04 1.60 1.56 170.39 97.35	12.36 21.60 26.79 31.10	0.42 0.31 0.27 0.25	7.25 12.68 15.73 18.25	0.47 0.32 0.27 0.25	0.06 0.01 0.00 0.00	0.05 0.01 0.00 0.00	8.56 15.91 20.39 24.10	1.85 4.57 6.60 8.27	1.31 3.23 4.67 5.86

Fig 9-1. Solids, Water, Copper and Nickel recoveries and Grades for all baseline recirculation tests.

	Reagents	Sample	Time, min	Mass Pull, g	Water Rec, g	Cum Mass, g	Cum Water, g	Ave cum Mass, g	Std dev	Std error	Ave cum wt Rec, g	Std dev	Std error	Copper %	Copper Mass	Cum Copper Mass	Copper Grade %	Copper Rec %	Ave Copper grade %	Std dev	Std error	Ave Copper rec %	Std dev	Std error	Nickel %	Nickel Mass	Cum Nickel Mass	Nickel Grade %	Nickel Rec %	Ave Nickel grade %	Std dev	Std error	Ave Nickel rec %	Std dev	Std error
RM 1.1	100 g/t SIBX 150 g/t Depramin 267 40 g/t DOW 200	C1 C2 C3 C4 F T T2 T3 Cc+Tl Mass Bal	2 6 12 20	22.60 37.63 35.44 30.57 1287.99 1128.74 16.23 16.78	193.04 409.58 487.41 559.67	22.60 60.23 95.67 126.24	193.04 602.62 1090.03 1649.70	18.68 59.60 97.34 127.39	5.29 2.21 3.11 1.23	2.65 1.10 1.55 0.61	161.20 555.41 1018.87 1492.37	72.05 40.92 99.24 201.89	41.60 23.63 57.30 116.56	0.20 0.04 0.02 0.02 0.01 0.00370 0.00370 0.009	4.56 1.34 0.69 0.57 8.89 0.06 0.06 11.46 128.93	4.56 5.91 6.59 7.16	0.20 0.10 0.07 0.06	39.82 51.55 57.55 62.48	0.25 0.10 0.07 0.06	0.06 0.01 0.00 0.00	0.03 0.00 0.00 0.00	39.91 54.92 62.11 66.88	9.54 10.02 11.24 11.03	5.51 5.78 6.49 6.37	0.45 0.21 0.18 0.16 0.12 0.11 0.11 0.123	10.28 7.97 6.21 5.02 155.07 1.81 1.87 158.90 102.47	10.28 18.25 24.46 29.48	0.45 0.30 0.26 0.23	6.47 11.48 15.39 18.55	0.51 0.32 0.26 0.24	0.06 0.01 0.01 0.01	0.03 0.01 0.00 0.00	5.73 11.52 15.72 18.74	1.23 0.87 0.86 0.73	0.71 0.39 0.51 0.42
RM 1.2	100 g/t SIBX 150 g/t Depramin 267 40 g/t DOW 200	C1 C2 C3 C4 F T T2 T3 Cc+Tl Mass Bal		20.79 40.63 39.50 27.76 1257.53 1095.84 16.23 16.78	211.85 318.26 531.19 501.39	20.79 61.42 100.92 128.68	211.85 530.11 1061.30 1562.69							0.24 0.04 0.02 0.02 0.01 0.00360 0.000000 0.008	4.89 1.65 0.86 0.45 11.82 0.06 0.00 9.88 83.58	4.89 6.54 7.40 7.85	0.24 0.11 0.07 0.06	49.50 66.19 74.91 79.43							0.50 0.23 0.19 0.17 0.13 0.12 0.11 0.129	10.42 9.42 7.34 4.59 162.98 1.94 1.89 162.60 99.77	10.42 19.84 27.18 31.77	0.50 0.32 0.27 0.25	6.41 12.20 16.72 19.54						
RM 1.3	100 g/t SIBX 150 g/t Depramin 267 40 g/t DOW 200	C1 C2 C3 C4 F T T2 T3 Cc+Tl Mass Bal		12.66 44.48 38.28 31.82 1299.34 1088.03 14.03 14.56	78.71 454.79 372.09 359.13	12.66 57.14 95.42 127.24	78.71 533.50 905.59 1264.72							0.32 0.05 0.02 0.02 0.01 0.0052 0.0047 0.010	4.07 2.22 0.91 0.65 12.60 0.07 0.07 13.39 111.00	4.07 6.30 7.21 7.87	0.32 0.11 0.08 0.06	30.42 47.03 53.86 58.73							0.58 0.25 0.18 0.16 0.13 0.12 0.13 0.130	7.31 11.08 7.07 5.22 175.15 1.67 1.88 169.30 100.97	7.31 18.39 25.46 30.67	0.58 0.32 0.27 0.24	4.32 10.66 15.04 18.12						
RM 2.1	100 g/t SIBX 150 g/t Depramin 267 40 g/t DOW 200	C1 C2 C3 C4 F T T2 T3 Cc+Tl Mass Bal	2 6 12 20	18.60 38.01 38.82 33.39 1217.72 1061.73 13.60 13.61	161.43 442.96 486.91 574.14	18.60 56.61 95.43 128.78	161.43 604.39 1091.30 1665.44	17.82 56.02 94.09 124.41	0.97 0.60 1.38 3.90	0.49 0.30 0.69 1.95	171.29 593.77 1079.83 1561.34	47.89 64.99 133.78 224.75	27.65 37.52 77.24 129.76	0.24 0.04 0.02 0.02 0.01 0.0048 0.00610 0.011	4.42 1.57 0.83 0.52 14.25 0.07 0.08 13.27 93.16	4.42 5.99 6.82 7.34	0.24 0.11 0.07 0.06	33.34 45.14 51.37 55.29	0.27 0.11 0.08 0.06	0.05 0.01 0.01 0.01	0.02 0.01 0.00 0.00	36.60 49.06 55.47 59.41	2.97 3.53 3.62 3.59	1.71 2.04 2.09 2.07	0.48 0.22 0.17 0.14 0.11 0.11 0.125	8.89 8.43 6.79 5.82 166.46 1.52 1.53 152.15 91.40	8.89 17.32 24.10 29.92	0.48 0.31 0.25 0.23	5.84 11.38 15.84 19.66	0.49 0.31 0.26 0.24	0.03 0.01 0.01 0.00	0.02 0.01 0.00 0.00	5.37 10.67 14.78 17.94	0.47 0.89 1.16 1.69	0.27 0.52 0.68 0.98
RM 2.2	100 g/t SIBX 150 g/t Depramin 267 40 g/t DOW 200	C1 C2 C3 C4 F T T2 T3 Cc+Tl Mass Bal		18.13 37.29 37.26 28.59 1261.27 1116.72 11.62 11.66	223.35 429.44 554.72 507.86	18.13 55.42 92.68 121.27	223.35 652.79 1207.51 1715.17							0.24 0.04 0.02 0.02 0.01 0.00350 0.00450 0.009	4.37 1.50 0.79 0.49 16.02 0.04 0.05 11.71 73.12	4.37 5.86 6.66 7.15	0.24 0.11 0.07 0.06	37.30 50.07 56.85 61.07							0.47 0.22 0.18 0.17 0.13 0.13 0.13 0.139	8.59 8.36 6.73 4.88 159.60 1.49 1.51 175.33 109.72	8.59 16.95 23.68 28.56	0.47 0.31 0.26 0.24	4.90 9.87 13.50 16.29						
RM 2.3	100 g/t SIBX 150 g/t Depramin 267 40 g/t DOW 200	C1 C2 C3 C4 F T T2 T3 Cc+Tl Mass Bal		16.73 39.30 38.14 29.01 1309.42 1096.95 14.12 15.66	129.10 395.02 416.57 362.72	16.73 56.03 94.17 123.18	129.10 524.12 940.69 1303.41							0.32 0.05 0.02 0.02 0.01 0.00460 0.00480 0.011	5.44 1.78 0.87 0.51 15.58 0.06 0.08 13.88 93.35	5.44 7.22 8.08 8.59	0.32 0.13 0.09 0.07	39.15 51.97 58.20 61.86							0.53 0.24 0.17 0.16 0.14 0.12 0.12 0.127	8.87 9.28 6.66 4.78 185.94 1.65 1.85 165.65 93.33	8.87 18.15 24.81 29.60	0.53 0.32 0.26 0.24	5.35 10.96 14.98 17.87						
RM 3.1	100 g/t SIBX 150 g/t Depramin 267 40 g/t DOW 200	C1 C2 C3 C4 F T T2 T3 Cc+Tl Mass Bal	2 6 12 20	20.60 37.58 34.72 27.64 1271.57 1114.09 18.47 18.47	203.14 477.37 543.74 611.96	20.60 58.18 92.90 120.54	203.14 680.51 1224.25 1836.21	18.60 58.03 94.41 123.50	3.93 4.77 4.32 5.42 0.04	2.27 2.75 2.49 3.13	181.24 661.54 1144.78 1631.54	19.02 71.55 95.50 178.49 0.11	10.98 41.31 55.14 103.05 0.06	0.25 0.04 0.02 0.02 0.01 0.0040000 0.003700 0.010	5.24 1.39 0.81 0.49 17.55 0.00 0.07 0.07 12.36 70.46	5.24 6.63 7.45 7.93	0.25 0.11 0.08 0.07	42.40 53.65 60.22 64.16	0.30 0.12 0.08 0.07	0.08 0.01 0.01 0.00	0.05 0.01 0.00 0.00	39.37 51.14 57.39 61.20	3.09 3.05 3.25 3.46	1.78 1.76 1.88 2.00	0.53 0.23 0.18 0.17 0.14 0.11 0.11 0.124	10.93 8.91 6.21 4.79 172.93 2.05 2.02 157.42 91.03	10.93 19.74 25.96 30.75	0.53 0.34 0.28 0.26	6.94 12.54 16.49 19.53	0.56 0.33 0.27 0.25	0.09 0.02 0.01 0.01	0.05 0.01 0.01 0.00	6.15 11.63 15.61 18.63	0.76 0.89 0.91 1.04	0.45 0.51 0.53 0.60
RM 3.2	100 g/t SIBX 150 g/t Depramin 267 40 g/t DOW 200	C1 C2 C3 C4 F T T2 T3 Cc+Tl Mass Bal		21.13 41.60 36.55 30.48 1256.29 1100.33 14.18 12.02	168.86 413.56 456.42 511.36	21.13 62.73 99.28 129.76	168.86 582.42 1038.84 1550.20							0.24 0.04 0.02 0.02 0.01 0.00960 0.00420 0.011	5.17 1.64 0.87 0.51 12.56 0.09 0.05 14.27 113.63	5.17 6.82 7.69 8.19	0.24 0.11 0.08 0.06	36.24 47.75 53.84 57.39							0.49 0.22 0.19 0.17 0.14 0.13 0.12 0.133	10.26 9.13 6.88 5.31 175.13 1.78 1.39 167.49 95.64	10.26 19.39 26.27 31.57	0.49 0.31 0.26 0.24	6.13 11.58 15.68 18.85						
RM3.3	100 g/t SIBX 150 g/t Depramin 267 40 g/t DOW 200	C1 C2 C3 C4 F T T2 T3 Cc+Tl Mass Bal	2 6 12 20	14.08 39.11 37.86 29.16 1309.77 1108.96 15.67 12.08	171.71 549.98 449.57 336.95	14.08 53.19 91.05 120.21	171.71 721.69 1171.26 1508.21	23.29 67.86 107.68 136.98	13.02 20.75 23.52 23.72	9.21 14.67 16.63 16.77	215.81 736.27 1221.04 1582.18	62.36 20.61 70.39 104.61	44.10 14.58 49.78 73.97	0.39 0.04 0.02 0.02 0.01 0.004000 0.00520 0.011	5.44 1.73 0.84 0.54 11.13 0.06 0.06 13.78 128.95	5.44 7.16 8.01 8.55	0.39 0.13 0.09 0.07	39.46 52.01 58.11 62.05	0.28 0.11 0.08 0.08	0.14 0.03 0.02 0.01	0.10 0.02 0.01 0.01	41.71 53.48 59.30 63.06	3.18 2.09 1.69 1.43	2.25 1.48 1.19 1.01	0.67 0.24 0.18 0.17 0.14 0.12 0.13 0.133	9.38 9.38 6.78 4.93 187.30 1.92 1.57 174.15 96.89	9.38 18.76 25.54 30.47	0.67 0.35 0.28 0.25	5.39 10.77 14.66 17.49	0.53 0.32 0.26 0.24	0.19 0.05 0.02 0.02	0.14 0.04 0.02 0.01	6.32 12.00 16.08 18.87	1.32 1.74 2.01 1.94	0.94 1.23 1.42 1.37

Fig 9-2. Solids, Water, Copper and Nickel recoveries and Grades for all float cell recirculation tests.

Test	Reagents	Sample	Time, min	Mass Pull, g	Water Rec, g	Cum Mass, g	Cum Water, g	Ave cum Mass, g	Std dev	Std error	Ave cum w Rec, g	Std dev	Std error
RF 1.1	100 g/t SIBX	C1	2	30.23	221.90	30.23	221.90	28.70	1.69	0.98	236.45	24.22	13.98
	150 g/t Depramin 267	C2	6	36.90	547.38	67.13	769.28	73.11	5.18	2.99	759.91	11.58	6.69
	40 g/t DOW 200	C3	12	50.80	568.68	117.93	1337.96	116.73	2.07	1.20	1313.47	75.88	43.81
		C4	20	32.09	603.46	150.02	1941.42	148.55	3.50	2.02	1841.18	166.83	96.32
		F		1258.20									
		T		1073.86									
		T1		14.03									
		T2		20.29									
		Cc+Tt											
		Mass Bal											
RF 1.2	100 g/t SIBX	C1		26.88	223.05	26.88	223.05						
	150 g/t Depramin 267	C2		49.36	540.45	76.24	763.50						
	40 g/t DOW 200	C3		41.68	610.57	117.92	1374.07						
		C4		33.16	559.45	151.08	1933.52						
		F		1310.42									
		T		1123.07									
		T1		22.24									
		T2		14.03									
		Cc+Tt											
		Mass Bal											
RF 1.3	100 g/t SIBX	C1	2	28.99	264.41	28.99	264.41	21.79	10.19	7.21	171.46	131.45	92.95
	150 g/t Depramin 267	C2	6	46.96	482.55	75.95	746.96	64.95	15.56	11.00	594.66	215.39	152.31
	40 g/t DOW 200	C3	12	38.39	481.41	114.34	1228.37	102.81	16.31	11.54	1033.66	275.37	194.72
		C4	20	30.21	420.22	144.55	1648.59	132.45	17.11	12.10	1400.13	351.38	248.46
		F		1326.37									
		T		1099.34									
		T2		12.14									
		T3		13.22									
		Cc+Tt											
		Mass Bal											
RF 2.1	100 g/t SIBX	C1	2	24.79	202.44	24.79	202.44	26.34	3.88	2.24	235.29	53.29	30.77
	150 g/t Depramin 267	C2	6	48.70	536.26	73.49	738.70	71.47	3.61	2.09	753.64	60.27	34.80
	40 g/t DOW 200	C3	12	41.08	588.00	114.57	1326.70	112.31	5.27	3.04	1338.15	119.60	69.05
		C4	20	31.91	577.74	146.48	1904.44	143.71	5.87	3.39	1857.86	149.11	86.09
		F		1276.84									
		T		1102.10									
		T1		14.23									
		T2		14.03									
		Cc+Tt											
		Mass Bal											
RM 2.2	100 g/t SIBX	C1		30.76	296.77	30.76	296.77						
	150 g/t Depramin 267	C2		42.86	523.20	73.62	819.97						
	40 g/t DOW 200	C3		42.46	643.09	116.08	1463.06						
		C4		31.60	515.07	147.68	1978.13						
		F		1258.84									
		T		1075.51									
		T1		15.78									
		T2		19.87									
		Cc+Tt											
		Mass Bal											
RF 2.3	100 g/t SIBX	C1	2	23.47	206.65	23.47	206.65	23.78	0.43	0.31	205.34	1.85	1.31
	150 g/t Depramin 267	C2	6	43.83	495.59	67.30	702.24	63.48	5.40	3.82	636.13	93.50	66.12
	40 g/t DOW 200	C3	12	38.99	522.44	106.29	1224.68	101.00	7.48	5.29	1115.12	154.94	109.56
		C4	20	30.67	466.34	136.96	1691.02	131.87	7.20	5.09	1590.00	142.87	101.03
		F		1314.68									
		T		1083.77									
		T2		10.64									
		T3		13.08									
		Cc+Tt											
		Mass Bal											
RM 3.1	100 g/t SIBX	C1	2	30.84	203.60	30.84	203.60	29.43	3.96	2.29	216.27	38.88	22.44
	150 g/t Depramin 267	C2	6	48.25	532.50	79.09	736.10	80.39	1.87	1.08	747.46	10.10	5.83
	40 g/t DOW 200	C3	12	41.68	597.33	120.77	1333.43	122.32	1.91	1.10	1315.58	37.48	21.64
		C4	20	22.52	539.76	143.29	1873.19	150.38	6.15	3.55	1798.83	125.73	72.59
		F		1261.70									
		T		1093.10								0.07	
		T1		12.03									
		T2		13.28									
		Cc+Tt											
		Mass Bal											
RM 3.2	100 g/t SIBX	C1		24.95	185.31	24.95	185.31						
	150 g/t Depramin 267	C2		54.60	570.13	79.55	755.44						
	40 g/t DOW 200	C3		42.19	585.36	121.74	1340.80						
		C4		32.37	528.84	154.11	1869.64						
		F		1292.62									
		T		1107.47									
		T1		12.51									
		T2		18.53									
		Cc+Tt											
		Mass Bal											
RM 3.3	100 g/t SIBX	C1	2	32.49	259.90	32.49	259.90	28.36	5.85	4.14	228.10	44.98	31.81
	150 g/t Depramin 267	C2	6	50.04	490.94	82.53	750.84	77.19	7.55	5.34	722.58	39.97	28.26
	40 g/t DOW 200	C3	12	41.93	521.68	124.46	1272.52	119.14	7.53	5.33	1257.18	21.69	15.34
		C4	20	29.29	381.15	153.75	1653.67	149.45	6.08	4.30	1661.95	11.70	8.28
		F		1313.61									
		T		1078.00									
		T2		10.61									
		T3		14.10									
		Cc+Tt											
		Mass Bal											

Test	Sample	Copper %	Copper Mass	Cum Copper Mass	Copper Grade %	Copper Rec %	Ave Copper grade %	Std dev	Std error	Ave Copper rec %	Std dev	Std error
RF 1.1	C1	0.21	6.41	6.41	0.21	44.65	0.23	0.04	0.02	44.67	3.34	1.93
	C2	0.02	0.82	7.23	0.11	50.38	0.11	0.02	0.01	54.74	4.64	2.68
	C3	0.02	1.09	8.32	0.07	57.96	0.08	0.01	0.01	60.82	3.03	1.75
	C4	0.02	0.55	8.87	0.06	61.78	0.06	0.01	0.01	64.52	2.84	1.64
	F	0.01	15.60									
	T											
	T1	0.0039	0.05									
	T2	0.006	0.12									
	Cc+Tt		0.011	14.35								
	Mass Bal			92.00								
RF 1.2	C1	0.20	5.37	5.37	0.20	41.34						
	C2	0.03	1.67	7.04	0.09	54.22						
	C3	0.02	0.82	7.86	0.07	60.50						
	C4	0.01	0.49	8.35	0.06	64.31						
	F	0.01	13.63									
	T											
	T1	0.00400	0.09									
	T2	0.00400	0.06									
	Cc+Tt		0.010	12.99								
	Mass Bal			95.33								
RF 1.3	C1	0.27	7.88	7.88	0.27	48.01	0.31	0.06	0.04	43.43	6.48	4.58
	C2	0.04	1.91	9.79	0.13	59.63	0.13	0.00	0.00	56.47	4.47	3.16
	C3	0.02	0.72	10.51	0.09	64.00	0.09	0.00	0.00	62.05	2.76	1.95
	C4	0.02	0.57	11.07	0.08	67.46	0.07	0.00	0.00	66.16	1.83	1.30
	F	0.01	12.34									
	T											
	T2	0.005	0.06									
	T3	0.005	0.06									
	Cc+Tt		0.012	16.42								
	Mass Bal			139.08								
RF 2.1	C1	0.22	5.39	5.39	0.22	38.25	0.20	0.02	0.01	38.25	1.13	0.65
	C2	0.03	1.69	7.08	0.10	50.28	0.10	0.00	0.00	49.30	0.90	0.52
	C3	0.02	0.85	7.93	0.07	56.29	0.07	0.00	0.00	55.65	0.57	0.33
	C4	0.02	0.50	8.43	0.06	59.87	0.06	0.00	0.00	59.55	0.44	0.26
	F	0.01	12.90									
	T											
	T1	0.01	0.07									
	T2	0.00500	0.07									
	Cc+Tt		0.011	14.08								
	Mass Bal			109.21								
RM 2.2	C1	0.18	5.66	5.66	0.18	39.38						
	C2	0.03	1.31	6.97	0.09	48.50						
	C3	0.02	0.96	7.94	0.07	55.20						
	C4	0.02	0.55	8.49	0.06	59.05						
	F	0.01	13.09									
	T											
	T1	0.0036	0.06									
	T2	0.01	0.14									
	Cc+Tt		0.011	14.38								
	Mass Bal			109.84								
RF 2.3	C1	0.20	4.80	4.80	0.20	37.12	0.29	0.12	0.08	44.65	10.64	7.53
	C2	0.04	1.55	6.35	0.09	49.12	0.14	0.06	0.04	55.43	8.92	6.31
	C3	0.02	0.82	7.17	0.07	55.45	0.09	0.04	0.03	61.51	8.57	6.06
	C4	0.02	0.56	7.73	0.06	59.74	0.08	0.03	0.02	65.36	7.94	5.62
	F	0.01	10.91									
	T											
	T2	0.0038	0.04									
	T3	0.01	0.07									
	Cc+Tt		0.010	12.93								
	Mass Bal			125.19								
RM 3.1	C1	0.21	6.36	6.36	0.21	43.46	0.24	0.06	0.03	44.20	12.51	7.22
	C2	0.04	1.86	8.22	0.10	56.15	0.11	0.03	0.01	55.46	12.99	7.50
	C3	0.02	0.81	9.03	0.07	61.71	0.08	0.02	0.01	60.59	12.70	7.33
	C4	0.02	0.40	9.43	0.07	64.46	0.07	0.02	0.01	63.57	12.55	7.25
	F	0.02	19.93									
	T		0.00									
	T1	0.004	0.05									
	T2	0.01	0.07									
	Cc+Tt		0.012	14.63								
	Mass Bal			73.41								
RM 3.2	C1	0.21	5.36	5.36	0.21	32.08						
	C2	0.03	1.68	7.04	0.09	42.15						
	C3	0.02	0.87	7.91	0.07	47.37						
	C4	0.02	0.54	8.45	0.05	50.59						
	F	0.01	15.90									
	T											
	T1	0.01	0.11									
	T2	0.01	0.10									
	Cc+Tt		0.013	16.71								
	Mass Bal			105.07								
RM 3.3	C1	0.33	10.60	10.60	0.33	57.07	0.27	0.07	0.05	48.18	12.57	8.89
	C2	0.04	2.05	12.64	0.15	68.10	0.13	0.04	0.03	59.66	11.93	8.44
	C3	0.02	0.86	13.50	0.11	72.70	0.09	0.03	0.02	65.63	10.01	7.08
	C4	0.02	0.55	14.05	0.09	75.65	0.08	0.02	0.02	69.09	9.29	6.57
	F	0.01	10.64									
	T											
	T2	0.0040	0.04									
	T3	0.0042	0.06									
	Cc+Tt		0.014	18.57								
	Mass Bal			182.46								

Test	Sample	Nickel %	Nickel Mass	Cum Nickel Mass	Nickel Grade %	Nickel Rec %	Ave Nickel grade %	Std dev	Std error	Ave Nickel rec %	Std dev	Std error
RF 1.1	C1	0.45	13.69	13.69	0.45	7.93	0.47	0.06	0.04	7.71	1.16	0.67
	C2	0.17	6.28	19.96	0.30	11.57	0.31	0.03	0.02	13.02	1.76	1.02
	C3	0.21	10.66	30.62	0.26	17.75	0.26	0.03	0.01	17.73	1.19	0.69
	C4	0.16	5.22	35.84	0.24	20.77	0.24	0.02	0.01	20.80	0.95	0.55
	F	0.13	168.85									
	T											
	T1	0.12	1.65									
	T2	0.13	2.62									
	Cc+Tt		0.137	172.54								
	Mass Bal			102.18								
RF 1.2	C1	0.41	11.10	11.10	0.41	6.45						
	C2	0.21	10.44	21.55	0.28	12.52						
	C3	0.17	6.93	28.47	0.24	16.54						
	C4	0.17	5.71	34.19	0.23	19.86						
	F	0.14	188.44									
	T											
	T1	0.12	2.62									
	T2	0.12	1.69									
	Cc+Tt		0.131	172.15								
	Mass Bal			91.36								
RF 1.3	C1	0.53	15.46	15.46	0.53	8.75	0.55	0.02	0.01	6.85	2.69	1.90
	C2	0.23	11.02	26.48	0.35	14.98	0.34	0.01	0.01	12.97	2.83	2.00
	C3	0.18	6.96	33.44	0.29	18.91	0.28	0.01	0.01	17.03	2.67	1.89
	C4	0.17	5.03	38.47	0.27	21.76	0.26	0.01	0.01	19.86	2.69	1.90
	F	0.14	179.33									
	T											
	T2	0.12	1.49									
	T3	0.12	1.63									
	Cc+Tt		0.133	176.81								
	Mass Bal			103.03								
RF 2.1	C1	0.45	11.12	11.12	0.45	6.64	0.44	0.01	0.01	6.92	0.98	0.56
	C2	0.22	10.51	21.63	0.29	12.92	0.29	0.01	0.00	12.66	1.02	0.59
	C3	0.18	7.54	29.17	0.25	17.42	0.25	0.00	0.00	16.99	1.18	0.68
	C4	0.16	5.19	34.35	0.23	20.52	0.23	0.00	0.00	20.13	1.41	0.82
	F	0.14	173.39									
	T											
	T1	0.12	1.69									
	T2	0.12	1.64									
	Cc+Tt		0.131	167.39								
	Mass Bal			96.54								
RM 2.2	C1	0.43	13.08	13.08	0.43	8.01						
	C2	0.21	9.00	22.08	0.30	13.52						
	C3	0.17	7.15	29.23	0.25	17.90						
	C4	0.18	5.57	34.80	0.24	21.31						
	F	0.14	175.36									
	T											
	T1	0.11	1.78									
	T2	0.12	2.35									
	Cc+Tt		0.130	163.30								
	Mass Bal			93.13								
RF 2.3	C1	0.44	10.31	10.31	0.44	6.11	0.48	0.06	0.04	6.86	1.05	0.75
	C2	0.21	9.14	19.45	0.29	11.53	0.32	0.04	0.03	11.98	0.63	0.44
	C3	0.18	6.97	26.41	0.25	15.66	0.27	0.03	0.02	15.95	0.40	0.28
	C4	0.16	4.89	31.30	0.23	18.56	0.24	0.02	0.01	18.97	0.57	0.41
	F	0.13	173.93									
	T											
	T2	0.12	1.33									
	T3	0.12	1.61									
	Cc+Tt		0.128	168.63								
	Mass Bal			102.42								
RM 3.1	C1	0.44	13.45	13.45	0.44	7.57	0.49	0.09	0.05	8.23	2.14	1.24
	C2	0.22	10.82	24.27	0.31	13.65	0.32	0.05	0.03	14.68	2.34	1.35
	C3	0.17	7.05	31.32	0.26	17.62	0.27	0.04	0.02	18.78	2.36	1.36
	C4	0.16	3.70	35.02	0.24	19.70	0.25	0.03	0.02	21.40	2.44	1.41
	F	0.15	185.34									
	T											
	T1	0.13	1.53									
	T2	0.13	1.71									
	Cc+Tt		0.141	177.73								
	Mass Bal			95.89								
RM 3.2	C1	0.45	11.15	11.15	0.45	6.50						
	C2	0.21	11.20	22.35	0.28	13.04						
	C3	0.17	7.17	29.52	0.24	17.22						
	C4	0.16	5.27	34.79	0.23	20.30						
	F	0.13	170.37									
	T											
	T1	0.13	1.58									
	T2	0.11	2.10									
	Cc+Tt		0.133	171.41								
	Mass Bal			100.61								
RM 3.3	C1	0.59	19.25	19.25	0.59	10.63	0.52	0.10	0.07	8.74	2.68	1.90
	C2	0.24	12.18	31.43	0.38	17.36	0.34	0.06	0.04	15.25	2.98	2.11
	C3	0.18	7.48	38.91	0.31	21.49	0.28	0.04	0.03	19.59	2.69	1.90
	C4	0.17	4.91	43.81	0.28	24.20	0.26	0.04	0.03	22.55	2.34	1.65
	F	0.14	183.38									
	T											
	T2	0.12	1.30									
	T3	0.13	1.79									
	Cc+Tt		0.138	181.05								
	Mass Bal			103.22								

Fig 9-3. Solids, Water, Copper and Nickel recoveries and Grades for all mill recirculation tests.

Appendix C. Material Data Safety Sheets of Reagents

AFROX

MATERIAL SAFETY DATA SHEET (MSDS)

AIR

(Please ensure that this MSDS is received by the appropriate person)

DATE: February 2017 Version2
Ref .No. MS104

1 PRODUCT AND COMPANY IDENTIFICATION

PRODUCT IDENTIFICATION

Product Name	AIR
Chemical Formula	21% Oxygen/ Balance Nitrogen
Trade Names	Air, Compressed. Dry Air Air, Instrument Grade Air, Instrument Grade, (Zero) Medical Air, Compressed
Colour Coding	Air Compressed & Dry French Grey (H.30) body Air Instrument grade French Grey (H.30) body with the "Instrument Grade" logo affixed to the body of the cylinder Air, Instrument grade, (ZERO). Protea Pink (P.58) body with the "Instrument Grade" logo and "ZERO" decal affixed to the body of the cylinder. Medical Air, Compressed French Grey (H.30) body, with white & black quadrants on the shoulder of the cylinder
Valve	All of the above grades have the 3 SO – Brass 5/8 inch right hand female valve fitted
Company Identification	African Oxygen Limited 23 Webber Street Johannesburg, 2001 Tel. No: (011) 490-0400
EMERGENCY NUMBER	**0860 020202 or (011) 873 4382 (24hrs)**

2 COMPOSITION/INFORMATION ON INGREDIENTS

Chemical Name	Air
Synonyms	Atmospheric Air
CAS No.	None
UN No.	1002
ERG No.	122
Hazard Warning	2C Non flammable gas

3 HAZARDS IDENTIFICATION

Main Hazards. All cylinders are portable gas containers and must be regarded as pressure vessels at all times. Air is non -flammable, but readily supports combustion. Never permit oil, grease, or other readily combustible substance to come into contact with air at high pressures.

Adverse health effects. None. Air is non-toxic and non-flammable. Of the constituents which make up air, only oxygen and nitrogen are necessary for life.

Chemical Hazards. In air which contains more than the normal 21% oxygen, combustible materials are easier to ignite and burn faster. The higher the concentration of oxygen, the greater the fire risk. In a compartment (such as a tunnel, caisson or chamber) filled with air under pressure, most combustible materials will ignite more readily and burn much more rapidly than they would in air at normal atmospheric pressure, because of the increase in partial pressure of oxygen, even though the air contains only the normal 21% of oxygen.

Biological Hazards	No known effect
Vapour Inhalation	No known effect
Eye Contact	No known effect
Skin Contact	No known effect
Ingestion	No known effect

4 FIRST AID MEASURES

Care should be taken with the exposure to either oxygen-deficient, or oxygen-enriched atmospheres. Conscious persons should be assisted to an uncontaminated area and inhale fresh air. They should be kept warm and quiet. Quick removal from the contaminated area is most important. The physician should be informed when a patient has experienced hyperoxia.

Eye Contact	No known effect
Skin Contact	No known effect
Ingestion	No known effect

5 FIRE FIGHTING MEASURES

Extinguishing media. As Air is non-flammable, but supports combustion, the correct type of extinguishant should be used depending on the combustible material involved.

Specific Hazards. Materials that would not normally burn in air could combust vigorously in atmospheres having high concentrations of oxygen.

Emergency Actions. All cylinders should be removed from the vicinity of the fire. Cylinders that cannot be removed should be cooled with water from a safe distance. Cylinders which have been exposed to excessive heat should be clearly identified and returned to the supplier. CONTACT THE NEAREST AFROX BRANCH.

Protective Clothing. Safety goggles, gloves and safety shoes should be worn when handling cylinders.

Environmental precautions. None

6 ACCIDENTAL RELEASE MEASURES

Personal Precautions. Avoid exposure to either oxygen deficient, or oxygen-enriched atmospheres.

Environmental precautions. Beware of oxygen enriched atmospheres coming into contact with readily combustible materials.

Small spills	No known effect.
Large spills	No known effect.

7 HANDLING AND STORAGE

Do not allow cylinders to slide or come into contact with sharp edges. Cylinders of air should not be stored near cylinders of acetylene or other combustible gases. Air cylinders may be stacked horizontally provided that they are firmly secured at each end to prevent rolling. Prevent dirt, grit of any sort, oil, or any other lubricant from entering the cylinder valves, and store cylinders well clear of any corrosive influence e.g. battery acid. Compliance with all relevant legislation is essential. Use a "first in - first out" inventory system to prevent full cylinders from being stored for excessive periods of time. Keep out of reach of children.

Fig 9-4. MSDS of air

SIGMA-ALDRICH sigma-aldrich.com

SAFETY DATA SHEET

according to Regulation (EC) No. 1907/2006
Version 6.0 Revision Date 30.03.2016
Print Date 07.09.2019
GENERIC EU MSDS - NO COUNTRY SPECIFIC DATA - NO OEL DATA

SECTION 1: Identification of the substance/mixture and of the company/undertaking

1.1 Product identifiers

Product name	:	Calcium nitrate tetrahydrate
Product Number	:	C1396
Brand	:	SIGALD
REACH No.	:	A registration number is not available for this substance as the substance or its uses are exempted from registration, the annual tonnage does not require a registration or the registration is envisaged for a later registration deadline.
CAS-No.	:	13477-34-4

1.2 Relevant identified uses of the substance or mixture and uses advised against

Identified uses	:	Laboratory chemicals, Manufacture of substances

1.3 Details of the supplier of the safety data sheet

Company	:	Merck (Pty) Ltd. 1 Friesland Drive Longmeadow Business Estate South MODDERFONTEIN 1645 SOUTH AFRICA
Telephone	:	+27 +27 (0) 8600 63725
Fax	:	+27 +27 (0) 860 522 329
E-mail address	:	Melissa.byrne@merckgroup.com

1.4 Emergency telephone number

Emergency Phone #	:	

SECTION 2: Hazards identification

2.1 Classification of the substance or mixture

Classification according to Regulation (EC) No 1272/2008
Acute toxicity, Oral (Category 4), H302
Serious eye damage (Category 1), H318

For the full text of the H-Statements mentioned in this Section, see Section 16.

2.2 Label elements

Labelling according Regulation (EC) No 1272/2008
Pictogram

Signal word Danger

Hazard statement(s)
H302 Harmful if swallowed.
H318 Causes serious eye damage.

Fig 9-5. MSDS for Calcium Nitrate Tetrahydrate adapted from (Sigmaalderich, 2019).

AFROX
A Member of the Linde Group

MATERIAL SAFETY DATA SHEET (MSDS)

AIR

(Please ensure that this MSDS is received by the appropriate person)

DATE: February 2017 Version2
Ref .No. MS104

1 PRODUCT AND COMPANY IDENTIFICATION

PRODUCT IDENTIFICATION

Product Name	AIR.
Chemical Formula	21% Oxygen/ Balance Nitrogen
Trade Names	Air, Compressed. Dry Air Air, Instrument Grade Air, Instrument Grade, (Zero) Medical Air, Compressed
Colour Coding	Air Compressed & Dry French Grey (H.30) body Air Instrument grade French Grey (H.30) body with the "Instrument Grade" logo affixed to the body of the cylinder Air, Instrument grade, (ZERO). Protea Pink (P.58) body with the "Instrument Grade" logo and "ZERO" decal affixed to the body of the cylinder. Medical Air, Compressed French Grey (H.30) body, with white & black quadrants on the shoulder of the cylinder
Valve	All of the above grades have the 3 SO – Brass 5/8 inch right hand female valve fitted
Company Identification	African Oxygen Limited 23 Webber Street Johannesburg, 2001 Tel. No: (011) 490-0400
EMERGENCY NUMBER	**0860 020202 or (011) 873 4382 (24hrs)**

2 COMPOSITION/INFORMATION ON INGREDIENTS

Chemical Name	Air
Synonyms	Atmospheric Air
CAS No.	None
UN No.	1002
ERG No.	122
Hazard Warning	2C Non flammable gas

3 HAZARDS IDENTIFICATION

Main Hazards. All cylinders are portable gas containers and must be regarded as pressure vessels at all times. Air is non -flammable, but readily supports combustion. Never permit oil, grease, or other readily combustible substance to come into contact with air at high pressures.

Adverse health effects. None. Air is non-toxic and non-flammable. Of the constituents which make up air, only oxygen and nitrogen are necessary for life.

Chemical Hazards. In air which contains more than the normal 21% oxygen, combustible materials are easier to ignite and burn faster. The higher the concentration of oxygen, the greater the fire risk. In a compartment (such as a tunnel, caisson or chamber) filled with air under pressure, most combustible materials will ignite more readily and burn much more rapidly than they would in air at normal atmospheric pressure, because of the increase in partial pressure of oxygen, even though the air contains only the normal 21% of oxygen.

Biological Hazards	No known effect
Vapour Inhalation	No known effect
Eye Contact	No known effect
Skin Contact	No known effect
Ingestion	No known effect

4 FIRST AID MEASURES

Care should be taken with the exposure to either oxygen-deficient, or oxygen-enriched atmospheres. Conscious persons should be assisted to an uncontaminated area and inhale fresh air. They should be kept warm and quiet. Quick removal from the contaminated area is most important. The physician should be informed when a patient has experienced hyperoxia.

Eye Contact	No known effect
Skin Contact	No known effect
Ingestion	No known effect

5 FIRE FIGHTING MEASURES

Extinguishing media. As Air is non-flammable, but supports combustion, the correct type of extinguishant should be used depending on the combustible material involved.

Specific Hazards. Materials that would not normally burn in air could combust vigorously in atmospheres having high concentrations of oxygen.

Emergency Actions. All cylinders should be removed from the vicinity of the fire. Cylinders that cannot be removed should be cooled with water from a safe distance. Cylinders which have been exposed to excessive heat should be clearly identified and returned to the supplier. CONTACT THE NEAREST AFROX BRANCH.

Protective Clothing. Safety goggles, gloves and safety shoes should be worn when handling cylinders.

Environmental precautions. None

6 ACCIDENTAL RELEASE MEASURES

Personal Precautions. Avoid exposure to either oxygen deficient, or oxygen-enriched atmospheres.

Environmental precautions. Beware of oxygen enriched atmospheres coming into contact with readily combustible materials.

Small spills	No known effect.
Large spills	No known effect.

7 HANDLING AND STORAGE

Do not allow cylinders to slide or come into contact with sharp edges. Cylinders of air should not be stored near cylinders of acetylene or other combustible gases. Air cylinders may be stacked horizontally provided that they are firmly secured at each end to prevent rolling. Prevent dirt, grit of any sort, oil, or any other lubricant from entering the cylinder valves, and store cylinders well clear of any corrosive influence e.g. battery acid. Compliance with all relevant legislation is essential. Use a "first in - first out" inventory system to prevent full cylinders from being stored for excessive periods of time. Keep out of reach of children.

Fig 9-6. MSDS for Calcium Chloride Dihydrate adapted from (Sigmaalderich, 2019).

AFROX

MATERIAL SAFETY DATA SHEET (MSDS)

AIR

(Please ensure that this MSDS is received by the appropriate person)

DATE: February 2017 Version2
Ref .No. MS104

1 PRODUCT AND COMPANY IDENTIFICATION

PRODUCT IDENTIFICATION

Product Name	AIR.
Chemical Formula	21% Oxygen/ Balance Nitrogen
Trade Names	Air, Compressed. Dry Air Air, Instrument Grade Air, Instrument Grade, (Zero) Medical Air, Compressed
Colour Coding	Air Compressed & Dry French Grey (H.30) body Air Instrument grade French Grey (H.30) body with the "Instrument Grade" logo affixed to the body of the cylinder Air, Instrument grade, (ZERO). Protea Pink (P.58) body with the "Instrument Grade" logo and "ZERO" decal affixed to the body of the cylinder. Medical Air, Compressed French Grey (H.30) body, with white & black quadrants on the shoulder of the cylinder
Valve	All of the above grades have the 3 SO – Brass 5/8 inch right hand female valve fitted
Company Identification	African Oxygen Limited 23 Webber Street Johannesburg, 2001 Tel. No: (011) 490-0400
EMERGENCY NUMBER	**0860 020202 or (011) 873 4382 (24hrs)**

2 COMPOSITION/INFORMATION ON INGREDIENTS

Chemical Name	Air
Synonyms	Atmospheric Air
CAS No.	None
UN No.	1002
ERG No.	122
Hazard Warning	2C Non flammable gas

3 HAZARDS IDENTIFICATION

Main Hazards. All cylinders are portable gas containers and must be regarded as pressure vessels at all times. Air is non -flammable, but readily supports combustion. Never permit oil, grease, or other readily combustible substance to come into contact with air at high pressures.

Adverse health effects. None. Air is non-toxic and non-flammable. Of the constituents which make up air, only oxygen and nitrogen are necessary for life.

Chemical Hazards. In air which contains more than the normal 21% oxygen, combustible materials are easier to ignite and burn faster. The higher the concentration of oxygen, the greater the fire risk. In a compartment (such as a tunnel, caisson or chamber) filled with air under pressure, most combustible materials will ignite more readily and burn much more rapidly than they would in air at normal atmospheric pressure, because of the increase in partial pressure of oxygen, even though the air contains only the normal 21% of oxygen.

Biological Hazards	No known effect
Vapour Inhalation	No known effect
Eye Contact	No known effect
Skin Contact	No known effect
Ingestion	No known effect

4 FIRST AID MEASURES

Care should be taken with the exposure to either oxygen-deficient, or oxygen-enriched atmospheres. Conscious persons should be assisted to an uncontaminated area and inhale fresh air. They should be kept warm and quiet. Quick removal from the contaminated area is most important. The physician should be informed when a patient has experienced hyperoxia.

Eye Contact	No known effect
Skin Contact	No known effect
Ingestion	No known effect

5 FIRE FIGHTING MEASURES

Extinguishing media. As Air is non-flammable, but supports combustion, the correct type of extinguishant should be used depending on the combustible material involved.

Specific Hazards. Materials that would not normally burn in air could combust vigorously in atmospheres having high concentrations of oxygen.

Emergency Actions. All cylinders should be removed from the vicinity of the fire. Cylinders that cannot be removed should be cooled with water from a safe distance. Cylinders which have been exposed to excessive heat should be clearly identified and returned to the supplier. CONTACT THE NEAREST AFROX BRANCH.

Protective Clothing. Safety goggles, gloves and safety shoes should be worn when handling cylinders.

Environmental precautions. None

6 ACCIDENTAL RELEASE MEASURES

Personal Precautions. Avoid exposure to either oxygen deficient, or oxygen-enriched atmospheres.

Environmental precautions. Beware of oxygen enriched atmospheres coming into contact with readily combustible materials.

Small spills	No known effect.
Large spills	No known effect.

7 HANDLING AND STORAGE

Do not allow cylinders to slide or come into contact with sharp edges. Cylinders of air should not be stored near cylinders of acetylene or other combustible gases. Air cylinders may be stacked horizontally provided that they are firmly secured at each end to prevent rolling. Prevent dirt, grit of any sort, oil, or any other lubricant from entering the cylinder valves, and store cylinders well clear of any corrosive influence e.g. battery acid. Compliance with all relevant legislation is essential. Use a "first in - first out" inventory system to prevent full cylinders from being stored for excessive periods of time. Keep out of reach of children.

Fig 9-7. MSDS for Sodium Chloride Tetrahydrate adapted from (Sigmaalderich, 2019).

AFROX
A Member of the Linde Group

MATERIAL SAFETY DATA SHEET (MSDS)

AIR

(Please ensure that this MSDS is received by the appropriate person)

DATE: February 2017 Version2
Ref .No. MS104

1 PRODUCT AND COMPANY IDENTIFICATION

PRODUCT IDENTIFICATION

Product Name	AIR
Chemical Formula	21% Oxygen/ Balance Nitrogen
Trade Names	Air, Compressed. Dry Air Air, Instrument Grade Air, Instrument Grade, (Zero) Medical Air, Compressed
Colour Coding	Air Compressed & Dry French Grey (H.30) body Air Instrument grade French Grey (H.30) body with the "Instrument Grade" logo affixed to the body of the cylinder Air, Instrument grade, (ZERO). Protea Pink (P.58) body with the "Instrument Grade" logo and "ZERO" decal affixed to the body of the cylinder. Medical Air, Compressed French Grey (H.30) body, with white & black quadrants on the shoulder of the cylinder
Valve	All of the above grades have the 3 SO – Brass 5/8 inch right hand female valve fitted
Company Identification	African Oxygen Limited 23 Webber Street Johannesburg, 2001 Tel. No: (011) 490-0400

EMERGENCY NUMBER **0860 020202 or (011) 873 4382 (24hrs)**

2 COMPOSITION/INFORMATION ON INGREDIENTS

Chemical Name	Air
Synonyms	Atmospheric Air
CAS No.	None
UN No.	1002
ERG No.	122
Hazard Warning	2C Non flammable gas

3 HAZARDS IDENTIFICATION

Main Hazards. All cylinders are portable gas containers and must be regarded as pressure vessels at all times. Air is non -flammable, but readily supports combustion. Never permit oil, grease, or other readily combustible substance to come into contact with air at high pressures.

Adverse health effects. None. Air is non-toxic and non-flammable. Of the constituents which make up air, only oxygen and nitrogen are necessary for life.

Chemical Hazards. In air which contains more than the normal 21% oxygen, combustible materials are easier to ignite and burn faster. The higher the concentration of oxygen, the greater the fire risk. In a compartment (such as a tunnel, caisson or chamber) filled with air under pressure, most combustible materials will ignite more readily and burn much more rapidly than they would in air at normal atmospheric pressure, because of the increase in partial pressure of oxygen, even though the air contains only the normal 21% of oxygen.

Biological Hazards	No known effect
Vapour Inhalation	No known effect
Eye Contact	No known effect
Skin Contact	No known effect
Ingestion	No known effect

4 FIRST AID MEASURES

Care should be taken with the exposure to either oxygen-deficient, or oxygen-enriched atmospheres. Conscious persons should be assisted to an uncontaminated area and inhale fresh air. They should be kept warm and quiet. Quick removal from the contaminated area is most important. The physician should be informed when a patient has experienced hyperoxia.

Eye Contact	No known effect
Skin Contact	No known effect
Ingestion	No known effect

5 FIRE FIGHTING MEASURES

Extinguishing media. As Air is non-flammable, but supports combustion, the correct type of extinguishant should be used depending on the combustible material involved.

Specific Hazards. Materials that would not normally burn in air could combust vigorously in atmospheres having high concentrations of oxygen.

Emergency Actions. All cylinders should be removed from the vicinity of the fire. Cylinders that cannot be removed should be cooled with water from a safe distance. Cylinders which have been exposed to excessive heat should be clearly identified and returned to the supplier. CONTACT THE NEAREST AFROX BRANCH.

Protective Clothing. Safety goggles, gloves and safety shoes should be worn when handling cylinders.

Environmental precautions. None

6 ACCIDENTAL RELEASE MEASURES

Personal Precautions. Avoid exposure to either oxygen deficient, or oxygen-enriched atmospheres.

Environmental precautions. Beware of oxygen enriched atmospheres coming into contact with readily combustible materials.

Small spills	No known effect.
Large spills	No known effect.

7 HANDLING AND STORAGE

Do not allow cylinders to slide or come into contact with sharp edges. Cylinders of air should not be stored near cylinders of acetylene or other combustible gases. Air cylinders may be stacked horizontally provided that they are firmly secured at each end to prevent rolling. Prevent dirt, grit of any sort, oil, or any other lubricant from entering the cylinder valves, and store cylinders well clear of any corrosive influence e.g. battery acid. Compliance with all relevant legislation is essential. Use a "first in - first out" inventory system to prevent full cylinders from being stored for excessive periods of time. Keep out of reach of children.

Fig 9-8. MSDS for Magnesium sulfate heptahydrate adapted from (Sigmaalderich, 2019).

SIGMA-ALDRICH

sigma-aldrich.com

SAFETY DATA SHEET

according to Regulation (EC) No. 1907/2006
Version 6.0 Revision Date 30.03.2016
Print Date 07.09.2019
GENERIC EU MSDS - NO COUNTRY SPECIFIC DATA - NO OEL DATA

SECTION 1: Identification of the substance/mixture and of the company/undertaking

1.1 Product identifiers

Product name : Calcium nitrate tetrahydrate

Product Number : C1396
Brand : SIGALD
REACH No. : A registration number is not available for this substance as the substance or its uses are exempted from registration, the annual tonnage does not require a registration or the registration is envisaged for a later registration deadline.
CAS-No. : 13477-34-4

1.2 Relevant identified uses of the substance or mixture and uses advised against

Identified uses : Laboratory chemicals, Manufacture of substances

1.3 Details of the supplier of the safety data sheet

Company : Merck (Pty) Ltd.
1 Friesland Drive
Longmeadow Business Estate South
MODDERFONTEIN
1645
SOUTH AFRICA

Telephone : +27 +27 (0) 8600 63725
Fax : +27 +27 (0) 860 522 329
E-mail address : Melissa.byrne@merckgroup.com

1.4 Emergency telephone number

Emergency Phone # :

SECTION 2: Hazards identification

2.1 Classification of the substance or mixture

Classification according to Regulation (EC) No 1272/2008
Acute toxicity, Oral (Category 4), H302
Serious eye damage (Category 1), H318

For the full text of the H-Statements mentioned in this Section, see Section 16.

2.2 Label elements

Labelling according Regulation (EC) No 1272/2008
Pictogram

Signal word Danger

Hazard statement(s)
H302 Harmful if swallowed.
H318 Causes serious eye damage.

Fig 9-9. MSDS for Sodium Carbonate adapted from (Sigmaalderich, 2019).

MATERIAL SAFETY DATA SHEET

PRINT DATE: 02.09.2013
REVISION DATE: JAN 2013

1. IDENTIFICATION OF THE PRODUCT AND COMPANY

Product Name: **DOWFROTH 200 FLOTATION FROTHER**

Company: **Betachem (Pty) Ltd.**
P.O. Box 2306
RANDBURG 2125
R.S.A.

Emergency telephone No.: + 27 (11) 782 6789 ***Fax:*** + 27 (11) 888 7458
+ 27 (31) 305 7161 Code 1715 (24 hr Response)

2. COMPOSITION/INFORMATION ON INGREDIENTS

Identification of the preparation:

	CAS #	EINECS #
Tri-propylene glycol methyl ether	20324-33-8	Listed
Di-propylene glycol mono-methyl ether	34590-94-5	252-104-2
Diethylene glycol monobutyl ether	203-961-6	
Triethylene glycol monobutyl ether	143-22-6	
Polyethylene glycol monobutyl ether	1559-34-8	

3. HAZARDS IDENTIFICATION

This product is not hazardous to health and environment according to EU criteria

4. FIRST AID MEASURES

Never give fluids or induce vomiting if patient is unconscious or is having convulsions

Inhalation: Remove to fresh air if effects occur. Consult a physician.

Skin Contact: Wash off in flowing water or shower

Eye Contact: Irrigate with flowing water immediately and continuously for 15 minutes. Consult medical personnel.

Ingestion: Induce vomiting if large amounts are ingested. Consult medical personnel

Note to Physician: No specific antidote. Supportive care. Treatment based on judgement of the physician in response to reactions of the patient.

5. FIRE FIGHTING MEASURES

Suitable extinguishing media: Water fog, carbon dioxide, alcohol resistant foam, dry chemical

Hazardous Combustion Products: None known. Complete combustion will give carbon dioxide and water

Special protective equipment: Wear positive pressure self-contained breathing apparatus and protective fire-fighting clothing (includes fire-fighting helmet, coat, trousers, boots and gloves)

* Trademark of the Dow Chemical Company under license to Nasaco International Limited

Fig 9-10. MSDS for DOW CORING 200 adapted from (DOW CORING, 2015)

SIGMA-ALDRICH

sigma-aldrich.com

SAFETY DATA SHEET

according to Regulation (EC) No. 1907/2006
Version 6.0 Revision Date 30.03.2016
Print Date 07.09.2019
GENERIC EU MSDS - NO COUNTRY SPECIFIC DATA - NO OEL DATA

SECTION 1: Identification of the substance/mixture and of the company/undertaking

1.1 Product identifiers

Product name	:	Calcium nitrate tetrahydrate
Product Number	:	C1396
Brand	:	SIGALD
REACH No.	:	A registration number is not available for this substance as the substance or its uses are exempted from registration, the annual tonnage does not require a registration or the registration is envisaged for a later registration deadline.
CAS-No.	:	13477-34-4

1.2 Relevant identified uses of the substance or mixture and uses advised against

Identified uses	:	Laboratory chemicals, Manufacture of substances

1.3 Details of the supplier of the safety data sheet

Company	:	Merck (Pty) Ltd. 1 Friesland Drive Longmeadow Business Estate South MODDERFONTEIN 1645 SOUTH AFRICA
Telephone	:	+27 +27 (0) 8600 63725
Fax	:	+27 +27 (0) 860 522 329
E-mail address	:	Melissa.byrne@merckgroup.com

1.4 Emergency telephone number

Emergency Phone #	:	

SECTION 2: Hazards identification

2.1 Classification of the substance or mixture

Classification according to Regulation (EC) No 1272/2008
Acute toxicity, Oral (Category 4), H302
Serious eye damage (Category 1), H318

For the full text of the H-Statements mentioned in this Section, see Section 16.

2.2 Label elements

Labelling according Regulation (EC) No 1272/2008
Pictogram

Signal word Danger

Hazard statement(s)
H302 Harmful if swallowed.
H318 Causes serious eye damage.

Fig 9-11. MSDS for SIBX Collector adapted from (Flottec, n.d.)

UĞUR SELÜLOZ KİMYA
MAKİNA VE GIDA SAN. VE TİC. A.Ş.
O.S.B. UMURLU / AYDIN
TURKEY

MATERIAL SAFETY DATA SHEET
FOR
CARBOXYMETHYL CELLULOSE

Version : 03-2
Date : 24.04.2007

SECTION 1 IDENTIFICATION OF SUBSTANCE

Product : CARBOXYMETHYL CELLULOSE, SODIUM also known as CMC
Commercial Name : USK
Manufacturer : UGUR SELULOZ KIMYA MAKINA ve GIDA SAN. ve TIC. A.Ş.
Address : O.S.B. Umurlu / AYDIN - TURKEY
Phone : +90 256 2591144
Fax : +90 256 2591004

SECTION 2 – COMPOSITION / INFORMATION ON INGREDIENTS

FORMULATION : Cellulose + NaOH+ MCA /SCMA → NaCMC+NaCl
CAS no : 9004-32-4

Components (dry basis)	Technical Grades %	Pure Grades %	Highly Purified Grades %
Carboxymethyl Cellulose (CMC)	min. 60	up to 99,5	min. 99,5
Sodium chloride (NaCl)	max. 40	min. 0,5	max. 0,5

SECTION 3 – HAZARDS IDENTIFICATION

- No particular hazards known, based on the available data the product is not dangerous.

SECTION 4 FIRST AID MEASURES

Skin Contact : In case of contact with skin wash with warm water.
Eye Contact : In case of contact with eyes rinse thoroughly with water.
Inhalation : In case of inhalation move person to fresh air and seek medical assistance.
Ingestion : In case of ingestion consult a doctor whether a stomach washout is necessary.

SECTION 5 FIRE-FIGHTING MEASURES

- Water Spray
- Foam
- Sand
- Extinguishing Powder
- Carbon Dioxide

SECTION 6 – ACCIDENTAL RELEASE MEASURES

Precautions : Extremely slippery wet material on walking grounds when mixed with water.
Environmental : Use of water is not recommended.
Methods for cleaning up : Collect by vacuum or shoveling while avoiding dust formation.

SECTION 7 HANDLING AND STORAGE

Handling : Keep formation of dust minimum. Use dust suction and ventilation.
Storage : Store in a dry place. Use original packing for humidity and water protection.
Explosion and fire : No special measures required.

Fig 9-12. MSDS for CMC adapted from (USK, 2007)

Sigma-Aldrich.

www.sigmaaldrich.com

SAFETY DATA SHEET

according to Regulation (EC) No. 1907/2006

Version 6.6
Revision Date 31.03.2020
Print Date 16.11.2020
GENERIC EU MSDS - NO COUNTRY SPECIFIC DATA - NO OEL DATA

SECTION 1: Identification of the substance/mixture and of the company/undertaking

1.1 Product identifiers

Product name : Phenol

Product Number : 242322
Brand : Sigma-Aldrich
Index-No. : 604-001-00-2
REACH No. : 01-2119471329-32-XXXX
CAS-No. : 108-95-2

1.2 Relevant identified uses of the substance or mixture and uses advised against

Identified uses : Laboratory chemicals, Manufacture of substances

1.3 Details of the supplier of the safety data sheet

Company : Merck (Pty) Ltd.
1 Friesland Drive
Longmeadow Business Estate South
MODDERFONTEIN
1645
SOUTH AFRICA

Telephone : +27 +27 (0) 8600 63725
Fax : +27 +27 (0) 860 522 329
E-mail address : Melissa.byrne@merckgroup.com

1.4 Emergency telephone number

Emergency Phone # : 0-800-983-611

SECTION 2: Hazards identification

2.1 Classification of the substance or mixture

Classification according to Regulation (EC) No 1272/2008
Acute toxicity, Oral (Category 3), H301
Acute toxicity, Inhalation (Category 3), H331
Acute toxicity, Dermal (Category 3), H311
Skin corrosion (Sub-category 1B), H314
Serious eye damage (Category 1), H318
Germ cell mutagenicity (Category 2), H341
Specific target organ toxicity - repeated exposure (Category 2), Nervous system, Kidney, Liver, Skin, H373
Long-term (chronic) aquatic hazard (Category 2), H411

Fig 9-13. MSDS for Phenol adapted from (Sigmaalderich, 2019).

Supelco

www.sigmaaldrich.com

SAFETY DATA SHEET

according to Regulation (EC) No. 1907/2006

Version 6.2
Revision Date 30.04.2021
Print Date 21.05.2021
GENERIC EU MSDS - NO COUNTRY SPECIFIC DATA - NO OEL DATA

SECTION 1: Identification of the substance/mixture and of the company/undertaking

1.1 Product identifiers

Product name : Sulfuric acid 95-97% for analysis EMSURE® ISO

Product Number : 1.00731
Catalogue No. : 100731
Brand : Millipore
Index-No. : 016-020-00-8
REACH No. : 01-2119458838-20-XXXX
CAS-No. : 7664-93-9

1.2 Relevant identified uses of the substance or mixture and uses advised against

Identified uses : Reagent for analysis, Chemical production

1.3 Details of the supplier of the safety data sheet

Company : Merck KGaA
Frankfurter Str. 250
D-64271 DARMSTADT

Telephone : +49 (0)6151 72-0
Fax : +49 6151 727780
E-mail address : TechnicalService@merckgroup.com

1.4 Emergency telephone

Emergency Phone # : +(44)-870-8200418 (CHEMTREC (GB))
+(353)-19014670 (CHEMTREC Ireland)
001-803-017-9114 (CHEMTREC India)

SECTION 2: Hazards identification

2.1 Classification of the substance or mixture

Classification according to Regulation (EC) No 1272/2008
Corrosive to Metals (Category 1), H290
Skin corrosion (Sub-category 1A), H314
Serious eye damage (Category 1), H318

For the full text of the H-Statements mentioned in this Section, see Section 16.

2.2 Label elements

Labelling according Regulation (EC) No 1272/2008

Fig 9-14. MSDS for Sulfuric acid adapted from (Sigmaalderich, 2019).

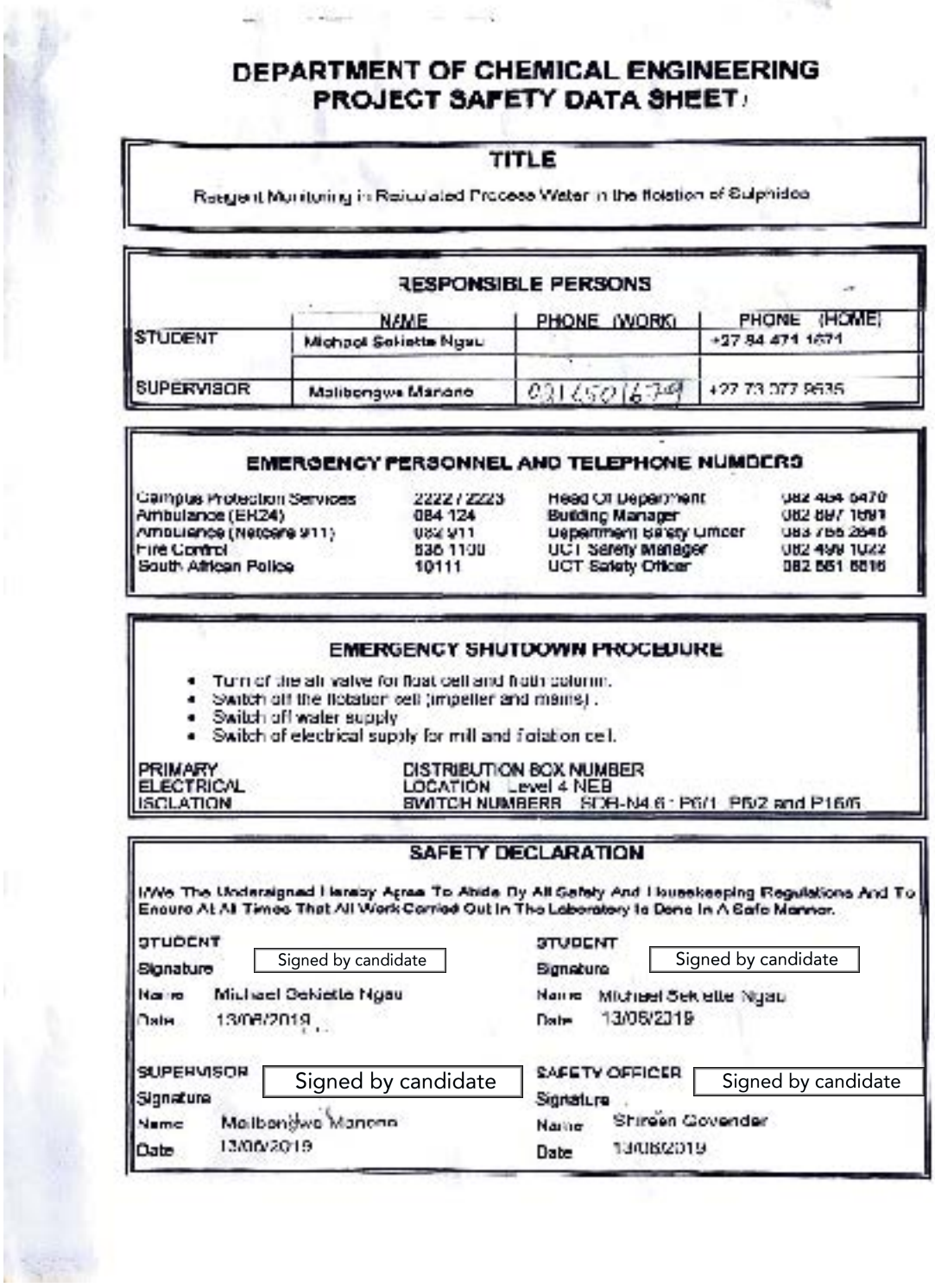

DEPARTMENT OF CHEMICAL ENGINEERING
PROJECT SAFETY DATA SHEET

TITLE

Reagent Monitoring in Recirculated Process Water in the flotation of Sulphides

RESPONSIBLE PERSONS

	NAME	PHONE (WORK)	PHONE (HOME)
STUDENT	Michael Sekitla Ngau		+27 84 474 1671
SUPERVISOR	Malibongwe Manono	0216502679	+27 73 077 9635

EMERGENCY PERSONNEL AND TELEPHONE NUMBERS

Campus Protection Services	2222 / 2223	Head Of Department	082 464 6470
Ambulance (EH24)	084 124	Building Manager	082 887 1691
Ambulance (Netcare 911)	082 911	Department Safety Officer	083 765 2646
Fire Control	535 1100	UCT Safety Manager	082 499 1042
South African Police	10111	UCT Safety Officer	082 551 5516

EMERGENCY SHUTDOWN PROCEDURE

- Turn of the air valve for float cell and froth column.
- Switch off the flotation cell (impeller and mains).
- Switch off water supply
- Switch of electrical supply for mill and flotation cell.

PRIMARY ELECTRICAL ISOLATION
DISTRIBUTION BOX NUMBER
LOCATION Level 4 NEB
SWITCH NUMBERS SDB-N4.6 : P6/1 P6/2 and P16/5

SAFETY DECLARATION

I/We The Undersigned Hereby Agree To Abide By All Safety And Housekeeping Regulations And To Ensure At All Times That All Work Carried Out In The Laboratory Is Done In A Safe Manner.

STUDENT
Signature Signed by candidate
Name Michael Sekitla Ngau
Date 13/06/2019

STUDENT
Signature Signed by candidate
Name Michael Sekitla Ngau
Date 13/06/2019

SUPERVISOR
Signature Signed by candidate
Name Malibongwe Manono
Date 13/06/2019

SAFETY OFFICER
Signature Signed by candidate
Name Shireen Govender
Date 13/06/2019

Fig 9-15.Project Safety Data Sheet

COMPANY: OCCUPATION: SafeCare Series Starter Pack

Occupational Risk & Exposure Profile ("OREP")

NAME: Michael Sekielte Ngau DATE: 13/06/2019

Brief job description: Batch flotation tests

SECTION: CMR DEPARTMENT: CHEM ENG DIVISION: EBE

Rate all aspects on a scale of 1-5. (/ = None; 1 = Low; 3 = Medium; 5 = High)

INHERENT REQUIREMENTS

Requirement scores ⇨	CAP	Requirement scores ⇨	CAP
THE SENSES		**COMPOSITE FUNCTIONS**	
Hearing	3	Fine motor control	5
Balance	3	Hand-eye co-ordination	5
Vision: Acuity - near	5	Hand-eye-foot co-ord	5
Acuity - far	3	Use of both hands required	5
Visual fields	3	Use of both feet required	5
Depth	3	Strength (power) (kg)	/
Colour	1	Endurance (fitness)	/
Night vision	/		
Smell	5		
Touch	5		
GENERAL		**SECONDARY TASKS**	✓
Clarity of speech	3	Company Driver (Code___)	/
Company Driver (______)	/	Forklift operator	/
Operator	/	Operate hazardous machinery	/
		Fire / Rescue Team	/
		Hazmat / Spill Team	/
		First Aid	5
PPE REQUIRED	REQ	**ENVIRONMENT / TASKS**	CAP
Hard Hat	/	Climbing ladders/stairs	/
Eye Protection	5	Work at heights	/
Face Shield	1	Confined spaces	/
Mask	5	Near dangerous machinery	/
Respirator	1	Prolonged sitting	/
Air hood/ Fume Hood/ Flow cabinet	3	Bending/squatting	/
Hearing Protection	1	Prolonged standing	3
Overall/ lab coat	5	Uneven or slippery terrain	/
Fleece-lined jacket	/	Poor lighting	/
Safety Belt/Harness	/	Shift work	/
Gloves	5	Other	/
Safety Boots	5		

BASE-LINE HAZARD EXPOSURE

Hazardous CHEMICAL Substances (Powders, liquids, fumes, dusts, etc.)

Group: [illegible]

Chemical Name	CONC	PROB	R-S#	GRP	Target Organs	SENSE
SIBX					skin, eyes, resp.	
SENDEP 30 D					skin, eyes, resp.	
SENDEP 516					skin, eyes, resp.	
SP3 WATER					skin, eyes	

Please continue on extra sheet

BIOLOGICAL Agents	CONC	PROB
Please continue on extra sheet		

DUST	CONC	PROB
Asbestos	4	/
Silica / Quartz	3	/
Grain / Wood / Chaff	2	/
Cotton / Flax	2	/
Animal Protein	2	/
Other		

PHYSICAL Agents	CONC	PROB
Noise	3	3
Heat	2	1
Cold	3	1
Glare	2	/
Vibration (Segmental)	3	3
Vibration (Whole)	2	/

PHYSICAL Agents	CONC	PROB
Radiation (ionising) - x-rays	4	/
- alpha / beta / gamma	4	/
Radiation (N-ion) - Laser	2	/
- UV (sun, welding)	4	/
- Infra Red (sun welding)	2	/
- Radio & micro	2	/
- V.F, ELF, mag	2	/
- EMF	2	/
Please continue on extra sheet		

ERGONOMIC Hazards	CONC	PROB
Abnormal posture		/
Truncal twisting		/
Static loading		
Static loading		

ERGONOMIC Hazards	CONC	PROB
Repetitive movements		1
Forceful movements		
Tasks at extremes of reach		

NOTES

Approved by: [signature] Position: Lab Manager Date: 13/06/2019

OREP Help snapshot.

Unauthorised reproduction prohibited. Licence Number: [illegible] | Reference: [illegible] | Written: [illegible] | Updated: [illegible] | Page 1 of 1 | Occupational Health Management Systems

Fig 9-16.OREP Form.

Appendix D. Ethics Application Form

Application for Approval of Ethics in Research (EiR) Projects
Faculty of Engineering and the Built Environment, University of Cape Town

ETHICS APPLICATION FORM

Please Note:
Any person planning to undertake research in the Faculty of Engineering and the Built Environment (EBE) at the University of Cape Town is required to complete this form **before** collecting or analysing data. The objective of submitting this application *prior* to embarking on research is to ensure that the highest ethical standards in research, conducted under the auspices of the EBE Faculty, are met. Please ensure that you have read, and understood the **EBE Ethics in Research Handbook** (available from the UCT EBE, Research Ethics website) prior to completing this application form: http://www.ebe.uct.ac.za/ebe/research/ethics1

APPLICANT'S DETAILS		
Name of principal researcher, student or external applicant		MICHAEL SEKIETTE NGAU
Department		CHEMICAL ENGINEERING DEPARTMENT
Preferred email address of applicant:		
If Student	Your Degree: e.g., MSc, PhD, etc.	MSc.Eng in Chemical Engineering
	Credit Value of Research: e.g., 60/120/180/360 etc.	180
	Name of Supervisor (if supervised):	Dr. Malibongwe Shadrach Manono, A/Prof. Kirsten Corin
If this is a researchcontract, indicate the source of funding/sponsorship		
Project Title		Recirculated Process Water in the Flotation of Sulphides

I hereby undertake to carry out my research in such a way that:

- there is no apparent legal objection to the nature or the method of research; and
- the research will not compromise staff or students or the other responsibilities of the University;
- the stated objective will be achieved, and the findings will have a high degree of validity;
- limitations and alternative interpretations will be considered;
- the findings could be subject to peer review and publicly available; and
- I will comply with the conventions of copyright and avoid any practice that would constitute plagiarism.

APPLICATION BY	Full name	Signature	Date
Principal Researcher/ Student/External applicant	Michael Ngau	Signed by candidate	13/06/2020
SUPPORTED BY	Full name	Signature	Date
Supervisor (where applicable)	Dr Malibongwe Shadrach Manono	Signed by candidate	17/06/2022

APPROVED BY	Full name	Signature	Date
HOD (or delegated nominee) Final authority for all applicants who have answered NO to all questions in Section 1; and for all Undergraduate research (Including Honours).	D Deglon	Signed by candidate	
Chair: Faculty EIR Committee For applicants other than undergraduate students who have answered YES to any of the questions in Section 1.			

Page **1** of **1**

Fig 9-17. Ethics Application Form